ANALYSIS OF EGF SIGNALING IN HEALTHY AGING PROMOTION IN *CAENORHABDITIS ELEGANS*.

by

SHIH-HUNG YU

A dissertation submitted to the

Graduate School-New Brunswick

Rutgers, The State University of New Jersey

and

The Graduate School of Biomedical Sciences

University of Medicine and Dentistry of New Jersey

In partial fulfillment of the requirements

For the degree of

Doctor of Philosophy

Graduate Program in Neuroscience

Written under the direction of

Monica Driscoll, Ph.D.

And approved by

_____

_____

_____

_____

New Brunswick, New Jersey

January, 2012

ABSTRACT OF THE DISSERTATION

ANALYSIS OF EGF SIGNALING IN HEALTHY AGING

PROMOTION IN *CAENORHABDITIS ELEGANS*

By

SHIH-HUNG YU

Dissertation Director:

Monica Driscoll, Ph.D.

The increase in longevity expectancy has been a focused issue goal of much current aging research. Many genes have been noted to modulate longevity of simple model systems, acting through distinct mechanisms. However, in principle, promotion of healthy aging of individual tissues can be accomplished without a major impact on the longevity endpoint. As such, healthspan-only genes may have been missed by genetic screens for longevity. New screens for tissue–specific betterment of aging phenotypes were anticipated to reveal a class of genes that might be manipulated for tissue-specific anti-aging outcomes. We identified two novel healthspan regulators, called HPA-1 and HPA-2 (for the high performance in old age locomotory phenotypes that their disruption confers) that delay age-associated locomotory

decline when they are knocked down by RNAi or by genetic deletion. Surprisingly, *hpa-1* and *hpa-2* do not regulate healthspan through canonical recognized longevity pathways. Instead, the structure of HPA proteins implicated a novel function of EGF signaling in anti–aging protection, and my genetic studies supported this mechanism. Activated EGF signaling confers a positive effect on multiple aging phenotypes, acting through the downstream branch of the EGF pathway involving PLCγ and the IP3 receptor. Further analysis defined the temporal and spatial benefits from EGF signaling. EGF/*lin-3* ligand is expressed into late life and acts throughout life to influence healthy aging. *lin-3* alternative slice variants, *lin-3S* and *lin-3XL* show healthspan promotion. Muscle and neuron are the most potent tissue for EGFR signaling on healthspan enhancement. I also identified global and tissue-specific modulators of healthy aging in the EGF pathway and identified candidate calcium-sensitive transducers of the anti-aging function of EGF signaling. Recent data in vertebrates suggest that EGF signaling might contribute to long-term maintenance. Thus, EGF signaling may exert a conserved impact on healthy aging and might be a plausible reagent for anti-aging therapies.

ACKNOWLEDGMENTS

First and most importantly, I would like to thank my Ph.D. supervisor, Dr. Monica Driscoll, for her extraordinary patience and guidance. She is my model of working in science. I benefited tremendously from her scientific expertise and enthusiasm. Moreover, she always thinks of students and knows what is best for us. Without her, I could not complete the Ph.D. program, be who I am today and mature as a scientist. She is the best mentor that I have ever met.

I would like to thank the members of my dissertation committee, Dr. Richard Padgett, Dr. John Pintar and Dr. Andrew Singson for their support, excellent advice and valuable guidance. With their help, I have more confidence in my Ph.D. dissertation and research.

In addition, I would like to thank all the past and present members of the Driscoll lab. Specially thank to Dr. Hiroaki Iwasa for his technical help and valuable discussion when initiating the EGF project and laying good foundation for the following interesting and supportive study in this direction. It has been a great time to cooperate with him on the EGF project; to Mr. Jian Xue for his help in constructing IGF receptor related RNAi clones and transgenic mutants used in this study; to Dr. Brian Onken for technical help and scientific discussion; and to all the members of the Driscoll lab; they have been a great support and created a great environment for my research.

Lastly, I would like to thank my family and friends for their fully support, especially my lovely family members in Taiwan and my sister currently in Cincinnati for their endless love, incredibly understanding and encouragement,

and always having faith in me throughout my graduate career. I am glad and honored to make them proud.

TABLE OF CONTENTS

LIST OF FIGURES

CHAPTER 4 : Summary and perspectives

LIST OF TABLES

CHAPTER I:

Introduction

Biology of aging

Aging can be defined as the gradual changes in an organism over time accompanied by progressive loss of physical function and increasing mortality with advancing age. The rapidly increasing elderly population suffers a diminished quality of life and consumes a disproportionate amount of health care resources. Therefore, understanding the biology of aging is centrally important for medical, political, and social reasons.

There are many factors involved in the aging process, including genetic and environmental components. Several conserved genes in model systems from yeast *Saccharomyces cerevisiae* to *C. elegans*, *Drosophila*, and mice exhibit remarkable effects on life span. For example, mutants that reduce activity of the insulin signaling pathway exhibit slowed locomotory decline and extended lifespan (Kenyon, 2010). Likewise, genes or conditions affecting dietary restriction (Lakowski and Hekimi, 1998; Panowski et al., 2007) or mitochondrial function (Dillin et al., 2002b; Feng et al., 2001) can alter lifespan. Furthermore, environmental signals such as stress (An and Blackwell, 2003; Apfeld et al., 2004; Hsu et al., 2003) and nutrient availability can affect organism longevity. Stochastic factors also are significant in aging and can explain how individuals with a uniform genetic background and environment can age either well or poorly (Herndon et al., 2002). Overall, genetic, environmental, and stochastic processes exert interconnected effects on quality of aging.

Sarcopenia is one of the most prevalent conditions in aging and genetic approaches toward understanding

Sarcopenia, the progressive decline of age-related muscle mass and strength with age, is a major problem of functional decline and frailty in the elderly. Sarcopenia initiates at midlife and causes significant loss so that individuals can expect nearly 50% muscle mass loss by age 90 (Evans, 1997). At the cellular level, sarcopenia is associated with disorganized change in muscle fibers, including sarcomere loss, and lipid content increase in the muscle tissue. There are several factors that are correlated with sarcopenia during aging such as contraction-related cellular injury, endocrine changes, reduced regenerative potential, and oxidative stress (Chow et al., 2006). However, the pathophysiology leading to the development of sarcopenia is not well investigated genetically or molecularly and preventative therapies are not available (Fisher, 2004).

The benefit of addressing aging biology in simple organisms

Analyses in invertebrate models have significantly advanced understanding of genetic and environmental influences that modulate aging process. Manipulating aging of higher organisms is difficult and time consuming. However, simple organism models (yeast (*S. cerevisae*), worms (*C. elegans*), flies (*D. melanogaster*), to mice (*M. musculus*)) can be good experimental sources in which to advance understanding of basic biological mechanisms. For instance, *C. elegans* lives only about three weeks in the lab, whereas humans live 10 decades. Many of these simple models share biologically relevant pathways with

mammals. Simple models are also easier to maintain and do not present experimental ethics barriers. Indeed, much insight into the basic biology of aging has been gleaned from studies of conserved pathways in simple model systems.

Caenorhabditis elegans – a powerful model organism for the study of aging

Caenorhabditis elegans is a small free-living, non-parasitic soil nematode that feeds mainly on bacteria. *C. elegans* have a life cycle that progresses through four larval stages: L1, L2, L3, and L4, then molt into reproductive adult (Figure 1). The animal exists primarily as a self-fertilizing hermaphrodite that reproduces the major proportion of *C. elegans* with a low frequency of males. Each hermaphrodite animal is fertile for approximately 4-8 days and can produce over 300 progeny. The progeny from hermaphrodite are genetically identical to the parent, yielding an extremely useful homogeneous genetic tool. However, there is also sexual reproduction between male worms and hermaphrodites to provide facile genetics studies.

C. elegans is a popular and powerful *in vivo* genetic model used to study the process of aging. The entire genome is sequenced and annotated, which facilitates conducting a broad range of molecular and genetic experiments. Many genetic mutants, RNAi knockdown gene libraries (Kamath and Ahringer, 2003), or DNA transgenic animals (for example, generating GFP reporter fusion) are available to manipulate gene expression. Plenty of data has been acquired and

much insight into basic biological mechanisms has been gained. The advantages of using *C. elegans* specifically for aging studies include the relatively short life cycle. Analysis of aging tissues can be simplified since all somatic cells are post-mitotic and there is no tissue regeneration. Numerous experiments have identified mutations that dramatically extend lifespan, and analyses of these mutants has provided a basis for understanding the mechanisms driving the aging process (Antebi, 2007; Kenyon, 2010).

Aging in *C. elegans*

Although multiple factors are involved in aging process in *C. elegans*, many single longevity related mutations known in yeast, flies, and mice dramatically extend the *C. elegans* lifespan (Longo and Finch, 2003)(Figure 2). In addition, there is a major stochastic component to how well animals age that is distinct from standard genetic programming and standard environmental factors (Herndon et al., 2002).

C. elegans has a basic biology of muscle structure and function that is remarkably similar to human skeletal muscle. Moreover, nematode sarcopenia bears striking similarity to human sarcopenia at the cell and phenomenological levels such as mid-life onset, sarcomere degeneration, and fat accumulation (Herndon et al., 2002). Interestingly, *C. elegans* muscle integrity deteriorates dramatically while the nervous system shows little obvious gross structural change in aging worms. Given the power of *C. elegans* genetic screens to

identify genes required for specific aging phenotypes, it is plausible to screen for genes that influence muscle healthspan by identifying those that accelerate or delay mobility decline (Iwasa et al., 2010; Schreiber et al., 2010).

Evaluation of healthy aging in *C. elegans*

As a focus of aging research progresses from concentration on the longevity endpoint to increased healthspan evaluation, the issue of how to measure healthy aging becomes a front-and-center challenge. One metric that most likely indicates healthspan at the organism level is measurement of survival of an aging population at middle and middle/late life--scores such as the 50% survival time point or mean lifespan. Genetic or drug manipulations that extend mean survivorship but not necessarily maximum lifespan are likely to be of value for extending the period of healthy life prior to decline. Analysis of mortality curves is another option for analysis of changes in the “rate of aging” (Johnson, 1987).

Several *C. elegans* behaviors decline with age (Bolanowski et al., 1981; Chow et al., 2006; Garigan et al., 2002; Glenn et al., 2004; Herndon et al., 2002; Huang et al., 2004) and the extent of change can be used as a measure of healthspan. Pumping of the pharynx, an organ through which the animal ingests its bacterial food, declines fairly precipitously with age (Chow et al., 2006; Huang et al., 2004). A two-day-old adult pumps on the order of 300 contractions/minute, a rate that progressively slows to essentially zero at about 12 days of adult life (Collins et al., 2008). Pharyngeal contractions are easily observed through the transparent

cuticle, and can be scored directly or with the aid of video analysis. Because the pharynx pumps by some autonomous mechanisms and includes specialized muscle that resembles mammalian heart muscle, the *C. elegans* pharynx is sometimes considered to model mammalian heart (Mango, 2007), and its age-associated decline to model mammalian cardiac aging.

The vigor of locomotion on solid support (agar plates in the lab) or in liquid (swimming) declines during *C. elegans* adult life. Diminished rates of movement can be measured by eye (body bends per unit time) or with computer programs that track locomotion (Huang et al., 2006; Schreiber et al., 2010; Tsechpenakis et al., 2008). Interestingly, locomotory behavior decline correlates with deterioration of body wall muscle, with fewer sarcomere units present over time and increased fat infiltration, reminiscent of mammalian sarcopenia (Garigan et al., 2002; Glenn et al., 2004). Although muscle exhibits markedly more dramatic cellular deterioration than do neurons, some neuronal influence on *C. elegans* sarcopenia appears operative (Glenn et al., 2004; Murakami et al., 2008).

Another conserved trait that tracks with age is the accumulation of fluorescent lipofuscin and advanced glycation end products (Gerstbrein et al., 2005), collectively referred to as age pigments. In *C. elegans* this fluorescence is concentrated in gut granules that appear to be secondary lysosomes (Clokey and Jacobson, 1986). Since extensively cross-linked lipofuscin cannot be degraded by lysosomal machinery, lysosomes accumulate this fluorescent material and are

thought to become progressively impaired as adults age. Interestingly, animals that age well (by locomotory criteria) tend to have low age pigment accumulation and those that age poorly accumulate relatively high levels (Gerstbrein et al., 2005). Likewise, animals that are long-lived (for example the *daf-2(rf*) insulin receptor mutant) tend to have lower age pigment scores than do progeric mutants such as *daf-16*/FOXO transcription factor. Thus, high age pigment scores suggest a poor healthspan and relatively low age pigments scores suggest a strong healthspan. Age pigments can be scored using an image analysis program that measures relative intensity of fluorescence in the 340nm range; a more precise approach is to use a fluorometer that can scan samples over a range of input wavelengths and quantitate emission spectra (typically peak emission is ~342 nm).

Although more detailed cellular phenotypes than those listed above can be characterized, use of the aforementioned relatively easily determined measures can indicate whether a population appears to be aging well or poorly relative to wild-type controls. Note that animals may exhibit system-wide evidence of a strong healthspan (all measures) or extended healthspan of individual tissues (only pharynx, body wall muscle, intestine, for example) for a given genetic or drug intervention.

The Insulin/IGF signaling pathway

Insulin/IGF signaling has multiple roles in biology functions. The insulin/IGF pathway affects cellular metabolism, development, and aging of living organisms. Importantly, the insulin signaling pathway is conserved from nematodes to humans. Dauer formation defects and longevity are the most observed phenotypes caused by insulin signaling pathway mutations in *C. elegans*. Some insulin signaling pathway molecules such as insulin-like receptor DAF-2, and downstream transcription factor FOXO/DAF-16 can regulate dauer formation (Gottlieb and Ruvkun, 1994). Interestingly, mutations involved in the insulin signaling pathway induce a conserved mechanism that promotes longevity in yeast, worms, fruit flies, and mammals (Kenyon, 2001). Previous studies have shown that down-regulation of *daf-2, age-1*, *pdk-1,* and *akt-1/akt-2* in the insulin/IGF-1 signaling pathway extends lifespan (Kimura et al., 1997; Morris et al., 1996; Paradis et al., 1999; Paradis and Ruvkun, 1998); while *daf-16* inactivation shortens life span (Lin et al., 1997; Ogg et al., 1997). In *C. elegans*, the insulin-like signaling pathway features 40 insulin-like ligands, the DAF-2 insulin like receptor, PI3 (phosphatidylinositol-3-OH) kinase AGE-1, kinases PDK-1, AKT-1/AKT-2, SGK-1 and downstream DAF-16/FOXO transcription factor (Figure 3). Mutations in the genes upstream of *daf-16* lower DAF-16 phosphorylation and DAF-16 translocates into the nucleus (Lin et al., 2001). In the nucleus DAF-16 affects longevity by turning on or repressing genes that regulate stress responses, development and metabolism. Some other signaling such as germline signaling (Hsin and Kenyon, 1999) and JNK signaling (Oh et al.,

2005) can also affect life span through DAF-16 only, but not the whole insulin signaling pathway.

EGF signaling is a conserved pathway in many organisms

The epidermal growth factor receptor (EGFR) is transmembrane receptor tyrosine kinase that belongs to the mammalian ErbB subfamily (EGFR, Erb-2/HER-2; Erb-3/HER-3; Erb-4/HER-4). When mammalian EGF family ligands bind (EGF, TGF-α, HB-EGF, amphiregulin, epiregulin, epigen, betacellulin, neuregulin) (Figure 4), EGFRs regulate cellular signal transduction pathways that regulate cell proliferation, survival, and migration (Citri and Yarden, 2006). Although different ligands can bind to different receptors to induce the signaling network, the ligands contain an EGF-like consensus sequence which consists of six cysteines, and the receptors include extracellular ligand binding domain (leucine-rich region; responsible for ligand binding; termed as L domain), transmembrane domain, and kinase domain.

EGF signaling is a conserved pathway and several genetic studies have studied EGF signaling in model organisms such as *Drosophila* and *C. elegans*. In *Drosophila,* EGF family signaling is mediated by TGFα-related ligands Spitz (ventral ectoderm patterning (Schweitzer et al., 1995)), Keren (Reich and Shilo, 2002), Gurken (oogenesis (Nilson and Schupbach, 1999)), and Vein (oogenesis role, neuregulin homolog (Schnepp et al., 1996)) and EGFR homolog DER (Shilo, 2003)(Figure 4). One secreted EGF-binding protein, Argos, is known to

sequester Spitz ligand to limit signaling (Klein et al., 2004). During embryogenesis, the ligands regulate the receptor activation temporally and spatially, maintaining gonad homeostasis and growth (Gilboa and Lehmann, 2006; Shilo, 2005).

In *C. elegans*, LIN-3 and LET-23 are the homologs of EGF ligand and EGFR, respectively (Aroian et al., 1990; Hill and Sternberg, 1992). There are three distinct downstream signal transduction pathways for EGF signaling (Figure 5). EGFR acts through the RAS-MAPK (*let-60-mek-1*) pathway to affect several cell fates, including the well-studied vulva development and male spicule formation (Moghal and Sternberg, 2003). In addition, EGFR acts through PLC-γ (*plc-3*) and IP3-inositol (1,4,5) trisphosphate (*itr-1*) signaling to affect ovulation and defecation (Clandinin et al., 1998; Yin et al., 2004). EGFR (LET-23) signaling also induces behavioral quiescence at the molt through *plc-3*, *unc-13*(diacylglycerol binding protein), and *tpa-1*(diacylglycerol binding protein). *unc-7* (gap junction innexin) is required for inhibition of feeding at the molt, and *egl-4* (cGMP dependent protein kinase) is required for inhibition of locomotion (Van Buskirk and Sternberg, 2007). However, no aging related information has ever been published on this pathway in nematodes.

Summary of thesis work

In this thesis I describe our efforts to identify factors that delay *C. elegans* sarcopenia, and how that work unexpectedly led us to discover that the EGF

pathway is a strong promoter for healthy aging in *C. elegans* (Chapter 2). Our initial work also showed identified novel negative regulators of EGF healthspan signaling, the HPA genes, which have primary sequences that suggest they might bind EGF ligand to limit signaling. We also defined the ITR-1 branch of the EGFR signal transduction pathways as critical for promoting healthspan.

I further investigated details of the mechanism by which EGF signaling promotes healthspan (Chapter 3). I identified splice isoforms EGF-S and EGF-XL as factors that can promote healthy aging, I showed that EGF acts both in development and during adulthood to influence aging, and I showed that EGFR(gf) expression in muscle, neurons and intestine can promote healthy aging. I also identified additional molecules that act in the pathway to extend healthspan, and I found some candidate proteins that might directly link cellular calcium changes to healthy aging. Overall, my thesis work began when the field did not know anything about EGF signaling effects on aging in any organism and ended with the identification of multiple gene activities in one specific sub-pathway that promote successful aging. Other recent discoveries in the field, including the establishment of a role of a different EGF subpathway for maintaining protein folding homeostasis (Liu et al., 2011) and a role of EGF in protecting against late-onset polyglutamine expansion disorders (Fryer et al., 2011), support that EGF signaling in general plays an important role in late-age maintenance.

Figure 1

A

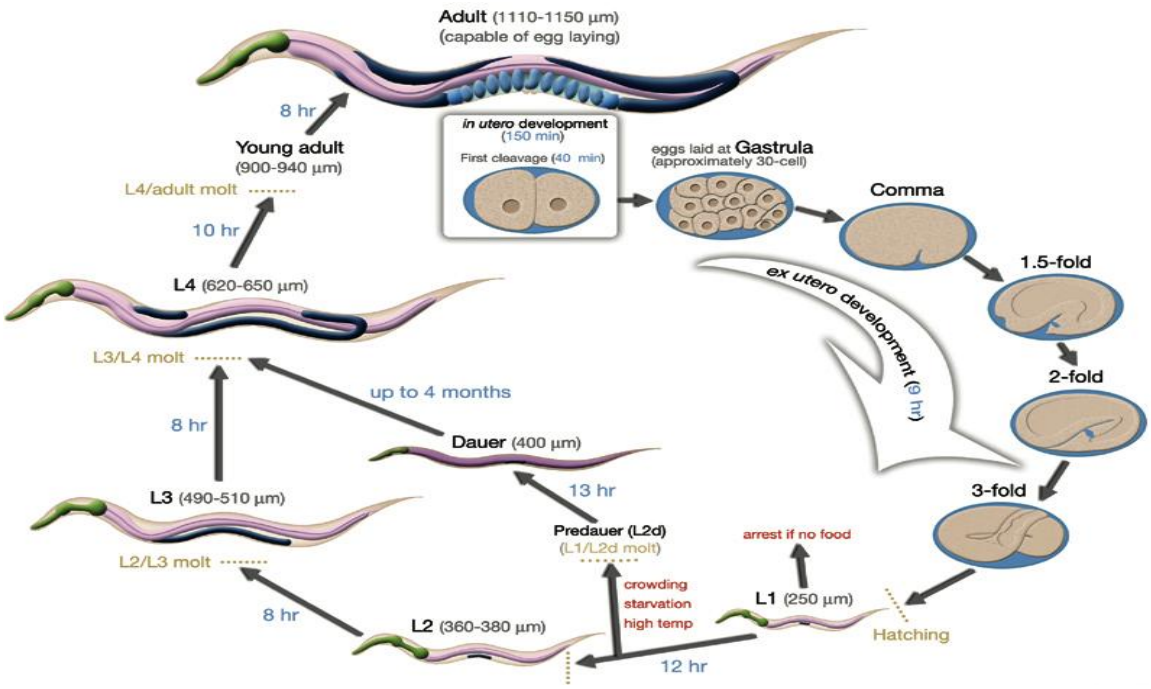

B

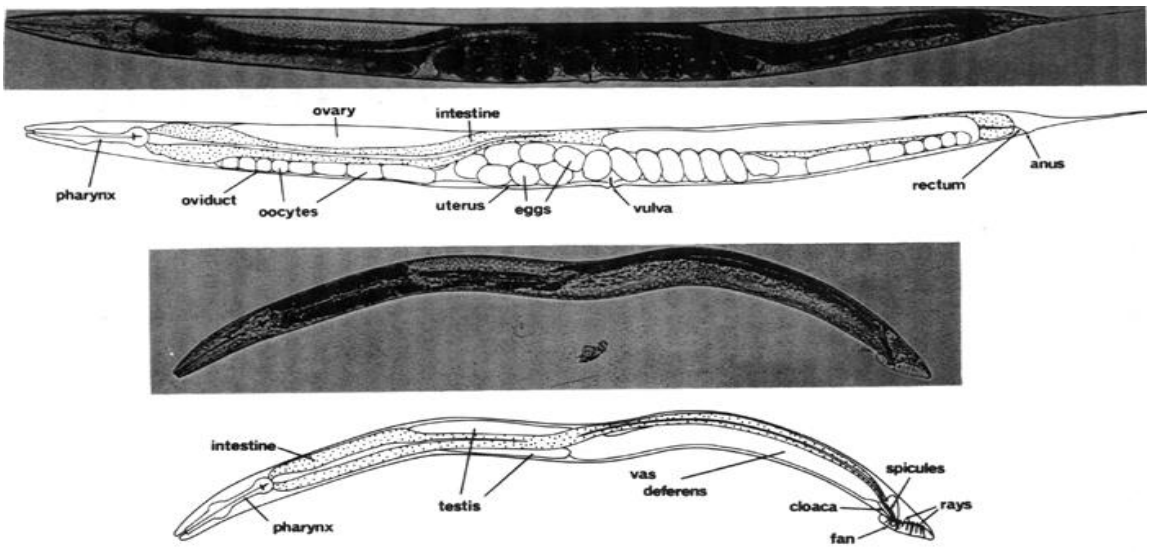

A. The life cycle of *C. elegans* (worm atlas)

B. The anatomy of *C. elegans* (*C.elegans II*)

Figure 2

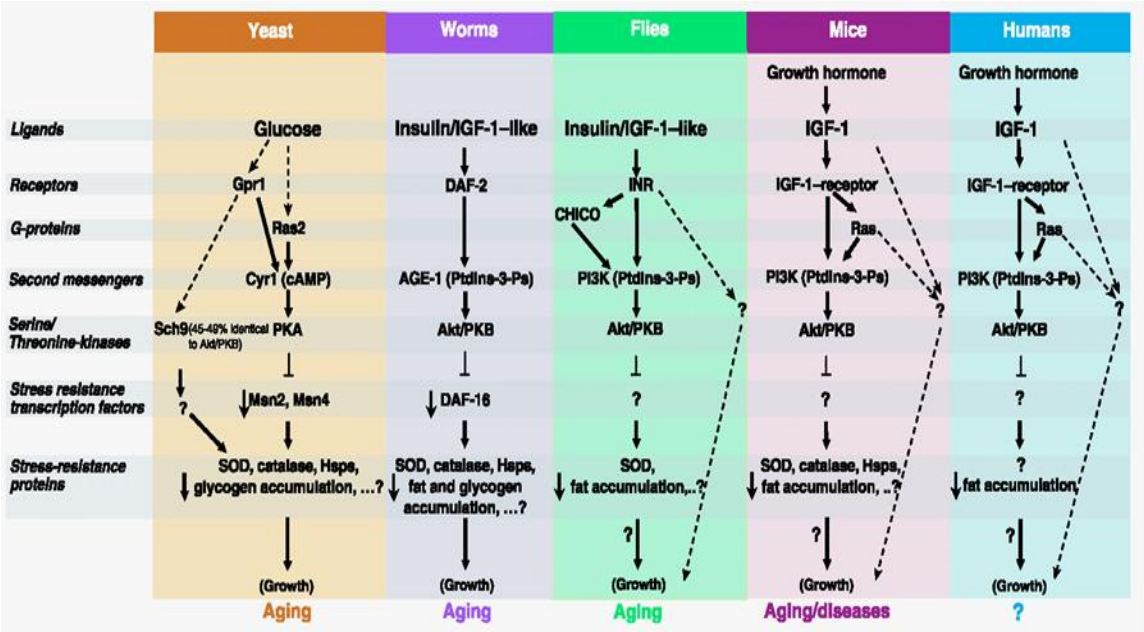

(Longo and Finch, 2003)

A conserved insulin-mediated pathway regulating lifespan. Certain components are still unknown in some simple and higher organisms but the general pathway is similar across species.

Figure 3

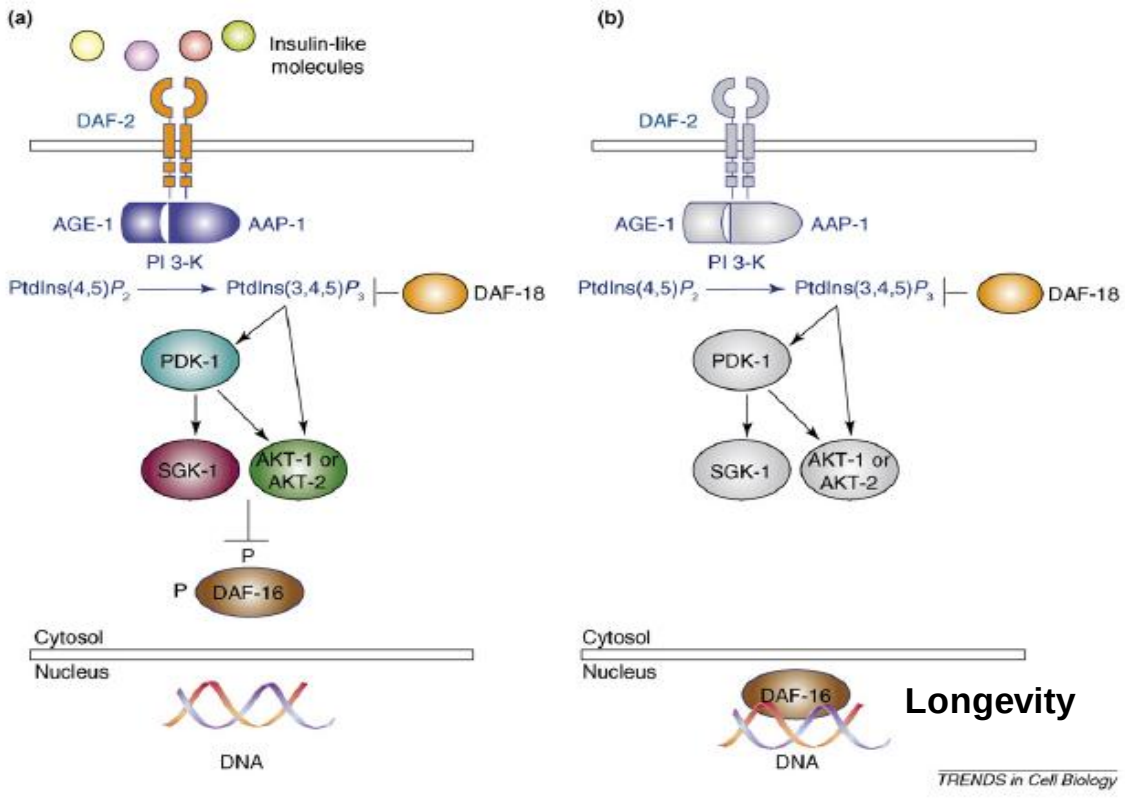

(Mukhopadhyay and Tissenbaum, 2007)

Insulin/IGF-like signaling pathway in *C. elegans*. The insulin signaling pathway is conserved from nematodes to humans. Panel (a) shows the complete signaling when insulin ligands binds to the receptor DAF-2 to transduce downstream signaling under favorable growth/reproduction conditions. Panel (b) shows how DAF-16 translocates into the nucleus during unfavorable environments associated with stresses.

Figure 4

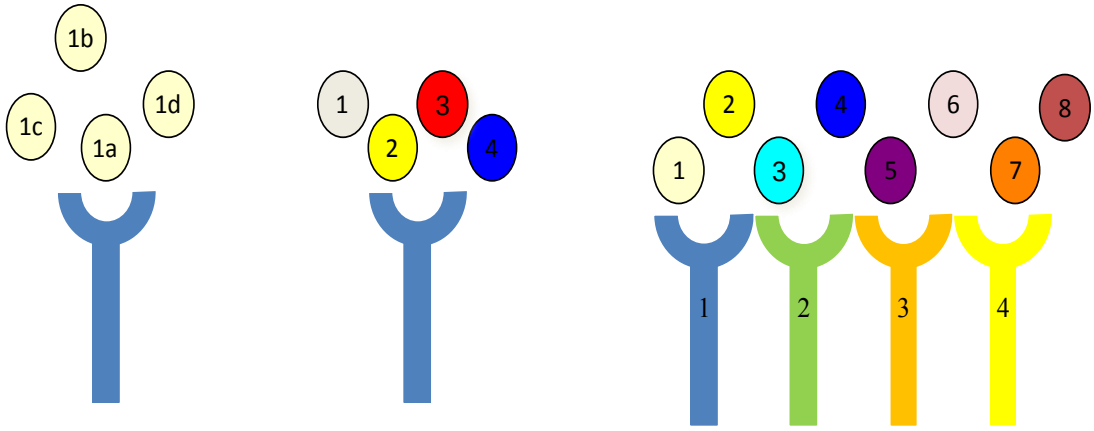

worm **fly** **human**

(Yu and Driscoll, 2011)

Summary of ligands and receptors in the EGF signaling pathways in *C. elegans*, *Drosophia melanogaster*, and humans. There is only one EGF ligand gene, *lin-3*, encoded by the *C. elegans* genome, although 4 splice-generated isoforms can be produced (noted a-d) (Van Buskirk et al., 2007). Four ligand genes are found in *Drosophila:* 1. Keren, 2. Spitz (TGF-α related), 3. Gurken, 4. Vein (neuregulin homolog). There are eight ligands in human: 1. EGF, 2. TGF-α, 3. Amphregulin, 4. Neuregulin, 5. Epigerulin, 6. Epigen, 7. Betacellulin, 8.HB-EGF. Both *C. elegans* and *Drosophila* genomes encode single EGFR receptors, LET-23 and DER respectively. Four ErbB subfamily receptors in human are: 1. EGFR , 2. HER-2 , 3. HER-3 , 4. HER-4. Human ligands cross-bind to multiple receptors.

Figure 5

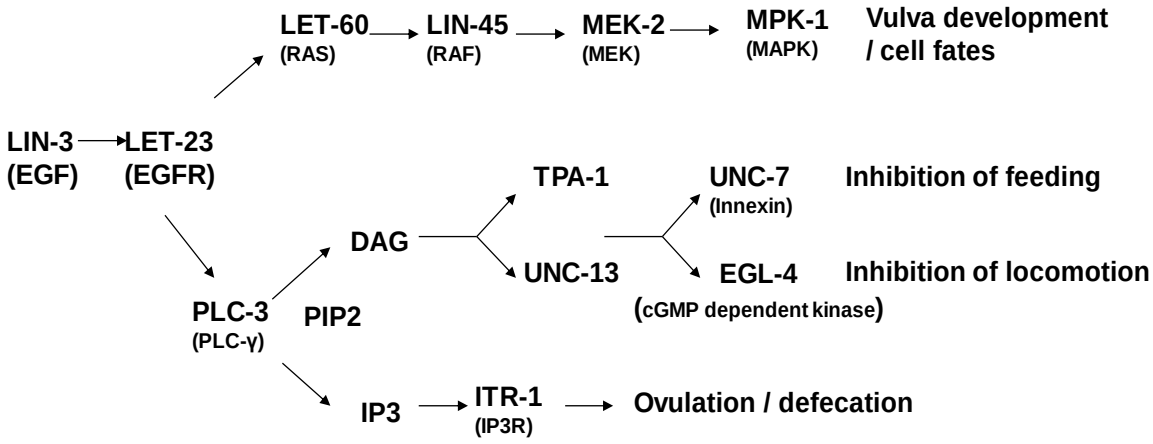

(Modified from Van Buskirk and Sternberg, 2007)

The EGFR signaling pathway in *C. elegans*. LIN-3 is the EGF ligand, and LET-23 is the EGF receptor. There are two separate signaling pathways downstream of *let-23*. The RAS signaling regulates cell fates such as vulva development. The PLC-γ signaling regulates ovulation/defecation through IP3 and behavioral quiescence through DAG.

CHAPTER II:

Novel EGF pathway regulators modulate *C. elegans* healthspan and lifespan via EGF receptor, PLC-γ, and IP3 receptor activation

In this chapter, I contributed to part of the results of the published paper in the journal Aging Cell. Here I briefly conclude my contribution to the published paper. The manuscript of Aging Cell paper is included in the Appendix.

1. I helped the screening of 54 clones of IGF receptor related genes, to test effects on locomotory decline rate by RNAi inactivation strategy. I did the screening for 1/3 of possible candidates (Figure 1; paper Table S1).
2. I found there is no developmental defect for the best two newly identified healthspan promoters, *hpa-1(tm3256)* and *hpa-2(tm3827)*. The pharyngeal pumping rate, defecation cycle, brood size, vulva formation, and dauer formation percentage are all similar to the matched control in both *hpa(RNAi)* and *hpa* deletion mutants. (paper FigureS2, TableS2)
3. I also examined the developmental phenotypes of double mutant, *hpa-2(tm3827); hpa-1(tm3256)*. Consistent with *hpa-1* RNAi, *hpa-2* RNAi, and single *hpa* deletion mutant phenotypes, the double deletion mutant did not change any basic behavior up to young adult (paper Figure S3).
4. Then I focused on the EGF signaling components on aging regulation. I conducted lifespan analysis and late-age locomotory prowess by *let-23(gf)* and *let-23(rf).* Note that Iwasa, the first author of the Aging Cell paper conducted these experiments at the same time too. Our results show the same trends for EGFR/*let-23* mutants. We found that the gain-of-function mutant of *let-23, let-23(sa62),* confers a more vigorous swimming behavior, and an extended survival curve. The lifespan data also implicated that *let-23(gf)* exerts more positive impact on mid-life survival (when ~ 50% of the

populations still survive). Conversely, *let-23(n1045)* exhibited faster decline in longevity. Similar to *let-23(gf)*, *let-23(rf)* survive less robustly in the mid-age of the life cycle (paper Figure 3A, 3G, 3H, TableS3).

5. I further analyzed the downstream EGF signaling branches. To identify which signaling branch that influences age-associated phenotypes, I conducted RNAi knockdown of genes encoding components acting downstream of the EGF signaling. My data indicated that inactivation of IP3 signaling components are deleterious to healthspan and IP3 signaling plays important roles in aging maintenance among downstream branches of EGF signaling (Figure 2). Note that this result was not included in the Aging Cell paper. However, a similar experiment was shown in the paper by *let-23(gf)* background with consistent outcome.
6. I further confirmed the age-associated phenotypes of *itr-1(gf)* and *itr-1(rf)* on late-age swimming and longevity curves. *itr-1(gf)* and *itr-1(rf)* show phenotypes conversely on delayed aging. *itr-1(gf)* promotes more vigorous locomotory mobility, and *itr-1(rf)* exhibits faster decline. Consistent with swimming prowess, increased ITR-1 activity extended lifespan, while shortened survival was observed in *itr-1(rf)*(paper Figure 4C, 4G,4H).

In sum, my results constituted a major contribution to deciphering the novel function of EGF signaling on healthspan and lifespan.

Figure 1

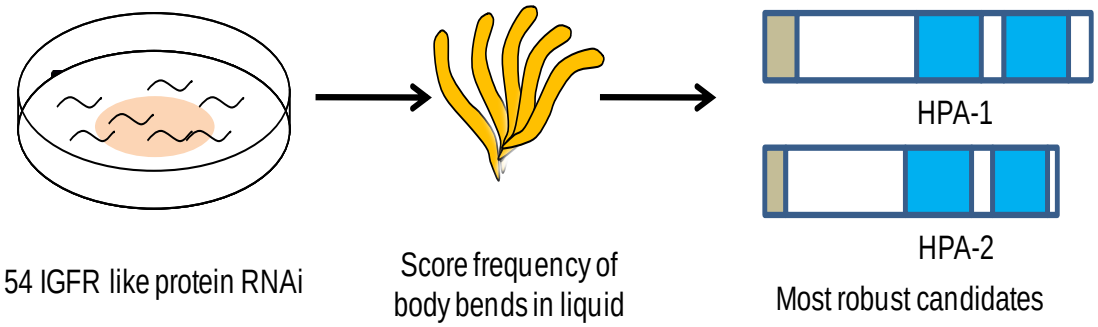

(Yu and Driscoll, 2011)

Figure 1. Summary of screen for RNAi interventions that improve late life swimming. *C. elegans* were fed with dsRNA to disrupt 54 IGF receptor-like genes (Dlakic, 2002) and scored for frequency of body bends in liquid on day11 (mid/late age) (Iwasa et al., 2010). Knockdown of 9 out of 54 genes resulted in better swimming in the population of old animals. Knockdown of *hpa-1* and *hpa-2* resulted in the most robust effects on late-life swimming. Signal sequences indicated in brown, L domains in blue.

Figure 2

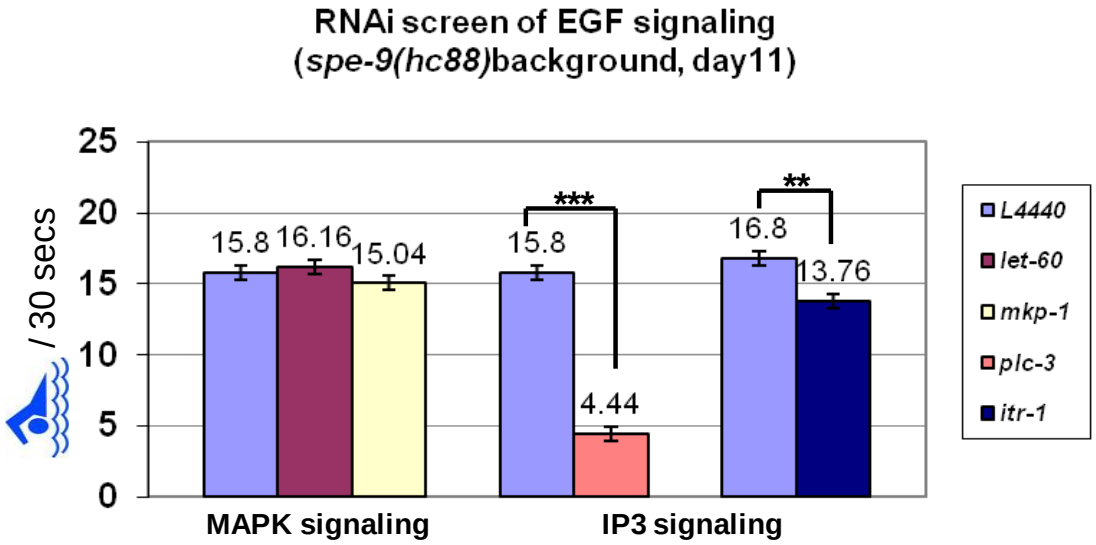

Figure 2. RNAi knockdown of key genes in the pathway downstream of EGF signaling implicated *plc-3/itr-1* signaling branch is related to in locomotory healthspan . Thrashing result of EGF signaling pathway by RNAi knockdown in *spe-9(hc88)* mutants. This result suggests RNAi knockdown of *plc-3* and *itr-1* has a significant difference compared to control L4440 and further indicates *itr-1*(IP3R) signaling rather than *let-60*(RAS) signaling has effect on healthspan. Note that *itr-1* RNAi was initiated from day3 (first day of adult) to avoid larval arrest. All pairwise comparisons are performed at 25°C. ***P < 0.0001 for *plc-3* RNAi compared to the same trial of control L4440; **P < 0.01 for *itr-1* RNAi compared to the same trial of control L4440.

CHAPTER III:

Deciphering mechanisms by which EGF signaling protects against the aging process

Simon Yu contributed all the experimental design and results in the figures. Hiroaki Iwasa made the transgenic mutants with extrachromosomal construct of *let-23(gf)* tissue specific lines for used in this chapter. Together with Jian Xue, I integrated these arrays for the studies reported here.

Introduction

The epidermal growth factor receptor (EGFR) transmembrane receptor tyrosine kinase belongs to the mammalian ErbB subfamily. When mammalian EGF family ligands bind, EGFRs regulate cellular signal transduction pathways that regulate cell proliferation, survival, and migration (Citri and Yarden, 2006).

EGF signaling pathways are conserved in nematodes and flies, and genetic studies on pathway activities have provided extensive insight into molecules in these pathways. In the nematode *C.elegans*, much is known about the effect of EGF signaling during development, including specification of multiple cell fates, regulation of ovulation, and control of behavioral quiescence. *lin-3* encodes for the sole EGF ligand (Hill and Sternberg, 1992). Four isoforms of *lin-3*, generated by alternative splicing, have been identified (Dutt et al., 2004; Hill and Sternberg, 1992; Van Buskirk and Sternberg, 2007). *let-23* encodes the only EGFR homolog (Aroian et al., 1990), and this receptor can act through three distinct downstream signal transduction pathways (MAPK pathway, IP3 receptor pathway, and DAG signaling) to influence cell fate and activity. Given the extensive effort devoted to the identification of longevity genes in the *C. elegans* field, it was surprising that no work had previously examined the role of EGF signaling in lifespan extension.

To address potential roles of the EGF pathway in healthy aging, we tested consequences of genetic manipulation of the EGF ligand /*lin-3* and EGF receptor/*let-23* (Iwasa et al., 2010). We found that an EGFR/*let-23(gf)* gain-of-

function mutant retained late-life swimming vigor and muscle integrity, maintained pharyngeal pumping capacity late into life, exhibited low rates of age pigment accumulation, and survived more robustly in midlife and late life than wild type, revealing a role for EGFR activation in organism-wide healthy aging. Conversely, a reduction-of-function mutation in EGFR/*let-23* confers accelerated swimming decline and diminished survival at mid life; as does mutation of EGF/*lin-3(rf)*. Thus, activation of EGF signaling positively influences healthspan as well as lifespan, and we showed that this signaling acts through the downstream branch of the EGF pathway involving the PLCγ and ITR-1/IP3 receptor (Iwasa et al., 2010). Recently, Liu et al (2011) reported an important role of MAPK signaling on lifespan extension by the activation of the ubiquitin-proteosome system (UPS) and repression of chaperone machinery. Thus EGF/EGFR action via two distinct downstream pathways can promote healthy maintenance.

Although our first analysis identified the skeleton of the EGF pathway that improved healthspan, many details remained to be added, including the identity and timing of the EGF ligand that promotes healthy aging, the tissue specificity of pathway activation required for healthy aging, and downstream effectors. Thus, to extend mechanistic understanding, I probed molecular and temporal ligand requirements, tested additional downstream EGF signaling components, and screening for downstream effectors that might link calcium changes to improved healthspan. I found that *lin-3* is expressed in the gonad system and pharynx

during the molts, but found that expression in the pharynx neurons persists late into adult life. Interestingly, though the expression pattern changes, either LIN-3 in larva or LIN-3 in adulthood can confer healthspan and lifespan promotion. Two isoforms of *lin-3* (LIN-3S and LIN-3XL) can promote locomotory mobility. The spatial requirement for EGF signaling is different for activation of downstream branches. For example, ALA neuronal EGFR/LET-23 activation mediates behavioral quiescence associated with developmental molts but PLCγ/*plc-3*) in the spermatheca regulates ovulation. Our data indicates that activation of EGFR in muscle, neuron, and the intestine can positively affect age-associated mobility decline and lifespan.

A component of calcium signaling -- ER calcium release that regulates intracellular calcium homeostasis -- promotes healthspan in *C. elegans* (Iwasa et al., 2010). The effectors that are the key factors to relay or propagate the calcium signal to promote healthspan are unknown. With the interest in identifying executors influenced by increase of calcium, I tested calcium sensitive genes for the potential to regulate locomotory healthspan and I identified candidate proteins that might mediate downstream effects of IP3R in healthspan promotion.

Material and Method

Strains and nematode growth

C. elegans were grown and maintained on nematode growth media (NGM) plates streaked with *Escherichia coli* OP50 at 20^{o}C as described (Brenner, 1974). The *C. elegans* Bristol strain, N2, was used as the wild type reference strain. Strains used in this study include:

PS4308 *unc-119(ed4) III;syIs107[unc-119(+) + lin-3(delta-pes-10)::GFP]*

AH380 *unc-119(e2498)III;zhEx84[plin-3::lin-3,unc-119(+),sur-5::gfp]*

AH364 *unc-119(e2498)III;zhEx68[plin-3::lin-3S,unc-119(+),sur-5::gfp]*

AH378 *unc-119(e2498)III;zhEx69[plin-3::lin-3L,unc-119(+),sur-5::gfp]*

AH589 *unc-119(e2498)III;zhEx70[plin-3::lin-3XL,unc-119(+),sur-5::gfp]*

AH357 *unc-119(e2498)III;zhEx72[plin-31::lin-3S,unc-119(+),sur-5::gfp]*

AH362 *unc-119(e2498)III;zhEx73[plin-31::lin-3L,unc-119(+),sur-5::gfp]*

AH354 *unc-119(e2498)III;zhEx74[plin-31::lin-3XL,unc-119(+),sur-5::gfp]*

PS2746 *dpy-20(e1282)IV;syEX234[MH86(dpy-20(+)+pBS+let-23::gfp]*

ZB40400 *bzIs147[pmyo-2::let-23(sa62gf),pmyo-2::gfp]*

ZB40401 *bzIs148[pmyo-2::let-23(sa62gf),pmyo-2::gfp]*

ZB40402 *bzIs149[pmyo-3::let-23(sa62gf),pmyo-2::gfp]*

ZB40403 *bzIs150[pmyo-3::let-23(sa62gf),pmyo-2::gfp]*

ZB40404 *bzIs151[punc-119::let-23(sa62gf),pmyo-2::gfp]*

ZB40405 *bzIs152[punc-119::let-23(sa62gf),pmyo-2::gfp]*

ZB40406 *bzIs153[pvha-6::let-23(sa62gf),pmyo-2::gfp]*

ZB40407 *bzIs154[pvha-6::let-23(sa62gf),pmyo-2::gfp]*

ZB40408 *bzIs155[pless::let-23(sa62gf),pmyo-2::gfp]*

PS3653 *ipp-5(sy605)*

PS1461 *ark-1(sy247)ts*

ZB40414 *itr-1(sy290)*

VC691 *ckk-1(ok1033)*

PY1589 *cmk-1(oy21)*

RB1081 *klf-2(ok1043*)

RB796 *sta-1(ok587)*

VC1270 *lin-31(g569)*

YT17*crh-1(tz2)*

RB746 *T05C1.4(ok515).*

Construction of mutants

Tissue-specific expression of *let-23(gf)* transgenic mutants were constructed by the following method. *pmyo-2::let-23(sa62)* is for pharynx-specific expression, constructed from vector pPD30.69 (containing the *myo-2* promoter) fused with *let-23(sa62)*. *pmyo-3::let-23(sa62)* is for body wall muscle-specific expression, constructed from vector pPD95.86 (containing the *myo-3* promoter) fused with *let-23(sa62). pvha-6::let-23(sa62)* is for intestine-specific expression, constructed from the *vha-6* promoter of Gateway plasmid, vector pPD95.75 fused with *let-23(sa62). punc-119::let-23(sa62)* is for neuronal-specific expression, constructed from vector pBY103 (containing the *unc-119* promoter) fused with *let-23(sa62).*

Each construct was injected into N2 worms at 100 ng/ul with *myo-2::GFP* and pBS. *myo-2::GFP*, which is used as marker DNA, is the *myo-2* promoter plasmid fused with GFP. pBS is the pBluescript, which was used as the carrier DNA. Extrachromosomal array *bzEX[tissue specific promoter::let-23(sa62gf)]* were integrated into *C. elegans* chromosome by X-ray irradiation at 4000 rad and were outcrossed at least five times with N2 to generate strains ZB40400-ZB40408.

RNAi feeding

RNAi feeding was similar to as described (Timmons and Fire, 1998). *Escherichia coli* (HT115) producing dsRNA for individual genes was seeded onto RNAi plates containing 25 mg/ml carbenicillin with 0.2 % lactose (20% STOCK) to induce the expression of the dsRNA for the gene of interest. The negative control was conducted by seeding the plates with HT115 containing empty vector pL4440. Synchronized eggs were placed onto each plate. Animals were grown at designated temperatures for distinct experiments. Worms were transferred to a new RNAi plate beginning at day3 (25°C) or day4 (for 20°C) until the end of reproductive period and cultured at the same condition. For *itr-1* dsRNA feeding, animals were fed with L4440 until reaching adult to avoid possible larva arrest caused by *itr-1* RNAi.

Locomotory evaluation--swimming prowess

Swimming assay was analyzed on young adult (first day adult, day3 or day4, depending on growing temperature) and mid/late-age animals (~5 or ~8 days

after reaching adulthood at 25°C) for synchronous reared *C. elegans*. Worms all grow at 25°C to the time point of assay after reaching adult. Total 20-30 adult worms/group were individually transferred into 1ml M9 buffer in a 24-well plate. We counted the frequency of body bends in 30 seconds for each fresh transferred worm under microscope manually.

Lifespan analysis

Synchronous *C. elegans* were grown on NGM plate spread with the OP50 or RNAi bacteria lawn in 20°C incubator throughout the whole experiment, except for in the experiment using temperature sensitive mutant *ark-1(sy247)* and matched control. After growing to the young adult stage, animals were transferred to either OP50 or RNAi fresh plates everyday until the end of the reproductive period to keep away from their progeny. The surviving animals were counted every other day until all the population was dead. Animals that died naturally or other reasons (i.e. bagging) were censored at the time of the event. Survival curves were analyzed using the GraphPad Prism 5 software, and median lifespan was automatically calculated. The statistical tests used for overall significance of difference were the log-rank (Mantel Cox) Test or the Gehan-Breslow-Wilcoxon Test. Maximum lifespan was counted by the mean age of the longest-lived 10% in the test population.

In vivo age pigment spectrofluorimetry

C. elegans were grown on NGM plates spread with the OP50 bacteria lawn in 25°C incubator throughout the whole experiment. Transferring worms to new plates is required daily from day3 (young adult) until the end of reproductive period to avoid contamination of progeny. Age pigment (AGE) and tryptophan (TRP) intensity were obtained by scanning worms at different excitation/emission pair (Gerstbrein et al., 2005). ~35 worms of each strain were used for age pigment (AGE) /tryptophan (TRP) ratio quatitation analysis.

Fluorescence microscopy

GFP expression pattern were visualized in *lin-3::gfp* and *let-23::gfp* animals by mounting young and aged animals with 1mM levamisole. Fluorescence images were observed and photographed using Zeiss Axio Imager Microscope with a QIMAGING digital camera by iVision software.

Results

lin-3/ EGF splice variants are expressed late into adult life

Previous studies, which focused primarily on developmental time points, showed *lin-3*/EGF is expressed in different cells and the expression is temporally regulated in these cells. *lin-3* is expressed in the anchor cell to influence vulva development at the L3 stage (Hill and Sternberg, 1992), in the vulF cell to influence the fate of uv1 cell during the early and mid L4 stage, and in the spermatheca valve and spermatheca to influence ovulation starting in the L3 to L4 stages (Hwang and Sternberg, 2004). Expression in the pharynx was observed throughout post-embryonic stages (Hwang and Sternberg, 2004) and another study showed that *lin-3* expression in the pharynx occurs in all larval stages and young adults, which might reflect expression of EGF that influences quiescence at the molt (Van Buskirk and Sternberg, 2007). Liu et al (2011) recently indicated that *lin-3* is also expressed in the intestine and hypodermis tissue at young fertile adult (24hr after L4 stage). It is important to note that previous studies focused on the expression pattern of *lin-3* more during early life, and virtually no information about *lin-3* expression in aging adults has been published.

To get an idea of when EGF might be available to influence healthy aging, I first examined broad expression of *lin-3::gfp* into late adulthood. As previously published, the *lin-3::GFP* reporter is expressed in the anchor cell at L3/L4 stages and in the pharynx area. Pharyngeal expression of *lin-3* can persist in the

pharynx region into late-age (Figure 1A). I quantitated by scoring GFP fluorescence at specific times in the anchor cell and in the pharyngeal area (Figure 1B).

My data suggest that *lin-3* is expressed from the pharynx region in older adults, which might be the source of EGF signaling into late-age. However, I observed the GFP signal in the region of the pharynx in a few dot-like structures that resemble pharyngeal neurons, unlike the previous report by Hwang et al. that observed whole pharynx muscle fluorescence in younger animals with the same construct. My data strongly suggest that in aging adult, EGF is expressed at high levels in pharyngeal neurons.

I further looked at the expression of *lin-3* by checking for transcriptional expression into adult life. Previous studies identified four distinct EGF isoforms (Dutt et al., 2004; Hill and Sternberg, 1992; Van Buskirk and Sternberg, 2007) (Sup figure 2A). EGF isoforms expression was previously assayed only in the development and early adult life, not in aged animals. I detected the expression timing of each isoform by RT-PCR (Sup figure 1). I was able to identify three of the four isoforms --- *lin-3S, lin-3L,* and *lin-3XL* (names based on the size of the transcripts and previously published names). However, I was unable to detect isoform *lin-3XXL* (Sup figure 2A) expression in any stage of the life cycle. Isoform *lin-3XXL* is much less abundant compared to other three isoforms in subclone collections from RT/PCR (data not shown—1/65 chance of *lin-3XXL* amplification

was found in one relative frequency of cloning/sequencing experiment I did). I found *lin-3S, lin-3L,* and *lin-3XL* in the L1/L2 stage (day 1 of life), young adult (day 3), and mid/late adult (day 10). Thus, multiple EGFs are expressed in the mature adult and aging *C. elegans*; these isoforms have the potential to continuously influence healthspan during adult life.

Specific *lin-3* splice isoforms, LIN-3S and LIN-3XL, confer anti-aging activity

lin-3, which encodes the ligand in the *C. elegans* EGF signaling pathway, is required for graceful aging by criteria of swimming ability, and lifespan (Iwasa et al., 2010). The EGF mutant *lin-3(n1058)* exhibits reduced locomotory mobility and shorter lifespan. Conversely, activation of the EGF pathway promotes healthy aging and a mutant activated EGFR/*let-23(gf)* can extend general healthspan (Iwasa et al., 2010). Previous LIN-3 dosage experiments indicated that different levels promote distinct vulva developmental cell fates (Katz et al., 1995). It is not known, however, whether elevated dosage of EGF/LIN-3 is enough to activate EGF signaling to extend healthspan and lifespan, especially since the HPA negative regulators that bind EGF may limit signaling in the adult (Iwasa et al., 2010). To address this issue, we tested whether overexpression of *lin-3* can be beneficial for healthspan.

We first expressed a genomic EGF/*lin-3* under the control of the native *lin-3* promoter from an extrachromosomal transgene array and tested for maintained

locomotory mobility prowess in late adult animals. We found that over-expression of the native *lin-3* gene did not confer healthspan benefits for swimming behavior (Figure 2A). Thus, in this experiment, modest overexpression from the native promoter could not over-ride negative regulation of EGF that can be exerted by HPA genes. However, I note that testing of additional transgene lines would help solidify this conclusion.

I next tested three available *lin-3* splice variant transgenes, termed LIN-3S, LIN-3L, and LIN-3XL (named for transcript size; one is termed LIN-3XXL, however, not available), that are distinct in the inclusion or exclusion of small exons in the region between the EGF repeat and the transmembrane domain (Sup figure 2A). I first tested the expression of specific isoforms from the native *lin-3* promoter, which should have expressed the genes in the normal cell and temporal pattern, but slightly elevated in concentration. I was not able to obtain enough animals carrying the *Ex[plin-3::lin-3S]* transgene, as these animals had a high degree of early adult bursting (possibly effects of LIN-3S on vulval fate specification—these animals had a severe Muv phenotype). I found that *Ex[plin-3::lin-3L]* overexpression did not improve locomotory aging (Figure 2B). In contrast, I found that *Ex[plin-3::lin-3XL]* confers some anti-aging protection, slowing mid-age locomotory decline (Figure 2C). These data suggest that the LIN-3XL EGF isoform may promote healthy aging.

I then tested for late age swimming phenotypes in transgenic animals that expressed distinct EGF/*lin-3* isoforms from the *lin-31* promoter in extrachromosomal transgene arrays. Previous studies revealed that LIN-3/EGF from vulva precursor cells can be the origin of the anchor cell independent *lin-3* signal (Dutt et al., 2004; Hill and Sternberg, 1992). *lin-31* is expressed in the vulva precursor cell (VPC) (similar expression as *let-23(gf)*), neurons, and the intestine.

We found that the transgenic line expressing *Ex[plin-31::lin-3S]* can enhance locomotory mobility at older age (Figure 2D). Interestingly, *Ex[plin-31::lin-3XL]* exerts a similar positive effect on maintenance of swimming vigor (Figure 2F). However, *Ex[plin-31::lin-3L]* still does not confer any protection against locomotory decline (Figure 2E), consistent with observations from over-expression of this isoform using the native *lin-3* promoter.

I conclude that at least 2 EGF isoforms, LIN-3S and LIN-3XL, can promote healthy lomocotory aging. Elevated expression of these EGFs in VPCs, neurons, and/or intestine is sufficient to confer benefits. Two independent lines that express LIN-3L from either the *lin-3* promoter or the *lin-31* promoter were not able to promote extended locomotory healthspan. Although testing with additional lines might improve expression levels and would more rigorously address the LIN-3L role, my data suggest that LIN-3L does not play a major role

in promoting healthy locomotory aging. Thus, it appears that specific LIN-3/EGFs have roles in extending adult swimming healthspan.

LIN-3/EGF acts during both larval development and adult life to promote healthy aging

The insulin signaling pathway influences longevity and developmental phenotypes such as reproduction and dauer formation. Notably, however, the insulin signaling pathway acts during adulthood to control aging but regulates diapause during development. Knockdown of some mitochondrial genes only during larva development can induce longevity phenotypes in adults (Dillin et al., 2002b). We identified enhanced EGF signaling as a previously unrecognized signaling pathway that can promote delayed aging phenotypes (Iwasa et al., 2010). As shown in Supplemental Figure 1, *lin-3* is expressed throughout *C. elegans* adult life. However, the temporal requirements for EGF signaling in healthspan promotion are unknown. We therefore analyzed the temporal requirements for LIN-3/EGF in regulation of aging phenotypes.

We used two approaches to alter EGF availability. In the first assay, we fed animals with L4440 empty vector control bacteria food during larval stages then switched their food to bacteria expressing *lin-3* dsRNA to knockdown *lin-3* expression during adult life (Figure 3A). Animals under this treatment have wild type *lin-3* expression in larva, but diminished *lin-3* expression during adult life.

We first confirmed that *lin-3(RNAi)* disruption up to the first day of adult life (day 3 from egg lay) does not disrupt young adult swimming (Sup figure 3A). Thus, *lin-3* is not critical for swimming per se and *lin-3(RNAi)* does not have a developmental consequence on swim behavior. We then compared animals that were reared on L4440 empty vector control, animals that were reared on control empty vector L4440 to day3 and then shifted to *lin-3(RNAi),* and animals subjected to *lin-3(RNAi)* for all life, scoring at day 8 for swimming prowess. As we have observed previously, *lin-3* knockdown throughout life accelerates swimming decline in adults (empty vector 27.9 +/- 0.4 body bends / 30 seconds vs. *lin-3(RNAi)* 17.3 +/- 1.3 body bends / 30 seconds). Animals subjected to *lin-3* knockdown only during adult life were significantly different from both non-treated and full-treated *lin-3(RNAi)* (22.8 +/- 1.5 body bends / 30 seconds). We conclude that *lin-3* expression is needed during adult life to promote locomotory maintenance. It might also be noteworthy that knockdown of *lin-3* only in the adult is less deleterious than lifetime knockdown, suggesting that LIN-3 might confer some protection against locomotory decline by acting early during development.

We further addressed a potential early-life role for LIN-3 in promoting later life mobility maintenance by inducing *lin-3(RNAi)* primarily in larval development. In these studies, we used *dcr-1(RNAi)* to rapidly impair the RNAi mechanism in treated young adults as had previously been shown (Dillin et al., 2002a). We find that *dcr-1(RNAi)* treatment alone exert no effect on age-associated locomotory

decline (Sup figure 3B). However, when we subjected animals to *lin-3(RNAi)* during larval development and then switched at day 3 of life to *dcr-1(RNAi)* to end *lin-3* knockdown, we find a significant reduction of later life swimming ability: *dcr-1(RNAi)* treatment throughout life swam at a rate of 26.4 +/- 0.3 body bends / 30 seconds and *lin-3(RNAi)* shifted to *dcr-1(RNAi)* at day3 swam at a rate of 19.2 +/- 1.1 body bends / 30 seconds. These data suggest that *lin-3* expression during larval stages can influence the quality of aging in later adult life. That limiting expression only during larval stages does not generally impair later swimming as much as limiting *lin-3* expression throughout life swimming (whole life *lin-3(RNAi)* knockdown rate of 16.2 +/- 0.8 body bends / 30 seconds) supports existence of a role for LIN-3 in maintaining locomotory function during the adult as well (Figure 3B).

Consistent with a broad positive effect of adult *lin-3* expression on aging at the organism level, we found that animals switched to *lin-3* RNAi during adult life had a shorter median lifespan (~18 days) than empty vector control (~22 days) (Figure 3C). Because adult-only *lin-3(RNAi)* was not as deleterious to survival as was full-life *lin-3(RNAi)* (median lifespan ~15 days), data also support that *lin-3* expression early in development can influence lifespan, conferring protective functions.

In sum, LIN-3 appears required both at larval stages and adult stages to influence maintained swimming performance and lifespan late in life. We find that:

1) EGF promotes maintenance throughout life: 2) effects of EGF signaling in development can have an impact later in life: and 3) EGF acts during adulthood to promote healthy aging.

Tissue-specific expression of EGFR/*let-23(gf)* suggests pathway activation in multiple tissue types can maintain locomotory function in later life

Low level insulin signaling pathway activation promotes longevity. Previous evidence indicated that DAF-2 insulin receptor expressed in neurons alone is sufficient to specify wild type life span and DAF-16 activity in the intestine can restore substantial longevity in *daf-16* deficient mutants (Libina et al., 2003; Wolkow et al., 2000). We have shown that activation of another signaling pathway, the EGF pathway, promotes healthy aging and that a mutant activated EGFR/*let-23(gf)* can extend general healthspan (Iwasa et al., 2010). The tissue-specific requirements for EGF signaling in healthy aging promotion, however, are unknown—in what tissues can EGFR be activated to extend healthspan? To address this question, we tested whether EGFR/*let-23(gf)* expressed in different tissues could confer healthspan benefits.

Previous studies showed *let-23*/EGFR is expressed in different cells to transduce EGF signaling during development. *let-23* is expressed in uv1 cell and vulva precursor cells during larval development, where it influences cell fate specification (Chang et al., 1999; Simske et al., 1996). LET-23/EGFR is also

expressed in the ALA neurons to influence behavioral quiescence induction, which accompanies molting during larval development (Van Buskirk and Sternberg, 2007). More recently, *let-23* expression was shown in the hypodermis & intestinal cell membrane in the young adult (Liu et al., 2011). It is important to note that previous studies focused on the expression pattern of *let-23* more during development, and not much information about adult expression, especially in aging adults, has been published.

I am still conducting a quantitative survey of LET-23::GFP expression in aging adults. I looked at mid age animal (around day 8) in which the expression is more obvious in the ALA neurons, the hypodermal expression is weak, and the intestinal membrane expression as described in Liu et al 2011 was not readily apparent. Low level expression might be hard to detect and all aspects of expression might not be observed with this GFP reporter.

Given our observation that *lin-3/*EGF must be expressed in the adult to promote healthy aging, we decided to address which tissue(s) might mediate locomotory healthspan benefits. We ectopically expressed the *let-23(gf)* EGF receptor in individual tissues: body wall muscle and neurons, which are directly involved in swimming behavior, as well as intestine and pharynx, which are not directly involved in locomotory control. We integrated transgene arrays, outcrossed strains, and then examined swimming prowess in two independent lines for each transgene construct.

We first tested whether tissue-specific expression of *let-23(gf)* up to day4 (20^{o}C, first day of adult life) alters young adult swimming (Figure 4A-4H). We find no significant difference between WT and lines harboring *let-23(gf)* expression constructs for any of the 8 tissue-specific expression constructs we analyzed. Thus, introduced transgenes neither disrupt development of neuromuscular systems that execute swimming nor improve the baseline vigor of swimming behavior.

We also compared the locomotory decline of wild type N2 and *Is[pless::let-23(gf)]* (no promoter region of *let-23* in the array) transgenic animals on day 4 and day 12. *let-23(gf*) should not be expressed in the promoter less transgenic line. Data collected from either day 4 or day 12 suggest no difference for locomotory mobility between WT and the line carrying promoter less *let-23(gf)* (Sup figure 4). Thus, the transgene backbone does not convey any age-associated phenotypes on its own. For historical reasons, I compared *let-23(gf)* transgenes against the N2 background.

I then compared N2 wild type vs. tissue-specific promoter::*let-23(gf)* for rate of body bending while swimming, scoring at day 12 (animals developed at 20^{o}C but were shifted to 25^{o}C for 8 more days of adult life, for reasons not relevant to this study. Animals at 25^{o}C are expected to age faster than those at 20^{o}C.). I found that transgenically elevated *let-23(gf)* expressed in muscle (Figure 4A, 4B) or

neurons (Figure 4C, 4D) slow late-life locomotory decline. Somewhat unexpectedly, transgenic lines with *let-23(gf)* expressed in the intestine or in pharynx also exert more vigorous swimming locomotion later in life than do their wild type counterparts (Figure 4E-4H).

I conclude that ectopic expression of *let-23(gf)* in multiple tissue types (muscle, neuron, intestine, and pharynx) can promote healthy locomotory aging. Furthermore, our tissue-specific expression analysis implies that EGF pathway activation can regulate locomotory vigor non-autonomously. Although body wall muscle and neurons can regulate locomotion directly, intestine and pharynx are not thought to directly control swimming. Thus, EGFR signaling in multiple tissue types appears to promote inter-tissue signaling that improves overall health and maintenance into older age.

Tissue-specific expression of EGFR/*let-23(gf)* activation in muscle and neuron confers multiple measures of favorable healthspan

Influence of tissue-specific let-23(gf) on longevity. Expression of EGFR/*let-23(gf)* in multiple tissues exerts delays age-associated locomotory decline (Figure 4). Previously, we found that EGFR/*let-23(gf)* mutants are long-lived (Iwasa et al., 2010). We were therefore curious as to how expression of EGFR/*let-23(gf)* in specific tissues altered lifespan. Is expression in just one

tissue sufficient to extend lifespan? What is the critical focus of action of EGFR signaling that maintains lifespan?

We examined two independent transgenic lines expressing *let-23(gf)* in body wall muscle, neurons, intestine or pharyngeal muscle. We compared cumulative survival curves and individual trial survival curves, using statistical tests to analyze overall differences (Figure 5, Sup figure 5) and median, mean, and max lifespan (Table1).

Transgenic lines that express *let-23(gf)* in body wall muscle under control of the *myo-3* promoter positively regulate median lifespan and lifelong survival. We noticed that the survival pattern is more robust in middle adulthood than the matched control: median lifespan: *bzIs149[pmyo-3::let-23(sa62gf)]*, 44% increase ; *bzIs150[pmyo-3::let-23(sa62gf)]*, 26% increase. Interestingly, *let-23(gf)* expressed in body wall muscle appears to promote healthspan more potently for mean rather than for maximum lifespan: *bzIs149[pmyo-3::let-23(sa62gf)]*, 3% more; *bzIs150[pmyo-3::let-23(sa62g)]*,12% less maximum lifespan (Figure 5A, 5B, Table1).

let-23(gf) expressed in neurons (*bzIs151[punc-119::let-23(sa62gf)]* and *bzIs152[punc-119::let-23(sa62gf)]*) can also exert a positive impact on median lifespan and overall survival. We also observed that benefits are most apparent for the middle age survival as seen from *pmyo-3::let-23(gf)* lines. Median survival

days are 31% and 11% extended, respectively, for line *bzIs151* and line *bzIs152*, but max survival days were -2% and 8% increased (Figure 5C, 5D, Table1).

Animals with *let-23(gf)* expressed in the intestine under control of the *vha-6* promoter exhibit enhanced median lifespan: N2 vs. *Is[pvha-6::let-23(gf)]*, 20% (line *bzIs153*) & 16% (line *bzIs154*) increase respectively. Note that from survival curve comparison, both *Is[pvha-6::let-23(gf)]* lines exhibit a positive influence on mid survival of life cycle. For both independently isolated lines, there appears to be a positive impact on survival early in adult life, that is not evident later (~>20 days). The late mortality rate accelerated (*bzIs153*) or remained the same as (*bzIs154*) the matched control group (Figure 5E, 5F, Table1).

In contrast, expression of *let-23(gf)* in pharynx under control of the *myo-2* promoter has no significant impact on survival at any point in the lifespan (Figure 5G, 5H, Table1).

We conclude that transgenic expression of activated EGFR/*let-23* in muscle, neurons and intestine can improve survival at some point during the lifespan, with greatest impact earlier in adult life. Data suggest that EGF pathway activation in any of these tissues may induce signaling that influences aging of the entire organism.

Influence of tissue-specific let-23(gf) on age pigment levels. I also tested whether age pigment accumulation with age was changed by by tissue-specific expression of *let-23(gf)*. Age pigment accumulation, is a phenotype directly observed in the gut, but which can report the organism-wide metabolic state.

Though the exact magnitude of AGE/TRP ratio showed some variation between repeated trials, we found that animals of independent lines with *let-23(gf)* expressed in body wall muscle or neuron exhibit lower AGE/TRP ratio at both early young adult life time and late life (Figure 5I-5L).

However, animals expressing *let-23(gf)* in the intestine or pharynx do not exert similar age pigment accumulation pattern between independent isolated lines, but rather either accelerated (*bzIs153[pvha-6::let-23(sa62gf)]*) or exhibited the same(*bzIs148[pmyo-2::let-23(sa62gf)]*) accumulation rate (Figure 5M-5P). The weakness of the effect in the intestine might be attributed to issues with the two specific transgenes. However, it is interesting that activating the EGFR pathway the intestine—the tissue in which age pigments accumulate most predominantly—actually may have a less dramatic effect than neurons or muscle. These data hint that pathway activation in diverse tissues can induce signals that influence aging rates across the body.

Data suggest that EGFR/LET-23 activated in muscle and neuron might directly modulate “physiological” age during the life cycle. In sum, we conclude that activated EGF signaling in muscle, neurons, and somewhat in intestine, can systemically influence aging quality phenotypes of locomotion, lifespan and age pigment accumulation.

Additional central modulators in the EGF/ITR-1 signaling pathway affect healthspan

Our previous data showed that activated EGFR acts via increased IP3 activity through the IP3 receptor and induced ER calcium release channel to confer healthspan benefits (Iwasa et al., 2010). Additional genes that act downstream of EGFR in this pathway have been identified in genetic studies (Moghal and Sternberg, 2003)(Figure 6A). *ark-1* encodes *A*ck-*r*elated tyrosine *k*inase and is an inhibitor of EGFR/*let-23* signaling that suppresses ovulation (Hopper et al., 2000). *ark-1* normally inhibits germline development and *ark-1(RNAi)* suppresses slow germline development for the *clk-1* mutant, which is involved in mitochondrial activity (Shibata et al., 2003). Both 5-phosphatase (*ipp-5*) and 3-kinase (*lfe-2*) can act to reduce IP3 levels, and modulate ovulation (Bui and Sternberg, 2002; Clandinin et al., 1998). No previous studies have tested the roles of these EGF pathway mutants in healthspan regulation. Here, I examined age-associated locomotory decline, age pigment accumulation, and survival curve properties as indicators of overall aging quality for these mutants.

My analysis of young adult locomotory prowess in three EGFR pathway mutant backgrounds *ark-1*, *lfe-2*, and *ipp-5* established that disruption of these genes does not alter young adult swimming. Studies at later life indicate that locomotory aging and age pigment accumulation phenotypes are improved when *ark-1* or *ipp-5* is mutant (Figure 6B, 6D, 6H, 6I), consistent with pathway activation when they are lacking, and positioning their activity in healthspan promotion. Interestingly, although the *ipp-5* mutant exhibits a longevity phenotype in addition to improved late age swimming and low age pigment accumulation, the *ark-1* mutant does not extend survival at any time over adult life (Figure 6B, 6C, 6D, 6E, 6H, 6I). Previously we have documented that EGF pathway negative regulator *hpa-2* influenced locomotory aging, but not age pigment accumulation; minimal impact on lifespan was noted. Thus, it is possible that, like *hpa-2*, *ark-1* acts in some healthy aging pathways, but not all. Affected pathways may be tissue-specific or certain deleterious consequences of *ark-1* deficiency might counter any positive effects on lifespan.

I did not observe any impact of *lfe-2(RNAi)* on averaged trials, monitoring mobility decline, age pigment accumulation, or lifespan (Figure 6F,6G). Thus, *lfe-2* does not appear to be an essential mediator of EGFR pathway healthspan benefits. Of course, it remains possible that *lfe-2* might be functionally redundant with another activity, or effects might require *lfe-2* in the nervous system with *lfe-2(RNAi)* particularly ineffective in neurons. However*, lfe-2* is expressed in pharynx, intestine and spermatheca, not in neurons so neuronal RNAi problems are not likely a cause of the lack of effect.

In general, my testing of additional genes that act downstream to execute EGFR signaling to the IP3 receptor identified two additional genes that can influence healthspan outcomes. One of these, *ark-1*, encodes a kinase that can down-regulate EGFR activity. Interestingly, although *ark-1* disruption can improve swimming maintenance and age pigment accumulation phenotypes, it does not exert an influence on lifespan. ARK-1 might regulate signaling relevant to a subset of healthspan pathways or might also confer deleterious consequences that counter any potential longevity outcomes. By contrast, *ipp-5* deficiency, which is predicted to increase IP3 concentrations available for signaling, increases late-age swimming proficiency, decreases age pigment scores, has some effect on longevity (although clearly not as much as an IP3R(gf) mutation (Iwasa et al., 2010)). These data support that IP3 signaling plays a central role in overall healthspan, and underscore the importance of the EGFR/IP3R pathway.

Multiple calcium-sensitive executors that could act downstream of EGF/ITR signaling to promote healthspan

We have shown that the HPA/*hpa-1* - EGF/*lin-3* – EGFR/*let-23* – IP3R/*itr-1* signaling pathway regulates ER calcium release and calcium homeostasis that promotes healthy aging. However, we do not know the downstream effectors in this pathway. Therefore I sought possible downstream regulators of the enhanced calcium signaling from the ER. Calmodulin (CaM), a ubiquitous EF hand binding protein, interacts with, and regulates kinases to alter transcriptional activity (Kimura et al., 2002). The Calmodulin-CaM kinase cascade (CaM-

CaMKK-CaMK) is activated after intracellular calcium elevation (Sup figure 6). Some transcription factors are known to be regulated by calcium.

I therefore first screened calmodulin-related cascade (CaMK cascade) and factors related to the cascade that might mediate calcium signaling generated by EGF activation. I used RNAi screening strategies to knockdown possible candidates categorized into groups (calmodulin-related, calcineurin-related, EF hand transcription factor, CREB-related) in sensitized *itr-1(sy290gf),* which mimics upstream EGF pathway activation. The idea was that if a given calcium-sensitive protein was required for *itr-1(gf)* healthspan benefits, its RNAi disruption would reduce late age swimming prowess. I found, however, that RNAi knockdown of the first candidate genes tested neither suppress the strong swimming performance of *itr-1(sy290gf)* at late age, nor enhance locomotory benefit in *itr-1(sy290gf)* (Table 2A). Thus, these genes may: 1) not be involved in aging regulation, 2) act in the nervous system in the pathway and thus are not readily disrupted by RNAi, 3) might be functionally redundant with other calcium responsive genes. Modest effects of *rcn-1*, *F23B12.7*, *crh-2* and *let-607* suggest a further look at these in nervous system-sensitized backgrounds, or in actual mutants, might be of future interest.

I further addressed a potential role of candidate genes in transducing calcium signaling or at least mediating signal after EGF activation by inducing *hpa-1(RNAi)*, using genetic calcium-associated mutants that were available as targets

(Table 2B). *hpa-1(RNAi)* activates the EGFR pathway, and increase late age swimming performance (Iwasa et al, 2010). I first asked whether *hpa-1(RNAi)* could extend healthspan of the mutants, comparing swimming with and without *hpa-1(RNAi)*.

I found that *lin-31(gk568)* does not suppress *hpa-1(RNAi)* locomotory benefits. This information underscores that *hpa-1* promotes locomotory healthspan distinct from EGF-MAPK signaling in which LIN-31 is the downstream transcription factor. *ckk-1*, the calmodulin kinase kinase (Kimura et al., 2002), also does not appear to be an essential downstream executor because *hpa-1(RNAi)* induces a benefit in this background.

In contrast, mutants disrupting the more downstream components of the CKK-1 cascade, CaMK1(*cmk-1*), and CREB(*crh-1*), do not exhibit the *hpa-1(RNAi)* effect on swimming healthspan extension late in life. This work suggests that *cmk-1* and *crh-1* could act downstream in the EGF pathway modulated by HPA-1 and suggest them as potential targets of ITR-1-influenced calcium changes, since ITR-1 is the known downstream effector for HPA-1 in healthspan regulation (Iwasa et al., 2010). An obvious follow-up for these studies, then, is to test how double mutants of these plus EGF pathway *lf* and *gf* mutations swim late in life. The prediction is that, if either was a critical downstream factor needed for healthspan promotion, *cmk-1* and *crh-1* defects should block *itr-1(gf)* benefits.

So, a control experiment question arises as to whether either *cmk-1* or *crh-1* is defective in old age swimming—either because they lack normal EGF protective mechanisms or because they impair some other pathway. I found that the body bend frequency of *crh-1(tz2)* is low at old age (~12.5 / 30 seconds), similar to what is observed for wild type. Previous study revealed that the *crh-1(nn3315)* null mutant did not confer extended lifespan (Mair et al., 2011). By contrast, *cmk-1(oy21)* swimming is much higher (~ 20/ 30 seconds) under RNAi (control or *hpa-1*) food feeding condition (Table 2B). Thus, cmk-1 might normally modulate negative signaling. Together, these data highlight *cmk-1* and *crh-1* as potential modulators of old age swimming. A first critical step will be to measure their swimming at young age. If they appear to be normal young adult swimmers, and specifically impacted at old age, a detailed analysis of how/if they fit into the HPA-1/LET-23/ITR1 pathway should be undertaken.

I further tested the transcription factor, *sta-1*, a homolog of STAT transcription factor in JAK-STAT signaling (Wang and Levy, 2006). Mammalian STAT proteins contain a conserved EF-hand-like domain. The motif can bind to calcium and possibly relay signal. I first found that *sta-1(ok587)* confers dramatic benefits on healthspan. The *sta-1(ok587)* allele encodes a deletion of exons 2 and 3, which creates an out of frame splice to exon4 to generate a stop codon. STA-1 immunoreactivity is not found in that strain (Wang and Levy, 2006), suggesting the allele could be a null. Thus, calcium signaling might normally negatively

regulate STA-1 activity to extend locomotory healthspan. Importantly, *sta-1* mutants swim normally in young adults, so the strain acts as a true aging mutant.

Somewhat paradoxically, the beneficial healthspan from *hpa-1(RNAi)* was diminished by *sta-1(ok587)* (Table 2B, 2C). This suggests that EGF pathway activation and health benefits require STA-1 activity. It will be critical to rescue *sta-1(ok587)* to confirm the healthy aging phenotype is conferred by the *sta-1* deficiency rather than from another mutation in the background. It is possible that the deletion allele, which takes out two exons but might get alternatively spliced later in life, has dominant negative activity.

Since my main purpose was to search for possible candidates that act downstream of *itr-1* and calcium elevation, I fed *sta-1(ok587)* mutants bacteria expressing *itr-1* dsRNA and compared to L4440 empty vector control bacteria. I observed no difference when *itr-1* was disrupted by RNAi. Thus, *sta-1(ok587)* effects are not dependent on ITR-1 activity. It is possible that *sta-1(ok587)* acts downstream to mediate effects, but it could also act in a parallel pathway (Table 2D). My data implicate STA-1 in healthy locomotory aging, and how this relates to possible downstream calcium signaling benefit remains to be worked out in detail.

I also tested other transcriptional genes, *T05C1.4* – a calmodulin binding transcriptional activator, and *klf-2*, kruppel-like transcription factor in my first–

pass screen. These two mutants exhibit more vigorous locomotion than N2 at late-age (Table 2C). Interestingly, the *klf-2* mutant also suppresses enhancement of healthspan of *hpa-1* RNAi (Table 2B). However, further tests to evaluate statistically significant changes remain to be conducted.

In sum, there are numerous mechanisms to maintain calcium homeostasis and factors that could execute ER release calcium signaling might be involved in the EGF healthspan pathway. Our data implicate part of the calmodulin(CaM)-CaMK cascade in response, suggesting calcium increase is likely to be involved in healthspan regulation. However, factors independent of the calmodulin cascade may also affect healthspan and be involved in the network of intracellular calcium balance. My work suggests that *cmk-1*, *crh-1*, *sta-1*, and possibly *klf-2* or *T05C1.4* can influence aging quality, and might be involved in the EGF-stimulated calcium changes that promote healthy aging. More detailed studies of the relationship of these genes to each other and to EGF pathway signaling are warranted.

Discussion

EGF/*lin-3* signaling regulates age-associated phenotypes and behavioral quiescence through different downstream branches of the pathway in a tissue-specific manner

There are three main downstream branches of the *C. elegans* EGF signaling pathway. EGF-EGFR acts through RAS-MAPK (*let-60-mek-1*) to affect cell fates by phosphorylating transcription factors—i.e., well studied vulva development. A second signaling branch utilizes PLC-γ (*plc-3*) - diacylglycerol binding proteins ((UNC-13 and TPA-1) - (UNC-7 (feeding related) and EGL-4 (locomotion related)) and mediates behavioral quiescence that accompanies the molt (Van Buskirk and Sternberg, 2007). A third downstream signaling branch, which we mainly focus on, involves IP3 (inositol-1, 4, 5 triphosphate) – IP3R – ER calcium release (Figure 5, Chapter I). This branch has been previously found to be in involved in ovulation (Bui and Sternberg, 2002). We found that activation of this signaling can enhance *C. elegans* locomotory mobility late in life (Iwasa et al., 2010). However, many mechanistic details of how this pathway influences healthy aging in general remained unknown.

Here we found that over-expression of certain *lin-3*/EGF isoforms can promote healthspan, and that tissue-specific pathway activation by *let-23(gf)* expression in muscle and neurons induces globally enhanced maintenance for multiple aging indicators. Van Buskirk et al (2007) reported that over-expression of LIN-3 severely decreases locomotion and pharyngeal pumping through activation of

LET-23 in the ALA neuron, inducing behavioral quiescence. The distinct (converse) phenotypes associated with EGF signaling suggest that cell and tissue-specific modes of EGF signaling transpire in response to activation of EGF/EGFR signaling. My activation of the pathway in all neurons using the *unc-119* promoter (which improves locomotion) also suggests that whole-nervous system pathway activation can over-ride the ALA-specific instructions for quiescence.

Different LIN-3 isoforms may have distinct functions

Alternative splicing has been documented for neuregulin isoforms, EGF family ligands in vertebrates (Chang et al., 1997), and these isoforms induce different consequences in response to different EGFR activation (Meyer et al., 1997). I have found that *lin-3* promoter-driven transgene *Ex[plin-3::lin-3XL]* and ectopic *lin-31* promoter-expressed transgenes *Ex[plin-31::lin-3S*], and *Ex[plin-31::lin-3XL]* confer healthspan extension (Figure 2). By contrast, LIN-3L does not appear effective. My data suggest that different isoforms play distinct roles in adult animals. Consistent with our observation, only *lin-3L*, but not *lin-3S* functions in the VPCs, dependent on *rom-1* activity (Dutt et al., 2004). Another observed difference in *lin-3* slice variants is that *lin-3S* (termed as *lin-3A* in the published paper) is not able to induce quiescence-but the other three *lin-3* isoforms can induce behavioral quiescence. Each *lin-3* isoform also induces different levels of excess vulval induction in development, suggesting that *lin-3S* and *lin-3XL* are more potent (Van Buskirk and Sternberg, 2007). Our results indicated a similar

phenomenon in *lin-3S* and *lin-3XL* as healthspan promoters. The splice variant LIN-3XL shares some conserved amino acids when compared with human EGF isoform sequences (Sup figure 2F), raising the question as to whether human splice variants also play critical roles in adult maintenance.

With transgenic expression, one must always consider whether the expression levels are at the correct level for gene activity. Too much or too little expression could induce non-physiological outcomes. In order to address how expression level influences outcome, we are interested in studying the correlation between proportional percentage changes and each individual isoform level by quantitative RT-PCR. Furthermore, the tissue-specific distribution of *lin-3* splice variants is not known yet. The source and localization of *lin-3* isoforms might be important in ligand activity, although ligands are thought to be able to diffuse. We might identify tissue-specific expression of individual isoforms by fusing GFP to the exons that distinguish the isoforms.

Either larva or adult expression appears enough for healthspan manipulation by EGF/*lin-3* signaling

I have shown by knocking down *lin-3/*EGF in adults only that EGF must be present in adults for maintaining locomotory function and survival in aging adults (Figure 3A). Conversely, knocking down *lin-3/EGF* primarily in larval stage animals followed by terminating knockdown beginning in young adulthood has an impact in mid-late life swimming prowess, without changing swimming proficiency

in young adults (Figure 3B). These data suggest that EGF signaling during development can impact aging quality later in life, without disrupting swimming behavior per se. Since whole life *lin-3(RNAi)* is more deleterious than adult life *lin-3(RNAi)* only, data also suggest that EGF signaling early may be also important for long lifespan. A test of the role of early EGF in lifespan would be to inactivate *lin-3* only in young animals, using the protocol outlined in figure 3B, followed by monitoring lifespan outcomes.

One of the very few genetic manipulations that can be executed early, but play out to confer late-life phenotypes, is mitochondrial gene knockdown (Dillin et al., 2002b). Our findings thus raise the question as to whether EGF signaling impacts mitochondrial activities, which might link to calcium signaling since part of the intracellular calcium is uptake into mitochondria (discussed later). It would be of interest to test whether identified mitochondrial longevity genes might require activation of the EGF pathway for lifespan extension; and conversely, whether the EGF pathway that we identified requires mitochondrial activity for healthspan benefit.

Tissue specific expression of *let-23(gf)* function can differentially impact age-associated phenotypes

let-23 is normally expressed in vulva-related cells, the ALA neuron, hypodermis, and the intestine (Chang et al., 1999; Liu et al., 2011; Simske et al., 1996). Our previous study revealed that *let-23(gf)* mutant is more vigorous in locomotory

mobility at old age, has lower age pigment levels, and has a longer lifespan (Iwasa et al., 2010). Here I found that EGF pathway activation by that ectopic *let-23(gf)* expression in muscle, neuron, and the intestine, can result in late-age locomotory mobility promotion but with different potencies. Survival curves showed muscle, neuronal, and intestinal, but not pharyngeal, expression can extend lifespan especially at mid-age. Differences with single tissue expression raise the issue of whether over-expression of *let-23(gf)* from the native promoter or ubiquitous promoter might confer more potent benefits than observed in single tissue over-expression.

The age-associated phenotypes were notably consistent with aging profiles in distinct lines. The locomotory body bends measured at day 12, 25^{o}C, is about the mid-age (~50% death) in the longevity curve. During this time of *C. elegans* life, the survival curves of transgenic lines revealed a greater impact on the mid-age than maximum and overall survival. For example, the expression of EGFR(gf) in the intestine may be beneficial for the first 20 or so days of life, but then not helpful or even deleterious. When comparing locomotory and lifespan results, tissues that seem most likely to influence locomotion (neurons and muscle) are the ones that most dramatically influence overall survival.

Although *lin-3/EGF* is expressed in the pharynx region (probably from neurons), ectopic *let-23(gf)* expression from muscle in this organ is the least potent in swimming vigor and does not confer lifespan benefits. These results suggest that

lin-3 probably does not activate EGF signaling locally but rather travels to other tissues instead. Also, we can expect the effect of ectopic *let-23(gf)* expression since *itr-1* is broadly expressed and could thus transduce signals from ectopic expression. However, we do not know the level to which LET-23 and ITR-1 activities are increased and how “activated” the pathway is.

Nonetheless, transgenic expression of activated EGFR/LET-23 in specific tissues suggests that expression in several tissues (body wall muscle, neurons, and intestine) can confer some longevity benefit. Since lifespan is an outcome that measures the summed influences on the animal, EGFR activation in one tissue might promote endocrine signaling that has positive outcomes for other tissues.

Additional central modulators might act through the EGF/ITR-1 signaling pathway on healthspan enhancement

The *ark-1* mutant increases swimming locomotion, decreases age pigment scores somewhat, but does not confer lifespan extension. There are two possible pathways by which *ark-1* acts on aging. The first one is negative regulation of *ark-1* on *let-23* (Hopper et al., 2000) which could include the involvement of *sem-5* (mutant 24% lifespan extension (Curran and Ruvkun, 2007)). Another mechanism might be *itr-1* inhibition by *ark-1* as occurs during germline development (Shibata et al., 2003) though this signal possibly acts during larva stages and in the gonad system. Thus *ark-1* could exert effects on aging through either a *let-23*-dependent or independent pathway. This should be easy to

decipher as there are *let-23 gf* and *rf* mutations that might be examined for *ark-1* effects.

In this study, we found that the *ipp-5* (phosphatase) mutant, which should maintain a higher intracellular IP3 level, confers improved locomotory healthspan and extended lifespan. Although *lin-3* acts through *let-23* then hydrolyzes PIP2 into IP3-IP3 receptor activation, there are other upstream inputs (i.e. G-protein coupled receptor, PLC-β) that can also produce IP3. Other experiments need to be performed to clarify the direct correlation between *ipp-5* and *let-23.*

Implication of multiple downstream signaling components that confer healthspan benefits of calcium balance modulation by ER

Our previous study implicated cellular calcium homeostasis in the promotion of nematode healthspan and lifespan (Iwasa et al., 2010). I screened some candidates that might relay the signal from increase of calcium in healthspan promotion. Calmodulin is a major EF hand calcium binding protein. There are six calmodulin (*cmd-1, cal-1, cal-2, cal-3, cal-4, cal-5*) in *C. elegans,* the precise role, however, are not clear yet. Although we obtain no difference in RNAi knockdown experiments, we are not able to rule out the possibilities of multiple calmodulins functioning redundantly.

Calcineurin, a calcium-dependent serine-threonine phosphatase, consists of catalytic subunit A and regulatory subunit B in *C.elegans*. Both *tax-6* reduction-

of-function and *cnb-1* null mutants displayed an extended lifespan through autophagy mechanism (Dwivedi et al., 2009). However, *rcn-1,* which binds and inhibits calcineurin function (Lee et al., 2003), and *ZK856.8* (phosphatase, similar to *cnb-1*) does not change *itr-1(gf)* health benefits. *tax-6* and *cnb-1* remain to be tested, although if they alter *hpa-1*/EGFR signaling outcomes, we will need to look carefully to distinguish different pathways that help healthy aging. Functional redundancy remains a potential confounding factor in testing activity requirements.

Although our preliminary data support that kinases (i.e. *cmk-1*) and kinase activated signaling (*sta-1*) might mediate intracellular calcium signaling. The interaction directly or indirectly between calcium and these candidates awaits biochemical confirmation. There is still no evidence of janus kinase in *C. elegans* (Rawlings et al., 2004). However, the crosstalk between JAK/STAT pathway and EGFR was documented. A cytokine receptor that activates JAK/STAT has been implicated in both positive and negative regulation of EGFR activity ((Moghal and Sternberg, 1999). Increased intracellular calcium also promotes EGFR activation (Moghal and Sternberg, 1999). Therefore multiple candidates discovered in our screening indicate that there is the possibility that each factor partially confers, but works together, with other healthspan promoters.

Figure 1

A

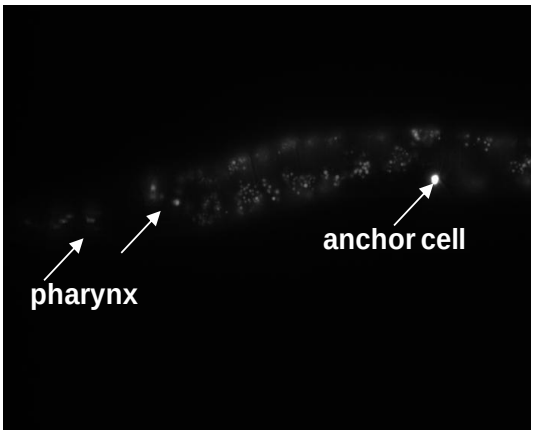

L3/L4 GFP

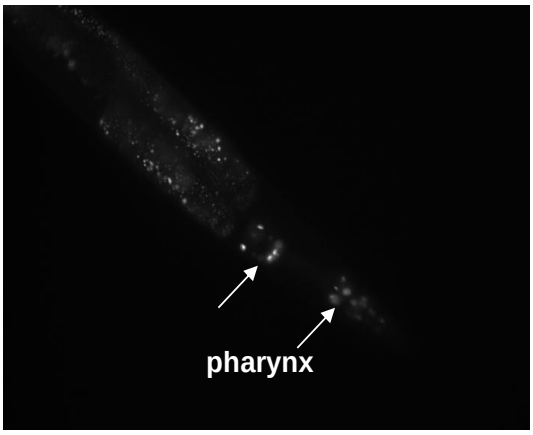

L4 head GFP

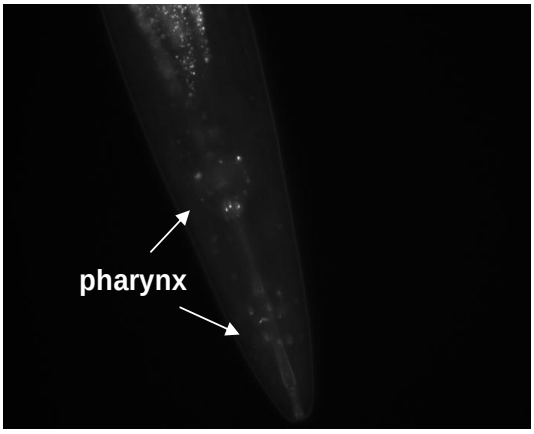

Mid-age head GFP

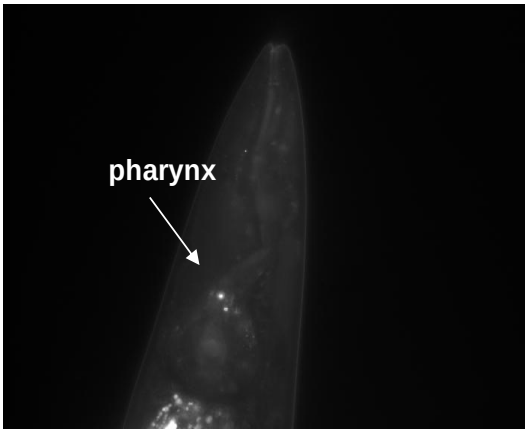

Late-age head GFP

B

stage	Expression sites	percentage
L3	Anchor cell	100%
L4	Anchor , Vulva related cell, Pharynx	100%
Mid-age(day6)	Pharynx(neuron?)	100%
Late-age(day10)	Pharynx(neuron?)	100%

Figure 1. *lin-3* EGF splice variants are expressed late into adult life

A. Temporal and spatial expression pattern of *lin-3*

Expression of *lin-3* is visualized at different stages (larva, mid-age adult, late-age adult) in *C. elegans* life by a GFP tag signal. *plin-3::gfp* animals were reared at 25ºC. Cells expressing *lin-3::gfp* are indicated by arrows. *lin-3* is expressed strongly in the anchor cell at the L3/L4 larva stage and expressed into late adult life in the pharynx region in cells likely to be neurons, with a possible nuclear localization. Note that this GFP reporter reflects expression of all *lin-3* splice isoforms (Sup figure 2A). Gut autofluorescence is apparent in the intestine, which might mask some expression there. Thus, it is unclear if any *lin-3::GFP* expression actually occurs in the gut. The *lin-3*::*gfp* construct was prepared by fusing *gfp* after the transmembrane domain of an inactive form of *lin-3*, in which nucleotides encoding two cysteine residues in the EGF domain were changed to those encoding serine residues (Hill and Sternberg, 1992). The construct contains 10 kb of 5′ upstream sequences from the first *lin-3* exon and is present as an integrated array (Hwang and Sternberg, 2004).

B. Quantitative measurement of *lin-3* expression pattern

15 animals reared at 25ºC were counted for *lin-3* expression sites at larva, mid-age (day 6), and late-age (day 10), respectively. *lin-3* is expressed throughout life in the pharynx region, but disappears from the anchor cell in adult life.

Note that the expression in the pharynx is mainly from a few cells (dot-like appearance) that are likely to correspond to pharyngeal neurons; pharyngeal

muscle does not express strongly. Details of the cell identification remain to be clarified. Also note that GFP expression patterns might not reveal the full gene expression pattern as all gene regulatory signals for the EGF gene might not be present and low level expression in the gut might be obscured by natural gut autofluorescence of age pigments.

Figure 2

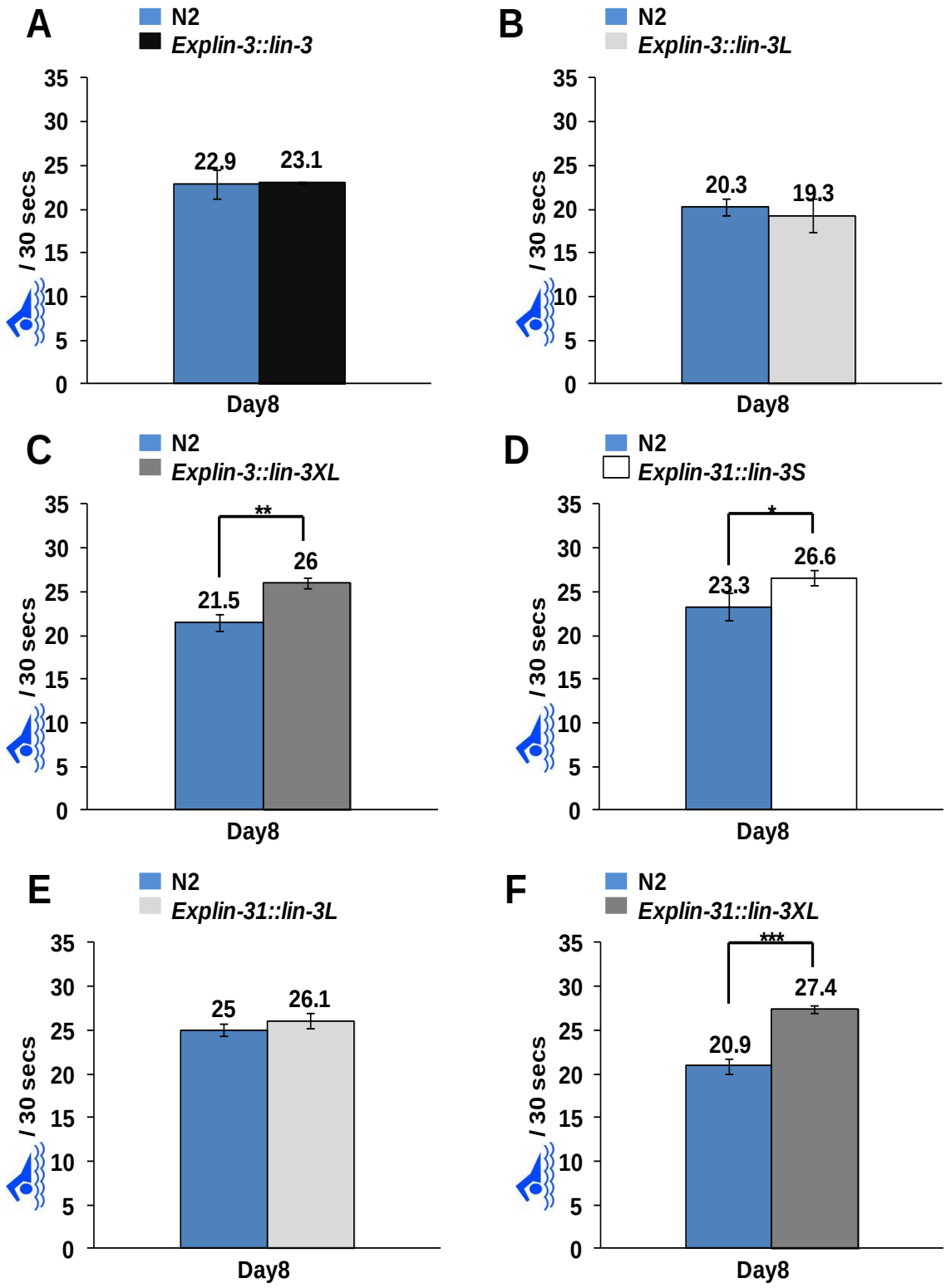
A
N2
Explin-3::lin-3
/ 30 secs
22.9
23.1
Day8
B
N2
Explin-3::lin-3L
/ 30 secs
20.3
19.3
Day8
C
N2
Explin-3::lin-3XL
/ 30 secs
**
21.5
26
Day8
D
N2
Explin-31::lin-3S
/ 30 secs
*
23.3
26.6
Day8
E
N2
Explin-31::lin-3L
/ 30 secs
25
26.1
Day8
F
N2
Explin-31::lin-3XL
/ 30 secs
***
20.9
27.4
Day8

Figure 2. Overexpression of specific *lin-3* splice isoforms implicates LIN-3S and LIN-3XL in anti-aging activity

Comparison of swimming measures for *C. elegans* transgenic lines overexpressing *lin-3* splice variants from extrachromosomal arrays including *unc-119(+)*, *sur-5::gfp*, and either the native *lin-3* promoter or the heterologous *lin-31* promoter fused to one of three *lin-3* splice variants in the *unc-119(e2498)* background. Data are given for day 8, 25ºC. Each trial scored 25-30 animals collected from a population of 200-250 synchronized animals. Shown are the averaged scores from repeat trials. Error bars represent the standard error of the mean (SEM). p-value by unpaired two tailed t-test, *p<0.05, **p<0.01, ***p< 0.001 for all pair-wise comparisons. Note that *lin-3S* expression from the *lin-3* promotor induced a strong young adult bursting Muv phenotype, and thus that line could not be tested (data not shown).

A. Overexpression of genomic *lin-3*, *Ex[plin-3::lin-3],* does not extend locomotory healthspan. The *Ex[plin-3::lin-3]* array consists of the genomic *lin-3* region driven by the native *lin-3* promoter. The extragenic array is expressed at high copy number. In this case, all *lin-3* isoforms may be overexpressed, presumably with correct tissue and temporal specificity as the native promoter. Blue bar, wild type animals; body bends 22.9 +/- 1.6 / 30 seconds at day 8. Black bar, animals with *Ex[plin-3::lin-3]* array; body bends 23.1 +/- 0.1 30 seconds at day 8. No significant difference from 4 repeat trials.

B. Overexpression of *lin-3L* splice variant, *Ex[plin-3::lin-3L]*, does not extend locomotory healthspan. The *Ex[plin-3::lin-3L]* array expresses alternative splicing variant *lin-3L* in high copy number driven by the native *lin-3* promoter. In this situation, *lin-3L* is the only isoform that will be overexpressed. Blue Bar, wild type animals; body bends 20.3 +/- 1.0 / 30 seconds at day 8. Light grey bar, animals with *Ex[plin-3::lin-3L]* array; body bends 19.3 +/- 1.9 30 seconds at day 8. We found no significant difference for the averaged score comparison from 3 repeat trials. However, *Ex[plin-3::lin-3L]* was modestly deleterious in some individual trials (data not shown).

C. Overexpression of the *lin-3XL* splice variant *Ex[plin-3::lin-3XL],* extends locomotory healthspan. The *Ex[plin-3::lin-3XL]* expresses alternative splicing variant *lin-3XL* in high copy number driven by the native *lin-3* promoter. In this situation, *lin-3XL* is the only isoform that will be overexpressed. Blue Bar, wild type animals; body bends 21.5 +/- 0.9 / 30 seconds at day 8. Dark grey bar, animals with *Explin-3::lin-3XL* array; body bends 26.0 +/- 0.6 30 seconds at day 8. The combined trial is $p<0.01$ from 2 repeat trials.

D. Ectopic overexpression of the *lin-3* splice variant *lin-3S* (*Ex[plin-31::lin-3S]),* extends locomotory healthspan. The high copy number *Ex[plin-31::lin-3S]* array expresses the alternative splicing variant *lin-3S* driven by the *lin-31* promoter. In this situation, *lin-3S* is the only isoform that is overexpressed in neurons and in the intestine. Blue Bar, wild type animals; body bends 23.3 +/- 1.6

/ 30 seconds at day 8. White bar, animals with *Ex[plin-31::lin-3S]* array; body bends 26.6 +/- 0.9 30 seconds at day 8. The combined trial $p<0.05$ from 4 repeat trials.

E. Ectopic overexpression of the *lin-3* splice variant *lin-3L* (*Ex[plin-31::lin-3L]*), does not extend locomotory healthspan. The high copy number *Ex[plin-31::lin-3L]* array expresses alternative splicing variant *lin-3L* driven by the *lin-31* promoter. In this situation, *lin-3L* is the only isoform that is overexpressed in neurons and in the intestine. Blue Bar, wild type animals; body bends 25.0 +/- 0.7 / 30 seconds at day 8. Light grey bar, animals transgenic for the *Ex[plin-31::lin-3L]* array; body bends 26.1 +/- 0.8 / 30 seconds at day 8. We found no significant difference in 4 repeat trials.

F. Ectopic overexpression of the *lin-3* splice variant *lin-3XL* (*Ex[plin-31::lin-3XL]*), extends locomotory healthspan. The high copy number array *Ex[plin-31::lin-3XL]* ectopically expresses alternative splicing variant *lin-3XL* from the *lin-31* promoter. In this situation, *lin-3XL* is the only isoform that will be overexpressed in neurons and in the intestine. Blue Bar, wild type animals; body bends 20.9 +/- 0.9 / 30 seconds at day 8. Dark grey bar, animals with the *Ex[plin-31::lin-3XL]* array; body bends 27.4 +/- 0.4 per 30 seconds at day 8. The combined trial is $p<0.001$ from 2 repeat trials.

Figure 3

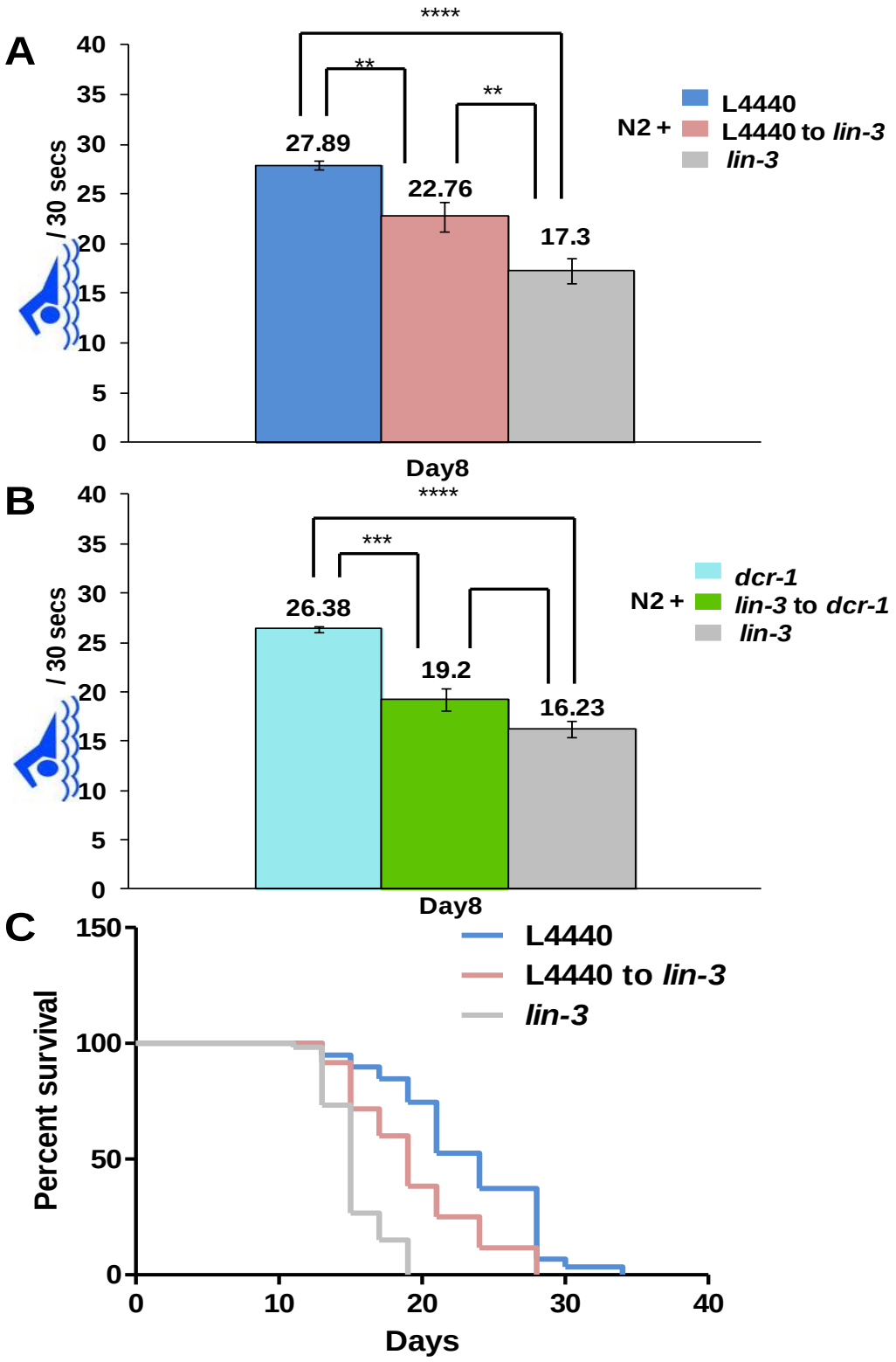
A
****
**
**
27.89
22.76
17.3
/ 30 secs
N2 +
L4440
L4440 to lin-3
lin-3
Day8
B
****
***
26.38
19.2
16.23
/ 30 secs
N2 +
dcr-1
lin-3 to dcr-1
lin-3
Day8
C
L4440
L4440 to lin-3
lin-3
Percent survival
Days

Figure 3. LIN-3/EGF acts during both larval development and adult life to promote healthy aging.

A. RNAi disruption of *lin-3* only during adult life diminishes swim performance later in life, revealing a need for adult-expressed LIN-3 in maintaining locomotory vigor.

Body bend frequency measurements are given at day 8 as measured from the time of egg lay, 25ºC. Blue bar, wild type animals reared on L4440 empty vector control bacteria; body bends 27.9 +/- 0.4 / 30 seconds. Pink bar, wild type animals reared on L4440 empty vector control bacteria during larval development and then transferred at day3 (young adult) to bacteria expressing *lin-3* dsRNA to induce *lin-3* transcript knockdown during adult life; body bends 22.8 +/- 1.5 / 30 seconds. Grey bar, wild type animals reared on bacteria expressing *lin-3* dsRNA over the entire life; body bends 17.3 +/- 1.3 / 30 seconds. Data are compiled from 4 independent trials, 30 animals collected from a population of 150-250 synchronized animals. Error bars represent the standard error of the mean (SEM); p-value for unpaired two tailed t-test, *p < 0.05 for every pairwise comparisons in all 4 repeats within individual trials; for combined trials here, **p <0.02 and ****p < 0.0001. Three experiments in which animals were shifted to *lin-3* RNAi on day2 (L4 larval stage, for possibly more robust impact in the adult) induced similar outcome, with mid-life shift to *lin-3(RNAi)* statistically different from whole life *lin-3(RNAi)* (data not shown, p <0.02 combined trials).

B. RNAi disruption of *lin-3* only during development impairs later life swim performance, suggesting a role for early-expressed LIN-3 in promoting later-age locomotory prowess. Measurements are day 8 mobility in liquid, 25^{o}C. Light blue bar, wild type animals reared on bacteria expressing *dcr-1* dsRNA throughout life; body bends 26.4 +/- 0.3 / 30 seconds. Green bar, wild type animals reared on bacteria expressing *lin-3* dsRNA during development and then shifted at young adulthood to bacteria expressing *dcr-1* dsRNA to rapidly end RNAi efficacy; body bends 19.2 +/- 1.1 / 30 seconds. Grey bar, wild type animals reared on bacteria expressing *lin-3* dsRNA throughout life; body bends 16.2 +/- 0.8 / 30 seconds. Shown is the average for 4 independent repeat trials; 30 animals per trial collected from a population of 150-250 synchronized animals. Error bars represent the standard error of the mean (SEM). p-value by unpaired two tailed t-test, ***p < 0.001 for *dcr-1(RNAi)* compared to *lin-3/dcr-1(RNAi);* p < 0.07 for average comparison of *lin-3(RNAi)/dcr-1(RNAi)* to whole life *lin-3(RNAi)*. In the 4 individual trials, the *lin-3/dcr-1(RNAi)* compared to whole life *lin-3(RNAi)* was different (whole life more potent) p <0.05 for 3 trials, but there was no significant difference between these two *lin-3* knockdown protocols in the 4th trial (data not shown).

C. *lin-3* acts during development and adulthood to regulate lifespan. Wild type animals were grown on RNAi bacteria to test the role of adult-expressed LIN-3 in promoting lifespan. Blue line, lifespan of wild type animals reared on control L4440 empty vector bacteria throughout life. Pink line, lifespan of wild

type animals reared on control L4440 empty vector bacteria during development and then transferred at young adulthood (day3) to bacteria expressing *lin-3* dsRNA to knockdown *lin-3* expression during adult life. Grey line, lifespan of wild type animals reared on bacteria expressing *lin-3* dsRNA in all life. P<0.001 for all pairwise comparisons, log rank test. In 4 repeat trials p value at least < 0.01 for whole life L4440 empty vector compared to shift to *lin-3(RNAi)* at young adult life; for 3 of 4 trials, *lin-3(RNAi*) shift at young adult life was different from *lin-3(RNAi)* over adult life (p<0.05); in 1 of 4 trials *lin-3(RNAi)* shift at young adult life was not different from *lin-3(RNAi)* over whole life.

Figure 4

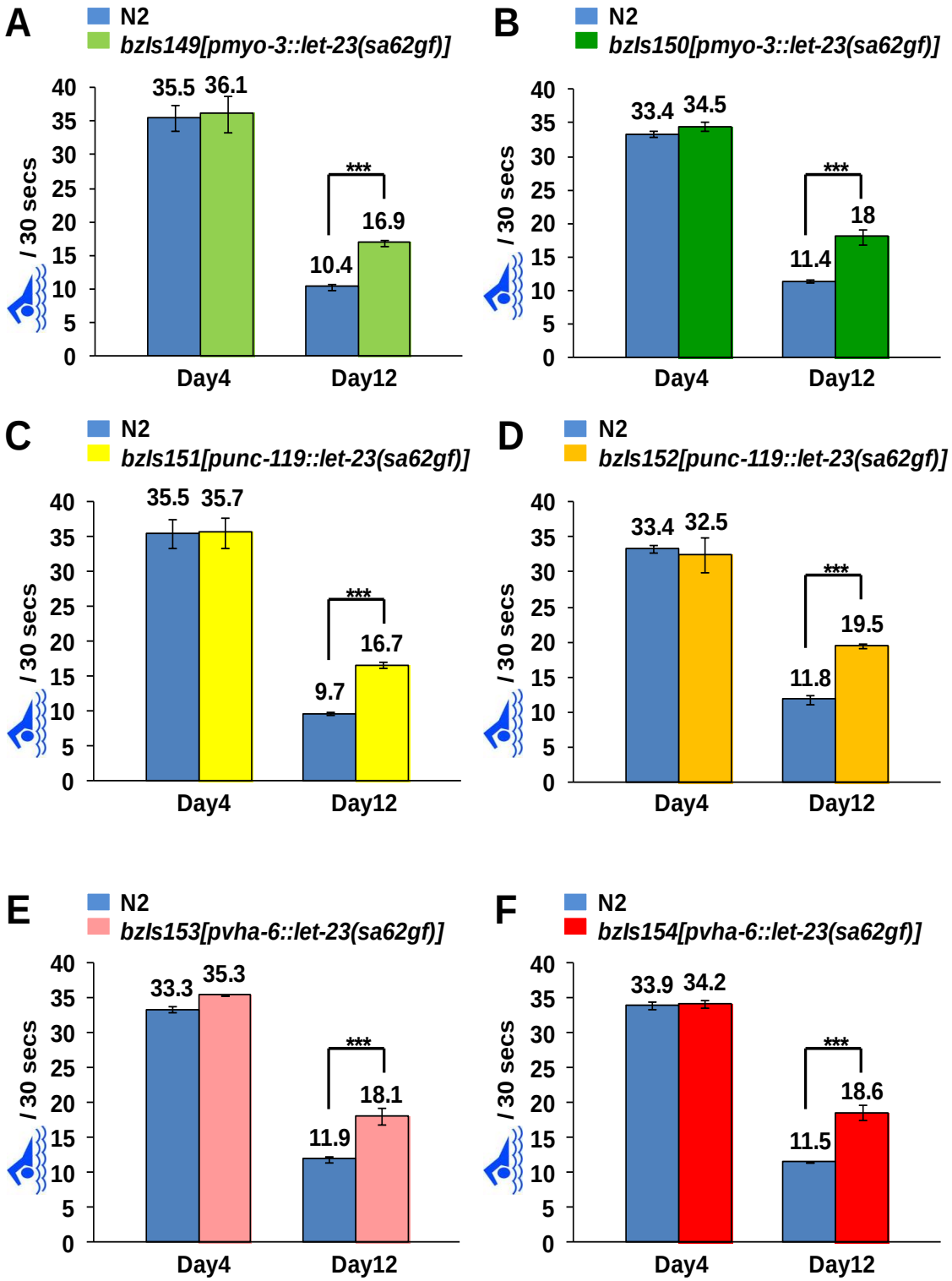
A
N2
bzIs149[pmyo-3::let-23(sa62gf)]
35.5
36.1
***
10.4
16.9
/ 30 secs
Day4
Day12
B
N2
bzIs150[pmyo-3::let-23(sa62gf)]
33.4
34.5
***
11.4
18
/ 30 secs
Day4
Day12
C
N2
bzIs151[punc-119::let-23(sa62gf)]
35.5
35.7
***
9.7
16.7
/ 30 secs
Day4
Day12
D
N2
bzIs152[punc-119::let-23(sa62gf)]
33.4
32.5
***
11.8
19.5
/ 30 secs
Day4
Day12
E
N2
bzIs153[pvha-6::let-23(sa62gf)]
33.3
35.3
***
11.9
18.1
/ 30 secs
Day4
Day12
F
N2
bzIs154[pvha-6::let-23(sa62gf)]
33.9
34.2
***
11.5
18.6
/ 30 secs
Day4
Day12

Figure 4

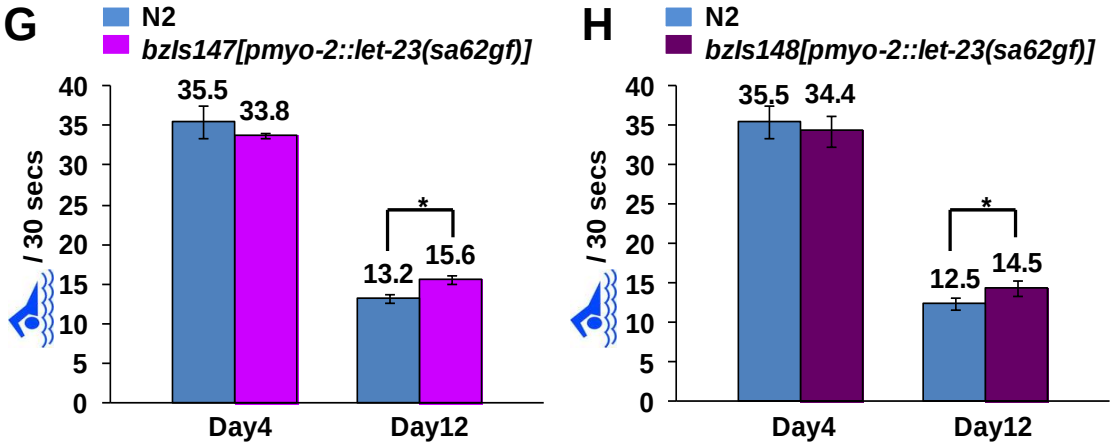
G
N2
bzIs147[pmyo-2::let-23(sa62gf)]
/ 30 secs
40
35
30
25
20
15
10
5
0
35.5
33.8
13.2
15.6
*
Day4
Day12
H
N2
bzIs148[pmyo-2::let-23(sa62gf)]
/ 30 secs
35.5
34.4
12.5
14.5
*
Day4
Day12

Figure 4. Tissue-specific expression of EGFR/*let-23(gf)* suggests pathway activation in multiple tissue types can maintain locomotory function in later life.

We constructed *C. elegans* transgenic lines overexpressing *let-23(gf)* under control of bodywall muscle, neuron, intestine, and pharyngeal muscle-specific promoters in the wild type N2 background and compared swim body bend rate to non-transgenic wild type N2. Data are given for day4, 20ºC (young adult, to test whether expression of *let-23(gf)* changes baseline swim behavior) and day 12, animals reared at 20ºC until young adult and shifted to 25ºC for adult life (late age). Each trial scored 25-30 animals collected from a population of 150-250 synchronized animals. Shown are the averaged scores from repeat trials (two trials for day 4 and at least two trials for day 12 in every transgenic line). Error bars represent the standard error of the mean (SEM). p-value by unpaired two tailed t-test, *p<0.05, **p<0.001, ***p< 0.0001 for all pair-wise comparisons.

A. Over-expression of *let-23(gf)* in bodywall muscle. Blue bar, wild type animals; body bends 35.5 +/- 1.9 / 30 seconds at day 4 and body bends 10.4 +/- 0.5 / 30 seconds at day12. Light green bar, *bzIs149[pmyo-3::let-23(sa62gf)]*; overexpression of *let-23(gf)* in body wall muscle, body bends 36.1 +/- 2.7 / 30 seconds at day 4 and body bends 16.9 +/- 0.5 / 30 seconds at day12. No significant difference at day 4; p<0.0001 for N2 vs. *bzIs149[pmyo-3::let-23(sa62gf)]* at day12.

B. Over-expression of *let-23(gf)* in bodywall muscle. Blue bar, wild type animals; body bends 33.4 +/- 0.6 / 30 seconds at day4 and body bends 11.4 +/- 0.2 / 30 seconds at day12. Dark green bar, *bzIs150[pmyo-3::let-23(sa62gf)]*; overexpression of *let-23(gf)* in body wall muscle, body bends 34.5 +/- 0.6 / 30 seconds at day4 and body bends 18.0 +/- 1.1 / 30 seconds at day12. No significant difference at day4; $p<0.0001$ for N2 vs *bzIs150[pmyo-3::let-23(sa62gf)]* at day12.

C. Over-expression of *let-23(gf)* in neurons. Blue bar, wild type animals; body bends 35.5 +/- 1.9 / 30 seconds at day4 and body bends 9.7 +/- 0.3 / 30 seconds at day12. Yellow bar, *bzIs151[punc-119::let-23(sa62gf)]*; overexpression of *let-23(gf)* in neurons, body bends 35.7 +/- 2.2 / 30 seconds at day4 and body bends 16.7 +/- 0.5 / 30 seconds at day12. No significant difference at day4; $p<0.0001$ for N2 vs *bzIs151[punc-119::let-23(sa62gf)]* at day12.

D. Over-expression of *let-23(gf)* in neurons. Blue bar, wild type animals; body bends 33.4 +/- 0.6 / 30 seconds at day 4 and body bends 11.8 +/- 0.7 / 30 seconds at day 12. Orange bar, *bzIs152[punc-119::let-23(sa62gf)]*; overexpression of *let-23(gf)* in neurons, body bends 32.5 +/- 2.5 / 30 seconds at day4 and body bends 19.5 +/- 0.3 / 30 seconds at day 12. No significant difference at day 4; $p<0.0001$ for N2 vs *bzIs152[punc-119::let-23(sa62gf)]* at day 12.

E. Over-expression of *let-23(gf)* in the intestine. Blue bar, wild type animals; body bends 33.3 +/- 0.5 / 30 seconds at day 4 and body bends 11.2 +/- 0.4 / 30 seconds at day 12. Pink bar, *bzIs153[pvha-6::let-23(sa62gf)]*; overexpression of *let-23(gf)* in the intestine, body bends 35.3 +/- 0.1 / 30 seconds at day 4 and body bends 18.1 +/- 1.2 / 30 seconds at day 12. No significant difference at day 4; $p<0.0001$ for N2 vs *bzIs153[pvha-6::let-23(sa62gf)]* at day 12.

F. Over-expression of *let-23(gf)* in the intestine. Blue bar, wild type animals; body bends 33.9 +/- 0.6 / 30 seconds at day4 and body bends 11.5 +/- 0.1 / 30 seconds at day12. Red bar, *bzIs154[pvha-6::let-23(sa62gf)]*; overexpression of *let-23(gf)* in the intestine, body bends 34.2 +/- 0.6 / 30 seconds at day4 and body bends 18.6 +/- 1.1 / 30 seconds at day12. No significant difference at day4; $p<0.0001$ for N2 vs *bzIs154[pvha-6::let-23(sa62gf)]* at day12.

G. Over-expression of *let-23(gf)* in pharyngeal muscle. Blue bar, wild type animals; body bends 35.5 +/- 1.9 / 30 seconds at day4 and body bends 13.6 +/- 0.5 / 30 seconds at day12. Purple bar, *bzIs147[pmyo-2::let-23(sa62gf)]*; over-expression of *let-23(gf)* in pharynx, body bends 33.8 +/- 0.4 / 30 seconds at day4 and body bends 15.6 +/- 0.6 / 30 seconds at day12. We find no significant difference for transgenic vs. WT at day4; $p<0.05$ for N2 vs *bzIs147[pmyo-2::let-23(sa62gf)]* at day12.

H. Over-expression of *let-23(gf)* in pharyngeal muscle. Blue bar, wild type animals; body bends 35.5 +/- 1.9 / 30 seconds at day4 and body bends 12.5 +/- 0.8 / 30 seconds at day12. Dark purple bar, *bzIs148[pmyo-2::let-23(sa62gf)]*; overexpression of *let-23(gf)* in pharynx, body bends 34.4 +/- 2.0 / 30 seconds at day4 and body bends 14.5 +/- 0.9 / 30 seconds at day12. No significant difference at day4; $p<0.05$ for N2 vs. *bzIs148[pmyo-2::let-23(sa62gf)]* at day12 (note that one out of four trial did not show significance).

Table 1

Cumulative trial	N2	*bzIs149[pmyo-3::let-23(sa62gf)]*	Change ratio
Median day	16	23	44%
Mean day	19.2+/-0.5	22.3+/-0.5	15% (p<0.0001)
Max day	32.6+/-0.6	33.6+/-0.7	3%(n.s.)
P value		p<0.0001	

Cumulative trial	N2	*bzIs150[pmyo-3::let-23(sa62gf)]*	Change ratio
Median day	15	19	27%
Mean day	17.9+/-0.5	19.5+/-0.5	9%(p<0.05)
Max day	32.9+/-1.0	28.9+/-0.7	-12%(p<0.01)
P value		p<0.001	

Cumulative trial	N2	*bzIs151[punc-119::let-23(sa62gf)]*	Change ratio
Median day	16	21	31%
Mean day	19.3+/-0.5	21.5+/-0.5	11%(p<0.01)
Max day	32.6+/-0.6	32.0+/-0.7	-2%(n.s.)
P value		p<0.001	

Cumulative trial	N2	*bzIs152[punc-119::let-23(sa62gf)]*	Change ratio
Median day	18	20	11%
Mean day	19.5+/-0.4	21.1+/-0.4	8%(p<0.01)
Max day	30.5+/-0.7	32.9+/-0.6	8%(p~0.01)
P value		p<0.001	

Table 1

Cumulative trial	N2	*bzIs153[pvha-6::let-23(sa62gf)]*	Change ratio
Median day	15	18	20%
Mean day	18.3+/-0.4	18.8+/-0.3	3%(n.s.)
Max day	32.3+/-0.6	28.5+/-0.7	-12%(p<0.0001)
P value		p<0.001	

Cumulative trial	N2	*bzIs154[pvha-6::let-23(sa62gf)]*	Change ratio
Median day	19	22	16%
Mean day	20.1+/-0.5	22.1+/-0.4	6%(p<0.05)
Max day	34.9+/-0.5	33.8+/-0/7	-3%(n.s.)
P value		p<0.01	

Cumulative trial	N2	*bzIs147[pmyo-2::let-23(sa62gf)]*	Change ratio
Median day	17	17	0%
Mean day	19.9+/-0.4	19.6+/-0.4	1% (n.s)
Max day	32.6+/-0.5	33.3+/-0.7	2%(n.s.)
P value		n.s.	

Cumulative trial	N2	*bzIs148[pmyo-2::let-23(sa62gf)]*	Change ratio
Median day	21	18	-14%
Mean day	21.8+/-0.6	20.8+/-0.6	-5%(n.s.)
Max day	34+/-0.8	34.4+/-0.9	1%(n.s.)
P value		n.s.	

Table 1. Details of lifespan for *let-23(gf)* tissue specific overexpression in *C. elegans*

C. elegans transgenic lines overexpressing *let-23(gf)* in a wild type background, driven under the control of various tissue-specific promoters, are compared to N2 wild type (20^{o}C). Shown here is the data of cumulative curves on mean, median and maximum lifespan. Maximum day is calculated by taking the mean age of the top 10% longest lived in the population. Curves are shown in Figure 5A-5H. Significance of differences between survival curves was calculated using the Gehan-Breslow-Wilcoxon test for all pair comparison.

Figure 5

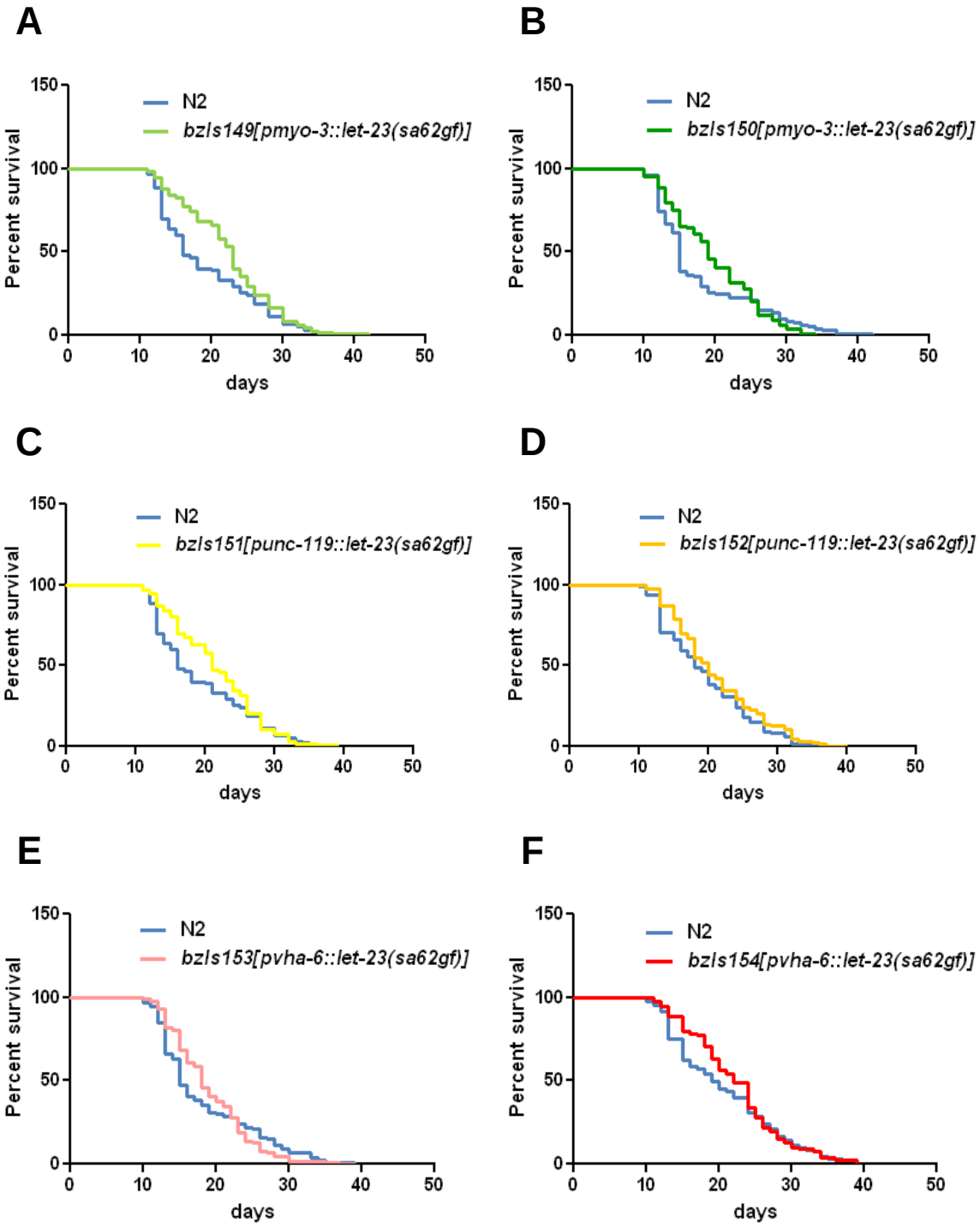
A
B
C
D
E
F
Percent survival
days
N2
bzIs149[pmyo-3::let-23(sa62gf)]
bzIs150[pmyo-3::let-23(sa62gf)]
bzIs151[punc-119::let-23(sa62gf)]
bzIs152[punc-119::let-23(sa62gf)]
bzIs153[pvha-6::let-23(sa62gf)]
bzIs154[pvha-6::let-23(sa62gf)]
0
50
100
150
0
10
20
30
40
50

Figure 5

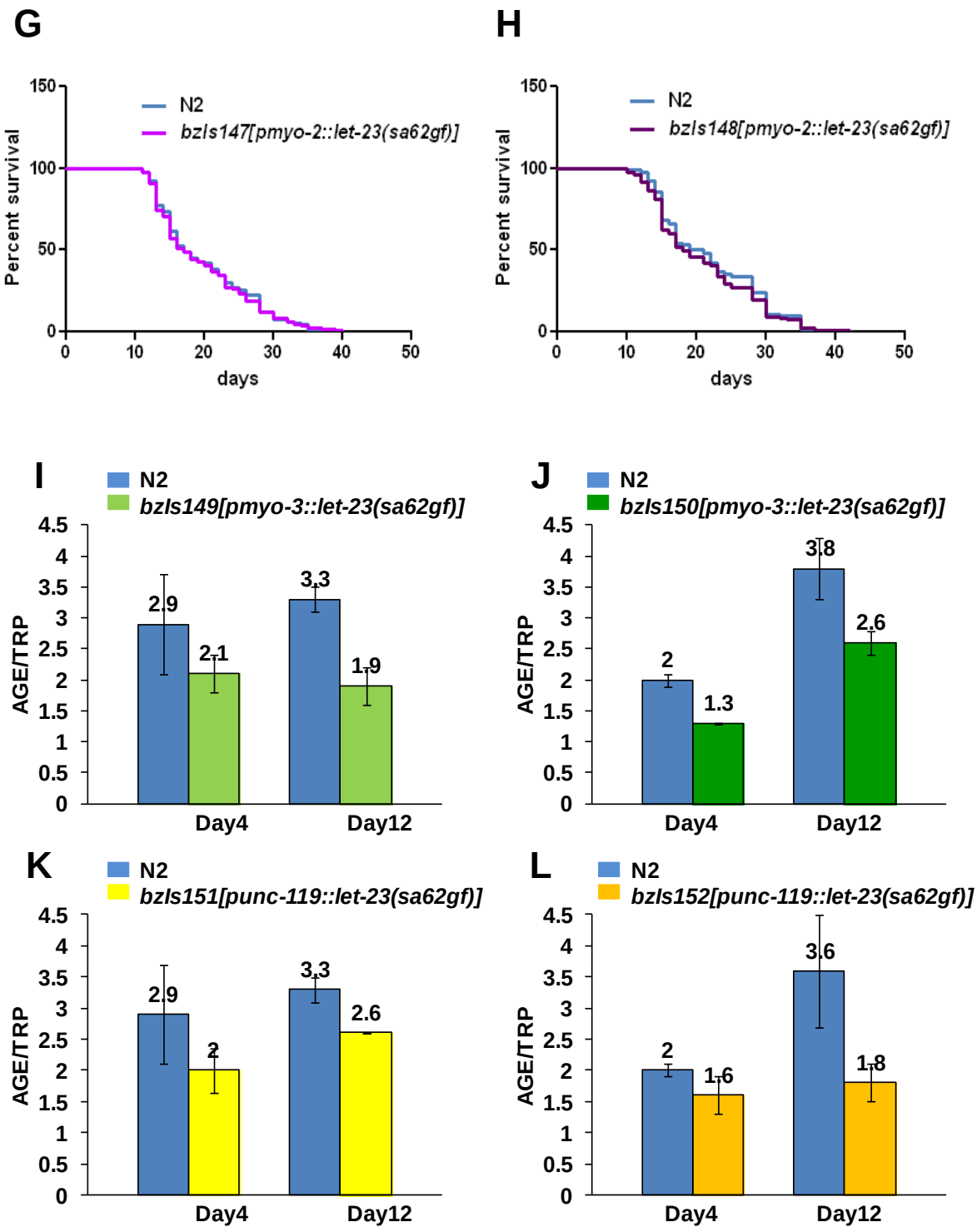
G
H
Percent survival
days
N2
bzIs147[pmyo-2::let-23(sa62gf)]
bzIs148[pmyo-2::let-23(sa62gf)]
I
J
K
L
AGE/TRP
Day4
Day12
bzIs149[pmyo-3::let-23(sa62gf)]
bzIs150[pmyo-3::let-23(sa62gf)]
bzIs151[punc-119::let-23(sa62gf)]
bzIs152[punc-119::let-23(sa62gf)]
2.9
2.1
3.3
1.9
2
1.3
3.8
2.6
2.9
2
3.3
2.6
2
1.6
3.6
1.8

Figure 5

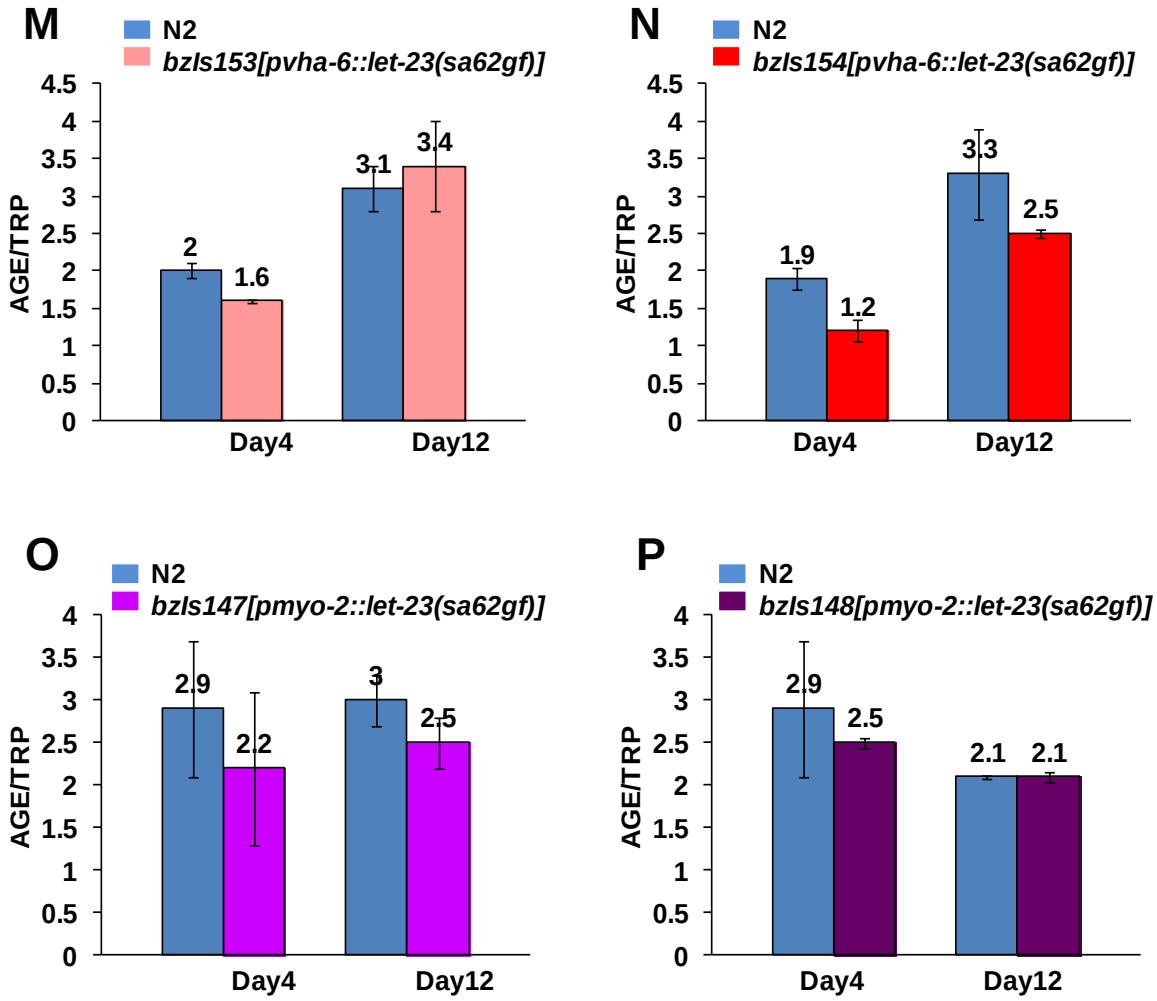
M
N2
bzIs153[pvha-6::let-23(sa62gf)]
AGE/TRP
4.5
4
3.5
3
2.5
2
1.5
1
0.5
0
2
1.6
3.1
3.4
Day4
Day12
N
N2
bzIs154[pvha-6::let-23(sa62gf)]
AGE/TRP
1.9
1.2
3.3
2.5
Day4
Day12
O
N2
bzIs147[pmyo-2::let-23(sa62gf)]
AGE/TRP
2.9
2.2
3
2.5
Day4
Day12
P
N2
bzIs148[pmyo-2::let-23(sa62gf)]
AGE/TRP
2.9
2.5
2.1
2.1
Day4
Day12

Figure 5. Tissue-specific expression of EGFR/*let-23(gf)* mutant activation in multiple age-associated performance.

(A-H) *C. elegans* transgenic lines overexpressing *let-23(gf)* in a wild type background, driven under the control of various tissue-specific promoters, are compared to N2 wild type (20^{o}C) to test whether activation of LET-23/EGFR in individual tissues can extend adult lifespan. Cumulative survival curves shown here are from multiple repeat trials. Survival curve data were collected from a population of 60 synchronized animals / trial. Significance of differences between survival curves was calculated using the Gehan-Breslow-Wilcoxon test for all pair comparison. Details of data on mean, median and maximum lifespan are summarized in Table 1.

A. *let-23(gf)* expressed in muscle extends median lifespan. Blue line, lifespan of N2 wild type; median lifespan is 16 days. Light green line, lifespan of *bzIs149[pmyo-3::let-23(sa62gf)]*; median lifespan is 23 days; cumulative curve is from 3 repeats with $p<0.0001$.

B. *let-23(gf)* expressed in muscle extends median lifespan. Blue line, lifespan of N2 wild type; median lifespan is 15 days. Dark green line, lifespan of *bzIs150[pmyo-3::let-23(sa62gf)]*; median lifespan is 19 days; cumulative curve is from 3 repeats with $p<0.001$.

C. *let-23(gf)* expressed pan-neuronally confers median lifespan extension. Blue line, lifespan of N2 wild type; median lifespan is 16 days. Yellow line, lifespan of *bzIs151[punc-119::let-23(sa62gf)]*; median lifespan is 21 days; cumulative curve is from 3 repeats with $p<0.001$.

D. *let-23(gf)* expressed pan-neuronally confers median lifespan extension. Blue line, lifespan of N2 wild type; median lifespan is 18 days. Orange line, lifespan of *bzIs152[punc-119::let-23(sa62gf)]*; median lifespan is 20 days; cumulative curve is from 4 repeats with $p<0.01$.

E. *let-23(gf)* expressed in the intestine confers median lifespan extension. Blue line, lifespan of N2 wild type; median lifespan is 15 days. Pink line, lifespan of *bzIs153[pvha-6::let-23(sa62gf)]*; median lifespan is 18 days; cumulative curve is from 6 repeats with $p<0.001$.

F. *let-23(gf)* expressed in the intestine confers median lifespan extension. Blue line, lifespan of N2 wild type; median lifespan is 19 days. Red line, lifespan of *bzIs154[pvha-6::let-23(sa62gf)]*; median lifespan is 22 days; cumulative curve is from 4 repeats with $p<0.01$. Note, however, that for both independently isolated lines, there appears to be a modest positive impact on survival early in adult life, but a deleterious effect later in life. Different medians, for *bzIs153* (12.3 day vs. 13.1 day) 6% longer, $p<0.001$; *bzIs154* (12.6 day vs. 14.4 day) 14% longer, $p<0.0001$.

G. *let-23(gf)* expressed in the pharynx does not confer lifespan extension. Blue line, lifespan of N2 wild type; median life span is 17 days. Purple line, lifespan of *bzIs147[pmyo-2::let-23(sa62gf)]*; median life span is 17 days. No difference was detected.

H. *let-23(gf)* expressed in the pharynx does not confer lifespan extension. Blue line, lifespan of N2 wild type; median lifespan is 21 days. Dark purple line, lifespan of *bzIs148[pmyo-2::let-23(sa62gf)]*; median lifespan is 18 days. No difference was detected.

(I-P) Impact of activation of LET-23(gf) in different tissues by quantitative measurement of age pigment accumulation. The age pigment score is normalized as the ratio of fluorescence units for age pigment/tryptophan fluorescence. Measurements are given at both day4 (young adult) 20ºC and day12 (8 days after young adult, which is fairly old) 25ºC. Each trial measurd 35 animals collected from a population of synchronized animals. Shown are the average ratios from repeat trials. Error bars represent the standard error of the mean (SEM).

I. Blue bar, N2 wild type animals. Light green bar, *bzIs149[pmyo-3::let-23(sa62gf)]*; overexpression of *let-23(gf)* in body wall muscle. 2 repeats were measured on day 4 and day 12 respectively.

J. Blue bar, N2 wild type animals. Dark green bar, *bzIs150[pmyo-3::let-23(sa62gf)]*; overexpression of *let-23(gf)* in body wall muscle. 2 repeats were measured on day 4 and 3 repeats on day 12 respectively.

K. Blue bar, N2 wild type animals. Yellow bar, *bzIs151[punc-119::let-23(sa62gf)]*; overexpression of *let-23(gf)* in neuron. 2 repeats were measured on day 4 and day 12 respectively.

L. Blue bar, N2 wild type animals. Orange bar, *bzIs152[punc-119::let-23(sa62gf)]*; overexpression of *let-23(gf)* in neuron. 2 repeats were measured on day 4 and day 12 respectively.

M. Blue bar, N2 wild type animals. Pink bar, *bzIs153[pvha-6::let-23(sa62gf)]*; overexpression of *let-23(gf)* in the intestine. 2 repeats were measured on day 4 and 4 repeats on day 12 respectively.

N. Blue bar, N2 wild type animals. Red bar, *bzIs154[pvha-6::let-23(sa62gf)]*; overexpression of *let-23(gf)* in the intestine. 2 repeats were measured on day 4 and day 12 respectively.

O. Blue bar, N2 wild type animals. Purple bar, *bzIs147[pmyo-2::let-23(sa62gf)]*; overexpression of *let-23(gf)* in the intestine. 2 repeats were measured on day 4 and 4 repeats on day 12 respectively.

P. Blue bar, N2 wild type animals. Dark purple bar, *bzIs148[pmyo-2::let-23(sa62gf)]*; overexpression of *let-23(gf)* in the intestine. 2 repeats were measured on day 4 and day 12 respectively.

Figure 6

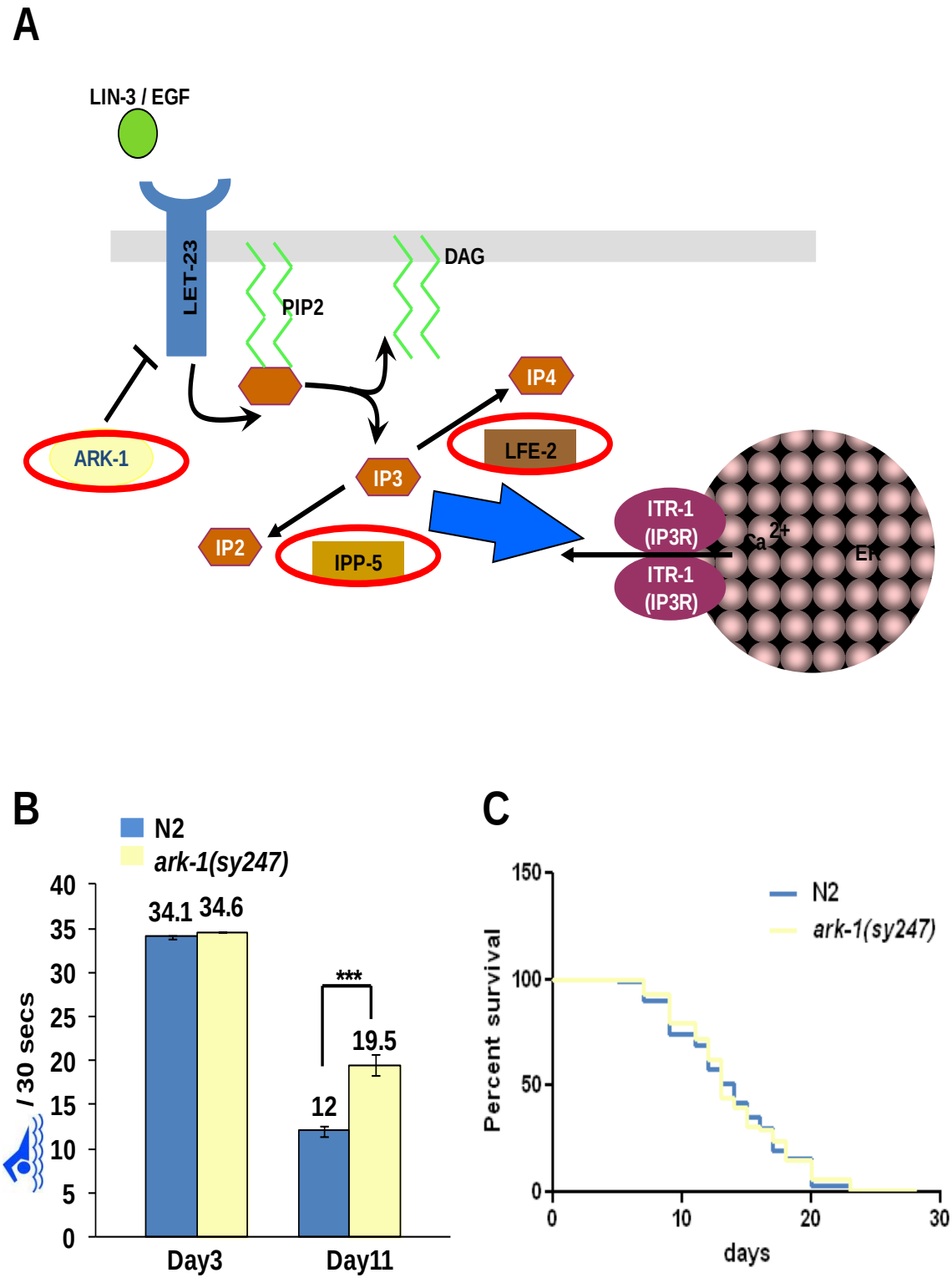
A
LIN-3 / EGF
LET-23
DAG
PIP2
IP4
LFE-2
ARK-1
IP3
IP2
IPP-5
ITR-1
(IP3R)
ITR-1
(IP3R)
Ca 2+
B
N2
ark-1(sy247)
34.1
34.6
***
19.5
12
/ 30 secs
Day3
Day11
C
N2
ark-1(sy247)
Percent survival
days

Figure 6

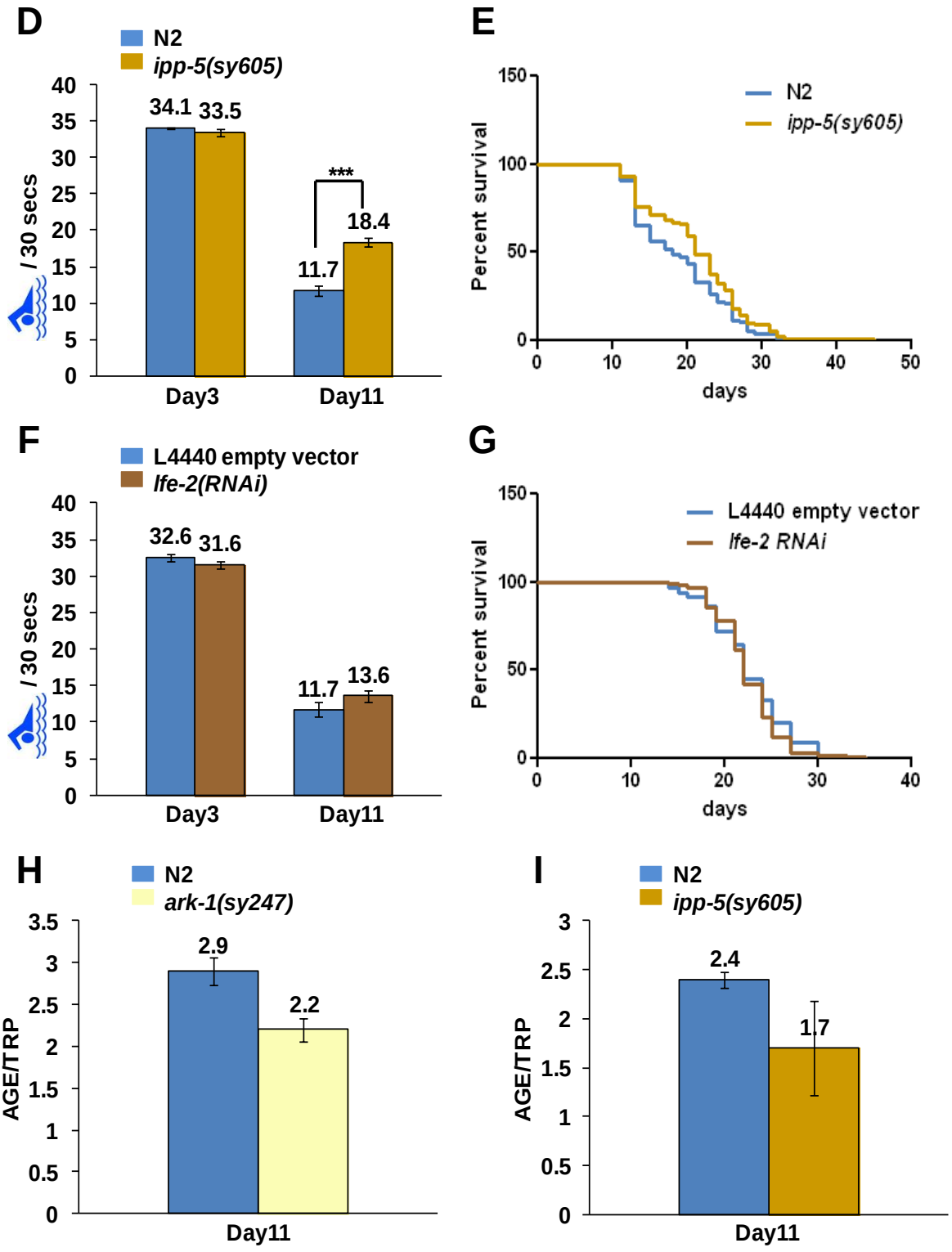
D
N2
ipp-5(sy605)
/ 30 secs
34.1
33.5
***
18.4
11.7
Day3
Day11
E
N2
ipp-5(sy605)
Percent survival
days
F
L4440 empty vector
lfe-2(RNAi)
/ 30 secs
32.6
31.6
11.7
13.6
Day3
Day11
G
L4440 empty vector
lfe-2 RNAi
Percent survival
days
H
N2
ark-1(sy247)
AGE/TRP
2.9
2.2
Day11
I
N2
ipp-5(sy605)
AGE/TRP
2.4
1.7
Day11

Figure 6. Additional central modulators in the EGF/ITR-1 signaling pathway affect *C. elegans* healthspan

A. Model of *C. elegans* modulators of EGF/ITR-1 signaling that influence ITR-1 activity. Highlighted are *ark-1*, *ipp-5*, and *lfe-2.* Under normal conditions, the ligand *lin-3*/EGF binds to the receptor *let-23*/EGFR, which results in the hydrolysis of PIP2 into IP3, which activates ITR-1 signaling by binding of IP3 to the IP3 receptor on the ER membrane. Calcium is consequently released. Genes of interest are circled with red. ARK-1 is a negative regulator of LET-23/EGFR. IPP-5 and LFE-2 control the IP3 level in the cell by catalyzing biochemical conversion pathways.

(B,D,F) Comparison of locomotory aging of wild type and EGF signaling mutants. Data are given for day 3, 25ºC (young adult, test of baseline swim behavior) and day 11 (8 days after reaching adulthood, late adult life). Each trial scored 25-30 animals collected from a population of 150-250 synchronized animals. Shown are the averaged scores from repeat trials (two trials for day 3 and at least three trials for day 11). Error bars represent the standard error of the mean (SEM). p-value by unpaired two tailed t-test, ***p< 0.0001 for pair-wise comparisons.

(C,E,G) Survival curve comparison of wild type and EGF signaling pathway mutants. Mutant survival curves were compared to N2 wild type survival curves to test the impact of genes *ark-1*, *ipp-5*, and *lfe-2* on adult lifespan extension.

Cumulative survival curves shown here combine data from multiple repeat trials. Survival curve data were collected from a population of 60 synchronized animals/trial. Significance of differences between survival curves was calculated using the Gehan-Breslow-Wilcoxon test for all pair comparisons.

(H,I) Quantitative measurement of age pigment accumulation of wild type and EGF signaling pathway mutants. The age pigment score is normalized as the ratio of fluorescence units for age pigment/tryptophan fluorescence. Measurements are reported for day 11 (8 days after young adult), 25ºC. Each trial measured 35 animals collected from a population of synchronized animals. Shown are the average ratios from repeat trials. Error bars represent the standard error of the mean (SEM).

B. Mutation of *ark-1(sy247),* a negative regulator of *let-23* signaling, confers enhanced locomotory mobility in later life. Blue bar, wild type animals; body bends 34.1 +/- 0.2 / 30 seconds at day 3 and body bends 12.0 +/- 0.6 / 30 seconds at day 11. Light yellow bar, *ark-1(sy247)* mutant; body bends 34.6 +/- 0.1 / 30 seconds at day 3 and body bends 19.5 +/- 1.2 / 30 seconds at day 11. We find no significant difference at day 3. The combined trial $p<0.0001$ for N2 and *ark-1(sy247)* comparison at day 11 from 3 repeated trials reveals improved swimming proficiency in old age for *ark-1*.

C. *ark-1(sy247)* does not confer lifespan extension. Blue line, lifespan of N2 wild type; median lifespan is 15 days. Light yellow line, lifespan of *ark-1(sy247)*;

median lifespan is 13 days. The comparison of curves was performed at 25ºC because the *sy247* allele is temperature-sensitive for certain phenotypes. The cumulative curve is from 3 repeat trials with no difference (a 20ºC trial shows similar results, data not shown).

D. Mutation in *ipp-5(sy605),* a negative regulator of IP3 signaling, causes enhanced locomotory mobility in later life. Blue bar, wild type animals; body bends 34.1+/- 0.2 / 30 seconds at day 3 and body bends 11.7 +/- 0.7 / 30 seconds at day 11. Brown bar, *ipp-5(sy605)* mutant; body bends 33.5 +/- 0.6 / 30 seconds at day 3 and body bends 18.4 +/- 0.6 / 30 seconds at day 11. We find no significant difference at day 3, supporting that development of swimming behavior is normal. The combined trial $p<0.0001$ for N2 and *ipp-5(sy605)* comparison at day 11, from 6 repeated trials. $p<0.0001$ for every pairwise comparison in 5 repeats within individual trials, except one individual trial $p<0.05$. Thus, disrupting *ipp-5* extends adult locomotory healthspan.

E. *ipp-5(sy605)* modestly extends lifespan. Blue line, lifespan of N2 wild type; median lifespan is 18 days. Brown line, lifespan of *ipp-5(sy605)*; median lifespan is 21 days. The cumulative curve data were obtained at 20ºC from 3 repeats with $p<0.01$. Note that in individual trials, 1/3 trials exhibited a significant lifespan extension by Wilcoxon statistics. Thus, impact on lifespan appears modest and sensitive to environmental conditions at best.

F. RNAi disruption of *lfe-2,* a negative regulator of IP3 signaling, does not improve locomotory mobility in later life.

Blue bar, wild type animals; body bends 32.6 +/- 0.5 / 30 seconds at day 3 and body bends 11.7 +/- 1.0 / 30 seconds at day 11. Dark brown bar, *lfe-2(RNAi)*; body bends 31.6 +/- 0.5 / 30 seconds at day3 and body bends 13.6 +/- 0.8 / 30 seconds at day 11. We found no significant differences at day 3 and day 11 (5 repeats).

G. *lfe-2(RNAi)* does not confer lifespan regulation. Wild type animals were grown on RNAi bacteria to test the role of *lfe-2* on lifespan regulation. Blue line, lifespan of wild type animals reared on control L4440 empty vector bacteria; median lifespan is 22 days. Dark brown line, lifespan of wild type animals reared on bacteria expressing *lfe-2* dsRNA; median lifespan is 22 days. Cumulative curve is from 2 repeats with no significant difference detected.

Note that the median lifespan day above cannot be compared directly between trials with different temperature and mutant/RNAi.

H. *ark-1(sy247)* exhibits modestly lower age pigment accumulation at old age. Blue bar, N2 wild type animals. Light yellow bar, *ark-1(sy247)*; 2 repeats were measured, day 11. Error bars show standard error of the mean.

I. *ipp-5(sy605)* exhibits modestly lower age pigment accumulation at old age. Blue bar, N2 wild type animals. Brown bar, *ipp-5(sy605)*; 3 repeats were measured on day 11. Error bars show standard error of the mean.

Table 2

A. Late-age swimming phenotypes consequent to RNAi knock-downs of possible downstream candidates calcium-sensitive effectors of EGF signaling in *itr-1(gf)*

Day 11, 25ºC, *itr-1(gf)* strain

RNAi gene name	Change ratio	p- value	n
Calmodulin related			
cal-1	-2%	n.s.	60
cal-2	2%	n.s.	60
cal-4	-1%	n.s.	30
cmd-1	4%	n.s.	60
aspm-1	4%	n.s.	60
Calcineurin related			
rcn-1	8%	n.s.	60
ZK856.8	3%	n.s.	60
EF hand transcription factor			
F23B12.7	-12%	two n.s. , one lower	90
CREB related			
crh-2	-7%	one n.s. , two lower	90
let-607	7%	one n.s. ,one higher	60

Table 2

B. Late-age swimming prowess consequent to RNAi knockdown of *hpa-1* in mutant backgrounds hypothesized to play a role in EGF healthspan promotion

Day11, 25ºC, *hpa-1(RNAi)*

Mutant gene name	Change ratio	p- value	n
Calmodulin related			
ckk-1(ok1033)	16%	P<0.05	60
cmk-1(oy21)	8%	n.s.	30
Transcription factor			
klf-2(ok1053)	-2%	n.s.	30
sta-1(ok587)	3%	n.s.	30
lin-31(gk569)	28%	P<0.01	60
CREB related			
crh-1(tz2)	4%	n.s.	30

Table 2

C. Late-age swimming prowess of *C. elegans* mutants being examined as candidate swimming healthspan modulators

Day3, 25ºC mutant strains without further manipulation

Mutant gene name	Change ratio	p- value	n
sta-1(ok587)	0%	n.s.	25

Day11, 25ºC

Mutant gene name	Change ratio	p- value	n
Calmodulin related			
cmk-1(oy21)	62%	P<0.01	60
T05C1.4(ok515)	35%	two good , one n.s.	72
Transcription factor			
klf-2(ok1053)	31%	one good ,one n.s.	60
sta-1(ok587)	71%	P<0.0001	120

D. Impact of *itr-1(RNAi)* against WT and *sta-1(ok587)*

Day11, 25ºC

Mutant gene name	% control	p- value	n
N2	-26%	P<0.01	20
sta-1(ok587)	-6%	n.s.	69

Table 2. Screening for calcium-sensitive executors that act downstream of EGF/ITR signaling to promote healthspan

A. Late-age swimming prowess consequent to RNAi knockdown of downstream candidates that might mediate responses to *C. elegans itr-1(gf)*

Four gene categories (calmodulin-related, calcineurin-related, EF hand transcription factor, CREB-related) were screened using an RNAi strategy in *itr-1(sy290gf)*, which has a large healthspan extension and is downstream in the HPA-1/2 modulated EGFR healthspan pathway. I initially sought calcium-responsive genes that might act downstream of ITR-1 and might therefore be required for ITR-1(gf) healthspan benefits. Body bend frequency measurements are given at day 11 as measured from the time of egg lay, 25ºC. *itr-1(sy290gf)* animals reared on L4440 empty vector control bacteria as control are compared with *itr-1(sy290gf)* animals reared on bacteria expressing specific dsRNA (i.e. *cal-1* in row 1) over the entire life. Data are compiled from repeated trials, and 30 animals / trial collected from a population of 150-250 synchronized animals. % change represents the difference of body bend frequency with a specific gene RNAi treatment divided by the body bend frequency with L4440 control RNAi treatment (i.e., *itr-1(gf)* + L4440 fed body bends number is normalized as the base line). p-value for unpaired two tailed t-test for pair-wise comparisons. n represents numbers of animals in trials.

B. Late-age swimming prowess consequent to *hpa-1(RNAi)* knockdown in potential calcium-responsive gene mutant backgrounds in *C. elegans*

Four categories of mutants (calmodulin-related, EF hand transcription factor, CREB-related, EGF-MAPK signaling) were treated with *hpa-1* RNAi. These data test the requirement for specific genes in the *hpa-1* EGF healthspan pathway. Body bend frequency measurements are given at day 11 as measured from the time of egg lay, 25ºC. Mutants reared on L4440 empty vector control bacteria are compared with mutants reared on bacteria expressing *hpa-1* dsRNA over the entire life. If the *hpa-1(RNAi)* benefit is enhanced or neutral, the gene suggested to act in parallel to the EGF pathway; if it is blocked, the gene becomes a candidate for acting in the pathway. Tests were repeated when significance was found in an individual trial and then data are shown here compiled from repeated trials. 30 animals / trial collected from a population of 150-250 synchronized animals. % change represents the difference of body bend frequency of single gene mutant + *hpa-1* RNAi and body bend frequency of single gene mutant + L4440 control RNAi divided by the body bend frequency of the single gene mutant + L4440 body bend number used to normalize as the base line. p-value for unpaired two tailed t-test for pair-wise comparisons. n represents numbers of animals in trials.

C. Late-age swimming prowess of selected calcium-responsive gene mutants in *C. elegans*

Comparison of locomotory aging of wild type and selected mutants that have disruptions in candidate calcium adaptor proteins for the EGF healthspan pathway. Body bend frequency measurements were scored at day 11 as measured from the time of egg lay, 25ºC. Data are compiled from repeated trials, 20-30 animals/trial collected from a population of 150-250 synchronized animals. % change represents the difference of body bend frequency of single gene mutant and the body bend frequency of N2 wild type divided vy N2 body bend numbernormalized as the base line). p-value for unpaired two tailed t-test for pair-wise comparisons. n represents numbers of animals in trials.

D. Late-age swimming prowess consequent to RNAi knockdown of *itr-1* in *C. elegans sta-1(ok587)*

sta-1(ok587) animals reared on L4440 empty vector control bacteria as control are compared with animals reared on bacteria expressing *itr-1* dsRNA over the entire life. These data address whether *sta-1* benefits require *itr-1*. Body bend frequency measurements are given at day 11 as measured from the time of egg lay, 25ºC. Data are shown compiled from repeated trials. 20-30 animals / trial collected from a population of 150-250 synchronized animals. % change represents the difference of body bend frequency of *sta-1(ok587)* and *itr-1* RNAi divided by the body bend frequency of *sta-1(ok587)* + L4440 control RNAi (here L4440 fed body bend rate is used as the base line for normalization). p-value for

unpaired two tailed t-test for pair-wise comparisons. n represents numbers of animals in trials.

Sup Figure 1

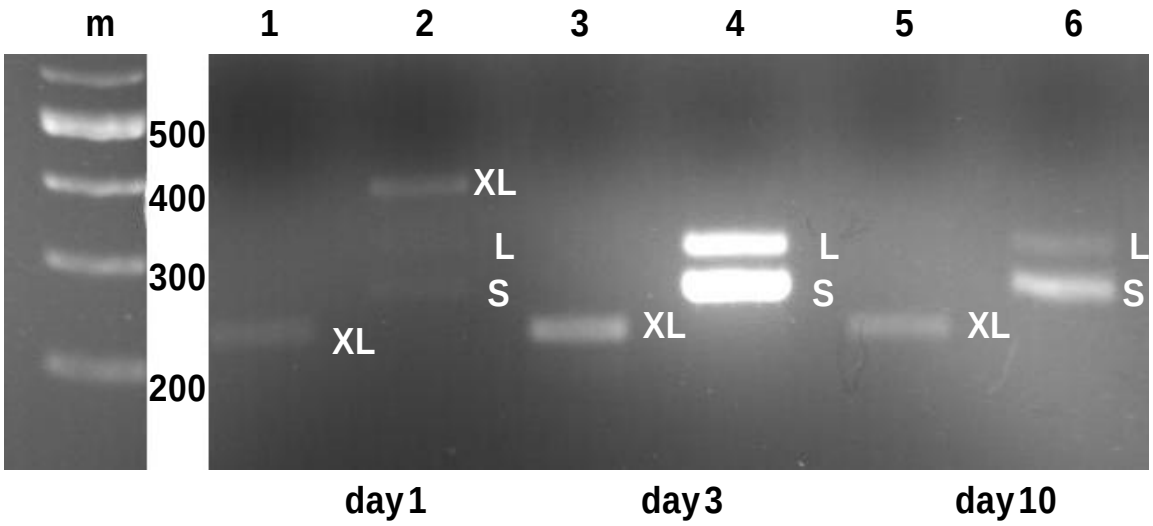

Supplemental figure 1. *lin-3* isoforms is expressed late into adult life. RT-PCR identification of *lin-3* isoform (Sup figure 2A) expression at different stages of life. RNA and cDNA were both collected from a *spe-9* mutant, reared at 25ºC to eliminate progeny production. Lanes 1 & 2 are day 1 (L1/L2); lanes 3 & 4 are day 3 (young adult); lanes 5 & 6 are day 11 (late-age). Primers flanking the alternative splicing region can yield three products shown in lanes 2, 4, 6. Primers within the alternative splicing region yield one product shown in lanes 1, 3, 5 that uniquely identifies lin-3XL, which is sometimes diminished in the three product reaction; lin-3XL and lin-3XXL should be visualized in this reaction. Three splice variants detected here are named *lin-3S, lin-3L, lin-3XL* by their sizes (as in Dutt et al., 2004). The undetected isoform *lin-3XXL* (Sup figure 2A)

has been difficult to find in other studies (as in Dutt et al., 2004). I sequenced 65 clones of amplified material and did find one copy of this seemingly rare transcript. Note that this experiment attempts detection, but data are not quantitative. Thus, relative amounts of amplified products are not necessarily present at their normal relative abundances.

Sup Figure 2

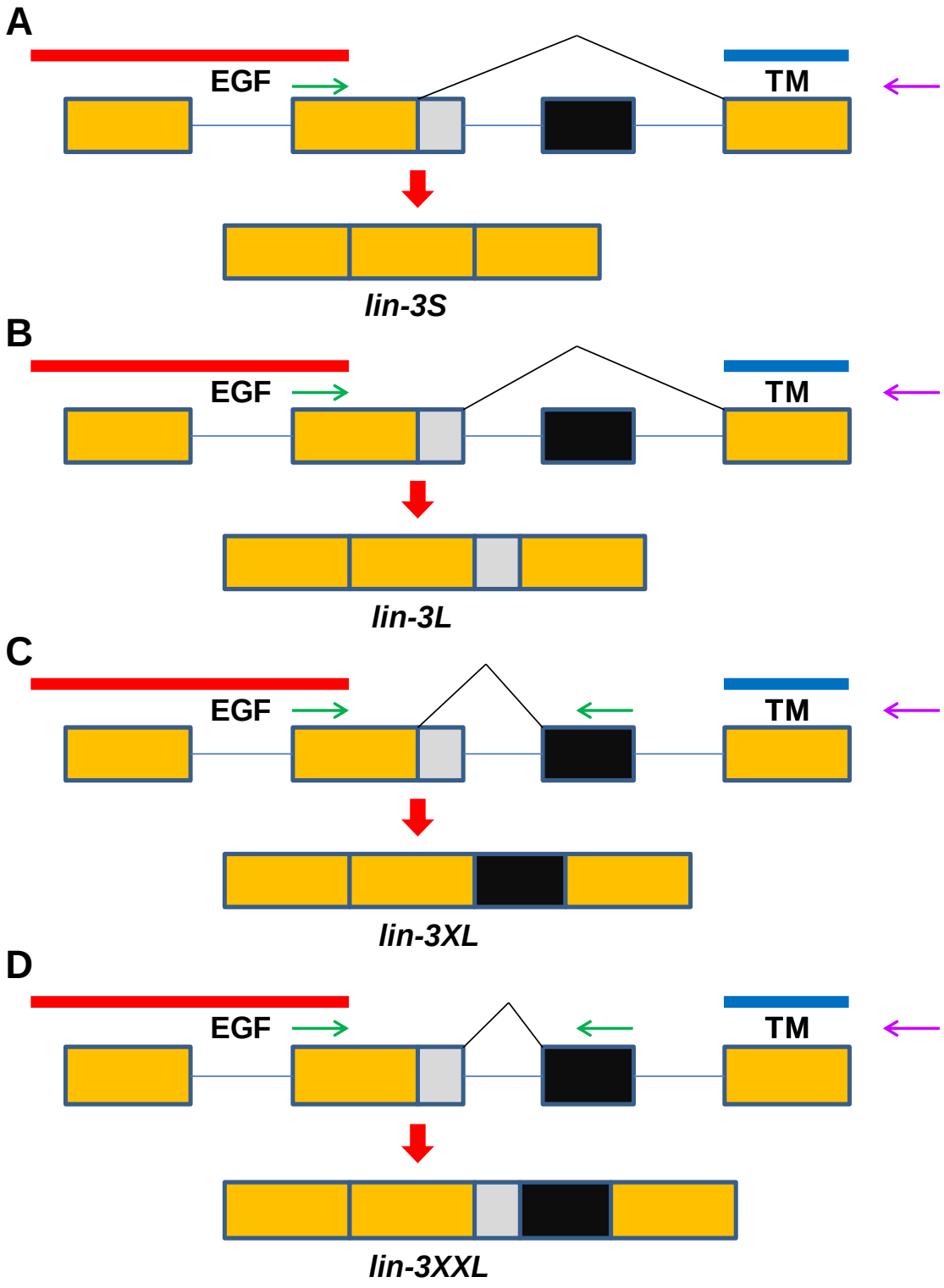

Sup Figure 2

E

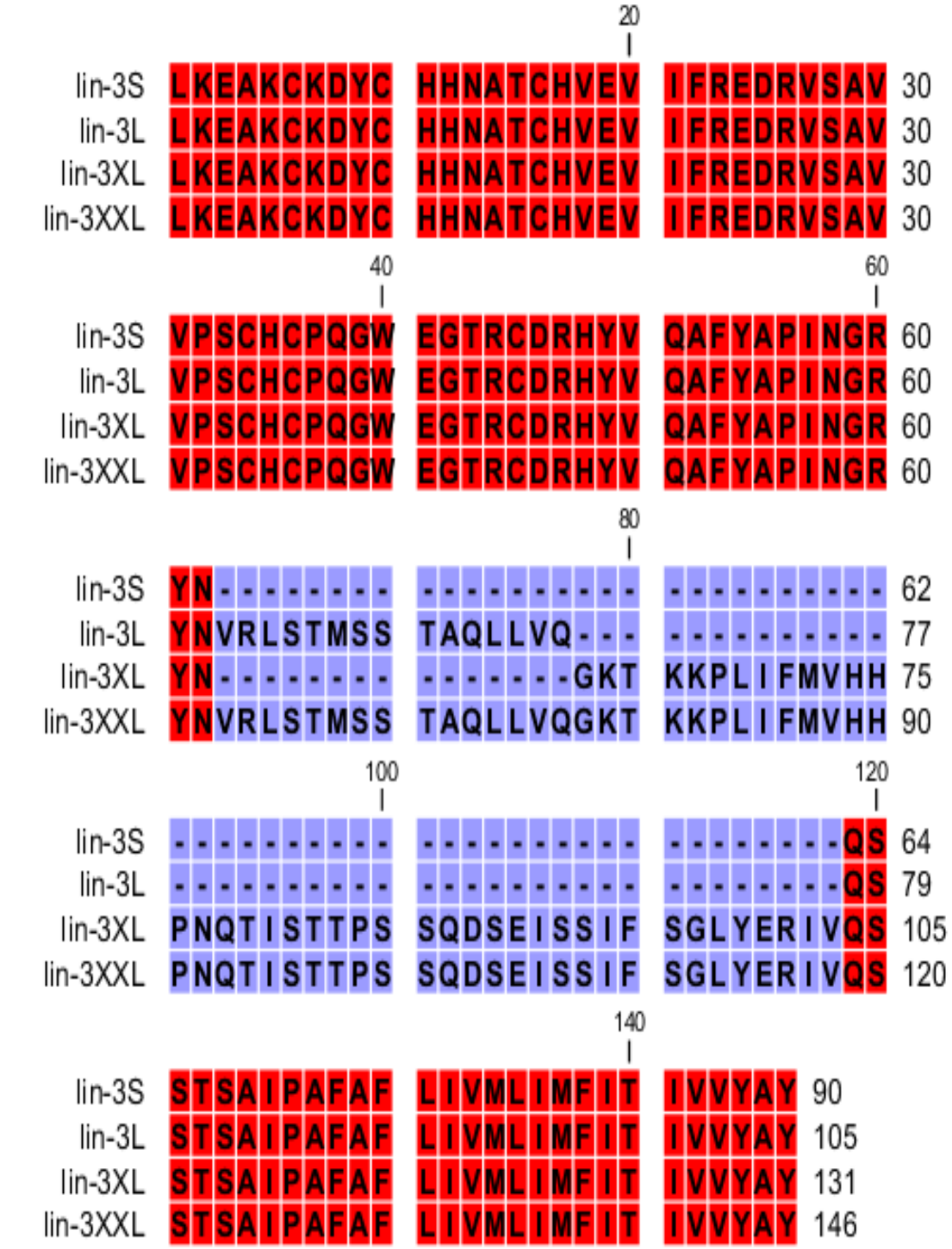

Sup Figure 2

F

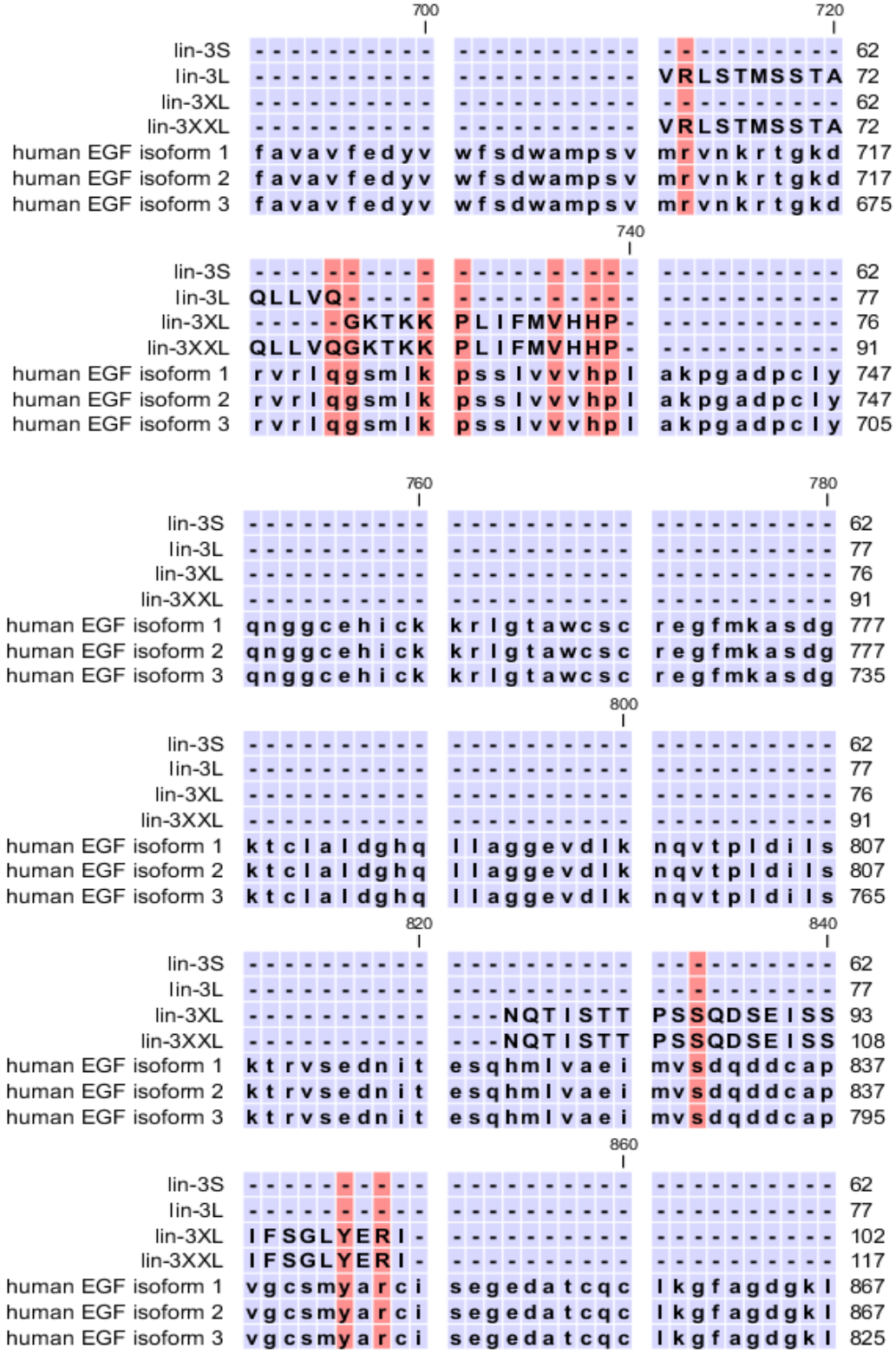

Sup Figure 2

G

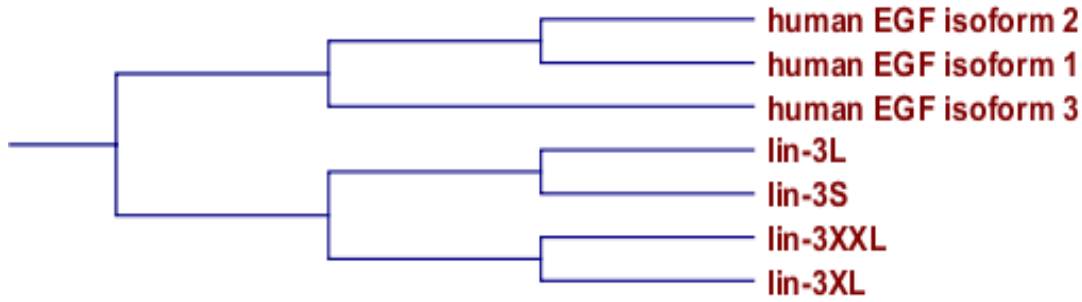

Supplemental figure 2. *lin-3* isoforms from alternative splicing.

(A-D) Four *lin-3* splice variants, termed *lin-3S*, *lin-3L*, *lin-3XL*, and *lin-3XXL* by transcript size, that are distinct in the two alternate exon region (grey and black boxes in the figure) between EGF repeat and transmembrane domain. Note that we overexpress *lin-3S*, *lin-3L*, *lin-3XL* in the swimming prowess tests. However, we do not have a *lin-3XXL* overexpression line available for testing. Arrows represent primers used for amplification.

A. Splice arrangement that generates *lin-3S*

B. Splice arrangement that generates *lin-3L*

C. Splice arrangement that generates *lin-3XL*

D. Splice arrangement that generates *lin-3XXL*

E. Sequence alignment of *lin-3* transcripts. Identical coding region are labeled with red background, while alternative splicing region is labeled with blue background. Shown here is the EGF domain, alternative splicing region, and transmembrane domain.

F. Sequence alignment of *lin-3* transcripts and human EGF. Alternative splicing region are shown in the alignment for *C. elegans* LIN-3/EGF and human EGF. Note that *lin-3XL* (and *lin-3 XXL*) contains more sequence match with human EGF isoforms within the alternative region. Shown here focus on the alternative splicing region.

G. Alignment tree of LIN-3 isoforms and human EGF.

Sup Figure 3

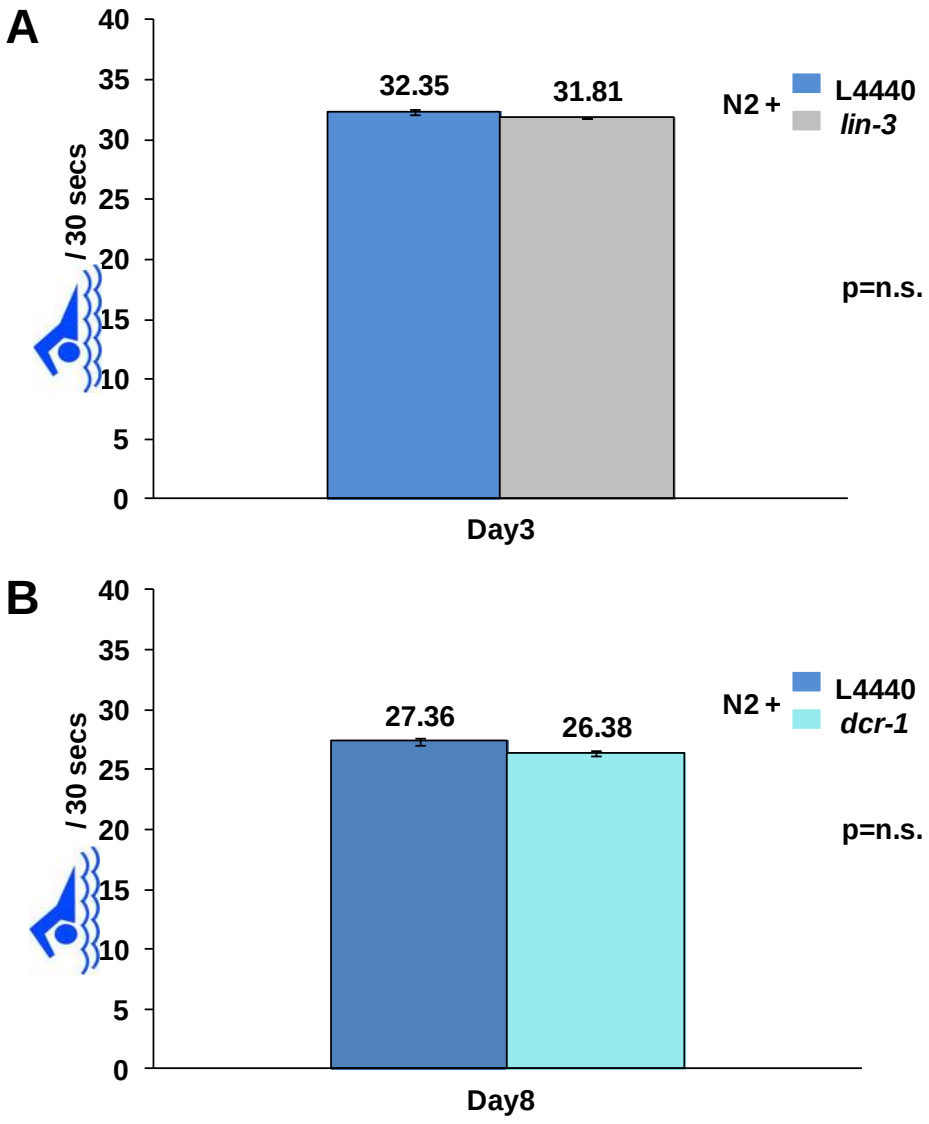
A
40
35
30
25
20
15
10
5
0
/ 30 secs
32.35
31.81
N2 + L4440
lin-3
p=n.s.
Day3
B
40
35
30
25
20
15
10
5
0
/ 30 secs
27.36
26.38
N2 + L4440
dcr-1
p=n.s.
Day8

Supplemental figure 3A. *lin-3* RNAi does not impair swimming of young adults, supporting that *lin-3* is not needed for development of normal swimming behavior. Measured is young adult (day 3) liquid mobility in number of body bends per 30 seconds. Each trial count was for 30 animals collected from a population of synchronized animals (two trials). Error bars represent the standard error of the mean (SEM); p-value by unpaired two tailed t-test. We found no significant difference between L4440 empty vector control and *lin-3(RNAi).*

Supplement figure 3B. Knockdown of dicer by RNAi does not alter normal age-associated locomotory decline. Comparison of L4440 empty vector control and *dcr-1* RNAi effect on day 8 animal liquid mobility, in number of body bends per 30 seconds. Each trial count was for 30 animals collected from a population of synchronized animals (three trials). Error bars represent the standard error of the mean (SEM). p-value by unpaired two tailed t-test. We noted no significant difference in locomotory decline when dicer was knocked down.

Sup Figure 4

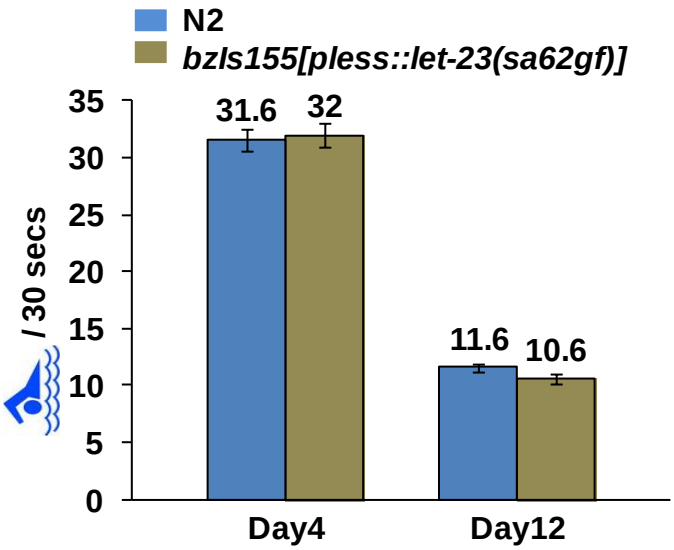

Supplemental Figure 4. Transgenic mutant carrying an integrated array of a promoter-less *let-23(gf*) does not cause any locomotory enhancement or defect.

C. elegans transgenic lines carrying an integrated transgene array without the promoter region of *let-23(gf)* in the wild type N2 background were compared to non-transgenic wild type N2 for swim body bend rates. Data are given for day 4, 20ºC (young adult to test whether expression of *let-23(gf)* changes baseline swim behavior) and day 12, animals reared at 20ºC until young adult and shifted to 25ºC for adult life (late age). Each trial scored 20-25 animals collected from a population of 150-200 synchronized animals. Shown are the averaged scores from repeat trials. Error bars represent the standard error of the mean (SEM). p-

value by unpaired two tailed t-test. Blue bar, wild type animals; body bends 31.6 +/- 1.0 / 30 seconds at day 4 and body bends 11.6 +/- 0.4 / 30 seconds at day12. Tan bar, *bzIs155[pless::let-23(sa62gf)]*; no *let-23(gf)* is expressed, body bends 32.0 +/- 1.0 / 30 seconds at day 4 and body bends 10.6 +/- 0.4 / 30 seconds at day12. No significant difference at day 4 and day 12.

Sup Figure 5

A

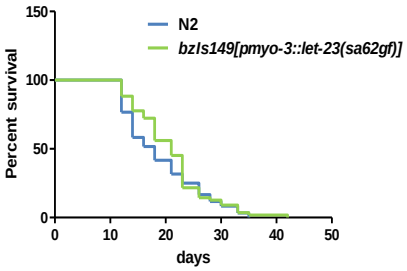

Trial 1	N2	bzIs149[pmyo-3::let-23(sa62gf)]
Median day	18	21
Mean	19.3+/-	20.9+/-
Max	33.2+/-0.7	34.3+/-1.7
P value (willcoxon)	0.08 , n.s.	

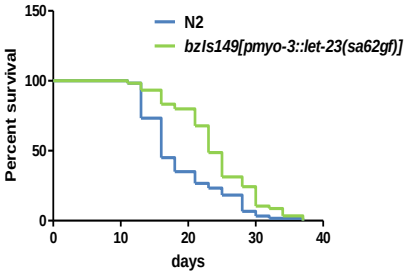

Trial 2	N2	bzIs149[pmyo-3::let-23(sa62gf)]
Median day	16	23
Mean	19.0+/-	24+/-
Max	30.8+/-1.4	34.7+/-0.8
P value (willcoxon)	<0.0001 ,yes	

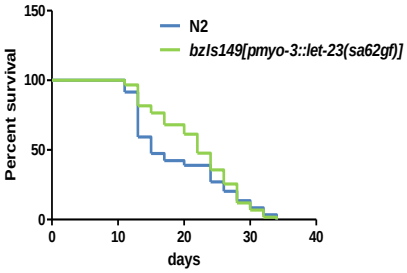

Trial 3	N2	bzIs149[pmyo-3::let-23(sa62gf)]
Median day	15	22
Mean	19.6+/-	21.9+/-
Max	33.7+/-1.0	31.6+/-0.6
P value (willcoxon)	0.02 , yes	

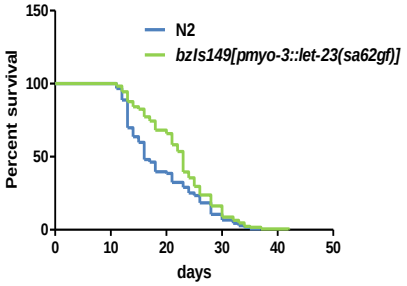

Cumulative trial	N2	bzIs149[pmyo-3::let-23(sa62gf)]
Median day	16	23
Mean	19.2+/-0.5	22.3+/-0.5
Max	32.6+/-0.6	33.6+/-0.7
P value (willcoxon)	<0.0001 , yes	

Sup Figure 5

B

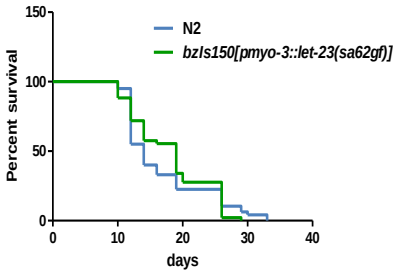

Trial 1	N2	bzIs150[pmyo-3::let-23(sa62gf)]
Median day	14	19
Mean	16.5+/-	17.8+/-
Max	30+/-1.1	26.5+/-0.5
P value (willcoxon)	0.27 ， n.s.	

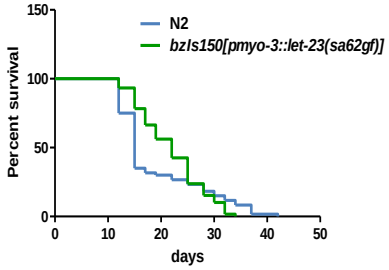

Trial 2	N2	bzIs150[pmyo-3::let-23(sa62gf)]
Median day	15	22
Mean	19.2+/-	21.9+/-
Max	37.3+/-1.1	32.3+/-0.3
P value (willcoxon)	0.0014 ， yes	

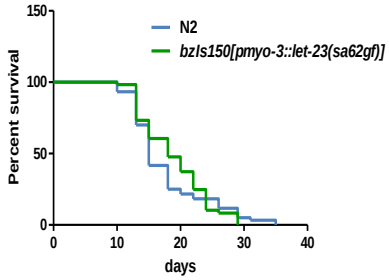

Trial 3	N2	bzIs150[pmyo-3::let-23(sa62gf)]
Median day	15	18
Mean	17.7+/-	18.5+/-
Max	31.3+/-1.2	27.6+/-0.9
P value (willcoxon)	0.12 ， n.s.	

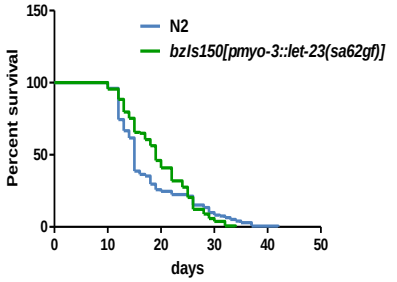

Cumulative trial	N2	bzIs150[pmyo-3::let-23(sa62gf)]
Median day	15	19
Mean	17.9+/-0.5	19.5+/-0.5
Max	32.9+/-1.0	28.9+/-0.7
P value (willcoxon)	0.0003 ， yes	

Sup Figure 5

C

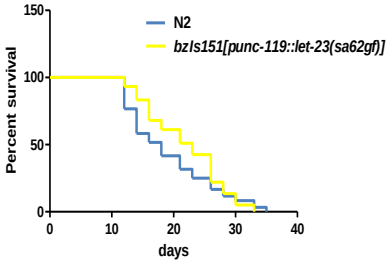

Trial 1	N2	bzIs151[punc-119::let-23(sa62gf)]
Median day	18	23
Mean	19.3+/-	21.9+/-
Max	33.2+/-0.7	31.5+/-0.7
P value (willcoxon)	0.012 , yes	

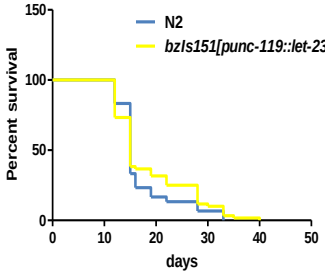

Trial 2	N2	bzIs151[punc-119::let-23(sa62gf)]
Median day	16	21
Mean	19.0+/-	20.7+/-
Max	30.8+/-1.4	31.2+/-1.8
P value (willcoxon)	0.06 , n.s.	

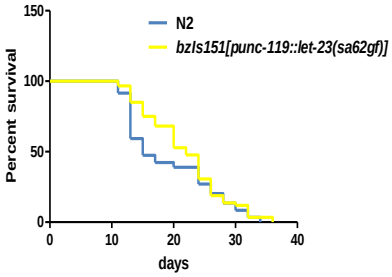

Trial 3	N2	bzIs151[punc-119::let-23(sa62gf)]
Median day	15	22
Mean	19.6+/-	21.8+/-
Max	33.7+/-1.0	33.3+/-0.8
P value (willcoxon)	0.045 , yes	

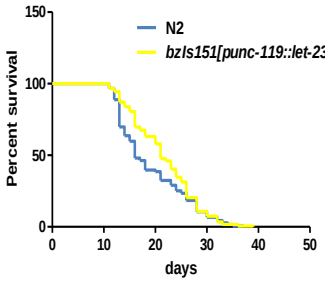

Cumulative trial	N2	bzIs151[punc-119::let-23(sa62gf)]
Median day	16	21
Mean	19.3+/-0.5	21.5+/-0.5
Max	32.6+/-0.6	32+/-0.7
P value (willcoxon)	0.0003 , yes	

Sup Figure 5

D

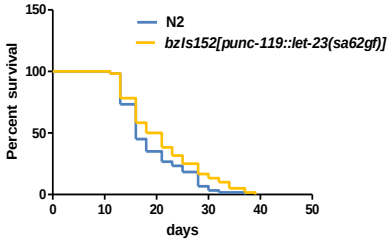

Trial 1	N2	bzIs152[punc-119::let-23(sa62gf)]
Median day	19	20
Mean	19.5+/-	21.2+/-
Max	30.8+/-0.7	34.3+/-1.2
P value (willcoxon)	0.16 ， n.s.	

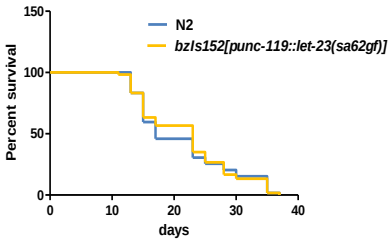

Trial 2	N2	bzIs152[punc-119::let-23(sa62gf)]
Median day	19	19
Mean	19.7+/-	20.3+/-
Max	28.0+/-0	31.3+/-1.6
P value (willcoxon)	0.59 ， n.s.	

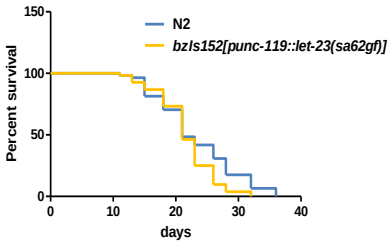

Trial 3	N2	bzIs152[punc-119::let-23(sa62gf)]
Median day	18	19
Mean	20.2+/-	21.2+/-
Max	34.3+/-1.3	33.8+/-1.3
P value (willcoxon)	0.19 ， n.s.	

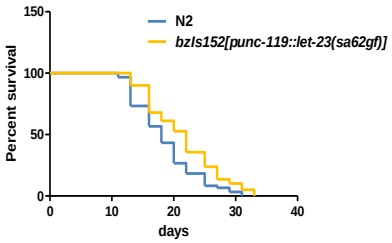

Trial 4	N2	bzIs152[punc-119::let-23(sa62gf)]
Median day	18	22
Mean	18.6+/-	21.4+/-
Max	28.7+/-1.0	32+/-0.4
P value (willcoxon)	0.005 ， yes	

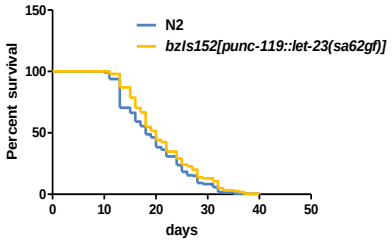

Cumulative Trial	N2	bzIs152[punc-119::let-23(sa62gf)]
Median day	18	20
Mean	19.5+/-0.4	21.1+/-0.4
Max	30.5+/-0.7	32.9+/-0.6
P value (willcoxon)	0.004 ， yes	

Sup Figure 5

E

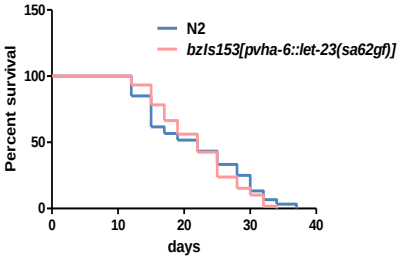

Trial 1	N2	bzIs153[pvha-6::let-23(sa62gf)]
Median day	14	19
Mean	16.5+/-	18.2+/-
Max	30.0+/-1.1	27.2+/-1.2
P value (willcoxon)	0.02 , yes	

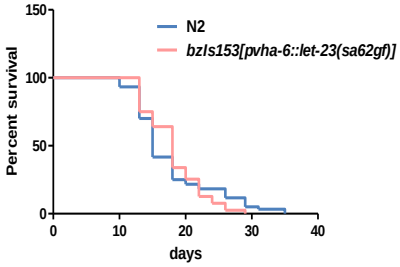

Trial 2	N2	bzIs153[pvha-6::let-23(sa62gf)]
Median day	15	18
Mean	17.7+/-	17.6+/-
Max	31.3+/-1.2	25.2+/-1.0
P value (willcoxon)	0.16 , n.s.	

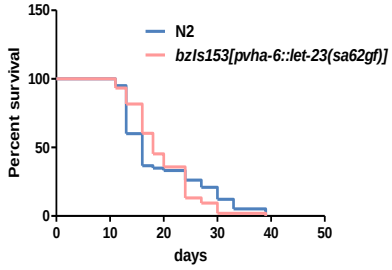

Trial 3	N2	bzIs153[pvha-6::let-23(sa62gf)]
Median day	16	18
Mean	19.4+/-	19.5+/-
Max	36+/-1.3	31+/-1.7
P value (willcoxon)	0.14 , n.s.	

Sup Figure 5

E

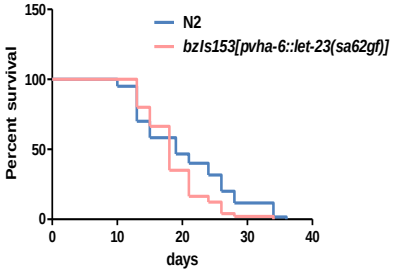

Trial 4	N2	bzIs153[pvha-6::let-23(sa62gf)]
Median day	19	18
Mean	20.5+/-	18.2+/-
Max	34.3+/-0.3	27.7+/-1.3
P value (willcoxon)	0.38 , n.s.	

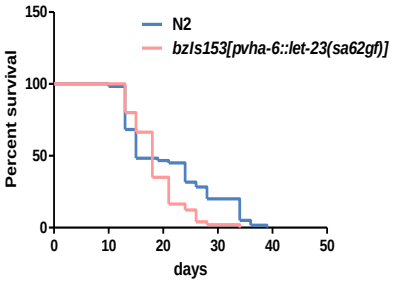

Trial 5	N2	bzIs153[pvha-6::let-23(sa62gf)]
Median day	15	16
Mean	17.1+/-	17.8+/-
Max	31.3+/-1.1	27.7+/-1.2
P value (willcoxon)	0.11 , n.s.	

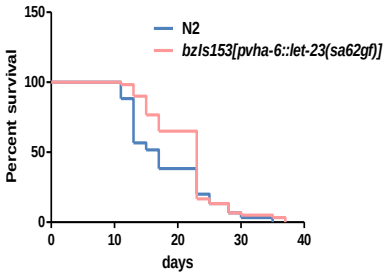

Trial 6	N2	bzIs153[pvha-6::let-23(sa62gf)]
Median day	17	23
Mean	18.3+/-	21.4+/-
Max	31+/-1.3	32.5+/-1.8
P value (willcoxon)	0.004 , yes	

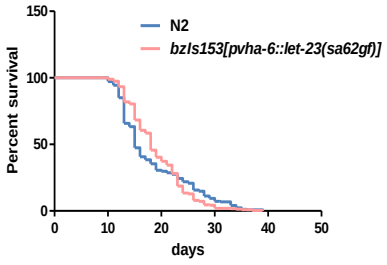

Cumulative trial	N2	bzIs153[pvha-6::let-23(sa62gf)]
Median day	15	18
Mean	18.3+/-0.4	18+/-0.3
Max	32.3+/-0.6	28.5+/-0.7
P value (willcoxon)	0.0001 , yes	

Sup Figure 5

F

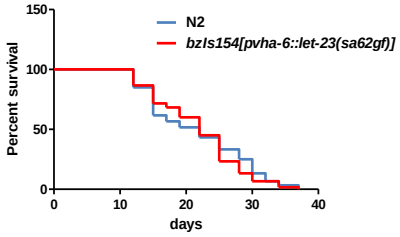

Trial 1	N2	bzIs154[pvha-6::let-23(sa62gf)]
Median day	22	22
Mean	21.8+/-	21.8+/-
Max	34.3+/-0.9	33.2+/-1.1
P value (willcoxon)	0.95 , n.s.	

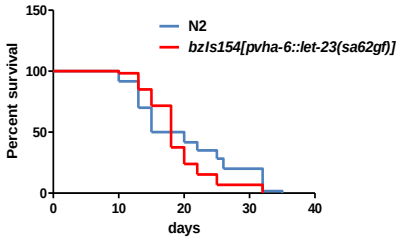

Trial 2	N2	bzIs154[pvha-6::let-23(sa62gf)]
Median day	18	20
Mean	19.9+/-	19.8+/-
Max	33+/-0.9	29.3+/-0.3
P value (willcoxon)	0.41 , n.s.	

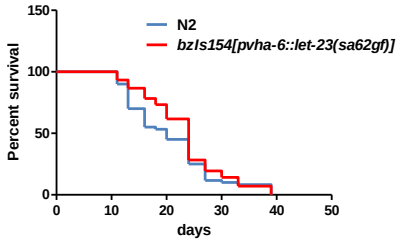

Trial 3	N2	bzIs154[pvha-6::let-23(sa62gf)]
Median day	20	24
Mean	20.8+/-	23.1+/-
Max	38+/-1.0	37+/-1.3
P value (willcoxon)	0.058 , n.s.	

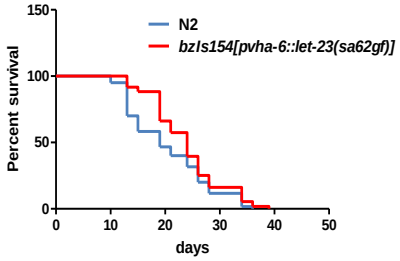

Trial 4	N2	bzIs154[pvha-6::let-23(sa62gf)]
Median day	19	24
Mean	20.5+/-	23.7+/-
Max	34.3+/-0.3	35.5+/-0.8
P value (willcoxon)	0.0099 , yes	

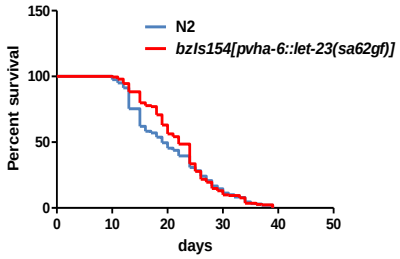

Cumulative Trial	N2	bzIs154[pvha-6::let-23(sa62gf)]
Median day	19	22
Mean	20.1+/-0.5	22.1+/-0.4
Max	34.9+/-0.5	33.8+/-0.7
P value (willcoxon)	0.006 , yes	

Sup Figure 5

G

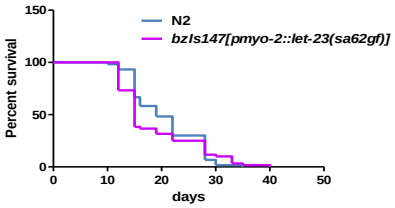

Trial 1	N2	bzIs147[pmyo-2::let-23(sa62gf)]
Median day	19	15
Mean	20.7+/-	18.8+/-
Max	30.2+/-1.0	34.5+/-1.1
P value (willcoxon)	0.015 , yes	

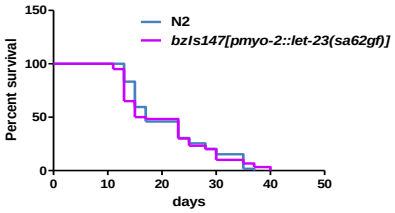

Trial 2	N2	bzIs147[pmyo-2::let-23(sa62gf)]
Median day	17	16
Mean	21.0+/-	20.5+/-
Max	35.3+/-0.3	37.3+/-0.9
P value (willcoxon)	0.25 , n.s.	

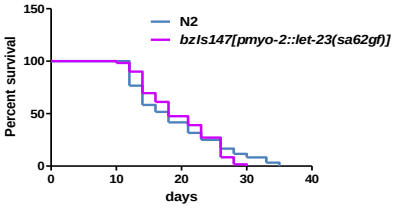

Trial 3	N2	bzIs147[pmyo-2::let-23(sa62gf)]
Median day	18	18
Mean	19.3+/-	19.5+/-
Max	33.2+/-0.7	28.0+/-0.5
P value (willcoxon)	0.36 , n.s.	

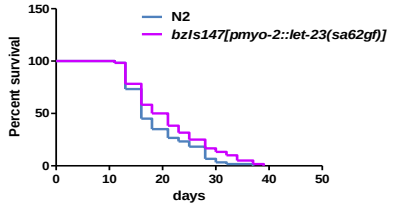

Trial 4	N2	bzIs147[pmyo-2::let-23(sa62gf)]
Median day	16	19.5
Mean	19.0+/-	21.1+/-
Max	30.8+/-1.4	35.8+/-0.9
P value (willcoxon)	0.82 , n.s.	

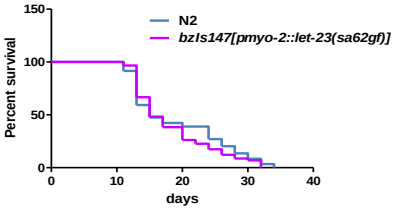

Trial 5	N2	bzIs147[pmyo-2::let-23(gsa62f)]
Median day	15	15
Mean	19.5+/-	18.1+/-
Max	33.6+/-1.0	31+/-0.7
P value (willcoxon)	0.92 , n.s.	

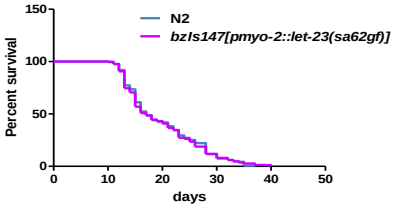

Cumulative trial	N2	bzIs147[pmyo-2::let-23(sa62gf)]
Median day	17	17
Mean	19.9+/-0.4	19.6+/-0.4
Max	32.6+/- 0.5	33.3+/-0.7
P value (willcoxon)	0.46 , n.s.	

Sup Figure 5

H

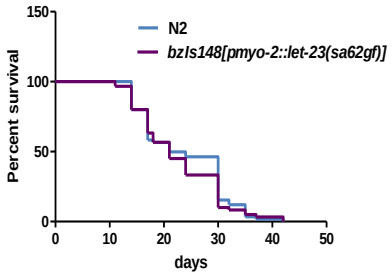

Trial 1	N2	bzIs148[pmyo-2::let-23(sa62gf)]
Median day	21	21
Mean	23.7+/-	22.7+/-
Max	36.5+/-1.1	37.2+/-1.7
P value (willcoxon)	0.54 , n.s.	

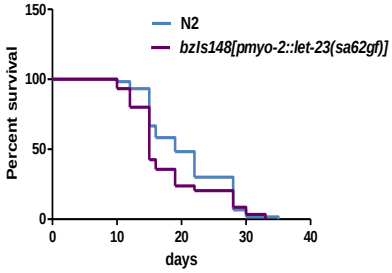

Trial 2	N2	bzIs148[pmyo-2::let-23(sa62gf)]
Median day	19	15
Mean	20.7+/-	18.0+/-
Max	30.2+/-1.0	30.7+/-0.8
P value (willcoxon)	0.007 , yes	

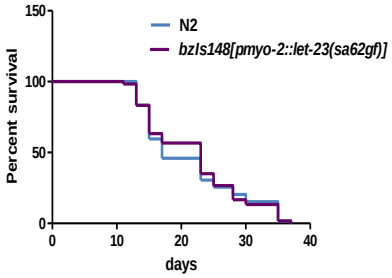

Trial 3	N2	bzIs148[pmyo-2::let-23(sa62gf)]
Median day	17	23
Mean	21.2+/-	21.8+/-
Max	35.3+/-0.3	35.3+/-0.3
P value (willcoxon)	0.6 , n.s.	

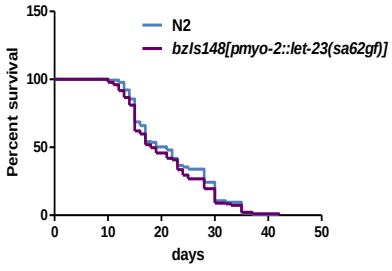

Cumulative trial	N2	bzIs148[pmyo-2::let-23(sa62gf)]
Median day	21	18
Mean	21.8+/-0.6	20.8+/-0.6
Max	34.0+/-0.8	34.4+/-0.9
P value (willcoxon)	0.82 , n.s.	

Supplemental figure 5. Tissue-specific expression of EGFR/*let-23(gf)* mutant activation in multiple lifespan performance.

(A-H) *C. elegans* transgenic lines overexpressing *let-23(gf)* in a wild type background, driven under the control of various tissue-specific promoters, are compared to N2 wild type (20^{o}C) to test whether activation of LET-23/EGFR in individual tissues can extend adult lifespan. Individual survival curves shown here are from different individual trials, and cumulative survival curves shown here are from multiple repeat trials. Survival curve data were collected from a population of 60 synchronized animals / trial. Significance of differences between survival curves was calculated using the Gehan-Breslow-Wilcoxon test for all pair comparison. Details of data on mean, median and maximum lifespan are summarized in the table next to the survival curve, respectively.

A. *let-23(gf)* expressed in muscle extends median lifespan. Blue line, lifespan of N2 wild type; light green line, lifespan of *bzIs149[pmyo-3::let-23(sa62gf)]*. 2/3 of individual curves shows significant difference, and cumulative curve is from 3 repeats with $p<0.0001$.

B. *let-23(gf)* expressed in muscle extends median lifespan. Blue line, lifespan of N2 wild type; dark green line, lifespan of *bzIs150[pmyo-3::let-23(sa62gf)]*. 1/3 of individual curves shows significant difference, and cumulative curve is from 3 repeats with $p<0.001$.

C. *let-23(gf)* expressed pan-neuronally confers median lifespan extension. Blue line, lifespan of N2 wild type; yellow line, lifespan of *bzIs151[punc-119::let-23(sa62gf)]*. 2/3 of individual curves shows significant difference, and cumulative curve is from 3 repeats with $p<0.001$.

D. *let-23(gf)* expressed pan-neuronally confers median lifespan extension. Blue line, lifespan of N2 wild type; orange line, lifespan of *bzIs152[punc-119::let-23(sa62gf)]*. 1/4 of individual curves shows a significant difference, however, cumulative curve is from 4 repeats with $p<0.01$.

E. *let-23(gf)* expressed in the intestine confers median lifespan extension somewhat. Blue line, lifespan of N2 wild type; pink line, lifespan of *bzIs153[pvha-6::let-23(sa62gf)]*. 2/6 of individual curves shows significant difference, but cumulative curve is from 6 repeats with $p<0.001$.

F. *let-23(gf)* expressed in the intestine confers median lifespan extension somewhat. Blue line, lifespan of N2 wild type; red line, lifespan of *bzIs154[pvha-6::let-23(sa62gf)]*. 1/4 of individual curves shows a significant difference, but cumulative curve is from 4 repeats with $p<0.01$.

G. *let-23(gf)* expressed in the pharynx does not confer lifespan extension. Blue line, lifespan of N2 wild type; purple line, lifespan of *bzIs147[pmyo-2::let-*

23(sa62gf)]. No better survival was detected in the transgenic line (one time N2 survives better). The cumulative curve is from 5 repeats.

H. *let-23(gf)* expressed in the pharynx does not confer lifespan extension. Blue line, lifespan of N2 wild type; dark purple line, lifespan of *bzIs148[pmyo-2::let-23(sa62gf)]*. No better survival was detected in the transgenic line (one time N2 survives better). The cumulative curve is from 3 repeats.

Sup Figure 6

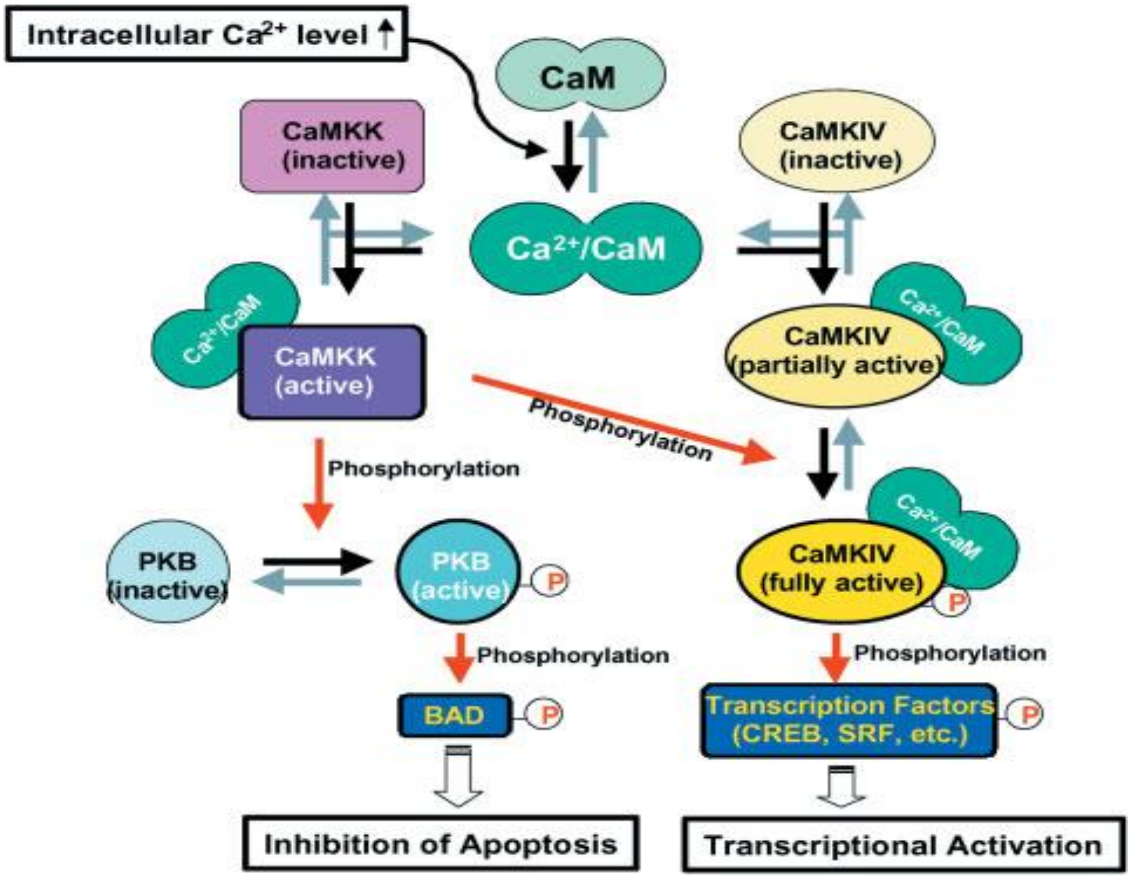

Supplemental figure 6. Schematic diagram of CaM-CamK cascade (Ikura et al., 2002).

When intracellular calcium concentration increases, calcium signaling is initiated by formation of calcium-calmodulin complex and further phosphorylation of kinases, resulting in activation of transcription.

CHAPTER IV:

Summary and perspectives

Summary and perspectives

Aging is influenced by genetic, environmental, and stochastic processes that exert interconnected effects on lifespan. Analyses in invertebrate models have significantly advanced understanding of genetic and environmental influences that modulate lifespan, including insulin/IGF signaling, dietary restriction, mitochondrial function, sensory activity, and metabolism (Kenyon, 2010; Antebi, 2007). A striking theme that has emerged is that many of the pathways that influence longevity exert effects conserved from invertebrates to mammals.

A key challenge in current aging research is to increase life expectancy coupled with significantly enhanced functionality later in life. Improved healthspan—the period of functional maintenance preceding debilitating decline--is increasingly being considered as an endpoint for aging studies. Indeed, many pathways that confer longevity, such as reduced insulin signaling, are associated with robustness of function later in life, although this is not always the rule.

My thesis work began with an emphasis on aging of mobility systems, but came to focus on how EGF signaling influences *C. elegans* quality of aging. EGF signaling was previously unknown as a factor in healthy aging—my work and recent studies in the field suggest EGF signaling may be a centrally important maintenance system. My work raises the question as to whether the EGF pathway might contribute to long-term maintenance in other organisms, a future topic to pursue in the field.

HPA genes, encoding likely secreted molecules that resemble insulin/IGF receptor binding domains, regulate aging through EGF signaling

Our investigations of potential roles for candidate insulin-binding proteins, HPA-1 and HPA-2, in promoting *C. elegans* healthspan led to the discovery of an unexpected, but major, role of EGF signaling for functional maintenance in aging nematodes. We studied *hpa-1* and *hpa-2,* for which both RNAi knockdown or genetic deletions improve old-age swimming. Insight into the mechanism of action came with the revisiting of the homologies of HPA-1 and HPA-2 to known signaling receptors. Close inspection suggested a greater sequence similarity of HPA-1 and HPA-2 to the EGF receptor EGF-binding domain than to the insulin receptor binding domain. Moreover, HPA-1 is most similar to mammalian EGF receptor-related protein (ERRP, homologous to mammalian EGFR), which is a secreted negative regulator of mammalian EGF family signaling (Yu et al., 2001). Sequence relationships thus suggested that, rather than insulin signaling, EGF signaling might be involved in *C. elegans* locomotory healthspan extension.

Interestingly, *hpa-1* and *hpa-2* do not impact healthy aging identically. *hpa-1* is involved in global organism benefits, while *hpa-2* is a tissue-specific modulator of swimming (body wall muscle) but not other healthspan indicators. *hpa-2* represents one of the first documented examples of a gene with tissue-specific effects on aging quality. It should be noted that the overall EGF signaling system

is likely to be very complex-with multiple *hpa-1*-like proteins (54) encoded in the *C. elegans* genome. Other members of this family might also regulate EGF signaling and modulate aging quality—in fact, a deletion of one studied by Dr. H. Iwasa suggests that deletion of at least one of these (T11F1.9) has a major healthspan benefits. Thus, investigating other family members may provide additional insight into molecular mechanisms that control EGF signaling. In addition, a major question that remains to be address with HPA proteins is whether they bind EGF ligand, and if so, how this occurs.

EGFR activation in different tissues can promote global or tissue-specific healthy aging

Basically EGFR signaling in multiple tissue types appears to improve and maintain locomotory healthspan. However, EGFR activation in muscle and neuron but not pharynx or the intestine are main the tissues that modulate lifespan and age pigment accumulation. The healthspan information suggests EGFR signaling may function broadly and differently when expressed in distinct tissues. Interestingly, some modulators in the EGF signaling influence locomotory healthspan without great effect on lifespan, exhibiting a similar pattern of tissue or phenotype specifcity like *hpa-2*. In other words, effects of some EGF signaling components fairly are specific to the aging of the locomotory system and do not confer systemic benefits.

Different EGF isoforms can promote healthy aging

EGF family isoforms (EGF isoforms and neuregulin isoforms) are found in mammals. Each ligand binds to different receptors and functions in different tissues. We found that EGF/*lin-3* isoforms have different capacities to enhance healthy aging. Over-expression of lin-3XL and lin-3S enhance locomotion at mid/late age. However, the mechanisms of action, including defining aspects of ligand that promote apparently different signaling from LIN-3L remain to be defined.

Continuous EGF signaling appears important for healthy aging, but even brief periods of pathway activation can confer healthspan benefits

The temporal requirement for *lin-3* (all isoforms) is at both larval and adult stages. Expression of EGF ligand only in development or only in the adult is better than no EGF expression, suggesting a need for continuous signaling. My data suggest the EGF signaling plays a dual role during development, not only for physiological growth and fate specification but also setting up an anti-aging maintenance system that can confer anti-aging protection throughout life.

A mitochondrial connection? The only known *C. elegans* gene system that acts in larvae to impact lifespan in adults affects mitochondrial respiration. Knockdown of several mitochondrial genes has been found to extend lifespan (Kenyon, 2010; Sedensky and Morgan, 2006). Two things suggest a connection for EGF signaling via ER calcium release and mitochondria. 1) Respiration

inhibition during development is the key timing for knockdown of these mitochondrial genes to increase lifespan (Dillin et al., 2002). We found that eliciting EGF/*lin-3* signaling only during larva stages can promote healthspan and longevity-- a similar aging protection pattern as mitochondrial respiration manipulation. 2) Mitochondria are recognized as playing a critical role in calcium signaling (Figure 1). When calcium is released from ER stores by IP3, a rapid increase in mitochondrial calcium occurs (Brini and Carafoli, 2000). Since our pathway work implicated calcium in downstream signaling (see below), mitochondrial activities could be targets of EGF signaling. Our findings thus raise questions: 1) whether mitochondria are the ultimate targets by which EGF induces healthy aging, and/or 2) whether the respiration inhibition mutants/RNAi interventions that cause longevity might activate EGF signaling. Cause and consequence, as well as relationship of the mitochondrial longevity pathway to the EGF pathway, can be pursued by knockdown of EGF signaling with RNAi in mitochondrial respiration mutants or vice versa.

I should note that our work has also indicated that EGF signaling promotes healthspan through a pathway distinct from insulin signaling and dietary restriction.

Activation of the EGFR signaling pathway extends *C. elegans* healthspan

Given the extensive effort devoted to the identification of longevity genes in the *C. elegans* field, it was surprising that no work had previously examined the role of EGF signaling in lifespan extension. However, elegant work by Sternberg and colleagues had characterized the *C. elegans* EGF pathway in other functions in detail. Thus, a wealth of genetic reagents was available for testing healthspan and lifespan phenotypes. An EGFR/*let-23(gf)* gain-of-function mutant retained late-life swimming vigor and muscle integrity, maintained pharyngeal pumping capacity late into life, exhibited low rates of age pigment accumulation, and survived more robustly in midlife and late life, revealing a role for EGFR activation in organism-wide healthy aging. Conversely, a reduction-of-function mutation in EGFR/*let-23* confers accelerated swimming decline and diminished survival at mid life; as does mutation of EGF/*lin-3(rf)*. *lin-3(rf)* and *let-23(rf)* both block healthspan benefits of *hpa-1* and *hpa-2*, linking all into one pathway. Thus, activation of EGF signaling positively influences healthspan as well as lifespan in *C. elegans*.

EGFR can be activated in muscle, neurons and intestine to confer healthspan benefits. We expressed EGFR(gf) in multiple tissue types and somewhat unexpectedly found that expression in body wall muscle, neurons or intestine could induce benefits for at least some indicators of healthy aging. The only tissue tested that appears refractory is pharyngeal muscle, which is

somewhat surprising because adult EGF seems expressed in the pharynx or pharyngeal neurons. I do note that I have not tested hypodermal expression yet, which is probably of interest because EGFR has been found to be normally expressed there. Liu et al (2011) reported that *let-23*is expressed in the hypodermis & intestinal cell membrane in the young adult. I personally observed obvious GFP signal in the ALA neurons and weak signal in hypodermal in mid-age animals (~day 8, 25°C).

Ectopic expression from heterologous promoters always must be analyzed with concerns for several things. First, transgenes might express at low levels in non-target tissues, and thus expression might be more broad than anticipated. Second, the timing of expression and expression levels induced are likely to be non-physiological. One could also anticipate that activation of a pathway in the incorrect tissue types could induce dysfunction of those tissues. Still, the fact that EGFR activation in nerve and muscle can induce positive effects on aging that appear non-autonomous (that is, longevity and age pigment phenotypes are not necessarily directly caused by muscle pathway activation, but require consequences in other tissues) strongly suggests that EGFR signaling promotes expression of other factors from multiple tissues that circulate to influence or coordinate aging throughout the body.

A specific downstream signaling pathway involving phopholipase C gamma and the ER IP3 receptor calcium-release channel mediates EGF healthspan benefits

There are three distinct downstream signal transduction pathways for *C. elegans* EGF signaling that act through LIN-3/EGF and LET-23/EGFR. Testing of representative genes in each downstream signaling branch established that it is the PLC-γ/*plc-3* and IP3 receptor/*itr-1* signaling that mediates healthy aging (Iwasa et al., 2010). Supporting data include that an IP3R gain-of-function shows a markedly enhanced general healthspan and significantly extended lifespan. Conversely, IP3R reduction-of-function confers a short life and accelerated swimming decline and RNAi knockdown can block the beneficial effects of EGFR activation. Because the IP3R modulates intracellular calcium by regulating ER calcium release, data implicate appropriate/maintained calcium homeostasis in healthy aging.

Reduction of function of other known factors that modulate EGFR (*ark-1,* as a negative regulator) and control IP3 level such as phosphatase (*ipp-5*) and ER calcium release confer a more active EGFR/ITR-1 signaling showing better locomotory mobility in late-age, consistent with the involvement of the core pathway in healthy aging.

There are numerous mechanisms that maintain calcium homeostasis and factors that could execute ER release calcium signaling might be involved in the EGF

healthspan pathway. My data implicate part of the calmodulin(CaM)-CaMK cascade in response, supporting that calcium increase is likely to be involved in healthspan regulation. Factors independent of the calmodulin cascade may also affect healthspan and be involved in the network of intracellular calcium balance. My work suggests that *cmk-1*, *crh-1*, *sta-1*, and possibly *klf-2* or *T05C1.4* can influence aging quality, and might be involved in the EGF-stimulated calcium changes that promote healthy aging. Future studies of the relationship of these genes to each other and to EGF pathway signaling should lead to much-needed understanding of the major downstream targets of EGFR/ITR-1 signaling.

A model for EGF signaling in maintaining aging *C. elegans*

Analysis of EGF signaling in *C. elegans* leads to a working model for this pathway in modulation of healthy aging (Figure 2). In the wild type aging adult, candidate EGF-binding proteins HPA-1 and HPA-2 bind circulating EGF to limit maintenance signaling. Disruption of HPA proteins releases EGF for increased EGFR binding and activation of downstream PLCγ/IP3R signaling. Activation of IP3R should increase ER calcium release, which might act in part through calmodulin kinase *cmk-1* to influence cellular maintenance. Transcription factors *crh-1, sta-1, klf-2* and *T05C1.4* might mediate some of EGFR induced healthspan benefits. Note that many details of this proposed mechanism remain to be addressed.

Might enhanced EGF family signaling promote healthy aging and maintained function across species?

EGF and EGFR mouse mutants. To date, there is not much evidence for roles of EGF signaling in healthy aging in other experimental models, and the specific question of age-associated maintenance has not yet been directly addressed. Mouse genetics indicated some results regarding mutant phenotypes of EGF/EGFR. Receptor knockouts have revealed developmental lethality but some ligand knockouts are viable. Knockout mice for TGF-α ligand exhibit excessive hair loss and weight loss with aging (Luetteke et al., 1999). Triple knockout of ligands EGF, TGF-α, and amphiregulin exhibit a higher penetrance of hair and weight loss compared to the TGF-α single knockout mutant (Luetteke et al., 1999). Whether these phenotypes might suggest accelerated segmental aging awaits a more focused look at phenotypes and an experimental separation of adult phenotypes from developmental defects by adult-specific and possibly tissue-specific disruption. A focus on potential anti-aging benefits of EGF family members might provide some insights from these available mutants.

Enhanced EGFR signaling has been associated with epithelial tumors in mammals (Herbst, 2004), which raises significant questions regarding value of enhanced EGF signaling as an anti-aging therapy. In *C. elegans*, cell divisions are completed by the time the animal reaches adulthood, which means that all aging studies are focused on post-mitotic cells. Thus, distinguishing EGF impact

on non-dividing cell types such as neurons might be critical for evaluating potential for age-associated maintenance.

EGF signaling may improve neuronal robustness. A fairly new study in a SCA1 (Spinocerebellar ataxia type 1, a neurodegenerative disease) mouse model suggested a possible link between neuronal health and EGF signaling (Fryer et al., 2011). In brief, the mouse model for poly-glutamine expanded ataxin-1, which causes SCA1 disease, was forced to exercise. Exercise increased brain levels of EGF, which was associated with decreased neurodegeneration. The data suggested that EGF is either directly or indirectly involved in anti-neurodegeneration protection. Since many neurodegenerative diseases are associated with protein folding challenges and have late onset, EGF might be associated with improved proteostasis later in life. Interestingly, in *C. elegans* Liu et al, 2011 reported that EGF signaling is involved in maintaining protein homeostasis by activating the ubiquitin-proteosome system (UPS) for protein degradation. Thus,a neuro-protection impact of activated EGF signaling might be conserved across species. An important set of experiments for us to do in the near future is to address how morphological neuronal aging in *C. elegans* responds to changes in EGF signaling.

EGF signaling could exert the benefits of exercise. Exercise shows clear benefit for the aging cardiovascular system and diabetes. In addition, exercise may slow the progression of neurodegenerative disease, such as

Alzheimer disease and Parkinson disease (Gitler, 2011). Recently in the Driscoll lab, we have been studying the effect of exercise on *C. elegans* longevity and/or healthspan. Although a definite difference for exercise on “trained” animals vs. “non- trained” samples need to be analyzed in detail by different age-associated phenotypes, our preliminary data suggested that swim exercise is beneficial for *C.elegans* healthspan. However, the mechanism by which the beneficial exercise acts remains to be solved. Fryer et al (2011) indicated EGF concentration increased in the brain tissue (~ 50% increase) in a mouse model after exercise. Changes were tissue-specific such that the increased level of EGF was found in the brainstem but not the cerebellum. The exercise-trained animals also exhibit extended lifespan (although they are a disease model). The longevity phenotype suggests that EGF signaling in species other than *C. elegans* might contribute to improving health.

Multiple EGF family ligands exist in mammals and the correlation between the increased EGF concentration and activation of EGF signaling in the mouse model mentioned above awaits more studies. However, the discovery in mice raises the question of a possible connection between exercise and EGF signaling in *C. elegans*. To compare the exercise benefits in wild type and EGF mutants by training could address whether EGF signaling is required for exercise benefits.

Fryer et al (2011) also suggested EGF might down-regulate Capicua protein (Cic), a high-mobility-group (HMG) transcription factor. The mild exercise

regimen in mice causes the decrease in Cic level (Fryer et al, 2011). *Drosophila* data indicated that Capicua is downstream of EGF signaling (Astigarraga et al., 2007; Tseng et al., 2007). In *C. elegans,* the capicua homolog, *gei-3*, encodes a member of the high mobility group (HMG) protein family that acts as a transcription factor (Tsuboi et al., 2002). However, not much is known about *gei-3*. Is there a connection between activated EGF/*lin-3*-EGFR/*let-23* and *gei-3*? Or can *gei-3* act downstream in the EGF signaling pathway to promote healthy aging? Such possibilities are readily tested in the *C. elegans* model and might underscore a connection between EGF signaling, healthy aging, and exercise.

Recently more evidence suggests the potential for EGF signaling potency in anti-aging maintenance. Serum levels of EGF decrease in normal human aging (Shurin et al., 2007). It is possible that a specific mammalian EGF family member might prove to be potent for maintenance signaling rather than proliferation.

A fairly new result indicates that long-lived rodents (naked mole-rats) had higher levels of ligand NRG-1 (neregulin-1) and receptor ErbB4 (Edrey et al., 2011). In this report, levels for NRG-1 and ErbB4 were sustained throughout development and adulthood (Edrey et al., 2011). Whether all mammalian EGF family members might promote maintenance remains to be addressed. However, our data for *lin-3* timing requirements match the sustained NRG-1 and ErbB4 logic since diminished *lin-3* expression either at larva or adult show accelerated aging phenotypes.

In sum, interesting evidence in *C. elegans* and in higher organisms now suggest a significant role in maintenance, which might prolong healthspan. This is an up-and-coming exciting area for future research. My thesis work has contributed to some of the first efforts in this area.

Figure 1

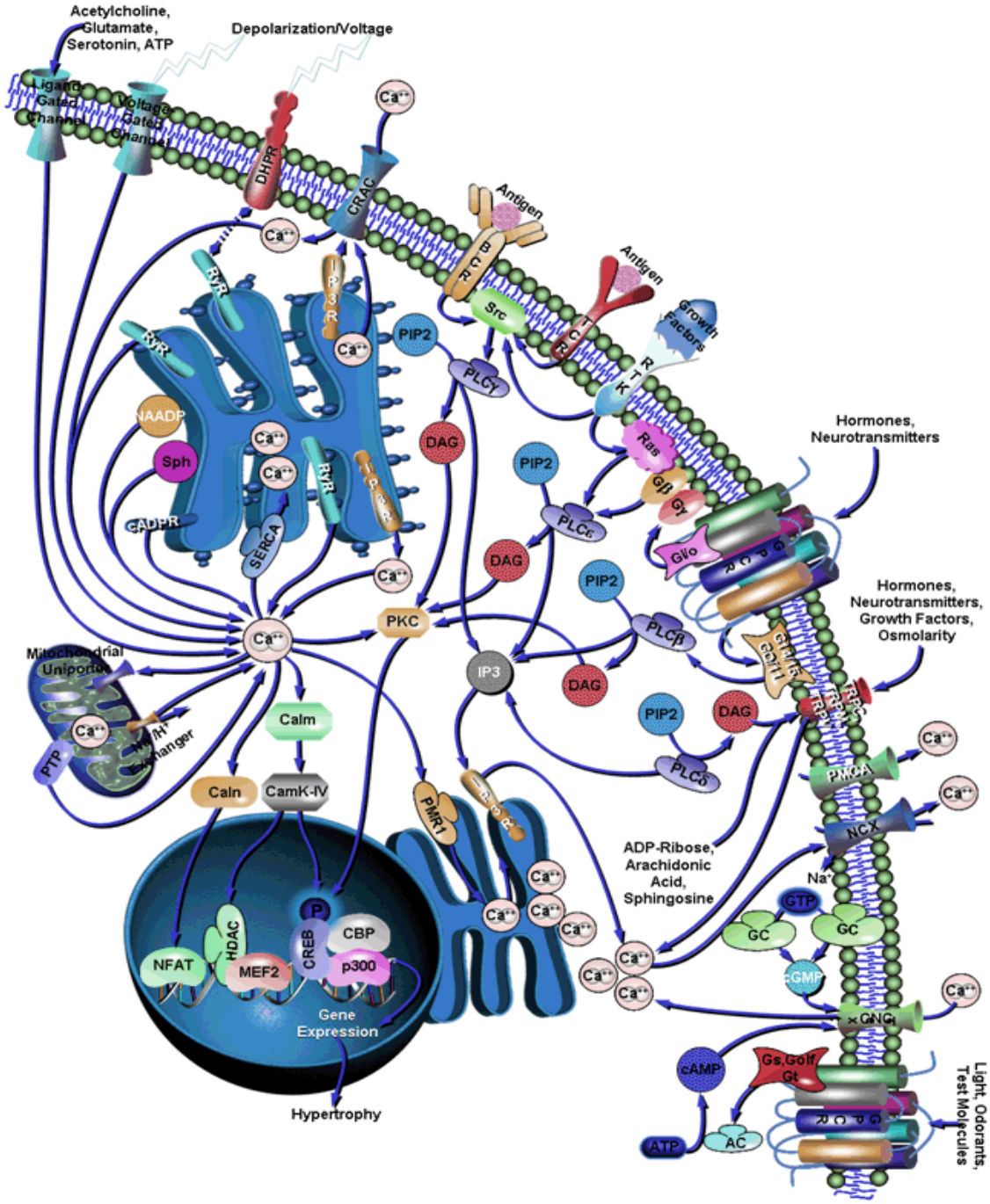

(adapted from SABiosciences)

Figure 2

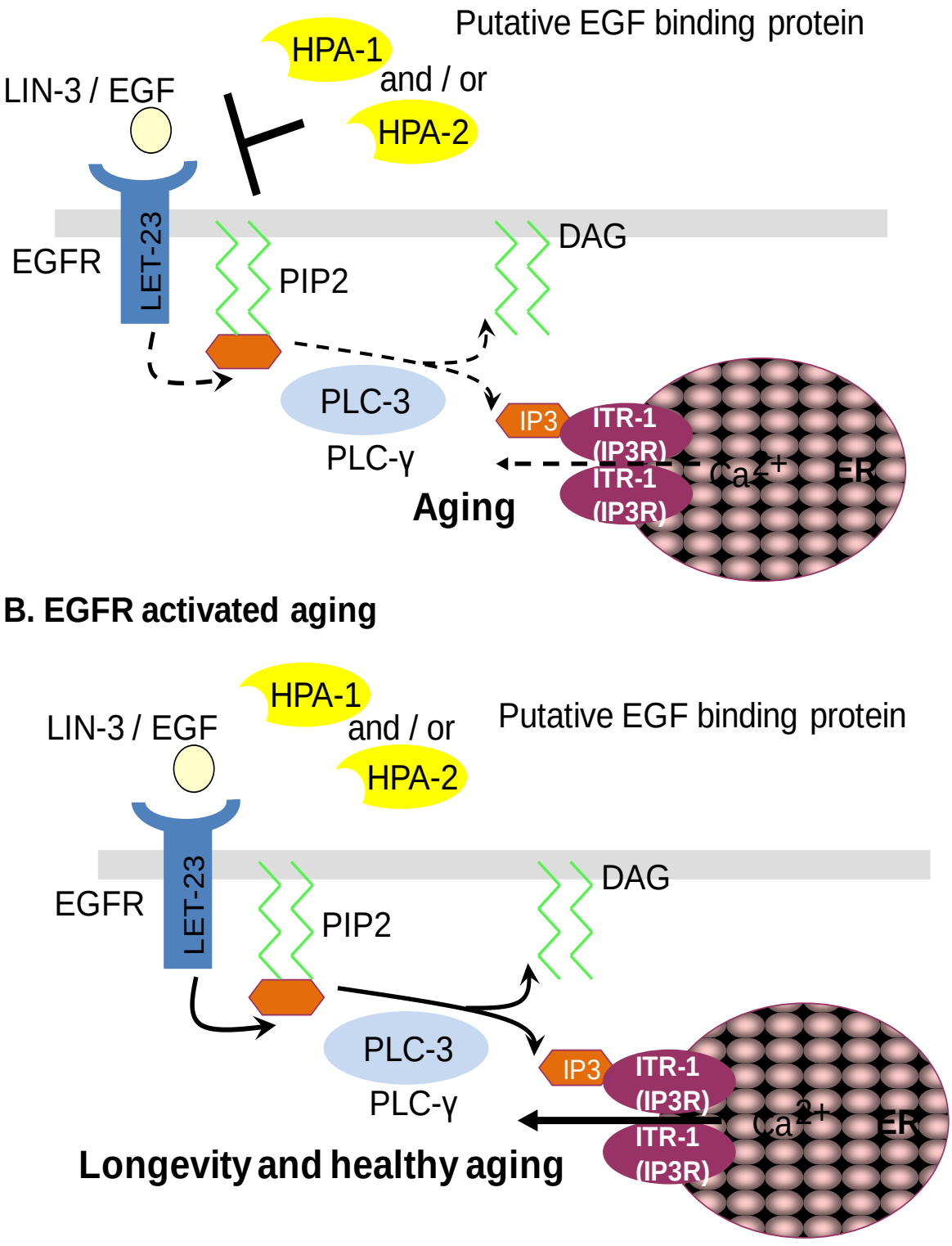
A. Normal aging
Putative EGF binding protein
HPA-1
and / or
HPA-2
LIN-3 / EGF
LET-23
EGFR
DAG
PIP2
PLC-3
PLC-γ
IP3
ITR-1
(IP3R)
ITR-1
(IP3R)
Ca2+
ER
Aging
B. EGFR activated aging
HPA-1
and / or
HPA-2
LIN-3 / EGF
Putative EGF binding protein
LET-23
EGFR
DAG
PIP2
PLC-3
PLC-γ
IP3
ITR-1
(IP3R)
ITR-1
(IP3R)
Ca2+
ER
Longevity and healthy aging

Figure 1. The complex illustration of intracellular calcium signaling.

Calcium is an ubiquitous intracellular messenger and calcium signaling is involved in multiple cellular activity such as cell proliferation, muscle contraction. Here we focus on ER release calcium through IP3 receptor induced IP3 binding and the consequent possible signaling effect on healthy aging promotion.

Figure 2. Model of *C. elegans* EGF pathway modulation in aging.

A. In wild type, putative EGF-binding proteins HPA-1 and HPA-2 function as negative regulators (possibly sequestering EGF ligand) to inhibit LIN-3/EGF LET-23/EGFR signal transduction, conferring the wild-type aging rate.

B. When HPA-1 or HPA-2 are knocked down or absent, EGF signaling through EGFR is increased, activating downstream phospholipase Cγ and IP3 receptor (more ER calcium release) to promote extended healthspan and lifespan. Note that HPA-1 knockdown impacts all assays of animal healthspan, whereas HPA-2 exerts its effect primarily on locomotory healthspan.

References

An, J.H., and T.K. Blackwell. 2003. SKN-1 links C. elegans mesendodermal specification to a conserved oxidative stress response. *Genes & development*. 17:1882-1893.

Antebi, A. 2007. Genetics of aging in Caenorhabditis elegans. *PLoS genetics*. 3:1565-1571.

Apfeld, J., G. O'Connor, T. McDonagh, P.S. DiStefano, and R. Curtis. 2004. The AMP-activated protein kinase AAK-2 links energy levels and insulin-like signals to lifespan in C. elegans. *Genes & development*. 18:3004-3009.

Aroian, R.V., M. Koga, J.E. Mendel, Y. Ohshima, and P.W. Sternberg. 1990. The let-23 gene necessary for Caenorhabditis elegans vulval induction encodes a tyrosine kinase of the EGF receptor subfamily. *Nature*. 348:693-699.

Astigarraga, S., R. Grossman, J. Diaz-Delfin, C. Caelles, Z. Paroush, and G. Jimenez. 2007. A MAPK docking site is critical for downregulation of Capicua by Torso and EGFR RTK signaling. *The EMBO journal*. 26:668-677.

Bolanowski, M.A., R.L. Russell, and L.A. Jacobson. 1981. Quantitative measures of aging in the nematode Caenorhabditis elegans. I. Population and longitudinal studies of two behavioral parameters. *Mechanisms of ageing and development*. 15:279-295.

Brenner, S. 1974. The genetics of Caenorhabditis elegans. *Genetics*. 77:71-94.

Brini, M., and E. Carafoli. 2000. Calcium signalling: a historical account, recent developments and future perspectives. *Cellular and molecular life sciences : CMLS*. 57:354-370.

Bui, Y.K., and P.W. Sternberg. 2002. Caenorhabditis elegans inositol 5-phosphatase homolog negatively regulates inositol 1,4,5-triphosphate signaling in ovulation. *Molecular biology of the cell*. 13:1641-1651.

Chang, C., A.P. Newman, and P.W. Sternberg. 1999. Reciprocal EGF signaling back to the uterus from the induced C. elegans vulva coordinates morphogenesis of epithelia. *Current biology : CB*. 9:237-246.

Chang, H., D.J. Riese, 2nd, W. Gilbert, D.F. Stern, and U.J. McMahan. 1997. Ligands for ErbB-family receptors encoded by a neuregulin-like gene. *Nature*. 387:509-512.

Chow, D.K., C.F. Glenn, J.L. Johnston, I.G. Goldberg, and C.A. Wolkow. 2006. Sarcopenia in the Caenorhabditis elegans pharynx correlates with muscle contraction rate over lifespan. *Experimental gerontology*. 41:252-260.

Citri, A., and Y. Yarden. 2006. EGF-ERBB signalling: towards the systems level. *Nature reviews. Molecular cell biology*. 7:505-516.

Clandinin, T.R., J.A. DeModena, and P.W. Sternberg. 1998. Inositol trisphosphate mediates a RAS-independent response to LET-23 receptor tyrosine kinase activation in C. elegans. *Cell*. 92:523-533.

Clokey, G.V., and L.A. Jacobson. 1986. The autofluorescent "lipofuscin granules" in the intestinal cells of Caenorhabditis elegans are secondary lysosomes. *Mechanisms of ageing and development*. 35:79-94.

Collins, J.J., C. Huang, S. Hughes, and K. Kornfeld. 2008. The measurement and analysis of age-related changes in Caenorhabditis elegans. *WormBook : the online review of C. elegans biology*:1-21.

Curran, S.P., and G. Ruvkun. 2007. Lifespan regulation by evolutionarily conserved genes essential for viability. *PLoS genetics*. 3:e56.

Dillin, A., D.K. Crawford, and C. Kenyon. 2002a. Timing requirements for insulin/IGF-1 signaling in C. elegans. *Science*. 298:830-834.

Dillin, A., A.L. Hsu, N. Arantes-Oliveira, J. Lehrer-Graiwer, H. Hsin, A.G. Fraser, R.S. Kamath, J. Ahringer, and C. Kenyon. 2002b. Rates of behavior and aging specified by mitochondrial function during development. *Science*. 298:2398-2401.

Dutt, A., S. Canevascini, E. Froehli-Hoier, and A. Hajnal. 2004. EGF signal propagation during C. elegans vulval development mediated by ROM-1 rhomboid. *PLoS biology*. 2:e334.

Dwivedi, M., H.O. Song, and J. Ahnn. 2009. Autophagy genes mediate the effect of calcineurin on life span in C. elegans. *Autophagy*. 5:604-607.

Edrey, Y.H., D. Casper, D. Huchon, J. Mele, J.A. Gelfond, D.M. Kristan, E. Nevo, and R. Buffenstein. 2011. Sustained high levels of neuregulin-1 in the longest-lived rodents; a key determinant of rodent longevity. *Aging cell*.

Evans, W. 1997. Functional and metabolic consequences of sarcopenia. *The Journal of nutrition*. 127:998S-1003S.

Feng, J., F. Bussiere, and S. Hekimi. 2001. Mitochondrial electron transport is a key determinant of life span in Caenorhabditis elegans. *Developmental cell*. 1:633-644.

Fisher, A.L. 2004. Of worms and women: sarcopenia and its role in disability and mortality. *Journal of the American Geriatrics Society*. 52:1185-1190.

Fryer, J.D., P. Yu, H. Kang, C. Mandel-Brehm, A.N. Carter, J. Crespo-Barreto, Y. Gao, A. Flora, C. Shaw, H.T. Orr, and H.Y. Zoghbi. 2011. Exercise and genetic rescue of SCA1 via the transcriptional repressor Capicua. *Science*. 334:690-693.

Garigan, D., A.L. Hsu, A.G. Fraser, R.S. Kamath, J. Ahringer, and C. Kenyon. 2002. Genetic analysis of tissue aging in Caenorhabditis elegans: a role for heat-shock factor and bacterial proliferation. *Genetics*. 161:1101-1112.

Gerstbrein, B., G. Stamatas, N. Kollias, and M. Driscoll. 2005. In vivo spectrofluorimetry reveals endogenous biomarkers that report healthspan and dietary restriction in Caenorhabditis elegans. *Aging cell*. 4:127-137.

Gilboa, L., and R. Lehmann. 2006. Soma-germline interactions coordinate homeostasis and growth in the Drosophila gonad. *Nature*. 443:97-100.

Gitler, A.D. 2011. Neuroscience. Another reason to exercise. *Science*. 334:606-607.

Glenn, C.F., D.K. Chow, L. David, C.A. Cooke, M.S. Gami, W.B. Iser, K.B. Hanselman, I.G. Goldberg, and C.A. Wolkow. 2004. Behavioral deficits during early stages of aging in Caenorhabditis elegans result from locomotory deficits possibly linked to muscle frailty. *The journals of gerontology. Series A, Biological sciences and medical sciences*. 59:1251-1260.

Gottlieb, S., and G. Ruvkun. 1994. daf-2, daf-16 and daf-23: genetically interacting genes controlling Dauer formation in Caenorhabditis elegans. *Genetics*. 137:107-120.

Herbst, R.S. 2004. Review of epidermal growth factor receptor biology. *International journal of radiation oncology, biology, physics*. 59:21-26.

Herndon, L.A., P.J. Schmeissner, J.M. Dudaronek, P.A. Brown, K.M. Listner, Y. Sakano, M.C. Paupard, D.H. Hall, and M. Driscoll. 2002. Stochastic and genetic factors influence tissue-specific decline in ageing C. elegans. *Nature*. 419:808-814.

Hill, R.J., and P.W. Sternberg. 1992. The gene lin-3 encodes an inductive signal for vulval development in C. elegans. *Nature*. 358:470-476.

Hopper, N.A., J. Lee, and P.W. Sternberg. 2000. ARK-1 inhibits EGFR signaling in C. elegans. *Molecular cell*. 6:65-75.

Hsin, H., and C. Kenyon. 1999. Signals from the reproductive system regulate the lifespan of C. elegans. *Nature*. 399:362-366.

Hsu, A.L., C.T. Murphy, and C. Kenyon. 2003. Regulation of aging and age-related disease by DAF-16 and heat-shock factor. *Science*. 300:1142-1145.

Huang, C., C. Xiong, and K. Kornfeld. 2004. Measurements of age-related changes of physiological processes that predict lifespan of Caenorhabditis elegans. *Proceedings of the National Academy of Sciences of the United States of America*. 101:8084-8089.

Huang, K.M., P. Cosman, and W.R. Schafer. 2006. Machine vision based detection of omega bends and reversals in C. elegans. *Journal of neuroscience methods*. 158:323-336.

Hwang, B.J., and P.W. Sternberg. 2004. A cell-specific enhancer that specifies lin-3 expression in the C. elegans anchor cell for vulval development. *Development*. 131:143-151.

Ikura, M., M. Osawa, and J.B. Ames. 2002. The role of calcium-binding proteins in the control of transcription: structure to function. *BioEssays : news and reviews in molecular, cellular and developmental biology*. 24:625-636.

Iwasa, H., S. Yu, J. Xue, and M. Driscoll. 2010. Novel EGF pathway regulators modulate C. elegans healthspan and lifespan via EGF receptor, PLC-gamma, and IP3R activation. *Aging cell*. 9:490-505.

Johnson, T.E. 1987. Aging can be genetically dissected into component processes using long-lived lines of Caenorhabditis elegans. *Proceedings of the National Academy of Sciences of the United States of America*. 84:3777-3781.

Kamath, R.S., and J. Ahringer. 2003. Genome-wide RNAi screening in Caenorhabditis elegans. *Methods*. 30:313-321.

Katz, W.S., R.J. Hill, T.R. Clandinin, and P.W. Sternberg. 1995. Different levels of the C. elegans growth factor LIN-3 promote distinct vulval precursor fates. *Cell*. 82:297-307.

Kenyon, C. 2001. A conserved regulatory system for aging. *Cell*. 105:165-168.

Kenyon, C.J. 2010. The genetics of ageing. *Nature*. 464:504-512.

Kimura, K.D., H.A. Tissenbaum, Y. Liu, and G. Ruvkun. 1997. daf-2, an insulin receptor-like gene that regulates longevity and diapause in Caenorhabditis elegans. *Science*. 277:942-946.

Kimura, Y., E.E. Corcoran, K. Eto, K. Gengyo-Ando, M.A. Muramatsu, R. Kobayashi, J.H. Freedman, S. Mitani, M. Hagiwara, A.R. Means, and H. Tokumitsu. 2002. A CaMK cascade activates CRE-mediated transcription in neurons of Caenorhabditis elegans. *EMBO reports*. 3:962-966.

Klein, D.E., V.M. Nappi, G.T. Reeves, S.Y. Shvartsman, and M.A. Lemmon. 2004. Argos inhibits epidermal growth factor receptor signalling by ligand sequestration. *Nature*. 430:1040-1044.

Lakowski, B., and S. Hekimi. 1998. The genetics of caloric restriction in Caenorhabditis elegans. *Proceedings of the National Academy of Sciences of the United States of America*. 95:13091-13096.

Lee, J.I., B.K. Dhakal, J. Lee, J. Bandyopadhyay, S.Y. Jeong, S.H. Eom, D.H. Kim, and J. Ahnn. 2003. The Caenorhabditis elegans homologue of Down syndrome critical region 1, RCN-1, inhibits multiple functions of the phosphatase calcineurin. *Journal of molecular biology*. 328:147-156.

Libina, N., J.R. Berman, and C. Kenyon. 2003. Tissue-specific activities of C. elegans DAF-16 in the regulation of lifespan. *Cell*. 115:489-502.

Lin, K., J.B. Dorman, A. Rodan, and C. Kenyon. 1997. daf-16: An HNF-3/forkhead family member that can function to double the life-span of Caenorhabditis elegans. *Science*. 278:1319-1322.

Lin, K., H. Hsin, N. Libina, and C. Kenyon. 2001. Regulation of the Caenorhabditis elegans longevity protein DAF-16 by insulin/IGF-1 and germline signaling. *Nature genetics*. 28:139-145.

Liu, G., J. Rogers, C.T. Murphy, and C. Rongo. 2011. EGF signalling activates the ubiquitin proteasome system to modulate C. elegans lifespan. *The EMBO journal*. 30:2990-3003.

Longo, V.D., and C.E. Finch. 2003. Evolutionary medicine: from dwarf model systems to healthy centenarians? *Science*. 299:1342-1346.

Luetteke, N.C., T.H. Qiu, S.E. Fenton, K.L. Troyer, R.F. Riedel, A. Chang, and D.C. Lee. 1999. Targeted inactivation of the EGF and amphiregulin genes reveals distinct roles for EGF receptor ligands in mouse mammary gland development. *Development*. 126:2739-2750.

Mair, W., I. Morantte, A.P. Rodrigues, G. Manning, M. Montminy, R.J. Shaw, and A. Dillin. 2011. Lifespan extension induced by AMPK and calcineurin is mediated by CRTC-1 and CREB. *Nature*. 470:404-408.

Mango, S.E. 2007. The C. elegans pharynx: a model for organogenesis. *WormBook : the online review of C. elegans biology*:1-26.

Meyer, D., T. Yamaai, A. Garratt, E. Riethmacher-Sonnenberg, D. Kane, L.E. Theill, and C. Birchmeier. 1997. Isoform-specific expression and function of neuregulin. *Development*. 124:3575-3586.

Moghal, N., and P.W. Sternberg. 1999. Multiple positive and negative regulators of signaling by the EGF-receptor. *Current opinion in cell biology*. 11:190-196.

Moghal, N., and P.W. Sternberg. 2003. The epidermal growth factor system in Caenorhabditis elegans. *Experimental cell research*. 284:150-159.

Morris, J.Z., H.A. Tissenbaum, and G. Ruvkun. 1996. A phosphatidylinositol-3-OH kinase family member regulating longevity and diapause in Caenorhabditis elegans. *Nature*. 382:536-539.

Mukhopadhyay, A., and H.A. Tissenbaum. 2007. Reproduction and longevity: secrets revealed by C. elegans. *Trends in cell biology*. 17:65-71.

Murakami, H., K. Bessinger, J. Hellmann, and S. Murakami. 2008. Manipulation of serotonin signal suppresses early phase of behavioral aging in Caenorhabditis elegans. *Neurobiology of aging*. 29:1093-1100.

Nilson, L.A., and T. Schupbach. 1999. EGF receptor signaling in Drosophila oogenesis. *Current topics in developmental biology*. 44:203-243.

Ogg, S., S. Paradis, S. Gottlieb, G.I. Patterson, L. Lee, H.A. Tissenbaum, and G. Ruvkun. 1997. The Fork head transcription factor DAF-16 transduces insulin-like metabolic and longevity signals in C. elegans. *Nature*. 389:994-999.

Oh, S.W., A. Mukhopadhyay, N. Svrzikapa, F. Jiang, R.J. Davis, and H.A. Tissenbaum. 2005. JNK regulates lifespan in Caenorhabditis elegans by modulating nuclear translocation of forkhead transcription factor/DAF-16. *Proceedings of the National Academy of Sciences of the United States of America*. 102:4494-4499.

Panowski, S.H., S. Wolff, H. Aguilaniu, J. Durieux, and A. Dillin. 2007. PHA-4/Foxa mediates diet-restriction-induced longevity of C. elegans. *Nature*. 447:550-555.

Paradis, S., M. Ailion, A. Toker, J.H. Thomas, and G. Ruvkun. 1999. A PDK1 homolog is necessary and sufficient to transduce AGE-1 PI3 kinase signals that regulate diapause in Caenorhabditis elegans. *Genes & development*. 13:1438-1452.

Paradis, S., and G. Ruvkun. 1998. Caenorhabditis elegans Akt/PKB transduces insulin receptor-like signals from AGE-1 PI3 kinase to the DAF-16 transcription factor. *Genes & development*. 12:2488-2498.

Rawlings, J.S., K.M. Rosler, and D.A. Harrison. 2004. The JAK/STAT signaling pathway. *Journal of cell science*. 117:1281-1283.

Reich, A., and B.Z. Shilo. 2002. Keren, a new ligand of the Drosophila epidermal growth factor receptor, undergoes two modes of cleavage. *The EMBO journal*. 21:4287-4296.

Schnepp, B., G. Grumbling, T. Donaldson, and A. Simcox. 1996. Vein is a novel component in the Drosophila epidermal growth factor receptor pathway with similarity to the neuregulins. *Genes & development*. 10:2302-2313.

Schreiber, M.A., J.T. Pierce-Shimomura, S. Chan, D. Parry, and S.L. McIntire. 2010. Manipulation of behavioral decline in Caenorhabditis elegans with the Rag GTPase raga-1. *PLoS genetics*. 6:e1000972.

Schweitzer, R., M. Shaharabany, R. Seger, and B.Z. Shilo. 1995. Secreted Spitz triggers the DER signaling pathway and is a limiting component in embryonic ventral ectoderm determination. *Genes & development*. 9:1518-1529.

Sedensky, M.M., and P.G. Morgan. 2006. Mitochondrial respiration and reactive oxygen species in C. elegans. *Experimental gerontology*. 41:957-967.

Shibata, Y., R. Branicky, I.O. Landaverde, and S. Hekimi. 2003. Redox regulation of germline and vulval development in Caenorhabditis elegans. *Science*. 302:1779-1782.

Shilo, B.Z. 2003. Signaling by the Drosophila epidermal growth factor receptor pathway during development. *Experimental cell research*. 284:140-149.

Shilo, B.Z. 2005. Regulating the dynamics of EGF receptor signaling in space and time. *Development*. 132:4017-4027.

Simske, J.S., S.M. Kaech, S.A. Harp, and S.K. Kim. 1996. LET-23 receptor localization by the cell junction protein LIN-7 during C. elegans vulval induction. *Cell*. 85:195-204.

Timmons, L., and A. Fire. 1998. Specific interference by ingested dsRNA. *Nature*. 395:854.

Tsechpenakis, G., L. Bianchi, D. Metaxas, and M. Driscoll. 2008. A novel computational approach for simultaneous tracking and feature extraction of C. elegans populations in fluid environments. *IEEE transactions on bio-medical engineering*. 55:1539-1549.

Tseng, A.S., N. Tapon, H. Kanda, S. Cigizoglu, L. Edelmann, B. Pellock, K. White, and I.K. Hariharan. 2007. Capicua regulates cell proliferation downstream of the receptor tyrosine kinase/ras signaling pathway. *Current biology : CB*. 17:728-733.

Tsuboi, D., H. Qadota, K. Kasuya, M. Amano, and K. Kaibuchi. 2002. Isolation of the interacting molecules with GEX-3 by a novel functional screening. *Biochemical and biophysical research communications*. 292:697-701.

Van Buskirk, C., and P.W. Sternberg. 2007. Epidermal growth factor signaling induces behavioral quiescence in Caenorhabditis elegans. *Nature neuroscience*. 10:1300-1307.

Wang, Y., and D.E. Levy. 2006. C. elegans STAT cooperates with DAF-7/TGF-beta signaling to repress dauer formation. *Current biology : CB*. 16:89-94.

Wolkow, C.A., K.D. Kimura, M.S. Lee, and G. Ruvkun. 2000. Regulation of C. elegans life-span by insulinlike signaling in the nervous system. *Science*. 290:147-150.

Yin, X., N.J. Gower, H.A. Baylis, and K. Strange. 2004. Inositol 1,4,5-trisphosphate signaling regulates rhythmic contractile activity of myoepithelial sheath cells in Caenorhabditis elegans. *Molecular biology of the cell*. 15:3938-3949.

Yu, S., and M. Driscoll. 2011. EGF signaling comes of age: promotion of healthy aging in C. elegans. *Experimental gerontology*. 46:129-134.

Yu, Y., A.K. Rishi, J.R. Turner, D. Liu, E.D. Black, J.A. Moshier, and A.P. Majumdar. 2001. Cloning of a novel EGFR-related peptide: a putative negative regulator of EGFR. *American journal of physiology. Cell physiology*. 280:C1083-1089.

Appendix

Novel EGF Pathway Regulators Modulate *C. elegans* Healthspan and Lifespan via EGF Receptor, PLC-γ and IP3R Activation

Hiroaki Iwasa, Simon Yu, Jian Xue and Monica Driscoll*

Department of Molecular Biology and Biochemistry
Rutgers, The State University of New Jersey
A232 Nelson Biological Laboratories
604 Allison Road
Piscataway, New Jersey, USA 08855

***To whom correspondence should be addressed**
E-mail: driscoll@biology.rutgers.edu
Phone: 732-445-7182
Fax: 732-445-7192

Summary

Improving health of the rapidly growing aging population is a critical medical, social, and economic goal. Identification of genes that modulate healthspan, the period of mid-life vigor that precedes significant functional decline, will be an essential part of the effort to design anti-aging therapies. Because locomotory decline in humans is a major contributor to frailty and loss of independence and because slowing of movement is a conserved feature of aging across phyla, we screened for genetic interventions that extend locomotory healthspan of *Caenorhabditis elegans*. From a group of 54 genes previously noted to encode secreted proteins similar in sequence to extracellular domains of insulin receptor, we identified two genes for which RNAi knockdown delayed age-associated locomotory decline, conferring a **h**igh **p**erformance in **a**dvanced age phenotype (Hpa). Unexpectedly, we found that *hpa-1* and *hpa-2* act through the EGF pathway, rather than the insulin signaling pathway, to control systemic healthspan benefits without detectable developmental consequences. Further analysis revealed a potent role of EGF signaling, acting via downstream phospholipase C-γ *plc-3* and inositol-3-phosphate receptor *itr-1,* to promote healthy aging associated with low lipofuscin levels, enhanced physical performance, and extended lifespan. This study identifies HPA-1 and HPA-2 as novel negative regulators of EGF signaling and constitutes the first report of EGF signaling as a major pathway for healthy aging. Our data raise the possibility that EGF family members should be investigated for similar activities in higher organisms.

Introduction

The increase in human life expectancy has been accompanied by a focused appreciation of the significant need to maintain general health and vigor late into life (Glatt *et al.*, 2007; Kirkland & Peterson, 2009). As such, extending healthspan—the period of maintained function and stress-resistance that precedes debilitating decline—has become a central goal of current aging research. Improving overall robustness as well as maintaining the integrity of individual organ systems are both likely to contribute to healthspan extension and an increased quality of life.

Locomotory decline is a conserved feature of aging animals that is typically accompanied by a progressive loss of muscle mass and muscle strength called sarcopenia (Fisher, 2004; Lang *et al.*, 2009). As an inescapable component of normal human aging, sarcopenia impacts the entire elderly population, and is thought to be a major underlying cause of loss of independence, frailty, and morbidity. Given the seemingly universal association of old age with diminished mobility, genetic analyses in invertebrate models may contribute novel insights into conserved molecular causes of locomotory decline (Augustin & Partridge, 2009; Tatar, 2009). Multiple studies in *C. elegans* have documented diminished locomotion with age scored as crawling on solid agar plates (Croll *et al.*, 1977; Bolanowski *et al.*, 1981; Johnson, 1987; Duhon & Johnson, 1995; Herndon *et al.*, 2002; Glenn *et al.*, 2004; Huang *et al.*, 2004; Hsu *et al.*, 2009). Another *C. elegans* locomotory phenotype, more easily quantitated by unaided observers, is

the rate of body bends /unit time when animals are placed in liquid (“swimming” (Pierce-Shimomura *et al.*, 2008)). Swimming rate progressively declines with age (Duhon & Johnson, 1995; Restif & Metaxas, 2008) (and data herein). Physical deterioration of muscle (without notable cell death) has been correlated with locomotory decline, with relatively subtle changes such as in actin filament organization (Glenn *et al.*, 2004) preceding a dramatic loss of sarcomere units and fat infiltration of muscle that resembles sarcopenia in higher organisms (Herndon *et al.*, 2002). A proportion of muscle deterioration might be attributed to diminished neuronal signaling--administration of muscarinic agonist arecoline can extend locomotory healthspan (Glenn *et al.*, 2004), and altering serotonin signaling can suppress early phases of locomotory aging (Murakami *et al.*, 2008). Lowering the strength of insulin receptor signaling prolongs locomotory healthspan and physical integrity of muscle (Herndon *et al.*, 2002) as well as extends lifespan. Dietary restriction regimens can also improve locomotory function in aging animals (Huang *et al.*, 2004; Hsu *et al.*, 2009). Overall, however, there has been little systematic evaluation of genetic influences on locomotory decline and much remains to be learned about the molecular systems modulating this process.

With an interest in identifying genes that impact locomotory decline, we screened sets of healthspan candidates by RNAi knockdown, scoring for enhanced swimming prowess in old age. Among genes suggested to encode insulin receptor-related proteins (Dlakic, 2002), we identified *hpa-1* and *hpa-2* (high

performance in advanced age), which proved to modulate multiple aging phenotypes in *C. elegans* healthspan. Effects of HPA-1 and HPA-2 occur largely independently of insulin signaling—instead, we show that *hpa-1* and *hpa-2* act through the EGF receptor/phospholipase Cγ/ IP3 receptor pathway. This work identifies novel upstream negative regulators of EGF pathway activities that are also noteworthy because their genetic manipulation exerts a greater proportionate impact on healthspan than on the longevity endpoint. In addition, this work is the first to document the impact of EGF signaling and the downstream PLCγ/IP3R signaling branch in *C. elegans* healthspan and lifespan. We suggest EGF signaling may be a conserved mechanism for adult maintenance and healthy aging.

Results

Inactivation of *hpa-1 and hpa-2* specifically extends locomotory capacity late in life

Although the problem of locomotory decline is a pervasive and universal component of aging biology, genetic influences on this process have not yet been systematically identified. In *C. elegans,* expression of individual genes can be knocked down by feeding animals the corresponding double stranded RNA expressed in bacterial food (Kamath & Ahringer, 2003). We initiated screening for gene knockdowns that altered adult locomotory healthspan by first testing selected sets of genes implicated in, or associated with, those genes known to influence longevity.

Among signaling pathways that modulate longevity, the insulin/IGF (IIS) pathway activity has emerged as a conserved and potent mechanism for modulating both healthspan and lifespan (Tatar *et al.*, 2003; Broughton & Partridge, 2009). The 40 insulin-like ligands encoded by the *C. elegans* genome (Malone & Thomas, 1994; Pierce *et al.*, 2001) are all thought to act via the sole DAF-2 insulin receptor homolog. Activation of the DAF-2 insulin receptor initiates a kinase cascade that includes AGE-1 (PI-3 kinase), and pathway activation ultimately phosphorylates FOXO family transcription factor DAF-16 to inhibit its activity (Tatar *et al.*, 2003). Conversely, decreased DAF-2 signaling promotes DAF-16 transcriptional functions and causes *daf-16*-dependent lifespan extension (Kenyon *et al.*, 1993; Hsu *et al.*, 2003). Additional, less-characterized molecular modulators of insulin

pathway activity are likely to also influence signaling. For example, a bioinformatic study identified 54 proteins related to the extracellular ligand binding domain of insulin receptor (Dlakic, 2002). These insulin receptor-related proteins share sequence similarities in the extracellular ligand-binding domain and contain secretion signal sequences, but lack the transmembrane domain and intracellular kinase domains characteristic of classic receptor kinases. Thus, this group of proteins resemble secreted proteins that might bind ligand more than they resemble intact transmembrane receptor kinases. Functional studies on this gene group have not yet been reported.

We constructed or obtained 54 clones for the IGF receptor-related genes and used these for food-delivered RNAi inactivation to test effects on locomotory healthspan (Fig. 1A; Table S1, Supporting Information). As a first-pass screen for changes in locomotory ability in aging adults, we scored body bend frequency (swimming rates) in aging post-reproductive adults (11 days from the hatch, 25^{o}C; day3 is the first day of reproductive adult life at this temperature and day11 is middle/late adult life of the ~ 20 day lifespan). We then verified that RNAi clones conferring statistically significant changes later in life did not impact locomotion rates in young adult life to rule out developmental or general behavioral effects of RNAi knockdown that might confer chronic hypo- or hyper-active swimming. In this way, we sought to identify genetic knockdowns that specifically changed swimming prowess in aging adults.

In the screen of 54 insulin receptor-related genes, we identified nine genes for which RNAi knockdown conferred enhanced swimming vigor in aging adults (Table S1, Supporting Information). Of these, we elected to focus on detailed analysis of H25K10.5 and T11F1.8 because RNAi directed against these consistently conferred strongest effects and because deletion alleles became available during the course of our study. We designate these receptor-related genes as *hpa-1* and *hpa-2*, respectively, for the phenotype of **h**igh **p**erformance in **a**dvanced age (*hpa*). For *hpa-1*(RNAi) and *hpa-2*(RNAi), animals swim at control rates in young day5 adults, but swim faster than wild type as older day11 adults (Fig. 1B). In young *hpa-1*(RNAi) and *hpa-2*(RNAi) adults pharyngeal pumping rates, defecation rates, dauer formation, vulval development, and brood size are all similar to controls (Fig. S2A-C and G; Table S2A, Supporting Information), supporting that *hpa-1* and *hpa-2* (RNAi) do not exert major impact on *C. elegans* development or basic behaviors up to young adulthood. Instead, phenotypes are apparent in aging adults.

We verified that 6x outcrossed deletion mutants of *hpa-1(tm3256)* and *hpa-2(tm3827)* exhibited increased swimming prowess at old age (Fig. 1C). For deletion mutants, swimming was indistinguishable from wild type on the first day of adult life (day3), with differences in swim vigor becoming already apparent at day5, and maintained later into adulthood (day11). (The different onsets for phenotype expression of deletion mutants vs. *hpa*(RNAi) might be attributed to the variable/partial knockdown capacities of RNAi). Consistent with *hpa-1* and

hpa-2 (RNAi) phenotypes, *hpa-1(tm3256)* and *hpa-2(tm3827)* deletions, as well as their double mutant combination, did not affect *C. elegans* development or basic behaviors up to young adulthood (Fig. S2D-F, H and Fig. S3; Table S2B, Supporting Information). We conclude that diminishing *hpa-1* and *hpa-2* activities extends swimming locomotory healthspan without a major impact on basic swimming or other functions during development.

We previously documented that WT *C. elegans* reared on agar plates progress through successive stages of crawling impairment, classifying animals that move vigorously in response to an eyelash hair touch as class A, those that are uncoordinated in response to touch as class B, and those that are virtually paralyzed except for the head as class C (Herndon *et al.*, 2002). To evaluate an independent measure of locomotory capacity when *hpa-1* and *hpa-2* are deficient, we scored the relative prevalence of ABC classes during adult life consequent to RNAi knockdown. We found that *hpa-1(RNAi)* and *hpa-2(RNAi)* animals exhibit diminished rates of decline in this comparative plate locomotion assay (Fig. S4, Supporting Information), in further support that locomotory aging is delayed when either *hpa-1* or *hpa*-2 is lacking.

hpa-1 and _hpa-2_ deficiencies improve multiple measures of favorable healthspan

hpa-1 and *hpa-2* might specifically impact locomotory aging or, alternatively, might systemically affect the overall quality of *C. elegans* aging. To address

whether *hpa-1* and *hpa-2* affect expression of other age-associated phenotypes, we monitored additional indicators that can reflect the quality of aging: age pigment accumulation (Gerstbrein *et al.*, 2005), pharyngeal pumping (Huang *et al.*, 2004; Chow *et al.*, 2006), and survival curve properties. Lipofuscin and advanced glycation end products (referred to here together as age pigments) accumulate in aging organisms across species (Perriere & Gouy, 1996; Ulrich & Cerami, 2001). We previously demonstrated via *in vivo* age pigment quantitation that age pigments accumulate at accelerated rates in aging *C. elegans* and that long-lived strains tend to have low levels of age pigments in early and middle adult life (Gerstbrein *et al.*, 2005). Moreover, same-age adults with low age pigment levels have longer life expectancy than age-matched siblings reared in the same environment that stochastically have high age pigment levels, suggesting that age pigment scores reflect a “physiological”, rather than chronological, age. Using *in vivo* fluorometric analysis, we precisely quantitated age pigment values in young and aging *hpa-1* and *hpa-2* adults (Fig. 1D,E). We find that *hpa-1* and *hpa-2* have low age pigment scores on the first day of adult life. Only *hpa-1,* however, maintains differences later into adulthood. Thus, *hpa-1* exhibits low age pigments though most of adult life, suggesting a systemic impact on healthy aging. The consequences of transiently low age pigments as found in *hpa-2* are not known, and thus we are unable to comment as to whether a transient low age pigment period early in life might be expected to influence the quality of aging in later adulthood.

As another measure of maintained tissue function/integrity over time, we analyzed pharyngeal pumping frequency in mid-life. Previous work documented that pumping frequency decline is dramatic in early adult life (Huang *et al.*, 2004). We find that *hpa-1* and *hpa-2* deficiencies slow this decline significantly without affecting pumping activity on the first day of adult life (Fig. 1F). Our data indicate improved maintenance of pharyngeal function as *hpa-1* and *hpa-2* mutant adults age.

We also compared survival curves of *hpa-1* and *hpa-2* deficient animals to those of wild type and long-lived *age-1* mutants. Analysis of deletion mutants supported that *hpa-1* and *hpa-2* deficiencies extend median and mean lifespan to improve mid-life survival in aging cultures (Fig. 1G). For example, in the lifespan trial in Fig. 1G, median lifespan of WT was 13 days, of *age-1* and *hpa-2* was 15 days, and of *hpa-1* was 17 days (15% increase in *age-1*, 31% increase in *hpa-1*, and 15% increase in *hpa-2*). Although the exact magnitude of mid-life survival showed some variation between repeat trials, we found that the median and mean lifespans for *hpa-1* and *hpa-2* were increased with statistical significance in all trials (Table S3, Supporting Information). Interestingly, for *hpa* mutant strains, the maximum lifespan changes (scored as the mean of the top 10% survivors) were more modest or lacking as compared to the median lifespan phenotypes (Max: N2 21.3 +/-0.1; *age-1* 32.3 +/-0.7 (51%); *hpa-1* 23.5+/-0.7 (10%); *hpa-2* 22.0+/- 0.6 (NS)). Thus, unlike *age-1* reduction-of-function, *hpa-1* and *hpa-2* deletions exert a proportionally greater impact on median lifespan as compared

to maximum lifespan.

We also calculated mortality rates over adult life for *hpa-1* and *hpa-2* deletion mutants (Johnson, 1987). Although like wt, mortality rates rise exponentially with age in *hpa* backgrounds, the rate of change in middle and late adulthood is slowed compared to wild type, supporting that *hpa-1* or *hpa-2* deficiency reduces the rate of aging (Fig. S5, Supporting Information).

In sum, on the basis of multiple assessments of organ and animal vigor in mid/late adult life, we conclude that HPA-1 and HPA-2 are newly identified modulators of healthy aging in *C. elegans*.

HPA-1 and HPA-2 can promote locomotory healthspan through a pathway distinct from insulin signaling and dietary restriction

HPA-1 and HPA-2 were initially identified by homology to extracellular ligand-binding regions of the insulin receptor (InsR) (Dlakic, 2002). To address whether *hpa-1* and *hpa-2* extend locomotory healthspan via the insulin/IGF signaling pathway, we first tested for a requirement for critical downstream IIS transcription factors in the execution of the *hpa-1* and *hpa-2* age-associated RNAi swimming phenotypes. Downstream transcription factor FOXO/DAF-16 is essential for the longevity phenotype of InsR/*daf-2(rf)* mutants (Kenyon *et al.*, 1993) and *daf-16* null mutants have early-onset age pigment elevation (Gerstbrein *et al.*, 2005), consistent with a progeric condition when *daf-16* is lacking. We find that *hpa-1* and *hpa-2* RNAi partially restored swimming prowess in young *daf-16* null

mutants (~29 bends/30min for *daf-16* vs. ~35 bends/30min for *hpa-1(RNAi) daf-16* and ~33 bends/30min for *hpa-2(RNAi) daf-16,* day5), suggesting that *hpa-1* and *hpa-2* knockdown effects are, at least in part, *daf-16*-independent.

Transcription factor HSF-1 is also required for *daf-2(rf)* to extend lifespan (Hsu *et al.*, 2003) and to protect against proteotoxic stress (Cohen *et al.*, 2006). We find that a shift of the temperature-sensitive *hsf-1* mutant to the non-permissive temperature accelerates swimming decline in young adults (Fig. 2A). *hpa-1* and *hpa-2* RNAi can extend swimming healthspan in the *hsf-1* mutant (~7 bends/30min day8 for *hsf-1* vs. ~13 bends/30min day8 for *hpa-1* and *hpa-2(RNAi) hsf-1*, day8). We conclude that *hsf-1* is needed for normal locomotory healthspan, and that knockdown of *hpa-1* and *hpa-2* extends locomotory healthspan via a mechanism that is at least in part *hsf-1*-independent.

Long-lived insulin receptor *daf-2(rf*) and PI3 kinase *age-1(rf)* (Herndon et al., 2002) exhibit extended locomotory healthspan. We knocked down *hpa-1* and *hpa-2* in *daf-2(rf)* and *age-1(rf)* mutants to show that this intervention further extends swimming healthspan (Fig. S6, Supporting Information). Although epistasis analysis on reduction-of-function mutations rather than deletion mutations is not definitive (Huang & Sternberg, 2006), the additive effects of low insulin pathway signaling and *hpa* knockdown are consistent with the interpretation that the two HPA proteins identified by similarity to insulin receptor ligand-binding sequences can modulate locomotory healthspan at least in part

via an IIS-independent pathway. The identity of this alternative pathway thus became a question of interest.

A second major pathway for longevity and healthspan benefit conserved across species is dietary restriction (DR), and thus we considered whether *hpa-1* and *hpa-2* RNAi might extend locomotory healthspan by activating DR. However, several lines of evidence argue against this possibility. First, as noted in Fig. S2, pharyngeal pumping is normal in young *hpa-1* and *hpa-2* RNAi and deletion mutants and enhanced in aging animals (Fig. 1F), so *hpa-1* or *hpa-2* deficiency does not physically limit feeding (Fig. S2A, D Supporting Information). Second, *hpa-1* or *hpa-2* deficiency exhibits the characteristic fluorometric shift in age pigment excitation maximum that exclusively characterizes DR mutants and animals treated with every DR regimen we have tested to date (Fig. 2B) (Gerstbrein *et al.*, 2005). Third, *hpa-1* and *hpa-2* (RNAi) do not cause the induction of a SKN-1::GFP reporter in the ASI neurons that occurs in WT under a modified food limitation DR protocol (Fig. 2D, E) (Bishop & Guarente, 2007). Finally, *hpa-1* and *hpa-2* RNAi further enhances the old-age swimming prowess of the *eat-2* feeding limited DR mutant (Lakowski & Hekimi, 1998), which suggests that *hpa-1* and *hpa-2* act via a mechanism distinct from, but additive with, feeding-limited DR (Fig. 2B). Thus, although we have not tested all DR regimens (Greer & Brunet, 2009), and genetic interactions with *eat-2* must be interpreted with attention to experimental concerns that DR might not be optimized in the *eat-2* background in this experiment (Huang & Sternberg, 2006;

Mair & Dillin, 2008), our compiled data fail to implicate *hpa-1* and *hpa-2* in any of several of probed DR mechanisms.

Activation of the conserved EGF signaling pathway confers healthspan benefits in *C. elegans*

Our genetic observations suggesting that HPA-1 and HPA-2 can act, at least in part, via a pathway distinct from the IIS pathway to influence locomotory healthspan prompted us to revisit bioinformatic analysis of HPA-1 and HPA-2. Alignments of HPA-1 and HPA-2 revealed primary sequence homologies to EGF receptor ligand-binding domains that appeared potentially more significant than the relationship to insulin receptor ligand-binding domains (Fig. S7A, Supporting Information). More specifically, HPA-1 and HPA-2, which are related in sequence to each other, are similar in ligand-binding Leucine Rich domains (L domains) to mammalian **E**GF **R**eceptor-**R**elated **P**rotein (ERRP), a secreted negative regulator of EGF receptor (EGFR), which itself exhibits homology to the extracellular domain of mammalian EGFR (Park *et al.*, 2001) (Fig. S7B, Supporting Information). This sequence relationship prompted us to address whether HPA-1 and HPA-2 might act via the EGF signaling pathway.

We first examined how the EGF signaling pathway itself impacts healthspan and lifespan—a question that, surprisingly, had not yet been addressed in the facile nematode model. The genetics of the *C. elegans* EGF pathway have been characterized in exquisite detail by Sternberg and colleagues, with a focus on

EGF signaling roles in development (Moghal & Sternberg, 2003), and a more recent observation of a role in behavioral quiescence (Van Buskirk & Sternberg, 2007). We found that a gain-of-function mutation affecting the EGF receptor, *let-23(sa62)*, increases swimming vigor later in life (Fig. 3A). Conversely, temperature-sensitive reduction-of-function of the EGF receptor mutant *let-23(n1045),* which is impaired at 20^{o}C, exhibits the opposite effect on swimming healthspan—an accelerated decline (Fig. 3B). *let-23(gf)* delays the decline in muscle nuclear GFP signal dimunition that characterizes sarcopenia in elderly MYO-3::GFP-NLS transgenic animals (Herndon *et al.*, 2002) (Fig. 3C, D), suggesting that both muscle function and integrity are maintained longer in EGFR/*let-23*(*gf)* mutants. The *let-23(gf)* mutant also exhibits low age pigment levels later in life, consistent with a general healthy aging trajectory (Fig. 3E, F). Finally, analysis of survival curves indicates that EGFR/*let-23(gf)* cultures survive more robustly in middle adulthood (i.e., 29% increase of median lifespan, 9% increase of maximum lifespan, and EGFR/*let-23(rf)* cultures survive less robustly in middle adulthood than matched wild type controls (i.e., 19% decrease of median lifespan, 8% decrease of maximum lifespan) (Fig. 3G, H). We conclude that EGF receptor activity modulates the quality of aging, with EGFR activation promoting extended healthspan, and EGFR inactivation associated with age-related declines. Consistent with this conclusion, we find that the reduction-of-function EGF mutant *lin-3(n1058)* exhibits reduced swimming vigor in mid-adulthood and a shortened median lifespan (Fig. S8A, C, Supporting Information).

The downstream branch of the EGF pathway involving phospholipase Cγ PLC-3 and IP3 receptor ITR-1 promotes healthy aging outcomes of EGFR activation

In *C. elegans*, EGF signaling activates distinct downstream signaling pathways (Fig. 4A) for specific functional outcomes (Moghal & Sternberg, 2003; Van Buskirk & Sternberg, 2007): EGFR signaling through the RAS-MAPK pathway determines cell fates that affect viability and development of the hermaphrodite vulva (Beitel *et al.*, 1990; Han & Sternberg, 1990; Lackner *et al.*, 1994; Wu & Han, 1994); EGF signaling through diacylglycerol (DAG) regulates behavioral quiescence in larvae at the developmental molts (Van Buskirk & Sternberg, 2007), and EGF signaling acts through phospholipase C-γ/*plc-3* and inositol-1,4,5-triphosphate (IP3) to regulate ovulation (Clandinin *et al.*, 1998; Merris *et al.*, 2004). To identify the downstream signaling branch of the EGF pathway that influences adult healthspan, we asked whether RAS/*let-60*, MAPK/*mpk-1*, DAG-binding protein/*unc-13,* PLC-γ/*plc-3*, or IP3 receptor/*itr-1* are required for the old-age swimming prowess observed in the EGFR/*let-23(gf)* mutant. We conducted these assays by performing feeding RNAi to knockdown gene activities in the EGFR/*let-23(gf)* background and measuring body bend frequency in middle/late adulthood. We found that *plc-3*(RNAi) and *itr-1*(RNAi) suppress the youthful swimming phenotype of the *let-23(gf)* mutant, but RNAi interventions affecting genes in other downstream branches of EGFR signaling do not (Fig. 4B). These data implicate the downstream PLC-γ/IP3 receptor pathway, rather than the RAS pathway used in vulval fate specification or the DAG pathway used in larval

quiescence at the molts, in mediating the positive EGFR effects on swimming healthspan.

To independently confirm that the IP3R pathway can influence multiple healthspan indicators, we examined *itr-1* alleles that decrease or increase IP3 receptor signaling for impact on late adult swimming prowess, age pigment accumulation rates and adult survival. We found that gain-of-function IP3 receptor *itr-1(sy290)* mutation conferred relatively youthful swimming in 11 day old animals (Fig. 4C), whereas reduction-of-function *itr-1(sa73)* mutants exhibited accelerated swimming decline (Fig. 4D). Gain-of-function mutation in IP3 receptor also reduced age pigment accumulation (Fig. 4E, F). Increased ITR-1 activity extends median and maximum lifespan (53% increase of median lifespan, 29% increase of maximum lifespan), whereas reduced ITR-1 activity shortens culture survival (i.e., -11% increase of median lifespan, -31% increase of maximum lifespan) (Fig. 4G, H). We find that the double mutant of progeric *lin-3(rf)* with healthy aging *itr-1(gf)* exhibits healthspan extension (Fig. S8B, Supporting Information) consistent with positioning of IP3R activity downstream of (or parallel to) EGF/LIN-3 action. Thus, both RNAi studies and analysis of mutant strains indicate that elevated signaling through the IP3 receptor extends *C. elegans* healthspan and lifespan.

Taken together, our perturbations of EGF pathway components support that beneficial effects of EGFR/LET-23 signaling occur via the IP3 receptor pathway

to promote healthy adult aging and longevity in *C. elegans.* This is a previously undescribed role for the EGF/IP3R pathway in aging biology.

HPA-1 and HPA-2 influence locomotory healthspan through the EGF pathway

Having established the positive impact of EGF signaling on healthspan and defined the downstream pathway operative, we returned to address the hypothesis that HPA-1 and HPA-2 act via the EGF pathway. We confirmed that the swimming healthspan phenotypes induced by *hpa-1*(RNAi) and *hpa-2*(RNAi) depend on the activity of the EGF signaling pathway by conducting RNAi inactivation in mutants defective for specific components of EGF signaling. In wild-type, *hpa-1*(RNAi) and *hpa-2*(RNAi) significantly increase late-life swimming vigor (Fig. 1B). In contrast, neither *hpa-1(RNAi)* nor *hpa-2*(RNAi) extends swimming healthspan in mutants bearing reduction-of-function alleles in EGF pathway genes EGF/*lin-3* (Fig. S8D, Supporting Information), EGFR/*let-23* (Fig. 5A) or IP3R/*itr-1* (Fig. 5B). Furthermore, neither *hpa-1(RNAi)* nor *hpa-2*(RNAi) can further extend the swimming prowess of gain-of-function mutations in EGFR/*let-23* or IP3R/*itr-1* (Fig. 5C, D). However, *hpa-1*(RNAi) and *hpa-2*(RNAi) significantly increase late-life swimming vigor in mutants of either the RAS pathway (*let-60(n1021)rf* and *let-60(n1046)gf*) or the DAG pathway (*unc-13(e51)rf* and *dgk-1(nu62)rf*) (Fig. S9, Supporting Information), consistent with roles for HPA-1 and HPA-2 in only the downstream ITR-1 signaling branch. We conclude that the EGF pathway must be operative for beneficial HPA-1 and HPA-

2 knockdown effects, and that HPA-1 and HPA-2 exert their most significant effects on healthspan via the EGFR/ITR1 pathway.

Adult EGF/IP3R signaling can modulate locomotory healthspan

Our studies of *itr-1(rf)* used a temperature-sensitive mutation with shifts to non-permissive temperature performed just prior to the reproductive adult stage to avoid developmental defects. Despite the fact that animals were disrupted for *itr-1* activity only during adulthood, these interventions still prevent the HPA-1 and HPA-2 RNAi–dependent healthspan effects (Fig. 5B). These experiments suggest that EGFR/IP3R signaling can be activated in the adult to maintain adult robustness in swimming. Our RT/PCR experiments do find EGF isoforms (Dutt *et al.*, 2004; Van Buskirk & Sternberg, 2007) expressed even in mid/late adult in synchronized populations (data not shown) and HPA-1 and HPA-2 translational GFP fusions are co-expressed strongly in adult in posterior intestine, and glial amphid and phasmid socket cells, and a few neurons (Fig. S11, Supporting Information). Thus, HPA-1, HPA-2, and EGF isoforms are expressed during adulthood, when they can act to influence healthspan.

In sum, we document a previously unreported pathway for the regulation of healthy aging and longevity in *C. elegans* (modeled in Fig. 6), revealing unexpected roles for proteins well known to promote cell specification and cell function, and suggesting unique regulatory mechanisms that control EGF/EGFR/PLC-γ/IP3R signaling relevant to adult maintenance. One possible

model for healthspan modulation by HPA-1 and HPA-2 deficiency, suggested by homologies to ligand binding domains of EGRR and EGFR, is that HPA-1 and/or HPA-2 normally bind EGF to limit EGFR signaling. If this negative regulation is relieved, the EGFR pathway involving the downstream EGFR/PLC-γ/IP3R branch is activated to promote healthy aging.

Discussion

Pursuing an initial interest in hypothesized aging-associated functions of proteins related to extracellular ligand binding domains of DAF-2 insulin receptor, we identified two receptor-related genes, *hpa-1* and *hpa-2*, for which RNAi conferred a **h**igh **p**erformance in **a**dvanced age (Hpa) phenotype for swimming behavior. Further analysis of these novel genes revealed an unexpected but potent role of EGF signaling in promoting system-wide healthy aging and longevity in the adult that appears largely distinct from insulin signaling mechanisms. To the best of our knowledge, this is the first report that EGF signaling constitutes a major healthspan and longevity pathway. Given conservation of EGF signaling pathways and data on mouse knockouts suggestive of roles for EGF in adult maintenance, we speculate that EGF family members may play a conserved role in maintaining adult health that might be exploited for anti-aging therapies.

Newly identified molecular modulators of EGF signaling are candidate secreted EGF binding proteins

We report that EGF signaling is limited by HPA-1 and HPA-2, and suggest this can occur during adult life. Eliminating the negative regulation mediated by HPA-1 and HPA-2 activates EGFR and promotes changes that are associated with improved healthy aging. HPA-1 and HPA-2 encode proteins of 516 and 472 amino acids, respectively, predicted to be secreted due to canonical signal sequences at their N-termini. HPA-1 and HPA-2 exhibit some sequence similarity to ligand binding domains of the EGF-binding EGF receptor-related

protein ERRP and to the EGF receptor itself. Rat ERRP is primarily expressed in intestine and liver (Park *et al.*, 2001) (interestingly, *hpa-1* and *hpa-2* are expressed in the worm intestine) and can negatively regulate EGFR activities in culture models (Park *et al.*, 2001; Marciniak *et al.*, 2004) as well as *in vivo* (Schmelz *et al.*, 2007). Although the mechanism of ERRP action has not yet been clearly defined, some evidence suggests ERRP sequesters EGFR ligand TGF- . to limit signaling. The similarity of HPA-1 and HPA-2 to proteins that bind EGF suggests that one mechanism of their action could be to bind and sequester EGF to negatively regulate EGFR activity. Such an EGF-sequestering regulatory mechanism has been documented for the secreted, but structurally distinct (Klein *et al.*, 2008), Argos protein that binds to *Drosophila* EGF/Spitz to downregulate EGF signaling (Klein *et al.*, 2004). Our study constitutes the first implication of putative secreted EGF binding proteins in any EGF signaling regulation in *C. elegans.* Whether HPA-1 and HPA-2 bind *C. elegans* EGF awaits biochemical confirmation. Regardless of the precise molecular mechanism by which HPA-1 and HPA-2 normally limit EGF signaling, it is noteworthy that these novel regulators of the EGF pathway exhibit a strong biological impact on age-associated phenotypes and without dramatic phenotypes on development.

We note that our RNAi screen identified 7 additional knockdowns of receptor-related proteins that also conferred statistically significant effects on swimming healthspan (Table S1, Supporting Information). Some of these additional *hpa* genes might also participate in EGF regulation that modulates locomotory aging.

Alternatively, some might function as insulin binding proteins as originally proposed (Dlakic, 2002) to influence locomotory aging via IIS.

hpa-1 and *hpa-2* function similarly, but not identically, to impact aging

It is somewhat striking that GFP reporters for *hpa-1* and *hpa-2* are expressed with the same timing and cell expression pattern (Fig. S11, Supporting Information), yet do not appear functionally redundant for basic phenotypes or for aging phenotypes (Fig. S3, Supporting Information). Moreover, we have noted that *hpa-1* and *hpa-2* RNAi knockdowns and mutants share many phenotypes and depend upon the same downstream signal transduction pathway, suggesting that they enact similar functions. Still, it should be underscored that age pigment accumulation patterns and maximum lifespan phenotypes differ between *hpa-1* and *hpa-2* (Fig 1D, G), and thus a subset of their activities, or the levels of activity required for specific functions, appear different.

hpa-1 and *hpa-2* exert proportionately greater impact on the quality of mid-life than on overall longevity, and might thus be identified as "healthspan" genes

hpa-1 and *hpa-2* genes have not been identified in previous genetic or RNAi screens for longevity. Indeed, maximum lifespan increase for *hpa-1(tm3256)* is only on the order of 10% and is essentially undetectable for *hpa-2(tm3827)*. For both *hpa* mutants, however, the general increases in mid-life vigor as measured by swimming locomotory prowess and mid-life survival are more substantial than

longevity phenotypes. Thus the *hpa* gene activities affect mid-life outcomes proportionately more than lifespan endpoints. The implications of this observation are worth underscoring: there may exist many genes with substantial effect on healthspan but relatively little effect on maximum lifespan. Such a gene class would most likely have been missed in previous screens focused on lifespan extension. Like the study we report here, future genetic screens that focus on healthspan phenotypes may thus uncover novel molecular strategies for healthy aging.

Downstream signaling that alters calcium balance can confer healthspan benefits

After EGFR activation, the downstream signal transduction pathway that promotes healthy aging involves PLC-γ/PLC-3 and IP3 receptor/ITR-1, which regulates ER calcium release and impacts cellular calcium homeostasis. This is the first implication of Ca^{2+} action through IP3 signaling in promoting nematode healthspan and lifespan. Calcium homeostasis undoubtedly plays an important role in adult maintenance (Imura *et al.*, 2007), and has been suggested to be modulated in the long-lived Klotho mouse (Kurosu *et al.*, 2005). The dramatic benefits of the *itr-1(gf)* mutation on healthspan and lifespan, more substantial than in individual *hpa* mutants, may reflect an optimal level of pathway activity in the *itr-1(gf)* mutant background. Such activity levels might be attained by further manipulation of EGF signaling levels in other *hpa* backgrounds or by adding inputs from other signaling pathways. Regardless of how optimal signaling is

attained, our data implicate IP3R as a plausible therapeutic target for healthspan extension.

EGF exerts mechanistically distinct effects on behavioral quiescence and healthy aging

EGF signaling has elegantly been shown to induce a state of behavioral quiescence that precedes the four larval molts that occur as *C. elegans* grows to adulthood (Van Buskirk & Sternberg, 2007). Over-expression of EGF under control of a heat shock promoter (hspEGF) causes rapid cessation of pumping and slowing of locomotion, even in young adults. This role of EGF signaling is distinct from the HPA-regulated EGF signaling we characterized that systemically affects healthy aging in that: 1) hspEGF is associated with locomotory impairment and cessation of pumping (Van Buskirk & Sternberg, 2007), whereas HPA-1/2 (RNAi)-induced EGFR activation does not impact pumping rates in young adults (Fig. S2, Supporting Information) and is associated with maintained pumping and locomotory activity late into life; and, 2) molecular requirements for downstream EGF signaling are different for quiescence vs. healthspan outcomes, with hspEGF acting via DAG receptor UNC-13 (Van Buskirk & Sternberg, 2007) rather than through the ITR-1/IP3 receptor that we document influences healthspan prowess (Fig. 4B; Fig. S8B and Fig. S9, Supporting Information). Another significant difference in the experimental paradigms of EGF signaling modulation in these two studies is that overexpression studies transiently express specific EGF isoforms under heat shock stress conditions, so that time

of expression, EGF concentration and particular isoforms overexpressed are likely different from the EGF signaling that occurs (or is prevented from occurring) as a component of normal aging. Despite the different pathways for EGF signaling in *C. elegans* aging and quiescence biology, the findings that EGF can promote healthy aging, that EGF can promote quiescence via a mechanism that also intersects in part with activities that influence sleep-like behavior (such as cGMP-dependent kinase EGL-4 (Raizen *et al.*, 2006; Van Buskirk & Sternberg, 2007; Raizen *et al.*, 2008)), and that sleep is known to have a significant affect on aging quality in humans (Neikrug & Ancoli-Israel, 2009), raise the question as to whether precisely modulated EGF signaling via multiple pathways might be a component of a fundamentally conserved rest/rejuvenation mechanism that promotes effective repair processes required for adult maintenance.

EGFs as conserved promoters of healthspan

In mammals, activated EGF signaling has been associated with epithelial and other cancers and secreted negative regulator ERRP has been used as a candidate anti-cancer therapeutic (Majumdar, 2003; Majumdar, 2005). Our data introduce a new way of thinking about EGF signaling in adults—effects on non-proliferating cells can clearly be beneficial. These effects may be conserved in mammals, a hypothesis that has not yet been directly tested. Interestingly, it has been reported that triple knock-out (TKO) of EGF ligands in mice causes accelerated hair and weight loss, dermatitis and skin ulceration with aging (Luetteke *et al.*, 1999), suggesting the possibility of EGF signaling for promoting

healthy aging in mammals. The implication of EGFR and IP3R activities in a pathway for healthspan and lifespan suggests antagonistic (i.e., targeted to mammalian ERRP) and agonistic (i.e., targeted to IP3 receptor) perturbations that might be considered in anti-aging strategies directed against functional disability in advanced age.

Experimental procedures

Strains and nematode growth: *C. elegans* were grown on nematode growth media (NGM) plates streaked with *Escherichia coli* OP50-1 (a streptomycin-resistant derivative of OP50) at 20^{o}C as described (Brenner, 1974), except that temperature sensitive strains containing *itr-1(sa73)* and *daf-2(e1368)* were routinely kept at the permissive temperature of 15^{o}C. Ts strains *hsf-1(sy441)*, *let-23(n1045),* and *spe-9(hc88)* were maintained at 20^{o}C. Strains used in this study include: BA708 *spe-9(hc88) ts*; CB138 *unc-24(e138)*; DA465 *eat-2(ad465)*; DA1116 *eat-2(ad1116)*; DR1572 *daf-2(e1368) ts*; GP555 *daf-16(mgDf50)*; JT73 *itr-1(sa73)*; KP1097 *dgk-1(nu62)*; LD001 *Is007*[*skn-1::GFP, rol-6(su1006)*]; MT2123 *let-23(n1045)*; MT2124 *let-60(n1046)*; MT2136 *lin-3(n1058)/unc-8(e49) dpy-20*; MT7929 *unc-13(e51)*; PS1524 *let-23(sa62)*; PS1631 *itr-1(sy290) dpy-20(e1282)*; PS3551 *hsf-1(sy441)*; PD4251 *dpy-20(e1282) ccIs4251* [$P_{myo\text{-}3}$NLS/GFP, *dpy-20(+)*];PS1378 *itr-1(sy290) lin-3(n1058)*; TJ1052 *age-1(hx546)*; TM3256 *hpa-1(tm3256)*; TM3827 *hpa-2(tm3827)* and N2 wild type. We outcrossed *hpa-1(tm3256)* and *hpa-2(tm3827)* six times with N2 to generate strains ZB2844 and ZB2845. The *hpa-1(tm3256)* and *hpa-2(tm3827)* alleles were tracked and/or sequenced by PCR amplification of genomic sequence encompassing the deletions with specific primers for *hpa-1(tm3256)* (5'CGGTTATCTAGGTGTGGCCT3' and 5'CCATGAGCAATATTACCCGA3') and for *hpa-2(tm3827)* (5'GTAGGTGGTAATTACGCCGA3' and 5' ACTCAAACAGCCGACATCGT3'), respectively.

Age synchronization: Egg-bearing animals were collected from NGM plates with OP50. Eggs were extracted in the cleaning solution (0.7 M NaOH with 2% Na-hypochlorite (household bleach)) and then washed with M9 buffer at least three times. Eggs were transferred to 7 ml M9 buffer in a 1 liter flask and incubated overnight at 20^{o}C with fairly vigorous shaking to obtain synchronous L1 animals. The day of egg preparation was scored as day 0. For strains containing either *daf-2(e1368)* or *itr-1(sa73)*, the temperature of incubation was kept at 15^{o}C.

RNAi feeding: RNAi feeding was similar to as described in (Timmons *et al.*, 2001; Kemp *et al.*, 2009). *Escherichia coli* (HT115) producing dsRNA for individual genes was seeded onto RNAi plates containing 25 mg/ml carbenicillin with 0.2 % lactose to induce the expression of the dsRNA for the gene of interest. The negative control was conducted by seeding the plates with HT115 containing empty vector pL4440. Synchronous L1-stage animals were placed onto each plate. After growing to the young adult stage, animals were transferred away from their progeny to fresh HT115-seeded plates every 1-2 days until the end of the reproductive period (except when animals were sterile, in which case they were transferred to fresh plates at the young adult stage and then were kept on the same plate). For targeting *itr-1*, animals were initially incubated with HT115 containing pL4440 because *itr-1* RNAi induces larval arrest. After growing to young adult stage, animals were transferred to fresh plates with HT115-expressing *itr-1* dsRNA every 1-2 day.

Dietary restriction (DR): For DR protocol, bacterial food deprivation treatments were carried out as described in reference (Gems & Riddle, 2000). Agar plates were spread with a suspension of HT115 bacteria and incubated overnight at room temperature. Plates were then irradiated in a UV Stratalinker (Stratagene, La Jolla, CA), with UV-killing verified by failure to form colonies upon streaking to Luria broth (LB) plate. For the assay, synchronous L1 animals were placed onto the NGM plate with UV-killed bacteria, and were incubated at 25^{o}C. At the L4 stage, animals were transferred to fresh NGM with UV-killed bacteria. RNAi treatments were conducted at 25^{o}C by using RNAi feeding protocol described above.

Swimming analysis: For RNAi screening of 54 insulin-related genes, we used the adult sterile strain, *spe-9(hc88)*, as the wild type control to avoid progeny overgrowth in age-synchronized population. Synchronous L1 animals containing *spe-9(hc88)* were incubated at 25^{o}C, the non-permissive temperature for adult sterility, and then were treated with RNAi feeding protocol as described above. Swimming assays for RNAi-screening were performed on day 11, a mid-to-late adult stage stage (~ 60 % alive).

For the swimming assay, single worms were picked off agar plates spread with a lawn of bacteria. If animals were buried into a thick bacterial lawn, they were gently mined with a platinum wire and allowed to crawl on an unseeded agar plate for about 30 seconds to remove adherent bacteria, a protocol that did not

change the frequency of body bends per minute (See Note1 in Supporting Information). We then transferred individual animals to 1 ml M9 buffer in a 24-well plate. After a 10-30 second recovery period, we counted the number of body bends during a 30 second trial using a stereomicroscope for observation. A body bend was defined as a change in the reciprocating motion of bending at the mid-body. Only animals that could move away after a touch and could thrash were used for the swimming assay (See Note 2 in Supporting Information).

Lifespan analysis: Synchronous L1 animals were placed onto an NGM plate with OP50, and were incubated at 20-25^{o}C. Lifespan assays were initiated at young adult stage as counted from the hatch. After growing to the young adult stage, animals were transferred away from their progeny to fresh OP50-seeded plates every 1-2 day until the end of the reproductive period. For the temperature-sensitive mutant *let-23(n1045)* as well as the control (N2 wild type), animals were grown at 25^{o}C (permissive temperature) until day 5, and then were maintained at 15^{o}C (non-permissive temperature). For temperature-sensitive mutant *itr-1(sa73)*, the temperature of incubation was kept at 15^{o}C (permissive temperature) during growth up to 5 days in both mutants and N2 wild type, and then shifted to 20^{o}C (non-permissive temperature). For RNAi lifespan experiments, age-synchronous animals were grown at 25^{o}C and were treated with the RNAi feeding protocol as described above. Animals that were lost, or exploded, or died from internal hatching of progeny were censored at the time of the event. Survival analyses were performed using the Kaplan Meier method on

censored data, and the significance of differences between survival curves calculated using the log rank test. The statistical software used was GraphPad Prism v.5.02 (GraphPad Software, Inc., La Jolla, CA 92037 USA), which also computed the median lifespan. Maximum lifespan was determined by taking the mean age at death of the longest-lived 10% of a given test population (Sutphin & Kaeberlein, 2008). The unpaired t-test was used to determine statistical significance and calculate P-values for the mean and maximum lifespan.

Pharyngeal pumping decline assays: Age-synchronous animals were grown at 25^{o}C on *E. coli* strains at 25^{o}C as described above. The number of contractions in the terminal bulb of pharynx was measured on Days 3, 5 and 7. For each strain, 10-15 different animals were scored during a 60 second trial.

***In vivo* spectrofluorimetric quantitation of age pigments:** Age-synchronized animals were grown and collected as described for swimming assays. Autofluorescent peaks corresponding to age pigments (which change with age, excitation/emission pair 340 nm/430 nm) and tryptophan (which remain constant with age, excitation/emission pair 290 nm/330 nm) were measured from 50 worms by using an *in vivo* spectrofluorimetory (SkinSkan, JY Horiba, Edison, NJ, USA), as described previously (Gerstbrein *et al.*, 2005). Often for analysis the ratio of AGE/TRP is compared to normalize. A Zeiss Axioplan 2 Microscope with a UV cube (excitation bondpass filter centered at 360 nm and 420 nm emission

longpass filter) was used to image animals and to verify fluorescence intensity with the results from the spectrofluorimeter.

Fluorescence microscopy: Animals were observed and photographed using a Zeiss Axioplan 2 Microscope with a Real-14 Precision Digital camera. Observations of GFP expression were recorded and color images were taken from the documentation of results with Magnafire software. For counting the number of GFP-labeled nuclei in the muscle, the transgenic strain PD4251 and its double-mutant strain, which carries a gain-of-function *let-23(sa62)* allele, were continuously grown at 25^{o}C after age-synchronized preparation, as described above. Animals were then observed using the 40x objective of a fluorescence microscope (Herndon *et al.*, 2002; Cao *et al.*, 2007).

Quantitation of fluorescence intensity in the ASI neuron: The strain LD001, which expresses *skn-1::GFP* in the ASI neurons, was observed as described in ref (Bishop & Guarente, 2007). Fluorescence images were collected from worms subjected to RNAi bacteria feeding or dietary restriction (DR) on day 4 at 25^{o}C. Fluorescence intensity in the ASI was quantitated by Image J software [available from part of National Institute of Health (NIH) website: http//rsb.info.nih.gov/ij/], as described previously.

Acknowledgments

We thank the following people and institutes for providing the strains used in this study: A. Fire for PS4251, P. Sternberg for PS1524, the National BioResource Project at Tokyo Women's Medical University School of Medicine for *tm3256* and the *Caenorhabditis* Genetic Center supported by NIH NCRR for many strains. We also thank A. Fire for plasmid vectors; J. Ahringer for RNAi library; B. Grant for helpful discussion; M. Barr and C. Rongo for critical reading of this manuscript; and H. Suda for advice on mortality rate analysis. This work was supported by grants from the National Institute on Aging (AG024882), The Ellison Medical Foundation, and The Paul Glenn Foundation.

Figure Legends

Fig. 1. *hpa-1* and *hpa-2* deficiencies promote healthy aging in *C. elegans*. (A) Summary of screen strategy for RNAi interventions that confer **h**igh **p**erformance in **a**dvanced age (*Hpa* phenotype). We fed bacteria expressing dsRNA to synchronized L1 larvae of ts sterile mutant *spe-9*, 25^{o}C, and counted the number of body bends during 30 second swim trials in M9 buffer at day 11 post-hatching (post-reproductive animals in mid/late adult life, slightly more than halfway through maximum wt adult lifespan at this temperature; ~ 60% alive).

(B) RNAi inactivation of *hpa-1* and *hpa-2* extends swimming healthspan in wild type N2. Negative control was fed with empty vector. Each trial count was for 30 animals collected from a population of 150-250 synchronized animals (three trials). Error bars represent the standard error of the mean (s.e.m.). Unpaired two tailed *t*-test (control versus *hpa-1*, *hpa-2* or positive control *age-1* RNAi on each day), ***P< 0.0001.

(C) *hpa-1(tm3256)* and *hpa-2(tm3827)* deletion mutants exhibit enhanced swimming performance in advanced age. *age-1(hx546)* mutants were used as a positive control for *Hpa* phenotype. Day 3 is the first day of adult life in animals raised at 25^{o}C, as indicated by egg-laying onset (two trials). Error bars represent s.e.m.. Unpaired two tailed *t*-test (N2 versus mutant on each day), ***P< 0.0001. Note that differences in onset of decline between RNAi-treated animals (panel

1B) and actual deletion mutants (panel 1C) may reflect the partial gene inactivation effects of RNAi.

(D) Quantitative measurement of AGE pigment levels for wild type N2, positive control *age-1(hx546), hpa-1(tm3256),* and *hpa-2(tm3827*), 25^{o}C. The AGE pigment score is normalized as the ratio of fluorescence units for AGE pigments / tryptophan fluorescence (three independent experiments, 50 animals per strain). Error bars, s.e.m., *P* values, unpaired two-tailed *t*-test, **P*< 0.05 and ***P*< 0.01. Although age pigment scores are low relative to wt on the first day of adult life in both *hpa-1* and *hpa-2*, only *hpa-1* maintains low age pigment levels later into adulthood.

(E) The *hpa-1* mutant has low age pigment levels in old age. Images are taken under fluorescent light with identical exposures, 25^{o}C. The gut houses autofluorescent lipofuscin, sequestered into lysosomes (Clokey & Jacobson, 1986). Top, N2; bottom, *hpa-1(tm3256).*

(F) The age-associated decline in pumping rate is delayed in aging *hpa-1* and *hpa-2* deletion mutants. *hpa-1(tm3256)* and *hpa-2(tm3827)* deletion mutants exhibit enhanced pumping performance in advanced age. At least fifteen animals were recorded for each trial (two trials). Day 3 is first day of adult life in animals raised at 25^{o}C, as indicated by egg-laying onset. Error bars represent s.e.m.. Unpaired two tailed *t*-test (N2 versus mutant on each day), ****P*< 0.0001.

(G) Comparative survival curves for wild type N2, *age-1(hx546)*, *hpa-1(tm3256),* and *hpa-2(tm3827)*. Details of data in Table S3, Supporting information.

Fig. 2. *hpa-1* and *hpa-2* (RNAi) can extend locomotory healthspan via a pathway distinct from insulin/IGF-1 signaling (IIS) and some dietary restriction (DR) indicators.

(A) Assays of *hpa-1* and *hpa-2* (RNAi) effects on representative mutants of the insulin signaling pathway. *daf-16(mgDf50)* is a progeric null mutant; *hsf-1(sy441)* is a progeric temperature-sensitive mutant. Mutants were fed with bacteria expressing indicated dsRNA; control is empty vector. Error bars represent s.e.m., unpaired two tailed *t*-test (control versus *hpa-1* or *hpa-2* RNAi on each day, **P*< 0.01, ***P*< 0.001, ****P*< 0.0001, NA; not available since population is largely dead). Note that to avoid developmental consequences of genetic disruption, temperature-sensitive *hsf-1(sy441)* mutants were grown at permissive temperature of 15-20^{o}C until day 5 after hatching (first day adults) and were then transferred to restrictive temperature 25^{o}C at the beginning of adult life. Thus *hsf-1* activities are disrupted only during adulthood. Since *hpa-1(RNAi)* and *hpa-2(RNAi)* can still extend locomotory healthspan when key donwstream transcription factors in the IIS pathway are deficient, *hpa-1* and *hpa-2* appear able to act, at least in part, independently of the IIS pathway. Note that temperature shifts required for some studies can influence lifespan both by

temperature and genetic changes; direct comparison between the same experimental days in different temperature regimens thus cannot be made.

(B) Effects of *hpa-1* and *hpa-2* RNAi on DR constitutive mutant *eat-2. eat-2(ad1116)* mutants were fed with bacteria expressing dsRNA (control is empty vector) at 25^{o}C. Error bars represent s.e.m., unpaired two tailed *t*-test (control versus *hpa-1* or *hpa-2* (RNAi) on each day, ****P*< 0.0001).

(C) The excitation maximum for the age pigment fluorescence shifts at 320 nm for DR-mimiced mutant *eat-2(ad465)*, while it remains constant at 340 nm for wild-type, *age-1(hx546)*, *hpa-1(tm3256)* and *hpa-2(tm3827)* animals.

(D) Representative images of SKN-1::GFP in the ASI neurons after RNAi treatments or DR. Note significant increase under food dilution DR.

(E) Activation of SKN-1 in the ASI neurons is induced by DR but not by *hpa-1* and *hpa-2* (RNAi). We quantitated fluorescence at 25^{o}C in the ASI neurons in adults harboring a *skn-1::gfp* reporter, which increases GFP expression under the DR conditions with UV-killed bacteria, consistent with a previous report (Bishop & Guarente, 2007). *hpa-1* and *hpa-2* RNAi treatments do not change the level of SKN-1::GFP in the ASI neurons, supporting that their knockdown is not associated this type of DR activation, or that if they do, SKN-1 activation occurs

upstream of HPA function. Error bars, s.e.m.; *p* value in unpaired two-tailed *t*-test ,***$P < 0.0001$.

Fig. 3. Activation of the EGF receptor LET-23 promotes healthy aging.

(A) Activation of the EGFR *let-23* extends swimming healthspan. The gain-of-function *let-23(sa62)* mutant strongly increases swimming performance in advanced age. Data are for 25^{o}C, though similar effects are observed also at 20^{o}C. Error bars represent s.e.m.. Unpaired two tailed *t*-test (N2 versus *let-23(sa62)* mutant on each day), ***$P< 0.0001$.

(B) Disruption of EGFR activity accelerates swimming decline in aging animals. For swimming assay, the reduction-of-function *let-23(n1045)rf* mutant and N2 wild type were grown continuously at restrictive temperature of 20^{o}C. Error bars represent s.e.m.. Unpaired two tailed *t*-test (N2 versus *let-23(n1045)* mutant on each day), ***$P< 0.0001$.

(C) Age-related deterioration of *C. elegans* body wall muscle as indicated by GFP fluorescence decline of a p_{myo-3}NLS::GFP fusion. The GFP reporter is localized to muscle nuclei, and becomes progressively sequestered and dims with age (Herndon *et al.*, 2002). Representative whole-animal view of the wild type and the *let-23(sa62)gf* mutant expressing GFP in the nuclei of body wall muscle at ages indicated (25^{o}C). When the EGFR is activated, signal dimming occurs more slowly, consistent with muscle healthspan extension.

(D) Quantitation of the number of fluorescent nuclei in the wild type and the *let-23(sa62)gf* mutant. 15 animals of each strain were scored in 2 independent trials. Error bars, s.e.m.. *P* value for unpaired two-tailed *t*-test, ***$P < 0.0001$.

(E) Age pigments accumulate at a reduced rate when EGFR is activated. Representative same-exposure photographs of fluorescent species in the intestine of wild type N2 versus *let-23(sa62)* mutants at day 11 (25^{o}C).

(F) Measurement of AGE pigment accumulation for wild type N2 and *let-23(sa62)gf*. AGE pigment scores were normalized as the relative fluorescence units for AGE pigments divided by tryptophan fluorescence. Data are from three independent experiments, 50 animals total for each strain; au arbitrary units, error bars, s.e.m.; *P* value, unpaired two-tailed *t*-test, *$P < 0.01$.

(G) The EGFR(gf) mutant exhibits enhanced lifespan, 20^{o}C. Details of data in Table S3, Supporting information.

(H) The EGFR(rf) mutant is short-lived. For lifespan assay, strains were grown at permissive temperature of 25^{o}C until day 5 after hatching, and then transferred to the non-permissive temperature of 15^{o}C. Details of data in Table S3, Supporting information.

Fig. 4. The PLC-γ/IP3 receptor signaling branch mediates EGFR healthy locomotory aging benefits.

(A) Epidermal growth factor (EGF) signaling activates multiple pathways in *C. elegans.* EGF ligands are encoded by the *lin-3* gene(Hill & Sternberg, 1992). EGF receptor LET-23 can activate at least three distinct downstream pathways. The LET-60/RAS MAP kinase pathway influences cell fate specification (Beitel *et al.*, 1990; Han & Sternberg, 1990; Lackner *et al.*, 1994; Wu & Han, 1994). Phospholipase C can act via diacyl glycerol binding protein UNC-13 to induce quiescent behavior during larval molts (Van Buskirk & Sternberg, 2007). The ER calcium release channel IP3 receptor acts in another pathway branch to influence ovulation (Clandinin *et al.*, 1998; Merris *et al.*, 2004).

(B) RNAi knockdown of key genes in pathways downstream of EGFR implicates the PLC-γ/IP3 receptor branch in healthy locomotory aging. EGFR/*let-23(sa62)gf* mutant swimming in mid/late age was assayed in feeding RNAi experiments for the indicated genes (25^{o}C). Note that *itr-1* RNAi was initiated on day 4 to avoid larval arrest caused by *itr-1(RNAi)*. The fact that this RNAi intervention blocks benefits of EGFR(gf) both supports that *itr-1* is a required downstream effector of LET-23(gf) and indicates that IP3 receptor activity is required during adult life for extended locomotory healthspan. Error bars represent s.e.m.. Unpaired two tailed *t*-test (control versus *let-60*, *mpk-1*, *plc-3*, *unc-13* or *itr-1* RNAi) ***P< 0.0001. Note that to cross-verify results from MAPK and DAG pathways, we performed RNAi in the “reverse” direction, testing *hpa-1*

and *hpa-2* (RNAi) on *let-60(rf), let-60(gf), unc-13* and *dgk-1(gf)* mutants, see Fig. S9, Supporting information).

(C-H) Genetic activation of IP3 receptor elicits healthy aging and longevity. (C) Activation of the IP3R *itr-1* elicits youthful swimming in old age. The *itr-1(sy290)gf* mutant exhibits markedly enhanced swimming performance in adulthood at 25^{o}C. Error bars represent s.e.m.. Unpaired two tailed *t*-test (N2 versus *itr-1(sy290)* mutant on each day): ****P*< 0.0001.

(D) Reduction of IP3 receptor/ITR-1 activity from early adulthood accelerates swimming decline in advanced age. For assay, *itr-1(sa73)rf* strains and N2 wild type were grown at permissive temperature of 15^{o}C until day 5 after hatching (first day of sexual maturity), and were then transferred to the non-permissive temperature (25^{o}C). Error bars represent s.e.m.. Unpaired two tailed *t*-test (N2 versus *itr-1(sa73)* mutant on each day): ****P*< 0.0001. Data indicate that limiting IP3R signaling in only the adult stage has deleterious consequences for locomotory aging.

(E-F) Age pigments are low in aging *itr-1(gf)* mutants. (E) Representative photographs of fluorescent species in the intestine of wild type N2 versus *itr-1(sy290)gf* worms at day 11. (F) Quantitative measurement of AGE pigment accumulation for wild type N2 and *itr-1(sy290)gf*. Indicated are AGE/TRP ratios; unpaired two tailed *t*-test, ***P*< 0.001, ****P*< 0.0001.

(G) Survival curve for *itr-1(sy290)gf* indicates extension of both mean and maximum lifespan, 20^{o}C. Details of data in Table S3, Supporting information.

(H) Survival curve for *itr-1(sa73)rf* reveals shortening of both mean and maximum lifespan. For lifespan assay, strains were grown at permissive temperature of 15^{o} C until day 5 after hatching, and then transferred to the non-permissive temperature of 20^{o} C. Details of data in Table S3, Supporting information.

Fig. 5. HPA-1 and HPA-2 influence locomotory aging through the EGF pathway.

Effect of EGFR and IP3R mutations on swimming vigor under conditions of *hpa-1* and *hpa-2* RNAi. (A) *let-23(n1045)rf* mutants. (B) *itr-1(sa73)rf* mutants. (C) *let-23(sa62)gf* mutants. (D) *itr-1(sy290)(gf)* mutant were introduced to indicated dsRNAs; control is empty vector. Error bars represent s.e.m., unpaired two tailed *t*-test (control versus *hpa-1* or *hpa-2* RNAi on each day: unlike wt strains, *P* values support no significant differences). Note: *let-23(n1045)rf* mutants were continuously grown at restrictive temperature of 20^{o}C. *itr-1(sa73)rf* strains were grown at permissive temperature of 15^{o}C until day 5 after hatching (first day of egg laying), and then transferred to the non-permissive temperature (25^{o}C). Other experiments were conducted at 25^{o}C.

Fig. 6. Model for HPA-1 and HPA-2 modulation of EGF signaling in aging *C. elegans*.

HPA-1 and HPA-2 are secreted proteins that might bind LIN-3/EGF via domains related to EGF binding regions of EGF receptor to limit signaling. Alternatively, HPA-1 and HPA-2 might interact with EGFR/LET-23 to prevent EGF/LIN-3 binding. In either case, the activities of HPA-1 and HPA-2 normally down-regulate EGF signaling. When HPA-1 or HPA-2 are disrupted, EGF signaling is increased, with the EGFR activating the downstream signaling pathway that includes phospholipase-C (PLC-3) and the IP3 receptor (ITR-1) to promote healthspan as evidenced by low age pigment accumulation, extended locomotory function, and increased median lifespans. Note that activation of ITR-1 signaling in the adult appears necessary to confer a healthspan benefit for locomotory aging. Activation of the EGF or IP3R pathways later in life could be a therapeutic consideration for combating sarcopenia and other aspects of age-related decline.

Figure 1

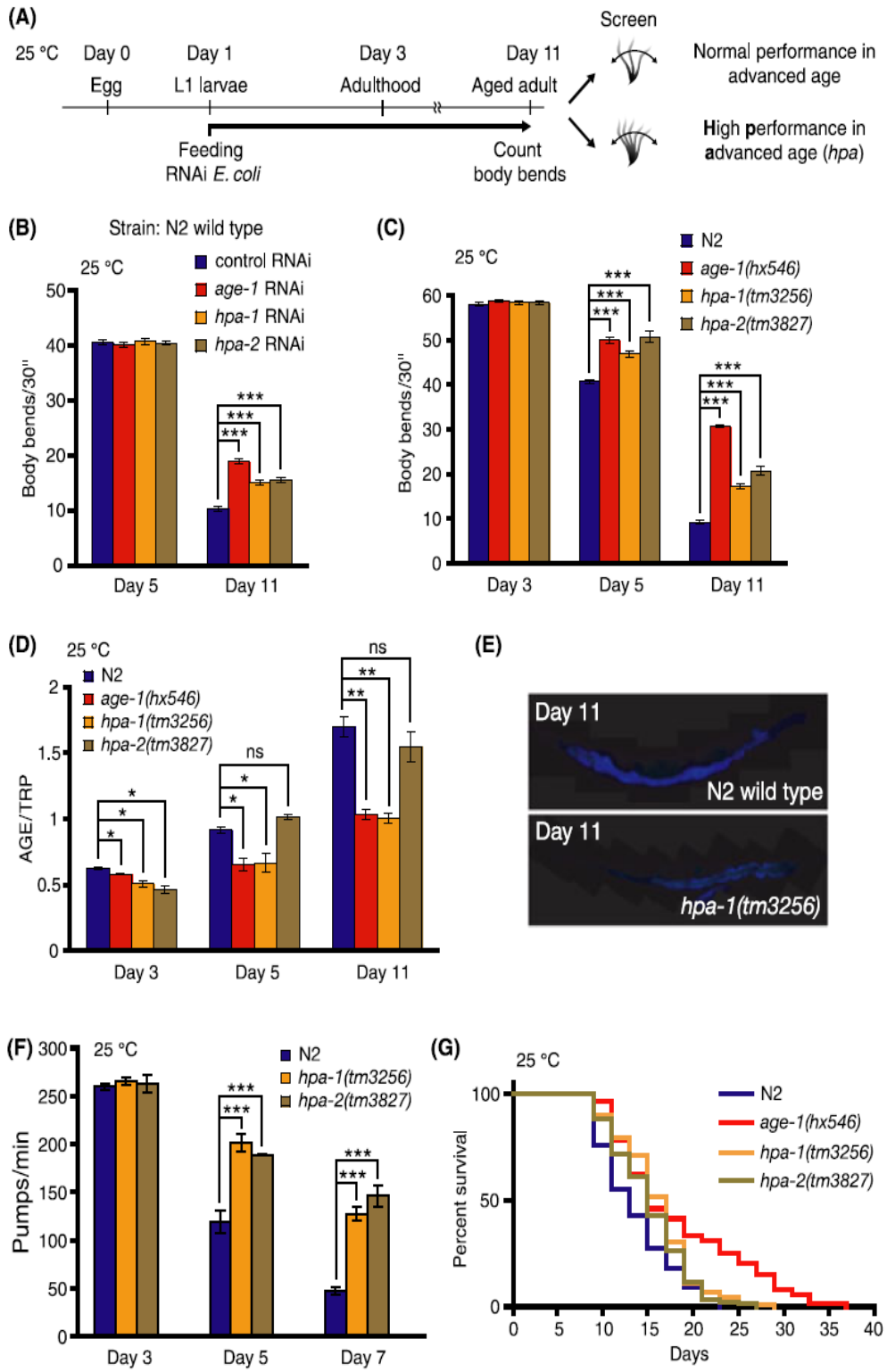
(A)
25 °C
Day 0
Egg
Day 1
L1 larvae
Day 3
Adulthood
Day 11
Aged adult
Screen
Normal performance in advanced age
High performance in advanced age (hpa)
Feeding RNAi E. coli
Count body bends
(B)
Strain: N2 wild type
25 °C
control RNAi
age-1 RNAi
hpa-1 RNAi
hpa-2 RNAi
Body bends/30''
Day 5
Day 11
(C)
25 °C
N2
age-1(hx546)
hpa-1(tm3256)
hpa-2(tm3827)
Body bends/30''
Day 3
Day 5
Day 11
(D)
25 °C
N2
age-1(hx546)
hpa-1(tm3256)
hpa-2(tm3827)
AGE/TRP
ns
Day 3
Day 5
Day 11
(E)
Day 11
N2 wild type
Day 11
hpa-1(tm3256)
(F)
25 °C
N2
hpa-1(tm3256)
hpa-2(tm3827)
Pumps/min
Day 3
Day 5
Day 7
(G)
25 °C
N2
age-1(hx546)
hpa-1(tm3256)
hpa-2(tm3827)
Percent survival
Days

Figure 2

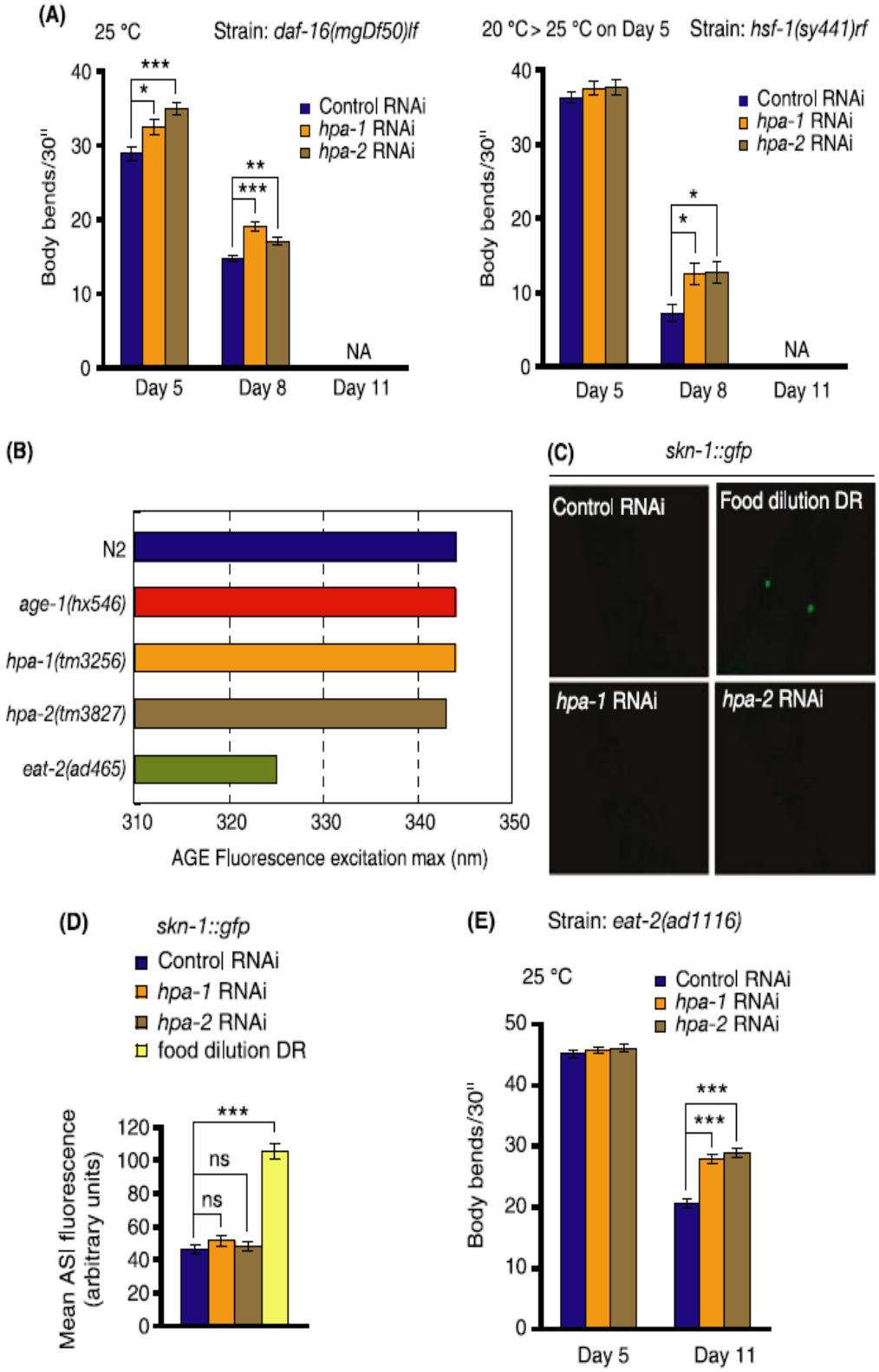
(A)
25 °C
Strain: daf-16(mgDf50)lf
20 °C > 25 °C on Day 5
Strain: hsf-1(sy441)rf
Body bends/30''
Control RNAi
hpa-1 RNAi
hpa-2 RNAi
Day 5
Day 8
Day 11
NA
(B)
N2
age-1(hx546)
hpa-1(tm3256)
hpa-2(tm3827)
eat-2(ad465)
AGE Fluorescence excitation max (nm)
(C)
skn-1::gfp
Control RNAi
Food dilution DR
hpa-1 RNAi
hpa-2 RNAi
(D)
skn-1::gfp
food dilution DR
Mean ASI fluorescence (arbitrary units)
ns
(E)
Strain: eat-2(ad1116)
25 °C

Figure 3

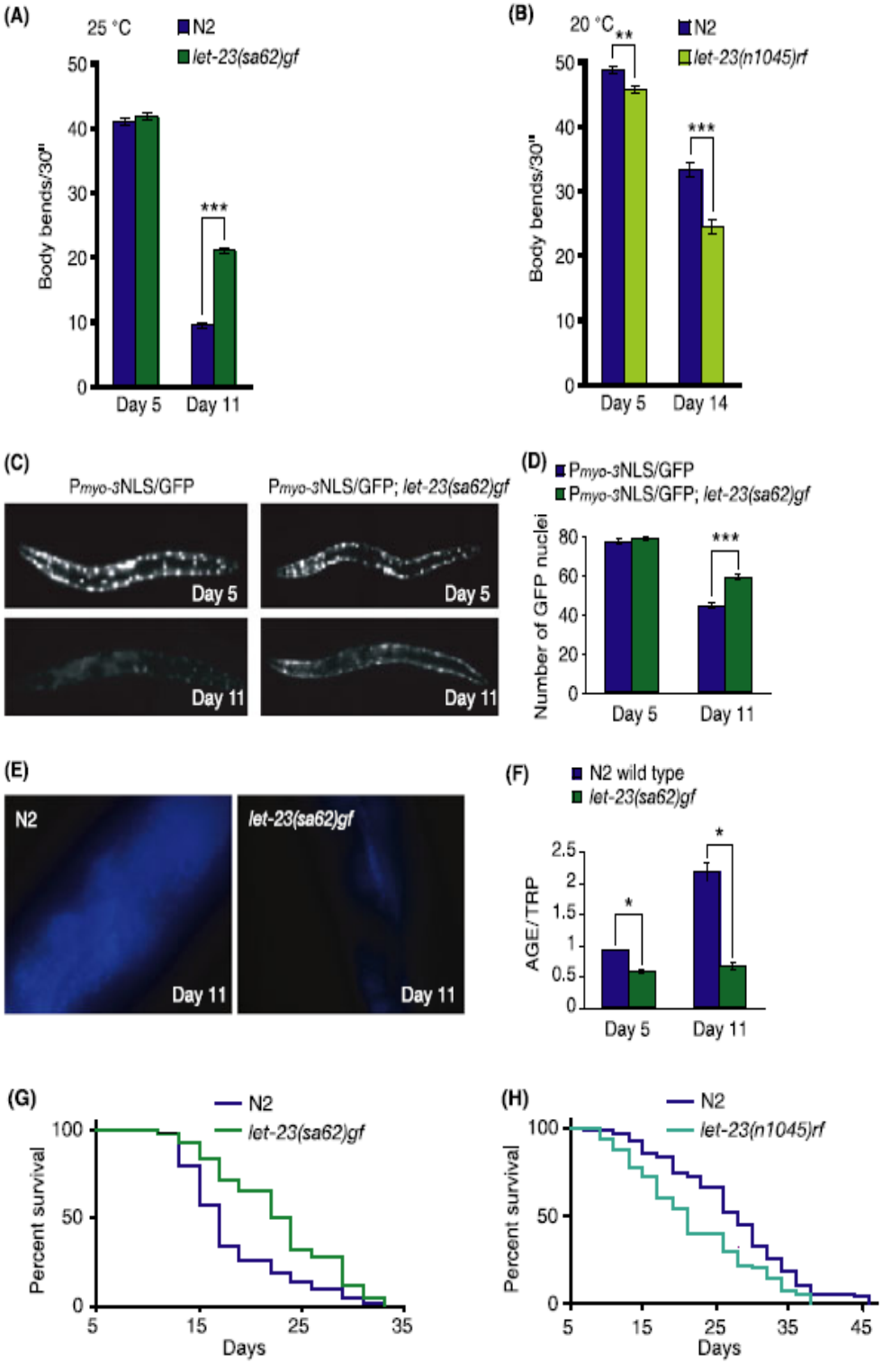
(A)
25 °C
N2
let-23(sa62)gf
Body bends/30"
50
40
30
20
10
0
***
Day 5
Day 11
(B)
20 °C
**
N2
let-23(n1045)rf
Body bends/30"
***
Day 5
Day 14
(C)
Pmyo-3NLS/GFP
Pmyo-3NLS/GFP; let-23(sa62)gf
Day 5
Day 5
Day 11
Day 11
(D)
Pmyo-3NLS/GFP
Pmyo-3NLS/GFP; let-23(sa62)gf
Number of GFP nuclei
80
60
40
20
0
***
Day 5
Day 11
(E)
N2
let-23(sa62)gf
Day 11
Day 11
(F)
N2 wild type
let-23(sa62)gf
AGE/TRP
2.5
2
1.5
1
0.5
0
*
*
Day 5
Day 11
(G)
N2
let-23(sa62)gf
Percent survival
100
50
0
5
15
25
35
Days
(H)
N2
let-23(n1045)rf
Percent survival
100
50
0
5
15
25
35
45
Days

Figure 4

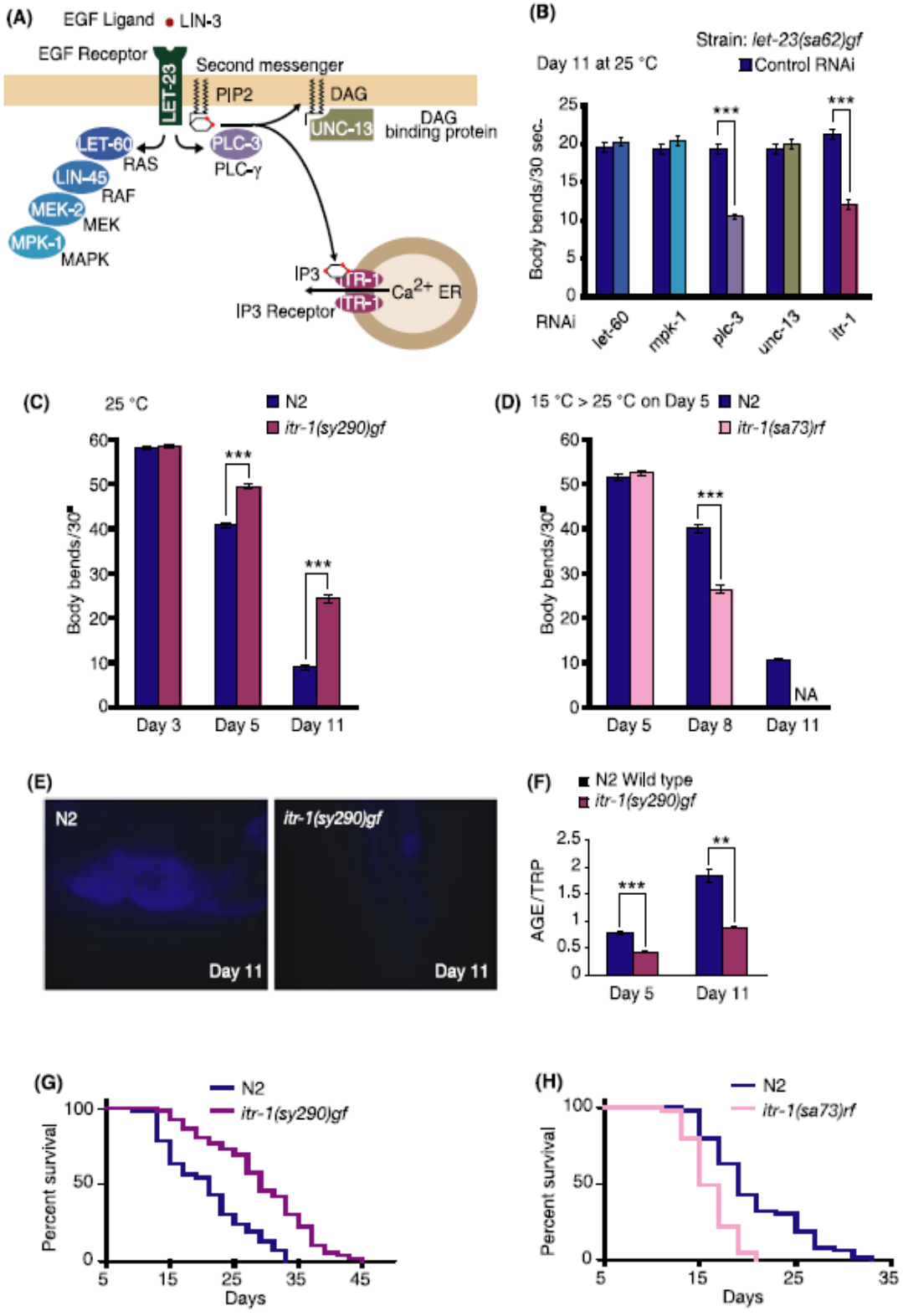
(A)
EGF Ligand
LIN-3
EGF Receptor
LET-23
Second messenger
PIP2
DAG
UNC-13
DAG binding protein
LET-60
RAS
PLC-3
PLC-γ
LIN-45
RAF
MEK-2
MEK
MPK-1
MAPK
IP3
ITR-1
Ca2+ ER
IP3 Receptor
(B)
Strain: let-23(sa62)gf
Day 11 at 25 °C
Control RNAi
Body bends/30 sec.
RNAi
let-60
mpk-1
plc-3
unc-13
itr-1
(C)
25 °C
N2
itr-1(sy290)gf
Body bends/30"
Day 3
Day 5
Day 11
(D)
15 °C > 25 °C on Day 5
N2
itr-1(sa73)rf
Body bends/30"
Day 5
Day 8
Day 11
NA
(E)
N2
itr-1(sy290)gf
Day 11
Day 11
(F)
N2 Wild type
itr-1(sy290)gf
AGE/TRP
Day 5
Day 11
(G)
N2
itr-1(sy290)gf
Percent survival
Days
(H)
N2
itr-1(sa73)rf
Percent survival
Days

Figure 5

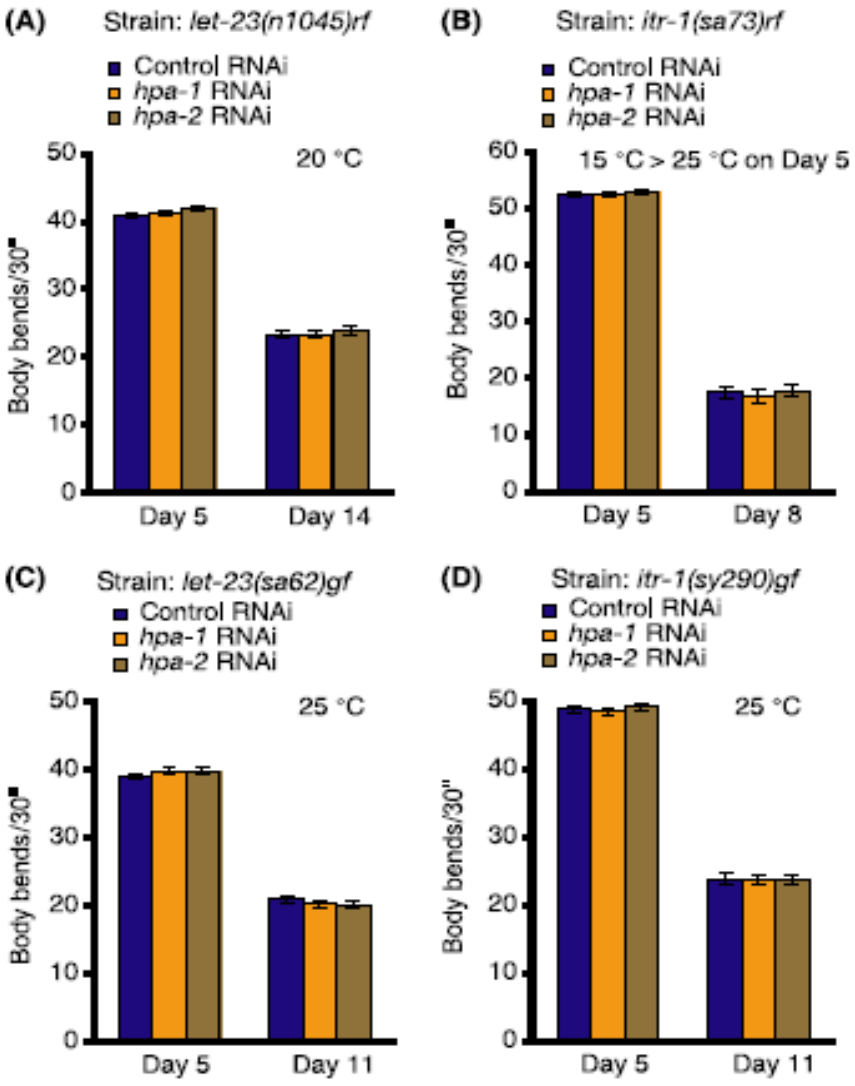
(A)
Strain: let-23(n1045)rf
Control RNAi
hpa-1 RNAi
hpa-2 RNAi
20 °C
Body bends/30"
Day 5
Day 14
(B)
Strain: itr-1(sa73)rf
Control RNAi
hpa-1 RNAi
hpa-2 RNAi
15 °C > 25 °C on Day 5
Body bends/30"
Day 5
Day 8
(C)
Strain: let-23(sa62)gf
Control RNAi
hpa-1 RNAi
hpa-2 RNAi
25 °C
Body bends/30"
Day 5
Day 11
(D)
Strain: itr-1(sy290)gf
Control RNAi
hpa-1 RNAi
hpa-2 RNAi
25 °C
Body bends/30"
Day 5
Day 11

Figure 6

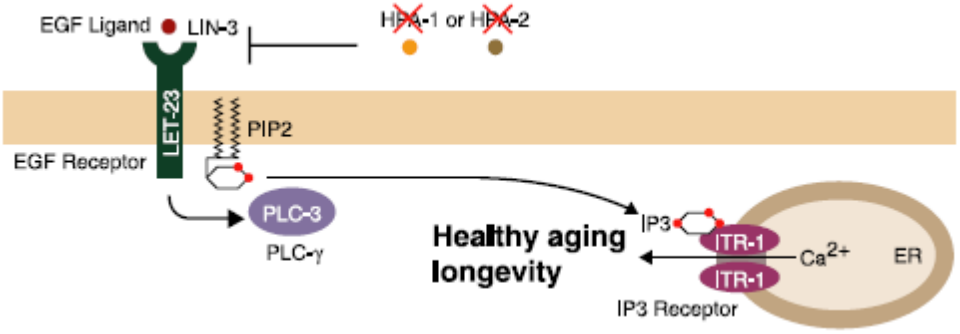
EGF Ligand
LIN-3
HPA-1 or HPA-2
LET-23
PIP2
EGF Receptor
PLC-3
PLC-γ
Healthy aging
longevity
IP3
ITR-1
ITR-1
Ca2+
ER
IP3 Receptor

Sup Figure 1

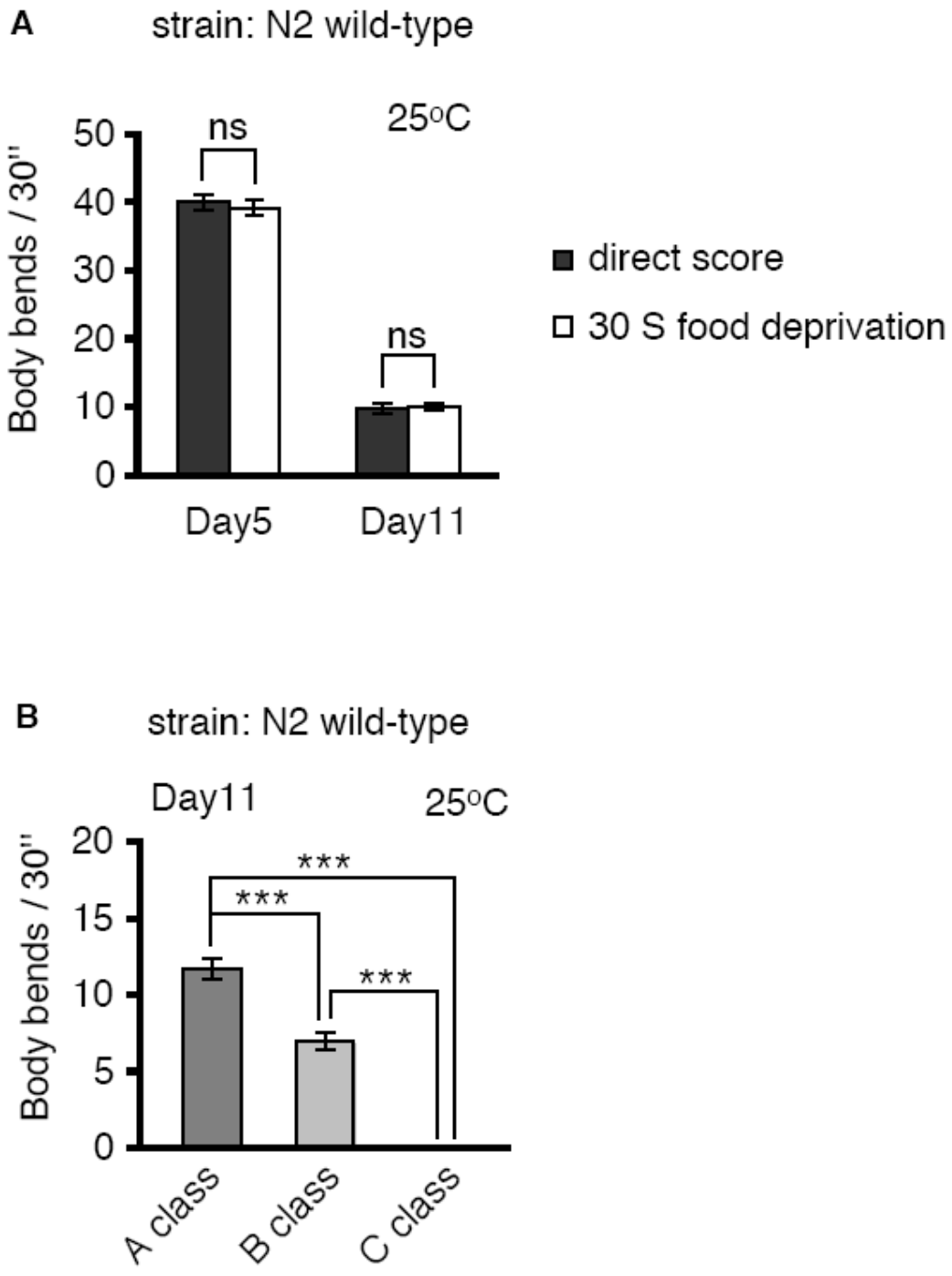
A
strain: N2 wild-type
25°C
Body bends / 30''
50
40
30
20
10
0
ns
ns
Day5
Day11
direct score
30 S food deprivation
B
strain: N2 wild-type
Day11
25°C
Body bends / 30''
20
15
10
5
0
***
***
***
A class
B class
C class

Sup Figure 2

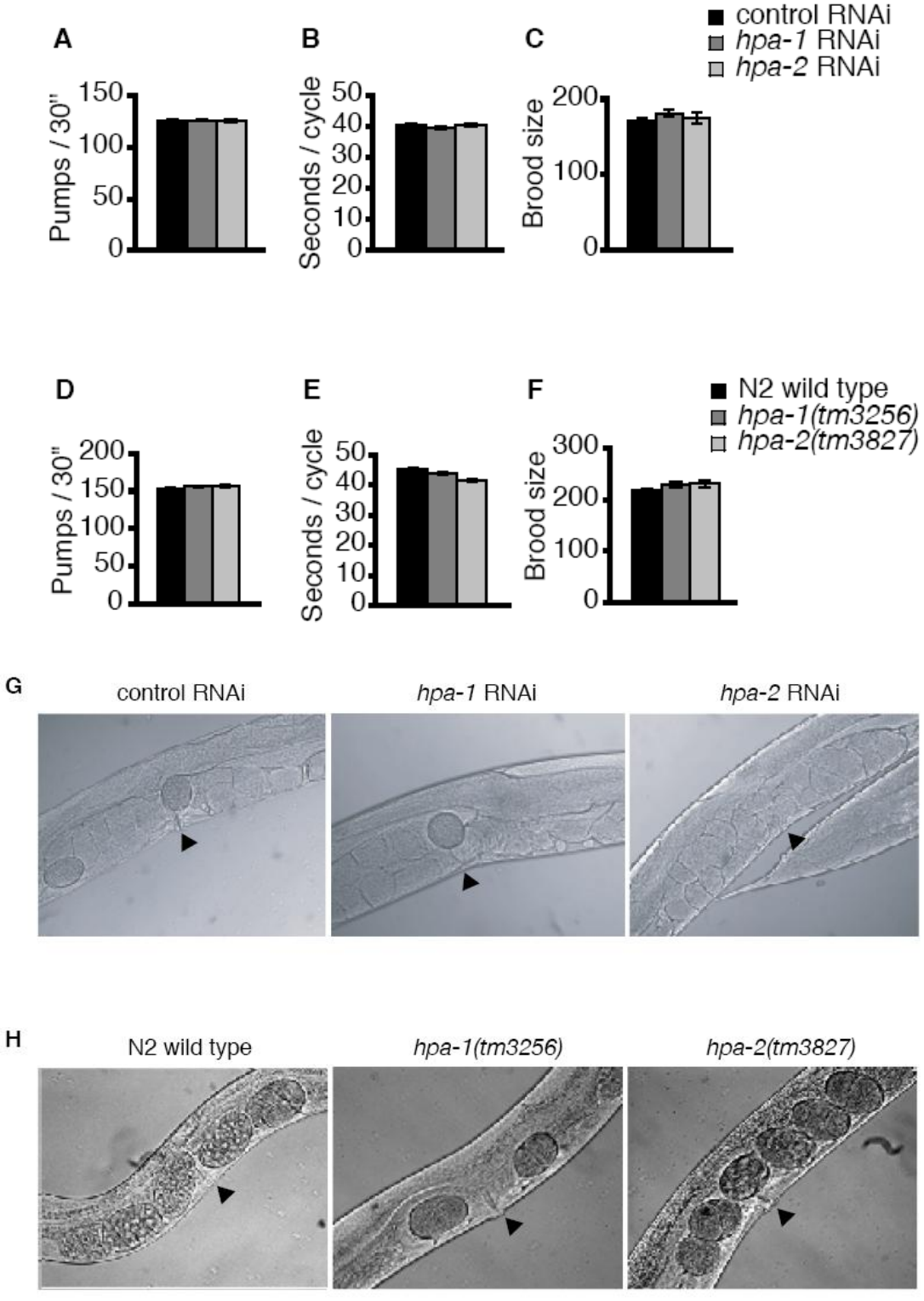
A
B
C
control RNAi
hpa-1 RNAi
hpa-2 RNAi
Pumps / 30"
150
100
50
0
Seconds / cycle
50
40
30
20
10
0
Brood size
200
100
0
D
E
F
N2 wild type
hpa-1(tm3256)
hpa-2(tm3827)
Pumps / 30"
200
150
100
50
0
Seconds / cycle
50
40
30
20
10
0
Brood size
300
200
100
0
G
control RNAi
hpa-1 RNAi
hpa-2 RNAi
H
N2 wild type
hpa-1(tm3256)
hpa-2(tm3827)

Sup Figure 3

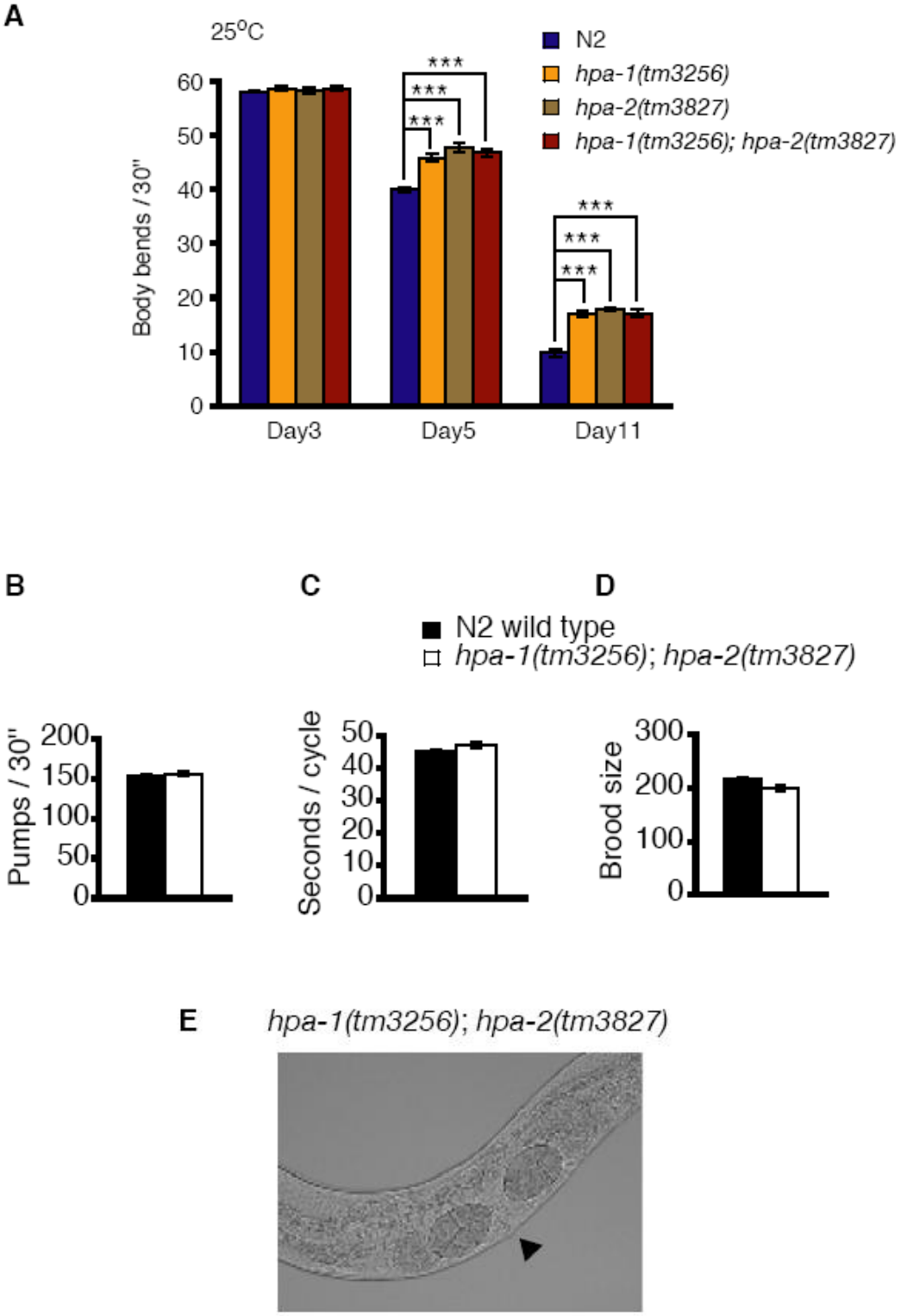
A
25°C
N2
hpa-1(tm3256)
hpa-2(tm3827)
hpa-1(tm3256); hpa-2(tm3827)
Body bends / 30''
0
10
20
30
40
50
60
***
***
***
***
***
***
Day3
Day5
Day11
B
Pumps / 30''
0
50
100
150
200
C
Seconds / cycle
0
10
20
30
40
50
D
N2 wild type
hpa-1(tm3256); hpa-2(tm3827)
Brood size
0
100
200
300
E
hpa-1(tm3256); hpa-2(tm3827)

Sup Figure 4

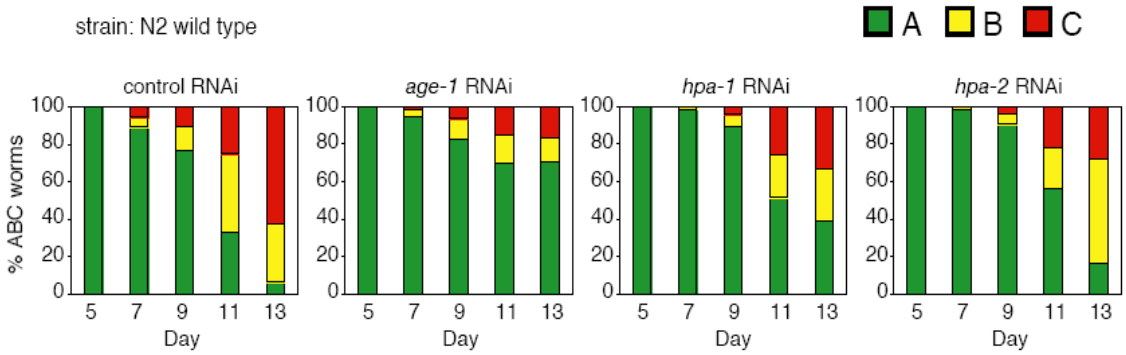

Sup Figure 5

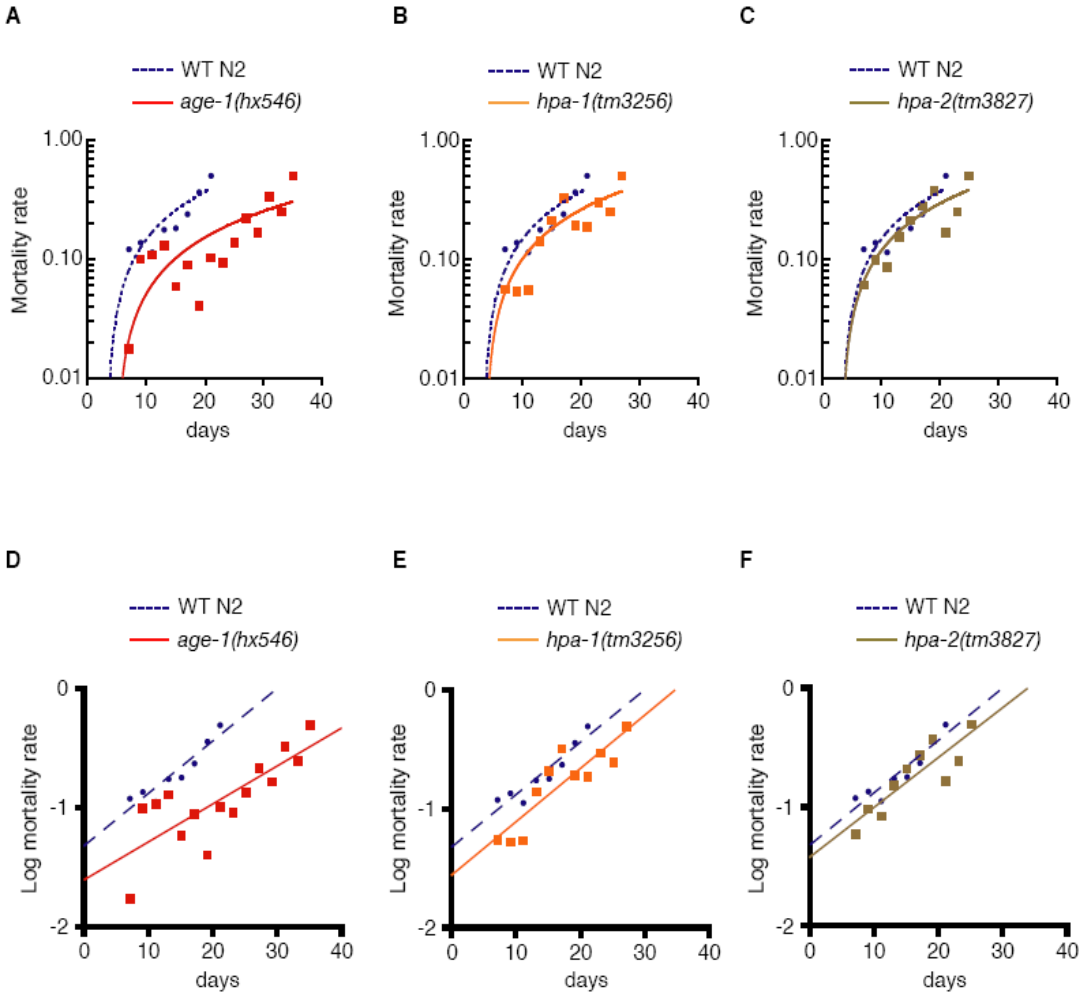

Sup Figure 6

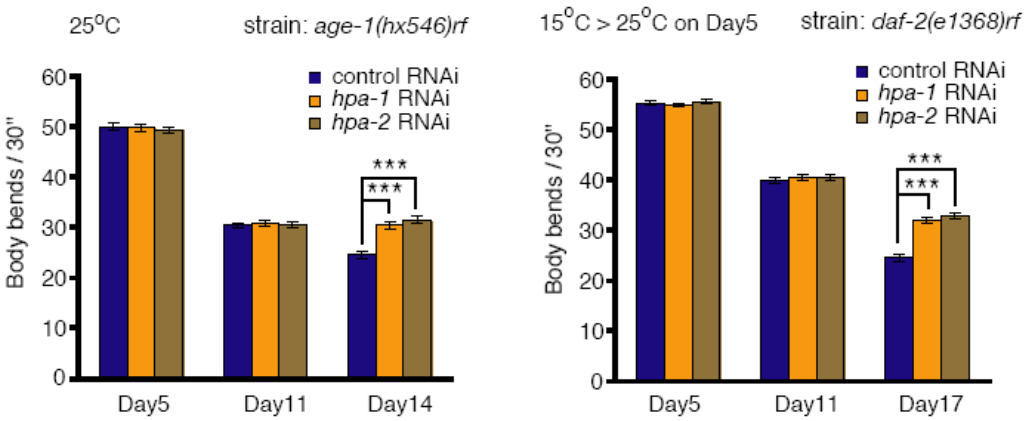

Sup Figure 7

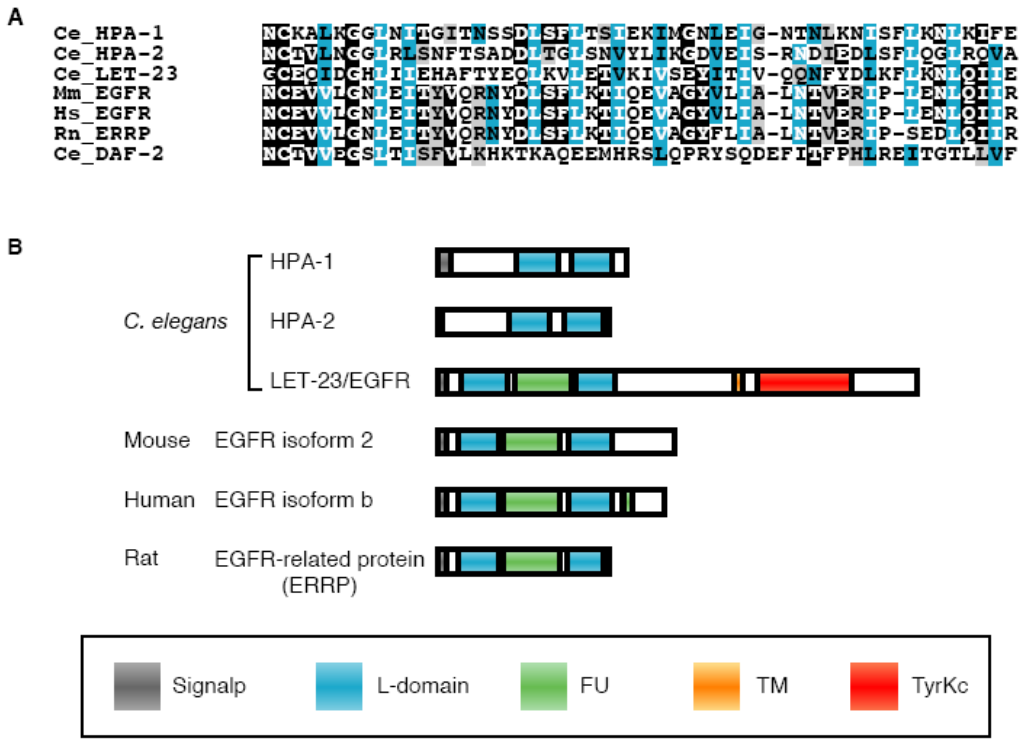

Sup Figure 8

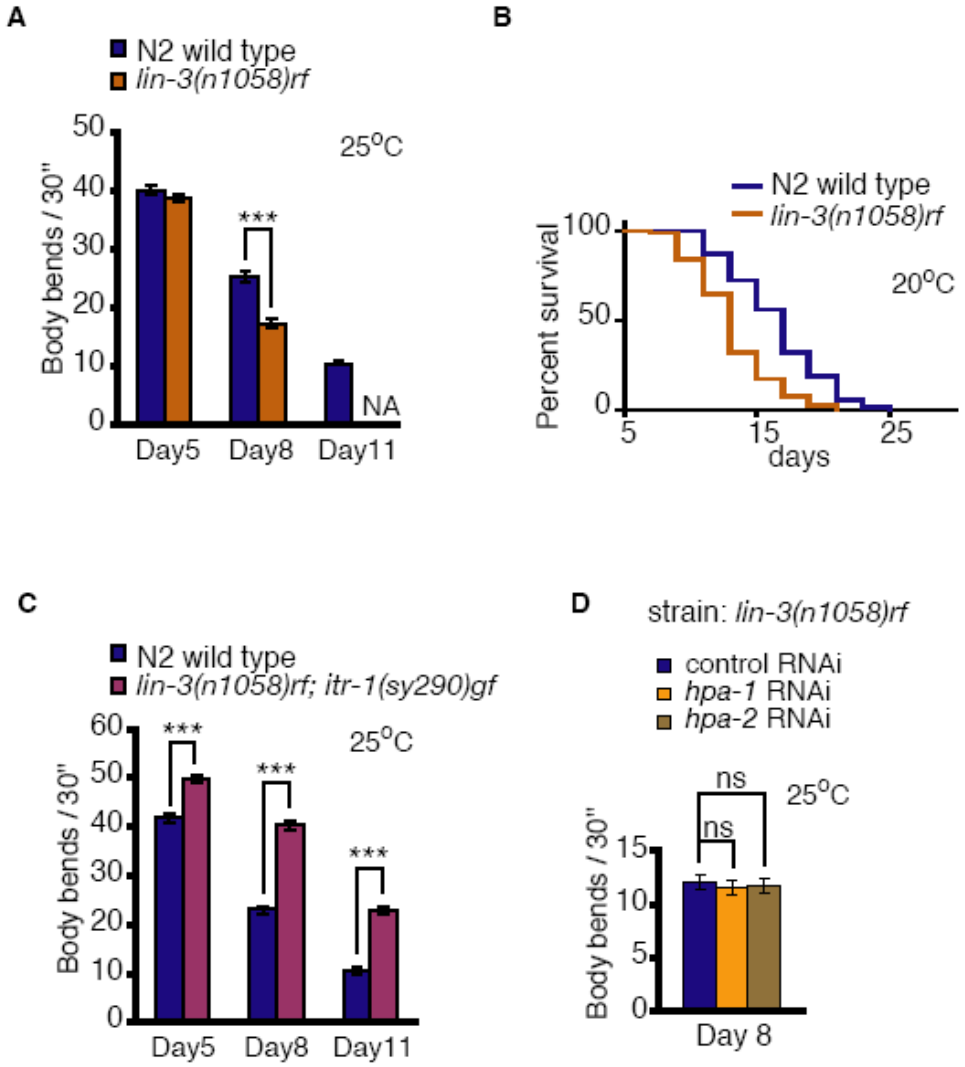
A
N2 wild type
lin-3(n1058)rf
25°C
Body bends / 30"
50
40
30
20
10
0
***
NA
Day5
Day8
Day11
B
N2 wild type
lin-3(n1058)rf
20°C
Percent survival
100
50
0
5
15
25
days
C
N2 wild type
lin-3(n1058)rf; itr-1(sy290)gf
25°C
Body bends / 30"
60
50
40
30
20
10
0
***
***
***
Day5
Day8
Day11
D
strain: lin-3(n1058)rf
control RNAi
hpa-1 RNAi
hpa-2 RNAi
ns
ns
25°C
Body bends / 30"
15
10
5
0
Day 8

Sup Figure 9

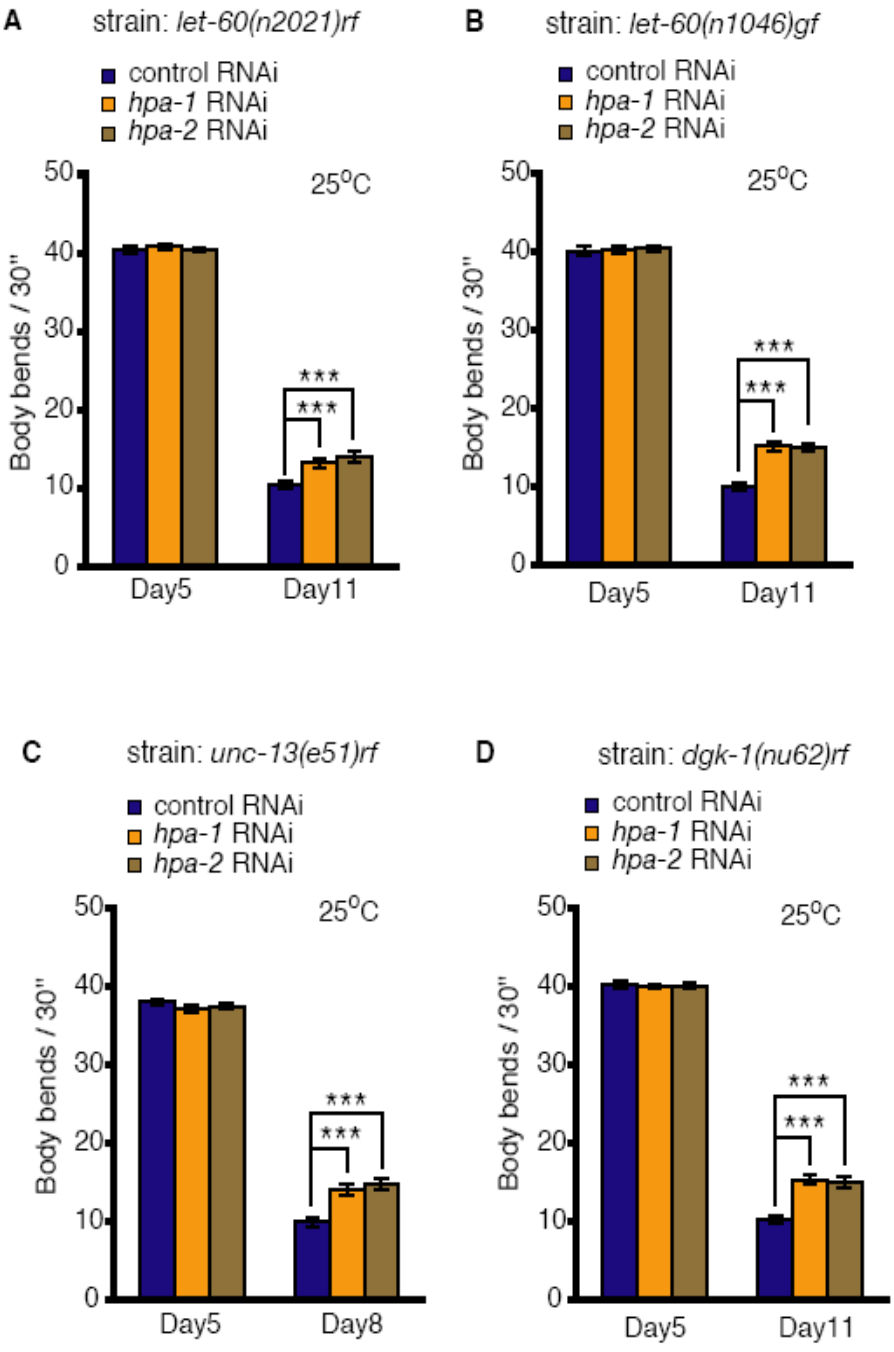
A
strain: let-60(n2021)rf
control RNAi
hpa-1 RNAi
hpa-2 RNAi
25°C
Body bends / 30"
50
40
30
20
10
0
***
***
Day5
Day11
B
strain: let-60(n1046)gf
control RNAi
hpa-1 RNAi
hpa-2 RNAi
25°C
Body bends / 30"
***
***
Day5
Day11
C
strain: unc-13(e51)rf
control RNAi
hpa-1 RNAi
hpa-2 RNAi
25°C
Body bends / 30"
***
***
Day5
Day8
D
strain: dgk-1(nu62)rf
control RNAi
hpa-1 RNAi
hpa-2 RNAi
25°C
Body bends / 30"
***
***
Day5
Day11

Sup Figure 10

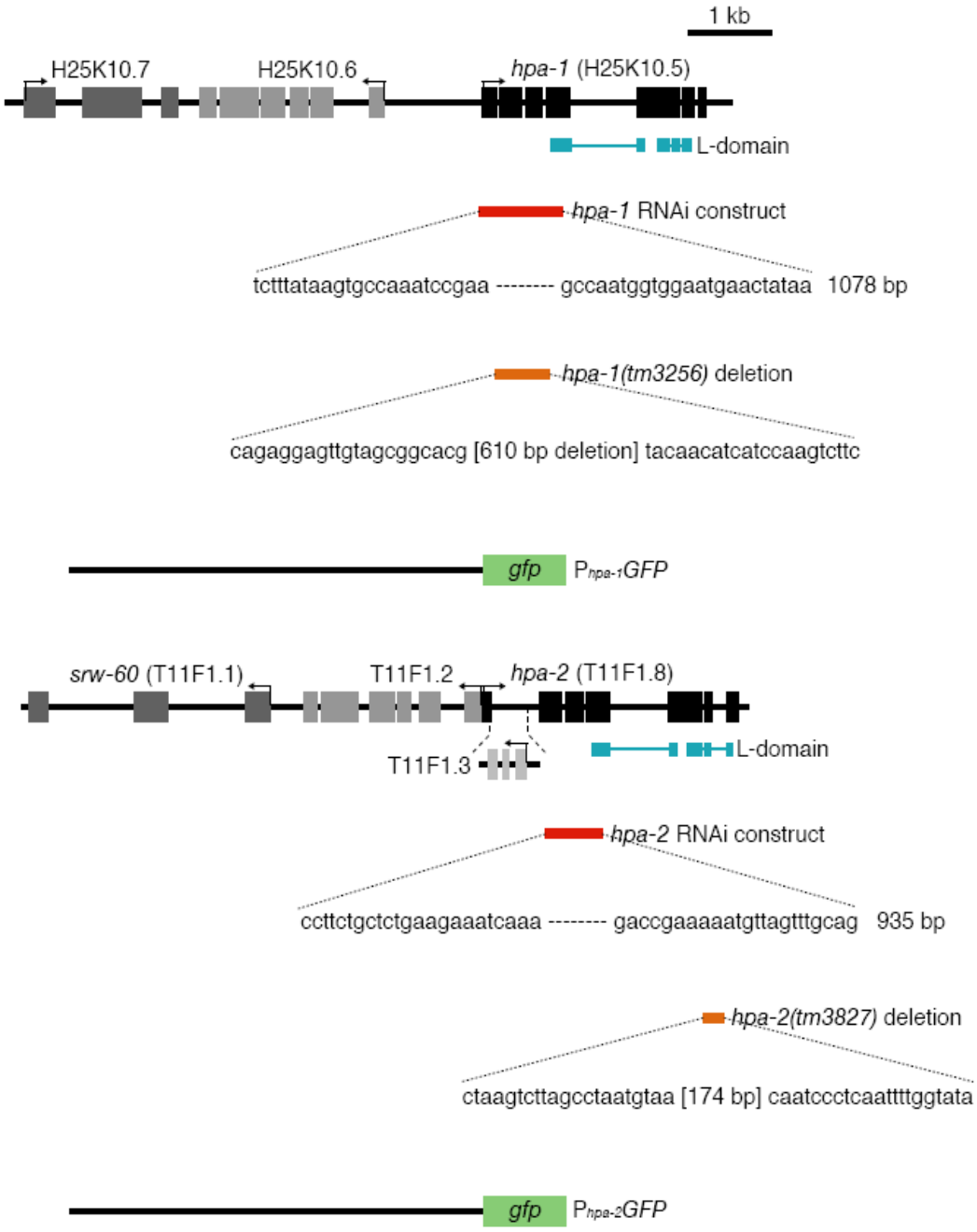

Sup Figure 11

Larval stage and young adult stage

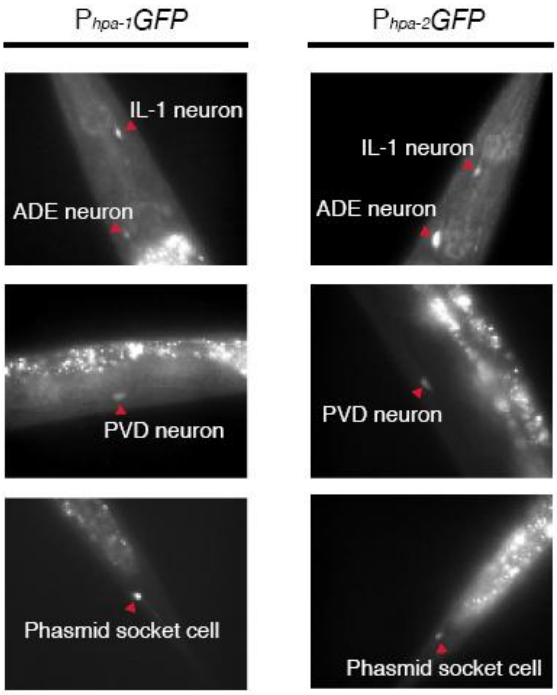

Reproductive and post-reproductive adult stage

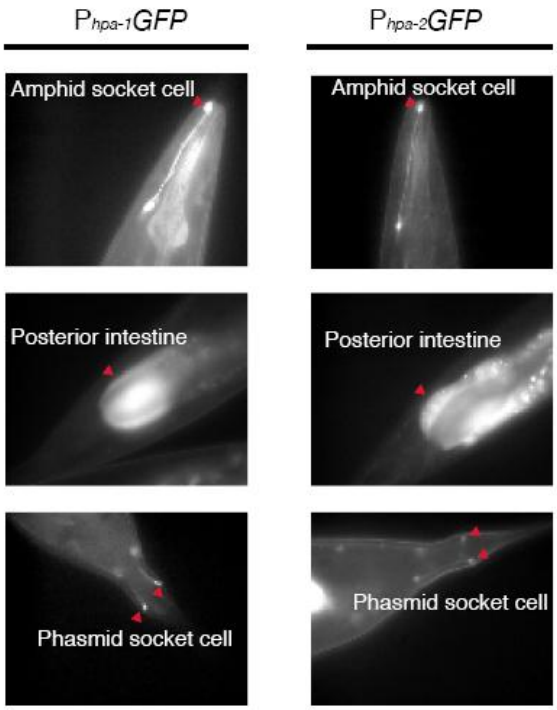

Table S1
Mid/late-age swimming phenotypes consequent to RNAi knockdowns of 54 putative insulin receptor-like genes in *C. elegans*

Gene Name	% control *	P-value	n	RNAi Library
C04G2.11	3%	ns: 0.6856	30	ref.2
C17E7.10	13%	< 0.05	30	ref.2
C30G4.6	-2%	ns: 0.6955	30	ref.2
C31E10.3	2%	ns: 0.8107	30	ref.2
C41G6.6	6%	ns: 0.7103	30	constructed
F02C12.4	-2%	ns: 0.7013	30	constructed
F11A5.7	9%	ns: 0.1670	30	ref.2
F14D2.6	-1%	ns: 0.9589	30	ref.2
F15E11.2	-20%	ns: 0.1118	30	constructed
F15E11.3	4%	ns: 0.4533	90	constructed
F15E11.4	26%	ns: 0.0790	30	ref.2
F15E11.5	12%	ns: 0.0736	90	ref.2
F15E11.11	23%	< 0.01	90	constructed
F45C12.1	2%	ns: 0.7949	30	ref.2
F45C12.16	-6%	ns: 0.2740	30	ref.2
F54G8.1	-6%	ns: 0.5941	30	ref.2
F56A4.9	7%	ns: 0.3656	30	ref.2
F58E1.4	1%	ns: 0.9408	30	ref.2
F58E1.7	18%	< 0.001	120	ref.2
F59D6.4	-16%	ns: 0.0971	30	ref.2
F59D6.6	6%	ns: 0.2655	30	ref.2
H25K10.5 (*hpa-1*)	28%	< 0.0001	150	ref.2
H25K10.6	-2%	ns: 0.8443	30	ref.2
K04F1.6	-8%	ns: 0.3766	30	constructed
K04F1.7	21%	< 0.05	30	constructed
K04F1.10	6%	ns: 0.5659	30	ref.2
K04F1.11	2%	ns: 0.8042	30	ref.2
K04F1.12	-3%	ns: 0.6002	30	constructed
K04F1.13	5%	ns: 0.7195	30	ref.2
K04F1.14	-13%	ns: 0.2831	30	ref.2
K12D9.12	-10%	ns: 0.3445	30	ref.2
R03G5.3	0%	ns: 0.9874	30	ref.2
T05A6.4	19%	ns: 0.0838	30	ref.2
T05A6.5	-3%	ns: 0.6779	30	constructed
T11F1.2	-12%	ns: 0.1181	30	ref.2
T11F1.6	13%	ns: 0.1882	30	ref.2
T11F1.7	23%	ns: 0.0570	30	ref.2
T11F1.8 (*hpa-2*)	43%	< 0.0001	150	ref.2
T26E4.1	9%	ns: 0.0685	30	ref.2
Y19D10A.7	7%	ns: 0.3656	30	constructed
Y19D10B.2	15%	< 0.01	120	constructed
Y37A1B.8	-8%	ns: 0.3726	30	ref.2
Y37A1B.9	0%	ns: 0.9556	30	constructed
Y70C5C.3	-6%	ns: 0.3758	30	ref.2
Y73F8A.18	7%	ns: 0.0825	30	constructed
ZC482.2	-2%	ns: 0.6784	30	constructed
ZC482.3	7%	ns: 0.5940	30	constructed
ZC482.4	-1%	ns: 0.9152	30	ref.2
ZC482.7	13%	< 0.05	90	constructed
ZK355.1	16%	ns: 0.0549	90	constructed
ZK355.4	19%	< 0.001	90	constructed
ZK355.5	-8%	ns: 0.5003	30	constructed
ZK355.6	-5%	ns: 0.6813	30	constructed
ZK1037.1	5%	ns: 0.7173	30	constructed

Table S2

hpa-1 and _hpa-2_ disruption does not affect development or dauer formation

Table S2A

hpa-1 and _hpa-2 RNAi_ does not confer developmental arrest in wild type N2

Genotype					
Background genes (Description)	RNAi	% dauer	% L4	% other†	n‡
N2 (Wild type)	control	0	99.1	0.9	225
	hpa-1	0	98.8	1.2	256
	hpa-2	0	99.5	0.5	190

Table S2B

hpa-1(tm3256) and _hpa-2(tm3827)_ deletion mutants do not confer developmental arrest

Genotype	% dauer	% L4	% other†	n‡
N2 (Wild type)	0	96.5	3.5	260
hpa-1(tm3256)	0	95.4	4.6	282
hpa-2(tm3827)	0	97.9	2.1	235
hpa-1(tm3256); hpa-2(tm3827)	0	98.2	1.8	167

Table S3
Lifespan data for Figures

Strain (Description)	Median Lifespan (days)	Mean Lifespan (days ± s.e.m.)	Maximum Lifespan (days ± s.e.m.)	P value log-rank (Mendel-Cox)	temperature (°C)	n	No of Exp.	Corresponding Figure
N2 (Wild type)	13	13.6 ± 0.4	21.3 ± 0.1		25	120/120	2	1G
age-1(hx546)	15 (15%)	18.1 ± 0.7 (33%, $p < 0.0001$)	32.7 ± 0.7 (51%, $p < 0.0001$)	< 0.0001	25	114/120	2	1G
hpa-1(tm3256)	17 (31%)	15.8 ± 0.4 (16%, $p < 0.0001$)	23.5 ± 0.7 (10%, $p < 0.05$)	< 0.001	25	116/120	2	1G
hpa-2(tm3827)	15 (15%)	14.9 ± 0.4 (10%, $p < 0.05$)	22.6 ± 0.6 (3%, ns)	< 0.05	25	116/120	2	1G
N2 (Wild type)	17	18.2 ± 0.4	27.6 ± 0.7		20	101/120	2	3G
let-23(sa62)gf (EGFR)	22 (29%)	21.9 ± 0.5 (20%, $p < 0.0001$)	30.1 ± 0.4 (9%, $p < 0.0001$)	< 0.0001	20	103/120	2	3G
N2 (Wild type)	26	26.7 ± 0.8	40.6 ± 0.9		25 > 15*	108/120	2	3H
let-23(n1045)rf (EGFR)	21 (-19%)	22.6 ± 0.8 (-15%, $p < 0.0001$)	37.5 ± 0.4 (-15%, $p < 0.01$)	< 0.005	25 > 15*	107/120	2	3H
N2 (Wild type)	17	16.4 ± 0.4	22.4 ± 0.5		20	98/122	2	S8C
lin-3(n1058)rf (EGF)	13 (-24%)	13.2 ± 0.2 (-20%, $p < 0.0001$)	19.0 ± 0.4 (-15%, $p < 0.0001$)	< 0.0001	20	147/171	2	S8C
N2 (Wild type)	19	19.7 ± 1.0	32.2 ± 0.4		20	101/120	2	4G
itr-1(sy290)gf (IP3R)	29 (53%)	29.0 ± 1.5 (47%, $p < 0.0001$)	41.4 ± 1.0 (29%, $p< 0.0001$)	< 0.0001	20	104/120	2	4G
N2 (Wild type)	18	19.3 ± 0.5	28.8 ± 0.7		15 > 20**	102/120	2	4H
itr-1(sa73)rf (IP3R)	16 (-11%)	15.5 ± 0.2 (-20%, $p < 0.0001$)	19.9 ± 0.2 (-31%, $p < 0.0001$)	< 0.0001	15 > 20**	116/120	2	4H

References

Augustin H , Partridge L (2009). Invertebrate models of age-related muscle degeneration. *Biochim Biophys Acta*. **1790**, 1084-1094.

Beitel GJ, Clark SG , Horvitz HR (1990). Caenorhabditis elegans ras gene let-60 acts as a switch in the pathway of vulval induction. *Nature*. **348**, 503-509.

Bishop NA , Guarente L (2007). Two neurons mediate diet-restriction-induced longevity in C. elegans. *Nature*. **447**, 545-549.

Bolanowski MA, Russell RL , Jacobson LA (1981). Quantitative measures of aging in the nematode Caenorhabditis elegans. I. Population and longitudinal studies of two behavioral parameters. *Mech Ageing Dev*. **15**, 279-295.

Brenner S (1974). The genetics of Caenorhabditis elegans. *Genetics*. **77**, 71-94.

Broughton S , Partridge L (2009). Insulin/IGF-like signalling, the central nervous system and aging. *Biochem J*. **418**, 1-12.

Cao Z, Wu Y, Curry K, Wu Z, Christen Y , Luo Y (2007). Ginkgo biloba extract EGb 761 and Wisconsin Ginseng delay sarcopenia in Caenorhabditis elegans. *J Gerontol A Biol Sci Med Sci*. **62**, 1337-1345.

Chow DK, Glenn CF, Johnston JL, Goldberg IG , Wolkow CA (2006). Sarcopenia in the Caenorhabditis elegans pharynx correlates with muscle contraction rate over lifespan. *Exp Gerontol*. **41**, 252-260.

Clandinin TR, DeModena JA , Sternberg PW (1998). Inositol trisphosphate mediates a RAS-independent response to LET-23 receptor tyrosine kinase activation in C. elegans. *Cell*. **92**, 523-533.

Clokey GV , Jacobson LA (1986). The autofluorescent "lipofuscin granules" in the intestinal cells of Caenorhabditis elegans are secondary lysosomes. *Mech Ageing Dev*. **35**, 79-94.

Cohen E, Bieschke J, Perciavalle RM, Kelly JW , Dillin A (2006). Opposing activities protect against age-onset proteotoxicity. *Science*. **313**, 1604-1610.

Croll NA, Smith JM , Zuckerman BM (1977). The aging process of the nematode Caenorhabditis elegans in bacterial and axenic culture. *Exp Aging Res*. **3**, 175-189.

Dlakic M (2002). A new family of putative insulin receptor-like proteins in C. elegans. *Curr Biol*. **12**, R155-157.

Duhon SA , Johnson TE (1995). Movement as an index of vitality: comparing wild type and the age-1 mutant of Caenorhabditis elegans. *J Gerontol A Biol Sci Med Sci*. **50**, B254-261.

Dutt A, Canevascini S, Froehli-Hoier E , Hajnal A (2004). EGF signal propagation during C. elegans vulval development mediated by ROM-1 rhomboid. *PLoS Biol*. **2**, e334.

Fisher AL (2004). Of worms and women: sarcopenia and its role in disability and mortality. *J Am Geriatr Soc*. **52**, 1185-1190.

Gems D , Riddle DL (2000). Genetic, behavioral and environmental determinants of male longevity in Caenorhabditis elegans. *Genetics*. **154**, 1597-1610.

Gerstbrein B, Stamatas G, Kollias N , Driscoll M (2005). In vivo spectrofluorimetry reveals endogenous biomarkers that report healthspan and dietary restriction in Caenorhabditis elegans. *Aging Cell*. **4**, 127-137.

Glatt SJ, Chayavichitsilp P, Depp C, Schork NJ , Jeste DV (2007). Successful aging: from phenotype to genotype. *Biol Psychiatry*. **62**, 282-293.

Glenn CF, Chow DK, David L, Cooke CA, Gami MS, Iser WB, Hanselman KB, Goldberg IG , Wolkow CA (2004). Behavioral deficits during early stages of aging in Caenorhabditis elegans result from locomotory deficits possibly linked to muscle frailty. *J Gerontol A Biol Sci Med Sci*. **59**, 1251-1260.

Greer EL , Brunet A (2009). Different dietary restriction regimens extend lifespan by both independent and overlapping genetic pathways in C. elegans. *Aging Cell*. **8**, 113-127.

Han M , Sternberg PW (1990). let-60, a gene that specifies cell fates during C. elegans vulval induction, encodes a ras protein. *Cell*. **63**, 921-931.

Herndon LA, Schmeissner PJ, Dudaronek JM, Brown PA, Listner KM, Sakano Y, Paupard MC, Hall DH , Driscoll M (2002). Stochastic and genetic factors influence tissue-specific decline in ageing C. elegans. *Nature*. **419**, 808-814.

Hill RJ , Sternberg PW (1992). The gene lin-3 encodes an inductive signal for vulval development in C. elegans. *Nature*. **358**, 470-476.

Hsu AL, Feng Z, Hsieh MY , Xu XZ (2009). Identification by machine vision of the rate of motor activity decline as a lifespan predictor in C. elegans. *Neurobiol Aging*. **30**, 1498-1503.

Hsu AL, Murphy CT , Kenyon C (2003). Regulation of aging and age-related disease by DAF-16 and heat-shock factor. *Science*. **300**, 1142-1145.

Huang C, Xiong C , Kornfeld K (2004). Measurements of age-related changes of physiological processes that predict lifespan of Caenorhabditis elegans. *Proc Natl Acad Sci U S A*. **101**, 8084-8089.

Huang LS , Sternberg PW (2006). Genetic dissection of developmental pathways. *WormBook*, 1-19.

Imura A, Tsuji Y, Murata M, Maeda R, Kubota K, Iwano A, Obuse C, Togashi K, Tominaga M, Kita N, Tomiyama K, Iijima J, Nabeshima Y, Fujioka M, Asato R, Tanaka S, Kojima K, Ito J, Nozaki K, Hashimoto N, Ito T, Nishio T, Uchiyama T, Fujimori T , Nabeshima Y (2007). alpha-Klotho as a regulator of calcium homeostasis. *Science*. **316**, 1615-1618.

Johnson TE (1987). Aging can be genetically dissected into component processes using long-lived lines of Caenorhabditis elegans. *Proc Natl Acad Sci U S A*. **84**, 3777-3781.

Kamath RS , Ahringer J (2003). Genome-wide RNAi screening in Caenorhabditis elegans. *Methods*. **30**, 313-321.

Kemp BJ, Church DL, Hatzold J, Conradt B , Lambie EJ (2009). Gem-1 encodes an SLC16 monocarboxylate transporter-related protein that functions in parallel to the gon-2 TRPM channel during gonad development in Caenorhabditis elegans. *Genetics*. **181**, 581-591.

Kenyon C, Chang J, Gensch E, Rudner A , Tabtiang R (1993). A C. elegans mutant that lives twice as long as wild type. *Nature*. **366**, 461-464.

Kirkland JL , Peterson C (2009). Healthspan, translation, and new outcomes for animal studies of aging. *J Gerontol A Biol Sci Med Sci*. **64**, 209-212.
Klein DE, Nappi VM, Reeves GT, Shvartsman SY , Lemmon MA (2004). Argos inhibits epidermal growth factor receptor signalling by ligand sequestration. *Nature*. **430**, 1040-1044.
Klein DE, Stayrook SE, Shi F, Narayan K , Lemmon MA (2008). Structural basis for EGFR ligand sequestration by Argos. *Nature*. **453**, 1271-1275.
Kurosu H, Yamamoto M, Clark JD, Pastor JV, Nandi A, Gurnani P, McGuinness OP, Chikuda H, Yamaguchi M, Kawaguchi H, Shimomura I, Takayama Y, Herz J, Kahn CR, Rosenblatt KP , Kuro-o M (2005). Suppression of aging in mice by the hormone Klotho. *Science*. **309**, 1829-1833.
Lackner MR, Kornfeld K, Miller LM, Horvitz HR , Kim SK (1994). A MAP kinase homolog, mpk-1, is involved in ras-mediated induction of vulval cell fates in Caenorhabditis elegans. *Genes Dev*. **8**, 160-173.
Lakowski B , Hekimi S (1998). The genetics of caloric restriction in Caenorhabditis elegans. *Proc Natl Acad Sci U S A*. **95**, 13091-13096.
Lang T, Streeper T, Cawthon P, Baldwin K, Taaffe DR , Harris TB (2009). Sarcopenia: etiology, clinical consequences, intervention, and assessment. *Osteoporos Int*.
Luetteke NC, Qiu TH, Fenton SE, Troyer KL, Riedel RF, Chang A , Lee DC (1999). Targeted inactivation of the EGF and amphiregulin genes reveals distinct roles for EGF receptor ligands in mouse mammary gland development. *Development*. **126**, 2739-2750.
Mair W , Dillin A (2008). Aging and survival: the genetics of life span extension by dietary restriction. *Annu Rev Biochem*. **77**, 727-754.
Majumdar AP (2003). Regulation of gastrointestinal mucosal growth during aging. *J Physiol Pharmacol*. **54 Suppl 4**, 143-154.
Majumdar AP (2005). Therapeutic potential of EGFR-related protein, a universal EGFR family antagonist. *Future Oncol*. **1**, 235-245.
Malone EA , Thomas JH (1994). A screen for nonconditional dauer-constitutive mutations in Caenorhabditis elegans. *Genetics*. **136**, 879-886.
Marciniak DJ, Rishi AK, Sarkar FH , Majumdar AP (2004). Epidermal growth factor receptor-related peptide inhibits growth of PC-3 prostate cancer cells. *Mol Cancer Ther*. **3**, 1615-1621.
Merris M, Kraeft J, Tint GS , Lenard J (2004). Long-term effects of sterol depletion in C. elegans: sterol content of synchronized wild-type and mutant populations. *J Lipid Res*. **45**, 2044-2051.
Moghal N , Sternberg PW (2003). The epidermal growth factor system in Caenorhabditis elegans. *Exp Cell Res*. **284**, 150-159.
Murakami H, Bessinger K, Hellmann J , Murakami S (2008). Manipulation of serotonin signal suppresses early phase of behavioral aging in Caenorhabditis elegans. *Neurobiol Aging*. **29**, 1093-1100.
Neikrug AB , Ancoli-Israel S (2009). Sleep Disorders in the Older Adult: A Mini-Review. *Gerontology*.
Park BJ, Lee DG, Yu JR, Jung SK, Choi K, Lee J, Lee J, Kim YS, Lee JI, Kwon JY, Lee J, Singson A, Song WK, Eom SH, Park CS, Kim DH,

Bandyopadhyay J , Ahnn J (2001). Calreticulin, a calcium-binding molecular chaperone, is required for stress response and fertility in Caenorhabditis elegans. *Mol Biol Cell*. **12**, 2835-2845.

Perriere G , Gouy M (1996). WWW-query: an on-line retrieval system for biological sequence banks. *Biochimie*. **78**, 364-369.

Pierce-Shimomura JT, Chen BL, Mun JJ, Ho R, Sarkis R , McIntire SL (2008). Genetic analysis of crawling and swimming locomotory patterns in C. elegans. *Proc Natl Acad Sci U S A*. **105**, 20982-20987.

Pierce SB, Costa M, Wisotzkey R, Devadhar S, Homburger SA, Buchman AR, Ferguson KC, Heller J, Platt DM, Pasquinelli AA, Liu LX, Doberstein SK , Ruvkun G (2001). Regulation of DAF-2 receptor signaling by human insulin and ins-1, a member of the unusually large and diverse C. elegans insulin gene family. *Genes Dev*. **15**, 672-686.

Raizen DM, Cullison KM, Pack AI , Sundaram MV (2006). A novel gain-of-function mutant of the cyclic GMP-dependent protein kinase egl-4 affects multiple physiological processes in Caenorhabditis elegans. *Genetics*. **173**, 177-187.

Raizen DM, Zimmerman JE, Maycock MH, Ta UD, You YJ, Sundaram MV , Pack AI (2008). Lethargus is a Caenorhabditis elegans sleep-like state. *Nature*. **451**, 569-572.

Restif C , Metaxas D (2008). Tracking the swimming motions of C. elegans worms with applications in aging studies. *Med Image Comput Comput Assist Interv Int Conf Med Image Comput Comput Assist Interv*. **11**, 35-42.

Schmelz EM, Xu H, Sengupta R, Du J, Banerjee S, Sarkar FH, Rishi AK , Majumdar AP (2007). Regression of early and intermediate stages of colon cancer by targeting multiple members of the EGFR family with EGFR-related protein. *Cancer Res*. **67**, 5389-5396.

Sutphin GL , Kaeberlein M (2008). Dietary restriction by bacterial deprivation increases life span in wild-derived nematodes. *Exp Gerontol*. **43**, 130-135.

Tatar M (2009). Can we develop genetically tractable models to assess healthspan (rather than life span) in animal models? *J Gerontol A Biol Sci Med Sci*. **64**, 161-163.

Tatar M, Bartke A , Antebi A (2003). The endocrine regulation of aging by insulin-like signals. *Science*. **299**, 1346-1351.

Timmons L, Court DL , Fire A (2001). Ingestion of bacterially expressed dsRNAs can produce specific and potent genetic interference in Caenorhabditis elegans. *Gene*. **263**, 103-112.

Ulrich P , Cerami A (2001). Protein glycation, diabetes, and aging. *Recent Prog Horm Res*. **56**, 1-21.

Van Buskirk C , Sternberg PW (2007). Epidermal growth factor signaling induces behavioral quiescence in Caenorhabditis elegans. *Nat Neurosci*. **10**, 1300-1307.

Wu Y , Han M (1994). Suppression of activated Let-60 ras protein defines a role of Caenorhabditis elegans Sur-1 MAP kinase in vulval differentiation. *Genes Dev*. **8**, 147-159.

Supporting Information

Note 1: Short food deprivation used to remove bacterial coating does not alter swimming locomotion.

C. elegans are reared on plates spread with live bacteria. To remove excess bacteria that coat the body, which we thought might physically interfere with swimming locomotion, we transferred individual worms to an unseeded agar plate for about 30 seconds to shake off bacteria prior to introduction to liquid. Because crawling locomotion rate increases after 5 minutes on plates lacking bacteria (Sawin *et al.*, 2000; Murakami *et al.*, 2008), we tested whether a short crawl without food might affect swimming rates. We examined the effect of 30 second food deprivation on swimming locomotion in well-fed N2 wild-type animals as young adults and mid/late adults (Fig. S1A, Supporting Information). We found no differences when we compared swim rates of direct observations to those of 30 second food deprivation. Thus, it is unlikely that this step in our protocol alters swimming behavior.

Note 2: Swimming rate decline is associated with aging.

We previously documented that same-age wild type cultures exhibit striking heterogeneity in crawling locomotory capabilities in middle and late life (Herndon et al., 2002), such that same-age animals can be identified as Class A (youthful locomotion), Class B (uncoordinated and lethargic) and Class C (paralyzed) (see also Fig. S3, Supporting Information). We find that swimming vigor exhibits a progressive decline with similar heterogeneity observed (Fig. S1B, Supporting Information). In fact, by 11 days of adulthood (25^{o}C) class C animals lost swimming ability, while the A class and B class animals still swim (A class for ~12

bends/30sec; B class for ~7 bends/30sec; C class for ~0 bends/30sec). In our scoring of older age swimming we did not include non-swimmers in the average score. We consider this focus on A and B swimmers somewhat akin to studies on aging human masters athletes (Tanaka & Seals, 1997; Donato *et al.*, 2003; Hawkins *et al.*, 2003; Tanaka & Seals, 2008) that track declining muscle/nerve performance in the absence of complications from other age-associated debilitation. Although this scoring likely over-estimates how well the general population is performing, it still provides a reproducible metric that reflects relative vigor of a strain associated with age.

Supporting Experimental Procedures

Construction of mutants: A single-mutant strain containing *itr-1(sy290)* was obtained from an *unc-24*/*itr-1 dpy-20* heterozygote, selecting non-Unc and non-Dpy progeny (presumed *itr-1*/*itr-1 dpy-20* or *itr-1*/*unc-24* recombinant arising by crossing over between *unc-24* and *dpy-20*), and then selecting the non-Unc and non-Dpy progeny to obtain the *itr-1* homozygote. The presence of *itr-1(sy290)* mutation in this strain was confirmed by DNA sequence analysis. A double-mutant strain containing *let-23(sa62)* and *ccIs4251* ($P_{myo\text{-}3}$*GFP/NLS*, *dpy-20*(+)) was obtained by constructing a *let-23/ccIs4251* heterozygote, and then selecting *let-23* multivulva (Muv) with GFP expression to obtain the *let-23* homozygote with the *ccIs4251* transgene array. Double-mutant strain *hpa-2(tm3827)*; *hpa-1(tm3256)* was obtained by constructing a *hpa-1(tm3256)/hpa-2(tm3827)* heterozygote, and then selecting the double deletion homozygote using PCR to identify deletion alleles, as described in main text methods section. The *hpa-1(tm3256)* and *hpa-2(tm3827)* alleles were tracked and/or sequenced by PCR amplification of genomic sequence encompassing the deletions with specific primers for *hpa-1(tm3256)* (5'CGGTTATCTAGGTGTGGCCT3' and 5'CCATGAGCAATATTACCCGA3') and for *hpa-2(tm3827)* (5'GTAGGTGGTAATTACGCCGA3' and 5' ACTCAAACAGCCGACATCGT3'), respectively.

RNAi bacteria: *Escherichia coli* (HT115) producing double-stranded RNA (dsRNA) were from the Ahringer library (Kamath & Ahringer, 2003), except for 21

insulin-related genes missing from that library that we constructed (Table S1). DNAs for dsRNA targeting 21 genes were constructed and inserted into empty vector (pL4440). Primer sequences of the template DNAs for dsRNA targeting 21 genes were as follows:

C41G6.6 forward, AAGGAAAAAAGCGGCCGCATGTTCGTTATCAAACTT

C41G6.6 reverse,

CGGGGTACCTTACTTACTGCACACTCTCCCGTCGAACGTC

F02C12.4 forward, AAGGAAAAAAGCGGCCGCATGAAATTGTTAAACACG

F02C12.4 reverse, CGGGGTACCGTCTTGGCATGACCTACCACA

F15E11.2 forward, AAGGAAAAAAGCGGCCGCATGCTCAAAACAATTTTC

F15E11.2 reverse, CGGGGTACCGTTCAACTTACTATCAAGATG

F15E11.3 forward, AAGGAAAAAAGCGGCCGCATGACTGAAAGCCAATTA

F15E11.3 reverse, CGGGGTACCAAACTTTATTGGAAAGAA

F15E11.11 forward, AAGGAAAAAAGCGGCCGCATGAACTTCTTGTTGATA

F15E11.11 reverse, CGGGGTACCCTTTAAATTTGGGACATTCAAATTAGT

K04F1.6 forward, AAGGAAAAAAGCGGCCGCATGTTTTCAAACAATTAT

K04F1.6 reverse, CGGGGTACCCTTACAACAATCAAGGCCATCAAA

K04F1.7 forward, AAGGAAAAAAGCGGCCGCATGTGGTGGCAGTTTTAT

K04F1.7 reverse, CGGGGTACCAAATGAAAAGAGCAGATTATG

K04F1.12 forward, AAGGAAAAAAGCGGCCGCATGCGTGAGAATAAAAAA

K04F1.12 reverse, CGGGGTACCTTTGATGTGGCGGCAATTTTTTCCTAA

T05A6.5 forward, CTCGAGTCTGTTTTGAGTTTGTCAGAGCAAAAAATGAACA

T05A6.5 reverse, CTCGAGACTTTCAGCATTTTCCAAGCATATAATTTTGCGT

Y19D10A.7 forward,

AAGGAAAAAAGCGGCCGCATGAAAATACTGATTTCACTAA

Y19D10A.7 reverse, CGGGGTACCAGTTAAAAGTTAAAATATGCTTC

Y19D10B.2 forward, AAGGAAAAAAGCGGCCGCATGTCGGCCGCGGCGAAA

Y19D10B.2 reverse, CGGGGTACCCACATTCAACTGCTTCCAATCCTGCC

Y37A1B.9 forward, CTCGAGATTTCCCCCAAACACATAATTTCGCATCATCAAA

Y37A1B.9 reverse, CTCGAGTTGAAAAACTATGAACAATGCCCCAACAAACTTT

Y73F8A.18 forward, AAGGAAAAAAGCGGCCGCATGAAAGAAAGTTTACTA

Y73F8A.18 reverse, CGGGGTACCGGTGTGGAAATTGTCGGATCGCACACGC

ZC482.2 forward, AAGGAAAAAAGCGGCCGCATGATATCAATAATCTAC

ZC482.2 reverse,

CGGGGTACCCATAATCCCATTTAATCCAACGTTTCTTAGATTT

ZC482.3 forward, AAGGAAAAAAGCGGCCGCATGAGAAGAAATATTCGC

ZC482.3 reverse, CGGGGTACCAAATTTACGCCAACTATGCACTCT

ZC482.7 forward, AAGGAAAAAAGCGGCCGCATGGTGTGCTCTTATATA

ZC482.7 reverse,

CGGGGTACCTATTTTGAAAAACAAACAAATAAAAAAAAACACGG

ZK355.1 forward, AAGGAAAAAAGCGGCCGCATGCAGTTTGTTTTTTCGAT

ZK355.1 reverse, CGGGGTACCAAATTCCTCAAAAGTCAGACAAAA

ZK355.4 forward, AAGGAAAAAAGCGGCCGCATGAAGTTTGGTGGGCTT

ZK355.4 reverse, CGGGGTACCCAATCTTTCATTAAACCCC

ZK355.5 forward, AAGGAAAAAAGCGGCCGCATGACTTTCGTTGTCTTA

ZK355.5 reverse, CGGGGTACCATTAATTTTCTCAAAACC

ZK355.6 forward, AAGGAAAAAAGCGGCCGCATGCGTTTTCTCTCCTGT

ZK355.6 reverse, CGGGGTACCATTCAAAGATGGAACAGCAAGCC

ZK1037.1 forward, AAGGAAAAAAGCGGCCGCATGTGCCTTTGGAGAAAT

ZK1037.1 reverse, CGGGGTACCTATCAAATTCGGCAAATTCAATTTGTT

Expression constructs: Transcriptional fusions P_{hpa-1}GFP and P_{hpa-2}GFP were generated by cloning 5 kb of upstream regulatory sequences of either gene into the pPD95.75 vector, which contains the green fluorescent protein (GFP) coding sequence and the 3' untranslated region of *unc-54*. Each construct was injected into N2 worms at 100 ng/μl with a dominant Roller marker, pRF4 containing *rol-6(su1006)* at 30 ng/μl. Primer sequences used in the construction of above plasmids as follows:

P_{hpa-1} forward,

CTGCAGTCGGCAATTTTTGAAATTTGCCGCACACACCACAAATTGG

P_{hpa-1} reverse,

CTGCAGTTTTGTCAAAACTTTCAAAATGCCTCGGGTAATATTGCTC

P_{hpa-2} forward,

CTGCAGCATTTTCATAAATTCACAGAGTTTTCCATAATGTTTTACA

P_{hpa-2} reverse,

CTGCAGACTAAAGTGAAGTTTGAGAGCAGAATGGCGATAACTTTAT

Phenotypic characterization of *hpa* knockdowns and mutants: Age-synchronous animals were grown at 20^{o}C and were treated with bacterial strains as described above. Pumping assays were performed on NGM plates with lawns of OP50-1 at room temperature. The number of contractions in the terminal bulb of the pharynx was measured at young adult stage (Day 4). For each strain, 10-15 different animals were scored during a 30 second period.

The defecation cycles of young adults were scored for each RNAi genotype and mutant as in Liu & Thomas, 1994. Cycles were observed at room temperature, and time was measured from one posterior body contraction to the next. For each strain, fifteen different animals were scored for 5-6 cycles each.

For developmental phenotypic analysis, the number of dauer progeny was scored 96 hr after the midpoint of egg laying at 20^{o}C. Brood size was measured by cloning ten L4 animals of each RNAi genotype and mutant, transferring egg-laying adults each day for 4 days to a new plate, and counting the resulting F1 progeny. For the observation of potential vulva phenotypes, all larvae on a plate were examined by differential interference contrast (DIC) optics when they were at the L4-young adult stage.

Behavioral scoring of aging nematodes: Age-synchronized animals were grown on *E. coli* strains at 25^{o}C as described above. When animals matured to

the young adult stage on day 5, they were scored every 2 days for class A, B and C as described in (Herndon *et al.*, 2002). In the reproductive phase, animals were transferred away from their progeny to fresh plates every 1-2 day to maintain an age-synchronized population.

Pharyngeal pumping decline assays: Age-synchronous animals were grown at 25^{o}C on *E. coli* strains at 25^{o}C as described above. The number of contractions in the terminal bulb of pharynx was measured on Days 3, 5 and 7. For each strain, 10-15 different animals were scored during a 60 second trial.

Supporting Figure legends

Fig. S1. Pilot experiments for swimming assays

(A) Effect of temporary food deprivation on swimming locomotion. Well-fed N2 wild type animals on a bacterial lawn plate were transferred to a fresh unseeded plate at 25° C and were allowed to crawl for 30 seconds, after which they were picked singly into wells of a microtiter plate containing M9 buffer. Swimming assays were carried out either directly, or after a 30 second crawl on an unseeded plate. Day 3 is first day of adult life in animals raised at 25^{o}C, as indicated by egg-laying onset. Error bars represent s.e.m.. Paired two tailed *t*-test (direct vs. after 30 second food deprivation) on each day; no statistical significance (ns).

(B) Swimming declines of age-synchronized old animals sorted according to mid-life crawling impairment. We sorted nematodes into A (youthful), B (partially impaired) and C (severely impaired, nearly paralyzed) classes based on locomotion and response to gentle touch (Herndon et al., 2002) and measured body bend rates. Day 3 is first day of adult life in animals raised at 25^{o}C, as indicated by egg-laying onset. Error bars represent s.e.m.. Paired two tailed *t*-test ***$P< 0.0001$. Note that all animals are of the same chronological age and A, B, C classes were first identified based on crawling ability on solid media.

Fig. S2. *hpa-1* and *hpa-2* RNAi knockdown or *hpa-1(tm3256)* and *hpa-2(tm3827)* deletion mutants do not have defects in pharyngeal pumping, defecation cycle, brood size or vulval development as assayed in young adult animals, suggesting no major developmental consequences of *hpa-1* and *hpa-2* disruption.

(A to C and G) Synchronized wt L1 larvae were fed bacteria expressing dsRNA, and grown at 20^{o}C. Worms were fed either bacteria not expressing dsRNA (empty vector; control) or bacteria expressing dsRNA that targeted the indicated transcripts. Note that *hpa-1* and *hpa-2* RNAi clones do not include any continuous homologous stretches longer than 12 nucleotides, and are thus highly unlikely to induce reciprocal transcript degradation. (D to F and H) cultures were reared at 20^{o}C under standard conditions.

(A) *hpa-1* and *hpa-2* RNAi does not alter pharyngeal pumping in young adults. Assay was carried on day 4 after hatching (first day of adult life at this temperature). At least ten animals were recorded for each trial (three trials). Error bars represent s.e.m..

(B) *hpa-1* and *hpa-2* RNAi does not alter defecation cycle time in young adults. Cycle time was measured from one posterior body contraction to the next. At least 15 animals were scored for six cycles each on day 4 after hatching (three trials). Error bars represent s.e.m..

(C) *hpa-1* and *hpa-2* RNAi does not impact brood size. Brood size was counted by transferring L4 larvae to individual plates and transferring adults every 24 hr for 4 days. The number of progeny on each plate was counted 1 day after egg hatching (10 parents total each trial, three trials). Error bars represent s.e.m..

(D) *hpa-1(tm3256)* and *hpa-2(tm3827)* deletion mutants are not defective in pharyngeal pumping in young adults. Assay was carried out on day 4 after hatching (first day of adult life at this temperature). At least ten animals were recorded for each trial (two trials). Error bars represent s.e.m..

(E) *hpa-1* and *hpa*-2 deletion mutants are not defective in defecation cycle time as young adults. Cycle time was measured from one posterior body contraction to the next. At least 15 animals were scored for six cycles each on day 4 after hatching (two trials). Error bars represent s.e.m..

(F) *hpa-1* and *hpa*-2 deletion mutants have normal brood sizes. Brood size was counted by transferring L4 larvae to individual plates every 24 hr for 4 days. The number of progeny on each plate was counted 1 day after egg hatching (10 animals total each trial, two trials). Error bars represent s.e.m..

(G) *hpa-1* and *hpa-2* RNAi does not impact vulval development. Panels show representative photos of adults for observations of more 200 worms total each.

Arrows indicate the positions of normal vulvae. We did not observe morphological defects or bagging.

(H) *hpa-1* and *hpa-2* deletion mutants do not impact vulval development. Panels show representative photos of observations of more than 200 adults total each. Arrows indicate the positions of normal vulvae. We did not observe morphological defects or bagging.

Fig. S3. The *hpa-2(tm3827)*;*hpa-1(tm3256)* double mutant exhibits phenotypes similar to single mutants.

(A) The *hpa-2(tm3827);hpa-1(tm3256)* double mutant exhibits enhanced swimming performance in advanced age that is similar in vigor to single mutants. Error bars represent s.e.m.. Unpaired two tailed *t*-test (N2 versus mutant on each day) ***$P < 0.0001$.

(B) The *hpa-2(tm3827);hpa-1(tm3256)* double mutant is not defective in pharyngeal pumping in young adults. Assay was carried on day 4 after hatching (first day of adult life at this temperature). At least ten animals of were recorded for each trial (two trials). Error bars represent s.e.m..

(C) The *hpa-2(tm3827);hpa-1(tm3256)* double mutant is not defective in defecation cycle time in young adults. Cycle time was measured from one

posterior body contraction to the next. At least 15 animals were scored for six cycles each on day 4 after hatching (two trials). Error bars represent s.e.m..

(D) The *hpa-2(tm3827);hpa-1(tm3256)* double mutant has normal brood sizes. Brood size was counted by transferring L4 larvae to individual plates every 24 hr for 4 days. The number of progeny on each plate was counted 1 day after egg hatching (10 parents total each trial, two trials). Error bars represent s.e.m..

(E) The *hpa-2(tm3827);hpa-1(tm3256)* double mutant is not defective in vulval development. Panels show representative photos of adults for observations of more 200 worms total each. Arrows indicate the positions of normal vulvae. We did not observe morphological defects or bagging.

Fig. S4. Plate locomotion decline appears delayed in aging *hpa-1* and *hpa-2* RNAi animals.

WT *C. elegans* transit through progressive stages of crawling impairment on solid media as they age, and can be sorted into groups that move vigorously in response to an eyelash hair touch (Class A, green); that are uncoordinated and sluggish in response to touch (Class B, yellow); or that are virtually paralyzed except for the head (Class C, red) (Herndon et al., 2002). Note that decline rates are variable among individual aging animals, but trends can be compared across populations. Class A animals have a greater life expectancy than Class C animals, despite having the same chronological age and same environment—

Class A are the graceful agers. We scored *hpa-1* and *hpa-2* RNAi-treated animals for plate locomotion phenotypes, using empty vector as a negative control and PI3 kinase *age-1* (RNAi) as a positive control. y-axis, percentage of animals in a given category; x-axis, days after hatch at 25^{o}C (75 worms for each assay). Although healthspan-promoting impact is not as robust as for *age-1(RNAi),* the *hpa-1* and *hpa-2* knockdown animals exhibit a slowed locomotory decline as compared to vector-only RNAi controls.

Fig. S5. Age-specific mortality rate analysis from the lifespan curves of Fig. 1F and G.

The age-specific mortality rates $q(x)$ for each 2 day period throughout life (interval $z = 2$) were calculated from $q(x) = (N(x) – N(x + z))/N(x)/z$, where $N(x)$ is the number of animals alive on day x. (A-C) Age-specific mortality rate for wild type N2, *age-1(hx546)*, *hpa-1(tm3256)* and *hpa-2(tm3827)*. The circles are the age-specific mortality rates in WT N2; squares are the age-specific mortality rates in either *age-1(hx546)*, *hpa-1(tm3256)* or *hpa-2(tm3827)*; ventral axis is log scale. (D-F) as above, with log of mortality rate plotted vs. age.

Fig. S6. *hpa-1* and *hpa-2* RNAi can extend locomotory healthspan of *age-1* and *daf-2* reduction-of-function mutants.

Assays of *hpa-1* and *hpa-2* RNAi effects on swimming of *age-1(hx546)* and *daf-2(e1368)ts* partial reduction-of-function mutants in the IIS pathway. Mutants were fed with bacteria expressing indicated dsRNA; control is empty vector.

Error bars represent s.e.m., unpaired two tailed *t*-test (control versus *hpa-1* or *hpa-2* RNAi on each day) *$P<$ 0.01, **$P<$ 0.001, ***$P<$ 0.0001. Note that to avoid developmental consequences of genetic disruption, temperature-sensitive *daf-2(e1368)ts* mutants were grown at permissive temperature of 15^{o}C until day 5 after hatching (first day adults) and were then transferred to restrictive temperature 25^{o}C at the beginning of adult life, so *daf-2* activities are disrupted only during adulthood. Since *hpa-1(RNAi)* and *hpa-2(RNAi)* can further extend locomotory healthspan in IIS mutant backgrounds late in life, they appear able to act, at least in part, independently of the IIS pathway. However, it should be noted that neither RNAi nor genetic mutants constitute a null situation, so data must be considered with regard to that caveat. That *hpa(RNAi)*-dependent differences in *age-1* and *daf-2* swimming become apparent only late adult life might reflect a maximum swimming capacity from summed pathways in mid-adult life or alternatively might suggest a mid-life requirement for insulin-like signaling in *hpa(RNAi)* activity. Still, the finding that *hpa-1* and *hpa-2* (RNAi) is additive with insulin pathway down-regulation later in life suggested that HPA-1 and HPA-2 act in part through a different pathway, which promoted us to examine HPA/receptor sequence relationships more closely (Fig. S7).

Fig. S7. HPA-1 and HPA-2 L domains exhibit sequence similarities to L domains of mammalian ERRP and EGFR proteins.

(A) Sequence alignment of L-domains of HPA-1, HPA-2, members of EGFR family and *C. elegans* InsR DAF-2. HPA-1 and HPA-2 have the Ixx-LxIxx-Nx-

Lxx-Lxx-Lxx-Lxx-like-repeat motif present in the L-domain of EGFR family proteins (Knight & Bass, 2001). Identical residues are shown based on ClustalW (Thompson et al., 1994) alignment of L-domains from *C. elegans* (Ce), *Homo sapiens* (Hs), *Mus musculus* (Mm) and *Rattus norvegicus* (Rn). Blue boxes indicate the conserved amino acids for the repeat motif. Residue identity between L-domains is highlighted in black, and similarity is highlighted in gray. We show the sequence alignment of L-domains for Ce_HPA-1 (GeneID: 186781, residue 215-330), Ce_HPA-2 (GeneID: 188415, residue 198-307), Ce_LET-23 (GeneID: 174462, residue 384-491), the *C. elegans* EGFR homologs Mm_EGFR (GeneID: 13649, residue 57-168), Hs_EGFR (GeneID: 1956, residue 57-168), Rn_ERRP (GeneID: 24329, residue 57-168), and the *C. elegans* InsR homolog Ce_DAF-2 (GeneID: 175410, residue 177-302).

(B) Schematic representations of HPA-1, HPA-2, *C. elegans* EGFR homolog LET-23, mammalian EGFR-related protein (ERRP), and truncated mammalian EGFR isoforms. Domain assignments are as follows: Signalp, cleaved signal peptide; L-domain, Leucine-rich repeats; FU, furin-like Cys-rich repeats; TM, transmembrane domain; TyrKc, protein tyrosine kinase domain. Note: The BLASTP program for HPA-1 picked up mammalian EGFR homolog (i.e., human EGFR isoform b (e-value = $5e^{-05}$)), although no significant similarity was found for the HPA-2 homolog. HPA-1 and HPA-2 are related in sequence to each other (e-value = $6e^{-85}$). HPA-2 was identified also on the Blast list as similar to EGFR-related protein (ERRP).

Fig. S8. EGF ligand disruption reduces healthy aging and blocks *hpa-1* and *hpa-2* RNAi benefits.

(A) Reduction of EGF/LIN-3 activity accelerates age-associated swimming decline. The *lin-3(n1058)rf* mutants were obtained from fertile heterozygote parents. For experiments, synchronized progeny were distributed one worm per plate and then sterile *lin-3(n1058)rf* homozygote adults were collected for assay. Error bars represent s.e.m.. Unpaired two tailed *t*-test (N2 versus *lin-3(n1058)* mutant on each day) ***$P < 0.0001$.

(B) Double mutants of EGF ligand *lin-3(n1058)rf* and IP3R gain-of-function *itr-1(sy290)gf* exhibit enhanced swimming vigor later in life. The *itr-1(sy290)gf lin-3(n1058)rf* double mutant has extended locomotory healthspan, suggesting ITR-1 acts downstream of LIN-3 signaling. Error bars represent s.e.m.. Unpaired two tailed *t*-test (N2 versus *lin-3(n1058)* mutant on each day) ***$P < 0.0001$.

(C) The EGF mutant *lin-3(n1058)rf* exhibits diminished mid-life survival. For lifespan assay, synchronized progeny were distributed one worm per plate and then sterile *lin-3(n1058)rf* homozygote adults were collected for assay at 20^{o} C. Detailed statistics from survival curves are given in Table S3.

(D) EGF reduction-of-function eliminates swimming vigor conferred by *hpa-1* and *hpa-2* RNAi. Indicated strains were fed with bacteria expressing indicated dsRNA; control is empty vector. Error bars represent s.e.m., unpaired two tailed

t-test (control versus *hpa-1* or *hpa-2* RNAi on 8 day), *P* values were not significant for any comparisons. The experiments were conducted at 25^{o}C.

Fig. S9. RNAi studies suggest that HPA-1 and HPA-2 do not impact locomotory aging through the RAS and DAG signaling pathways. Tested are effects of RAS and DAG signaling mutations on swimming vigor under conditions of *hpa-1* and *hpa-2* RNAi. (A) *let-60(n2021)rf* mutants, (B) *let-60(n1046)gf* mutants, (C) *unc-13(e51)rf* mutants, and (D) *dgk-1(nu62)rf* mutants (DAG kinase/*dgk-1(rf)* is predicted to increase DAG levels, consequently up-regulating UNC-13 functions(Nurrish *et al.*, 1999)) were fed with bacteria expressing indicated *hpa-1* and *hpa-2* dsRNA; control is empty vector. Error bars represent s.e.m., Unpaired two tailed *t*-test (control versus *hpa-1* or *hpa-2* RNAi on each day). All experiments were conducted at 25^{o}C. Note that the swimming performance of *unc-13(e51)* animals seemed normal in young stage, but was not assayed on day 11 since population was prematurely dead.

Fig. S10. Descriptions of *hpa-1* and *hpa-2* deletions, RNAi clones and promoter GFP fusions. Black boxes represent the exon structures of *hpa-1* (H25K10.5) and *hpa-2* (T11F1.8). Gray boxes represent the exon structures of neighboring genes. Blue boxes show the L-domains encoded by *hpa-1* and *hpa-2*. Green boxes indicate *gfp* coding sequences fused with 5 kb upstream regions of *hpa-1* and *hpa-2* (black lines). Sequences used in *hpa-1* and *hpa-2* RNAi constructs are indicated by red lines. The *hpa-1(tm3256)* mutation deletes the N-terminal region of HPA-1 (orange line: cagaggagttgtagcggcacg [610 bp deletion]

tacaacatcatccaagtcttc). Allele *tm3256* deletes part of exon 1 to exon 3, resulting in a frameshift that could create a stop codon at amino acid 66. The *hpa-2(tm3827)* mutation deletes the C-terminal part of HPA-2 (orange line: ctaagtcttagcctaatgtaa [174 bp deletion] caatccctcaattttggtata). Note that ORF T11F1.3 is transcribed in the opposite direction of *hpa-2* and is not expected to be targeted by RNAi experiments for *hpa-2* knockdown.

Fig. S11. *hpa-1* and *hpa-2* GFP reporters are co-expressed in specific neurons, glia and intestine.

$P_{hpa\text{-}1}$*GFP* and $P_{hpa\text{-}2}$*GFP* are expressed in strikingly similar tissue and cell-specific patterns. Panels show representative fluorescence images of larval to adult animals expressing either $P_{hpa\text{-}1}$*GFP* or $P_{hpa\text{-}2}$*GFP*. Arrowheads indicate the GFP signals. During larval stage and young adult stage (Day 2-3, 25 ^{o}C), we observed expression in the head IL-1 neurons and ADE neurons, and in the body midsection PVD neuron. In rare cases, we also observed expression in the phasmid socket cells during larvae and young adult. In the reproductive stage (Day 4-5, 25 ^{o}C) we find expression in posterior intestine and glia-like cells amphid (head) and phasmid (tail) socket cells. *hpa-1* and *hpa-2* GFP reporters appear expressed with identical cell specificities during the reproductive stage. Because RNAi is relatively ineffective in the nervous system (Timmons et al., 2001) and because *hpa-1* and *hpa-2* RNAi effects were robust, we speculate that non-neuronal expression is critical for the *hpa-1* and *hpa-2* influence on aging. HPA-1 and HPA-2 are probably secreted from their cellular sites of origin as

they include signal sequences. Note that since fusions are transcriptional, it is possible that some sequences that normally regulate expression are missing from expression constructs.

Supporting Table Legends

Table S1. Middle/late-age swimming phenotypes consequent to RNAi knockdown of 54 insulin receptor-like genes in *C. elegans*

RNAi inactivation of some insulin receptor extracelular ligand binding domain-related genes (Dlakic, 2002) conferred high swimming performance in advanced age (*Hpa* phenotype). Swimming assays were carried out 11 days after hatching, 25^{o}C, which is 8 days after animals become sexually mature adults; this is middle/late adult life in the ~ 20 day lifespan at this temperature (Ibanez-Ventoso et al., 2006). The strain used for the screen was ts sterile *spe-9(hc88),* (previously characterized to age similarly to N2 wild type) to eliminate progeny at 25^{o}C (Fabian & Johnson, 1994). The % difference between mean body bends of indicated RNAi clones and those of their respective control (empty vector) is shown in the third column (*P* value, unpaired two-tailed *t*-test; n, total number of animals for experiments). The control assay was always performed in parallel with the experiments for each clone to control for possible daily environmental changes.

We selected H25K10.5 (*hpa-1)* and T11F1.8 (*hpa-2*) (gray highlight) for full indepth analysis because RNAi reliably conferred the strongest locomotory phenotypes, because swimming rates were wild type in young adults, and because deletion alleles became available during the course of our study (details on deletions in Fig. S10. However, we note that there were 7 other tested genes that confer *Hpa* phenotypes with statistical significance, suggesting that there

may be several members of this gene class that can modulate the quality of locomotory aging.

Table S2. *hpa-1* and *hpa-2* disruption does not affect development or dauer formation.

Table S2A. *hpa-1* and *hpa-2 RNAi* does not confer developmental arrest in wild type N2.

For developmental phenotypic analysis, the number of dauer and other arrested progeny were scored 96 hr after the midpoint of egg laying at 20^{o}C (Hopper, 2006).

† Primarily unhatched eggs, L1s, or clear, unhealthy-looking L2s.

‡ Total number of progeny scored.

Table S2B. *hpa-1(tm3256)* and *hpa-2(tm3827)* deletion mutants do not confer developmental arrest.

For developmental phenotypic analysis, the number of dauer and other arrested progeny were scored 96 hr after the midpoint of egg laying at 20^{o}C (Gems et al., 1998).

† Primarily unhatched eggs, L1s, or clear, unhealthy-looking L2s.

‡ Total number of progeny scored.

Table S3. Lifespan data analyses for survival curves presented.

(%) percentage of lifespan extension relative to the control strain or wild type and (p) probability of being identical to the control strain or wild type (unpaired two-tailed *t*-test).

* Strains were grown at permissive temperature of 25^{o}C until day 5 after hatching, and then transferred to the non-permissive temperature of 15^{o}C.

** Strains were grown at permissive temperature of 15^{o} C until day 5 after hatching, and then transferred to the non-permissive temperature of 20^{o} C.

Supporting References

Dlakic M (2002). A new family of putative insulin receptor-like proteins in C. elegans. *Curr Biol*. **12**, R155-157.

Donato AJ, Tench K, Glueck DH, Seals DR, Eskurza I , Tanaka H (2003). Declines in physiological functional capacity with age: a longitudinal study in peak swimming performance. *J Appl Physiol*. **94**, 764-769.

Fabian TJ , Johnson TE (1994). Production of age-synchronous mass cultures of Caenorhabditis elegans. *J Gerontol*. **49**, B145-156.

Gems D, Sutton AJ, Sundermeyer ML, Albert PS, King KV, Edgley ML, Larsen PL , Riddle DL (1998). Two pleiotropic classes of daf-2 mutation affect larval arrest, adult behavior, reproduction and longevity in Caenorhabditis elegans. *Genetics*. **150**, 129-155.

Hawkins SA, Wiswell RA , Marcell TJ (2003). Exercise and the master athlete--a model of successful aging? *J Gerontol A Biol Sci Med Sci*. **58**, 1009-1011.

Herndon LA, Schmeissner PJ, Dudaronek JM, Brown PA, Listner KM, Sakano Y, Paupard MC, Hall DH , Driscoll M (2002). Stochastic and genetic factors influence tissue-specific decline in ageing C. elegans. *Nature*. **419**, 808-814.

Hopper NA (2006). The adaptor protein soc-1/Gab1 modifies growth factor receptor output in Caenorhabditis elegans. *Genetics*. **173**, 163-175.

Ibanez-Ventoso C, Yang M, Guo S, Robins H, Padgett RW , Driscoll M (2006). Modulated microRNA expression during adult lifespan in Caenorhabditis elegans. *Aging Cell*. **5**, 235-246.

Kamath RS , Ahringer J (2003). Genome-wide RNAi screening in Caenorhabditis elegans. *Methods*. **30**, 313-321.

Knight SW , Bass BL (2001). A role for the RNase III enzyme DCR-1 in RNA interference and germ line development in Caenorhabditis elegans. *Science*. **293**, 2269-2271.

Liu DW , Thomas JH (1994). Regulation of a periodic motor program in C. elegans. *J Neurosci*. **14**, 1953-1962.

Murakami H, Bessinger K, Hellmann J , Murakami S (2008). Manipulation of serotonin signal suppresses early phase of behavioral aging in Caenorhabditis elegans. *Neurobiol Aging*. **29**, 1093-1100.

Nurrish S, Segalat L , Kaplan JM (1999). Serotonin inhibition of synaptic transmission: Galpha(0) decreases the abundance of UNC-13 at release sites. *Neuron*. **24**, 231-242.

Sawin ER, Ranganathan R , Horvitz HR (2000). C. elegans locomotory rate is modulated by the environment through a dopaminergic pathway and by experience through a serotonergic pathway. *Neuron*. **26**, 619-631.

Tanaka H , Seals DR (1997). Age and gender interactions in physiological functional capacity: insight from swimming performance. *J Appl Physiol*. **82**, 846-851.

Tanaka H , Seals DR (2008). Endurance exercise performance in Masters athletes: age-associated changes and underlying physiological mechanisms. *J Physiol*. **586**, 55-63.

Thompson JD, Higgins DG , Gibson TJ (1994). CLUSTAL W: improving the sensitivity of progressive multiple sequence alignment through sequence weighting, position-specific gap penalties and weight matrix choice. *Nucleic Acids Res*. **22**, 4673-4680.

Timmons L, Court DL , Fire A (2001). Ingestion of bacterially expressed dsRNAs can produce specific and potent genetic interference in Caenorhabditis elegans. *Gene*. **263**, 103-112.

CURRICULUM VITAE

SHIH-HUNG YU

Education

1996-2000
Bachelor of Science in Medical Technology, Department of Medical Technolgy, National Taiwan University, Taiwan

2003-2004
Graduate student in Neuroscience program, University of Medicine and Dentistry of New Jersey

2004-2011
Program in Neuroscience, Rutgers, the State University of New Jersey

Working experience

2002-2003
Research Associate, National Taiwan University Hospital, Department of Genetic Medicine, Taipei, Taiwan

Teaching experience

2006
General Biology Lab, Teaching Assistant, The Division of Life Science, Rutgers University

2007
Genetics, Teaching Assistant, The Division of Life Science, Rutgers University

2007-2009
Genetics Lab, Teaching Assistant, The Division of Life Science, Rutgers University

2009-2011
Mentor, Daniel Burke, B.S., Undergraduate Honor Thesis, Rutgers University

Publications

Yu SH, Chiang WC, Shih HM, Wu KJ (2004) Stimulation of c-Rel transcriptional activity by PKA catalytic subunit beta. *Journal of Molecular Medicine* Sep;82(9):621-628

Iwasa H, **Yu S**, Xue J, Driscoll M (2010) Novel EGF pathway regulators modulate *C. elegans* healthspan and lifespan via EGF receptor, PLC-gamma, and IP3R activation. *Aging Cell* Aug;9(4):490-505

Yu S, Driscoll M (2011) EGF signaling comes of age: promotion of healthy aging in *C. elegans*. *Experimental Gerentology* Feb-Mar;46(2-3):129-134